Université de Liège

UNIVERSITY OF LIEGE
Faculty of Medicine
Laboratory of Analytical Chemistry
Professor Philippe HUBERT

New pharmaceutical applications involving Near Infrared spectroscopy as a PAT compliant process analyzer


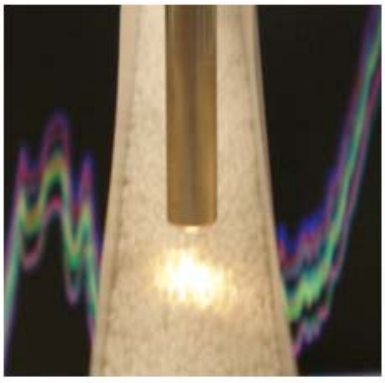
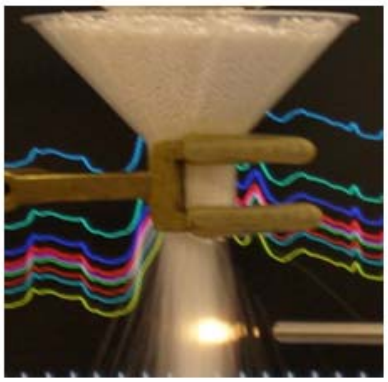
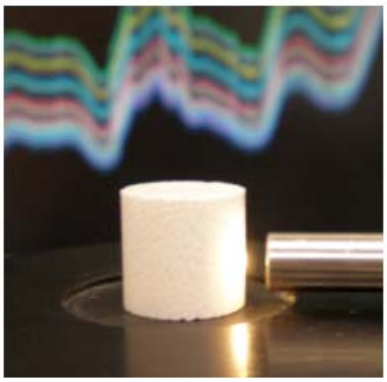

Jérôme MANTANUS
Pharmacist

Doctoral thesis in Biomedical and Pharmaceutical Sciences

Academic year 2011-2012

It is a great pleasure to thank those who made this thesis possible.

First of all, I owe my deepest gratitude to Prof. Philippe Hubert and Mr. Bruno Streel who gave me the opportunity to start and achieve this project.

I am heartily thankful to my supervisor, Dr Eric Ziémons. His every day high quality guidance and support, and always valuable advices were key elements for me to achieve this project.

I am also thankful to Dr Eric Rozet for sharing with me his solid expertise in analytical method validation.

Special thanks go to Prof. Jukka Rantanen and his team in Copenhagen for sharing with me their major expertise in PAT.

I would like to show my gratitude to SMB-Galephar for always providing me interesting and challenging PAT projects. Thanks go especially to Régis Klinkenberg for providing me technical support and always valuable advices.

I am grateful to Dr Attilio Ceccato, Dr Fabienne Wijzen and Dr Kathy Van Butsele from Odyssea pharma for the scientific meetings and technical advices we had on a nice PAT project.

I would like to show my gratitude to SMB-Galephar and to the Walloon Region for their financial support during the entire PhD. Thanks also go to the Fonds Léon Fredericq which provided me the financial support for my scientific training in Copenhagen.

I would like to thank all the members of the Laboratory of Analytical Chemistry from Liège, especially my colleagues of the 'IR team office': PhD student Pierre Lebrun and Dr Benjamen Debrus whose always valuable advices and great sense of humour made life enjoyable during the 4 years of PhD.

Special thanks go to the members of the Pharmaceutical Technology Laboratory of Liège for the scientific and non-scientific discussions during the coffee breaks.

Lastly, I would also like to thank my family for creating an environment in which following this path seemed so natural.

Table of contents

Chapter I

Introduction

I.1. Process Analytical Technology

Nowadays, conventional pharmaceutical manufacturing is generally accomplished using batch processing with laboratory testing conducted on randomly collected samples to evaluate their conformity. The latter approach slows down the batch release step as most of those conformity tests are carried out on end-product samples. Moreover, most manufacturing processes are performed with frozen process parameters, any changes in the manufacturing procedure requiring a new regulatory submission. Based on the previous considerations, FDA proposed a new concept: Process Analytical Technology (PAT) which can be defined as "*a system for designing, analyzing, and controlling manufacturing through timely measurements (i.e., during processing) of critical quality and performance attributes of raw and in-process materials and processes, with the goal of ensuring the final product quality*" [1], forming the basis of the pharmaceutical Good Manufacturing Practice (GMP) of the 21st century [2].

To ensure the final product quality, PAT requires adequate process analyzers. These analyzers should be used first to identify the processing steps impacting the most on the targeted product performance. Next, the real time monitoring of the identified critical processing steps should be achieved with analytical method developed on the selected process analyzers. Based on the collected data, the product critical quality attributes can be monitored and if necessary adjusted in real time by means of feed-back and feed-forward control loops enabling to keep the manufacturing within the defined product specifications.

Depending on the proximity between the manufacturing line and the process analyzers, *off-line*, *at-line*, *on-line* and *in-line* measurements can be performed. *Off-line* defines a measurement where the sample is removed, isolated from, and analyzed away from the process stream. The concept is the same for the *at-line* measurement except that the analysis is performed in close proximity to the process stream. *On-line* characterizes a measurement where the sample is diverted from the manufacturing process, and may be returned to the process stream. If the manufacturing line and process analyzers allow it, *in-line* measurements are the shortest and ideal way to monitor the insight of a process as the sample is not removed or diverted from the process stream. This measurement can be invasive or non-invasive. The data gathered during the production will provide a better process understanding and may also enable the Real Time Release (RTR) of the pharmaceutical batches which is defined by "*the ability to evaluate and ensure the acceptable quality of in-process and/or final product based on process data*" [1].

Facing the requirements of the PAT tools, there is a need for analytical techniques being able to acquire a large amount of data within seconds during all the critical steps of a pharmaceutical manufacturing process. The advantages of vibrational spectroscopic

techniques such as NIR and Raman spectroscopy, which will be discussed in the next sections, match the requirements of the PAT framework.

Together with PAT, there is also an increasing demand from the regulatory authorities towards the pharmaceutical industries to gain a comprehensive understanding of their processes together with an accurate estimation of their robustness and reliability. Instead of providing solutions to meet these demands and requirements, authorities have published guidelines establishing the philosophy to achieve these expectations [1-5]. In the ICH Q8(R2) guideline on pharmaceutical development [3], the emphasis is put on the "*Quality by Design*" concept, stating that the quality should not be tested into products, but should be built in. The Design Space concept is also introduced in this guideline, which is "*the multidimensional combination and interaction of input variables (e.g., materials attributes) and process parameters that have been demonstrated to provide assurance of quality*". Furthermore, ICH indicates that as long as the process and formulation parameters are kept within the defined Design Space, no regulatory post approval change is needed. Furthermore, the Design Space of a process also guarantees its reliability and robustness, supporting the quality risk management system.
Facing the challenges and expectations of the ICH Q8(R2) guideline on the pharmaceutical development, the process analyzers as described in the PAT concept can be advantageously integrated in a general Quality by Design quality system to provide reliable real time information helping to define the process design space.
Accordingly, this combination of real time analysis together with advanced process understanding and improved quality risk management are clearly promoting factors to achieve consistent product performance as requested by the ICH Q10 guideline on the pharmaceutical quality system [5].

Besides, in addition of being highly encouraged, the key concepts and recommendations appearing in the ICH Q8(R2), Q9 and Q10 guidance to industry are now becoming more and more mandatory: this can be read in the recent Manual of Policies and Procedures (MAPP) 5016.1 document for the chemistry, manufacturing, and controls (CMC) reviewers in the Office of the Pharmaceutical Science (OPS) [6]. The document is effective since 2nd August of this year and clearly highlights the use of PAT and QbD as follows:

> *"Reviewers should determine whether an application includes sufficient enhanced knowledge that demonstrates the applicant's understanding of materials attributes, manufacturing processes, and controls for product quality to support the proposed flexible regulatory approaches. Examples of flexible regulatory approaches are as follows:*
> - ***Manufacturing process improvements without regulatory notification (e.g., movement within a design space).***
> - *…*

- ***In-process tests in lieu of end product testing, including real time release testing approaches (e.g., "PAT – A Framework for Innovative Pharmaceutical Development, Manufacturing, and Quality Assurance," September 2004)."***

The subject of the present thesis being the use of NIR spectroscopy for pharmaceutical applications, the emphasis will be mainly put on NIR spectroscopy as a process analyzer while a potential application using Raman spectroscopy will also be considered. Indeed, the latters have been applied in numerous PAT applications to monitor pharmaceutical processes such as blending [7-11], granulation [12-16], coating [9, 17-23], drying [24], tabletting [9-10, 21, 23, 25-36], pelletization [37], hot-melt extrusion [38], freeze-drying [39-43] and fermentation [44].

I.2. Near Infrared Spectroscopy

I.2.1. History

While observing the dispersion of the sunlight through a glass prism, William Herschel noticed in 1800 that the area below the red end of the visible spectrum provided a significant heating effect [45]. The near infrared (NIR) radiation was discovered.
In 1881, Abney and Festing, using photographic plates, recorded the spectra of organic solvants within the 1000-1200 nm wavelength range [46]. Their observations highlighted the importance of the hydrogen bond in the NIR spectrum.
Combining a rock salt prism with a thermopile connected to a galvanometer, Coblentz created the first NIR spectrometer. Even though each substance had its own fingerprint, Coblentz found out that defined functional groups experienced some specific trend in their spectral features suggesting the possibility to extract structural information out of the NIR spectra [47].

The first quantitative application using NIR spectroscopy was developed in 1912 by Fowle who determined the atmospheric moisture content [48]. Later on, Ellis and Bath studied the interaction between water and gelatine in 1938 [49].

NIR spectroscopy made a step forward when the lead sulphide semi-conductor detector became commercially available in the 1950s. However, NIR research activities were slower than in the mid-infrared (MIR) field. This was linked to the fact that the wide absorption bands observed in the NIR field made spectral visual interpretation difficult. Consequently, parallel to the improvement of the optics, there was a need for new tools to extract the relevant information out of the NIR spectra. Therefore, the recent developments of NIR spectroscopy were enabled by advances in micro-computing which allowed performing advanced data analysis based on Chemometrics.

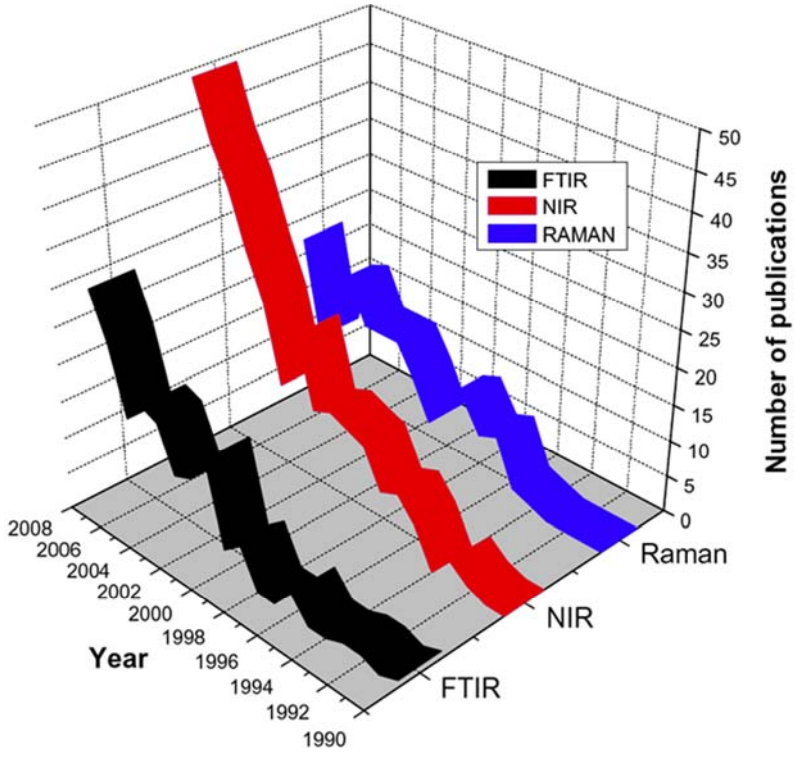

Fig. 1 - Number of publications involving multicomponent analysis by vibrational spectroscopy during the last decade [50].

Figure 1 clearly shows that vibrational spectroscopy has been increasingly involved in multicomponent analysis during the last decade [50]. In terms of publication number, among FT-IR and Raman techniques, NIR spectroscopy seems to stand on the first place for multicomponent analysis. Reasons for this increasing success may be first the improvements made in Chemometrics: data exploration and interpretation is now facilitated with stand-alone chemometric software based on user friendly point-and-click environment. Second, the availability of NIR spectrometers dedicated to various applications such as routine use, research and development and process monitoring together with the emergence of chemical imaging broadens the applicability of NIR spectroscopy. Indeed, it is now being used in the food [51-52], fuel [53-54] and pharmaceutical industry [55-57]. Within the pharmaceutical industry, NIR spectroscopy has been used to monitor critical quality attributes such as the API content [9-10,25-36,38], the moisture content [12-16,24,34,37,39,40-43], solid state[18, 37 38, 40, 43], blend uniformity [7-11], bulk density [16], hardness [25, 31, 36], coating [9,17,19-21,23] and particle size distribution [13,16,31]. Moreover, compared to tedious and time consuming reference methods (e.g. HPLC, dissolution bath testing, ...) , the fact that NIR and Raman spectroscopy allows simultaneous analysis of multiple sample critical quality attributes from the same sample in a single spectral acquisition without sample preparation and environmental sides effects may also justify their increasing success. Finally, as discussed previously, the use of process analyzers such as NIR and Raman spectroscopy to support the pharmaceutical quality system is more and more encouraged in the recent regulatory documents [1,3,6].

I.2.2. Principles of Near Infrared Spectroscopy

I.2.2.1. The NIR spectral region

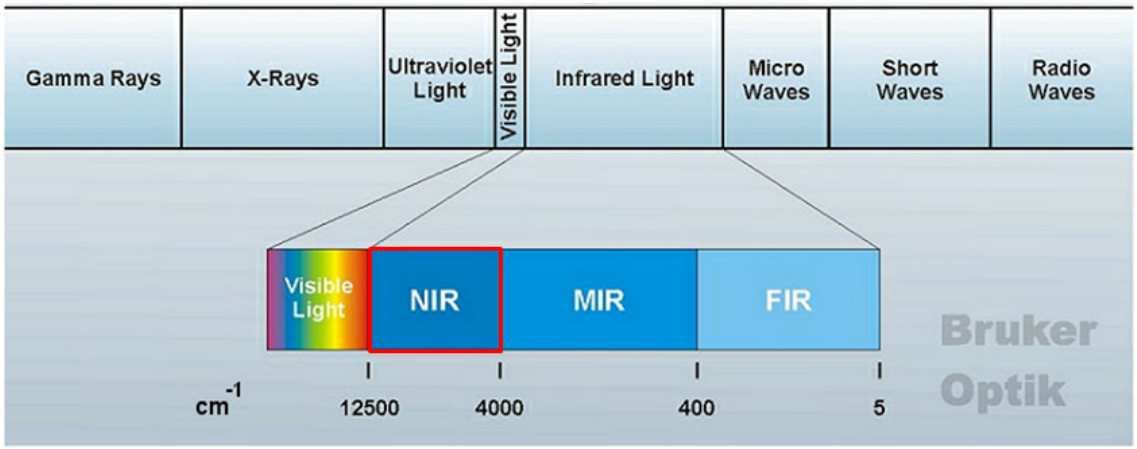

Fig. 2 - Location of the NIR spectral region in the electromagnetic spectrum.

As can be seen from Figure 2, NIR spectroscopy encompasses the spectral region located between 12500 and 4000 cm^{-1} (2500 – 500 nm). Mid infrared (MIR) as well as NIR spectroscopy are both part of vibrational spectroscopy and belong to absorption techniques.

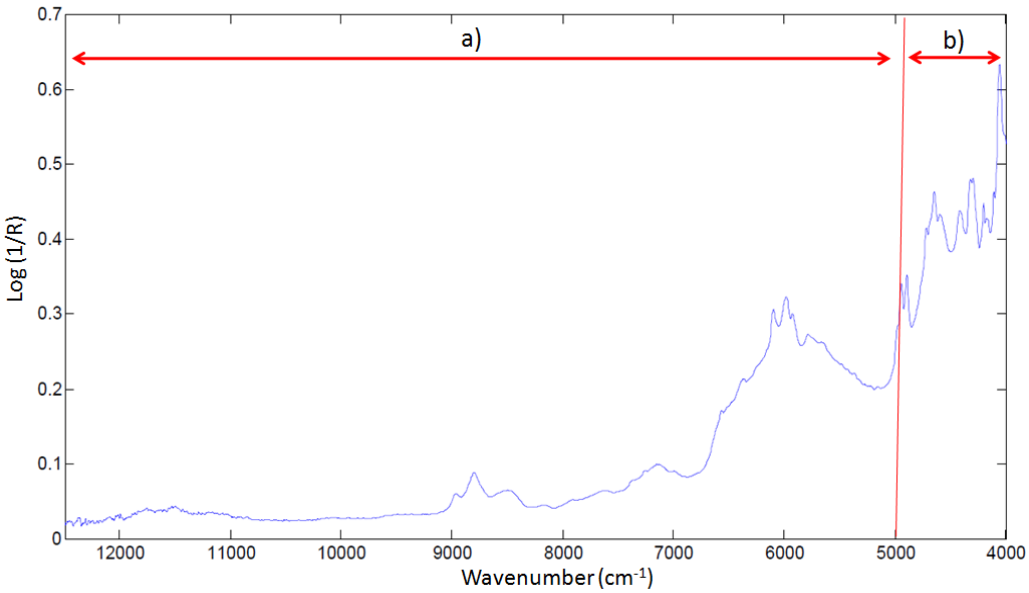

Fig. 3 - Spectral areas related to overtones (a) and combinations bands (b) in the NIR reflectance spectrum of acetaminophen PVP3.

However, contrary to MIR where transitions consist in fundamental vibrations, overtone and combination bands are observed in the NIR region, leading to large overlapping absorption bands. As an example, Figure 3 displays the NIR reflectance spectrum of acetaminophen PVP

3, i.e. acetaminophen mixed with 3 % povidone. In the NIR spectrum, overtones absorption bands are located in the 12500-5000 cm^{-1} spectral area while combination absorption bands are found in the 5000-4000 cm^{-1} spectral range [58-59].

I.2.2.2. The electromagnetic wave

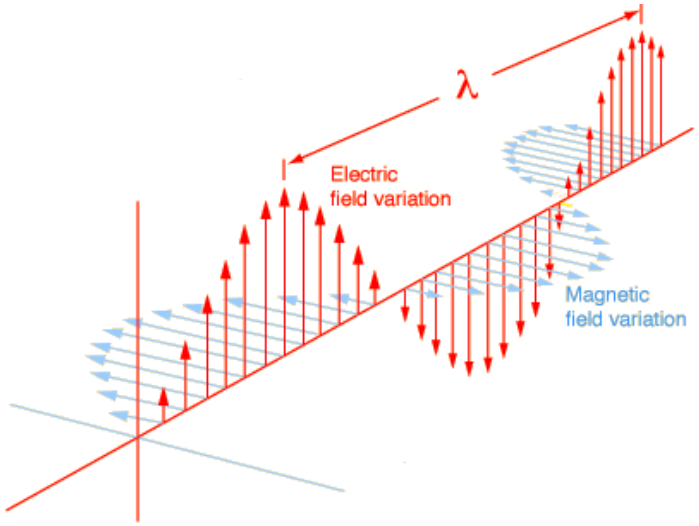

Fig. 4 - Electromagnetic wave propagation.

Light is a radiation consisting in the combination of an electric and magnetic field perpendicular to each other and also perpendicular to the propagation direction corresponding to the light direction (Figure 4).Both electric and magnetic fields exhibit a sinusoidal variation in space which can be defined by the following equation:

$$Y = A \sin 2 \pi \nu t \quad (1)$$

Where *Y* is the moving distance whose maximum is designated by the amplitude *A*, *v* is the wave frequency and *t* is the time.

The Wavelength λ is defined by the accomplished distance between two successive minima or maxima, it can be defined by the following equation:

$$\lambda = c / \nu \quad (2)$$

Where *c* is the speed of light in vacuum.

Besides NIR spectra are usually represented as the absorbance as a function of the wavenumber "$[\tilde{\nu}]$" which is expressed by the following equation:

$$[\tilde{\nu}] = 1 / \lambda \quad (3)$$

I.2.2.3. The absorption phenomenon of NIR spectroscopy

To take into account the absorption phenomenon, it is necessary to consider the electromagnetic wave as a protons flux which energy is proportional to the wave frequency. 2 physical models exist to explain the vibrations observed in the infrared region: the harmonic and anharmonic oscillators.

- *The harmonic oscillator*

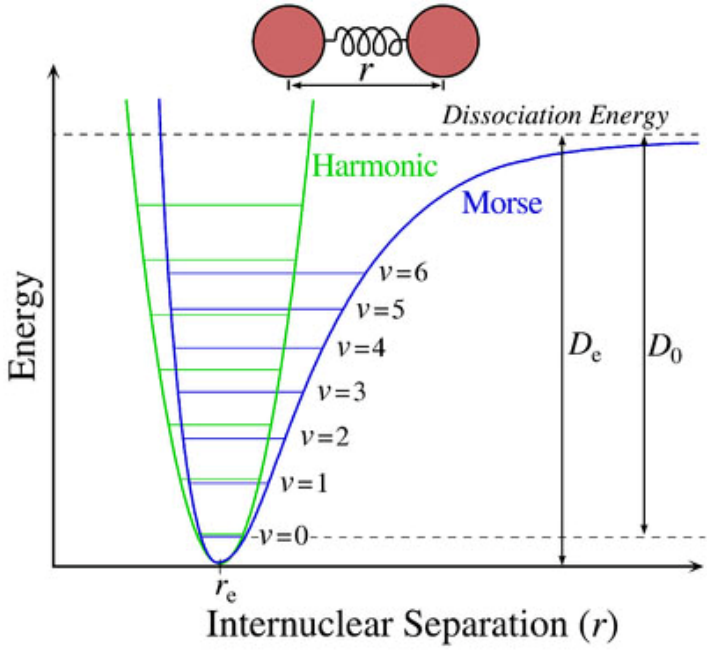

Fig. 5 - Potential energy curves of harmonic (green) and anharmonic (blue) oscillators.

Considering two masses, two atoms, bound together and vibrating. The vibrations lead to change in internuclear distance. According to the Hooke's law, the potential energy can be represented by the following equation:

$$V = ½ k (r-r_e)^2 = ½ kq^2 \quad (4)$$

Where *V* is the potential energy, *k* is the force constant of the bond, *r* is the internuclear distance during the vibration, r_e is the equilibrium internuclear distance, and $q = (r-r_e)$ is the displacement coordinate. Figure 5 displays the potential energy curve which is parabolic and symmetrical.

The model vibrational frequence is expressed as follows:

$$\nu = (1/2\pi)\sqrt{(k/m)} \quad (5)$$

Where the reduced mass *m* is given by:

$$m = (m_1 m_2)/(m_1+m_2) \quad (6)$$

If a transition occurs between the non-excited state (V=0) and the first excited state (V=1), the transition corresponds to the fundamental absorption.
From this model, it is observed that 2 elements are required for the vibration to exist, a dipole moment is needed. The previous consideration leads to the fact that MIR has a discriminant ability for polar groups.
However, the harmonic oscillator has major limitations: a chemical bond does not have only one but multiple vibration frequencies: the fundamental, the overtones and the combinations bands. Besides this model does not take into account the possibility of dissociation when the vibrating bond is strongly extended and the repulsive forces between the atoms [58].

- *The anharmonic oscillator*

For the anharmonic oscillator, the energy levels are no longer equidistant (Figure 5). The potential energy is represented by the Morse function:

$$V = D_e [1-\exp(a(r_{eq}-r))]^2 \quad (7)$$

Where *V*, D_e, *a* and r_{eq} are respectively the potential energy, the dissociation energy, a specific constant of the atomic bonds and the equilibrium internuclear distance.

This model provides a real representation of the atomic bond energy according the inter atomic distance: the overtones and combinations bands are modelled. The absorption bands close to 2 ν and 3 ν are called first and second overtones. In addition to the overtones, combination bands also occur due to the interaction between at least 2 vibration modes of the same molecule. The frequency of these absorption bands represent the sum or difference of fundamental frequencies multiples.

I.2.2.4. Chemical nature of the NIR absorption bands

As can be seen from Table 1, common and poorly specific X-H atomic bonds involving C, O, N and S as X give birth to NIR absorption bands. Based on Figure 3 and Table 1, one can easily understand that visual identification directly from the NIR spectra is rather difficult. This latter issue is caused mainly by the nature of the atomic bonds involved in the NIR signal and by an overlapping between the absorption bands which is explained by the overtones and combination bands occurring in the NIR spectral region. Accordingly, Chemometrics is needed to extract the information of interest out of the physico-chemical data contained in the NIR spectra [58-59].

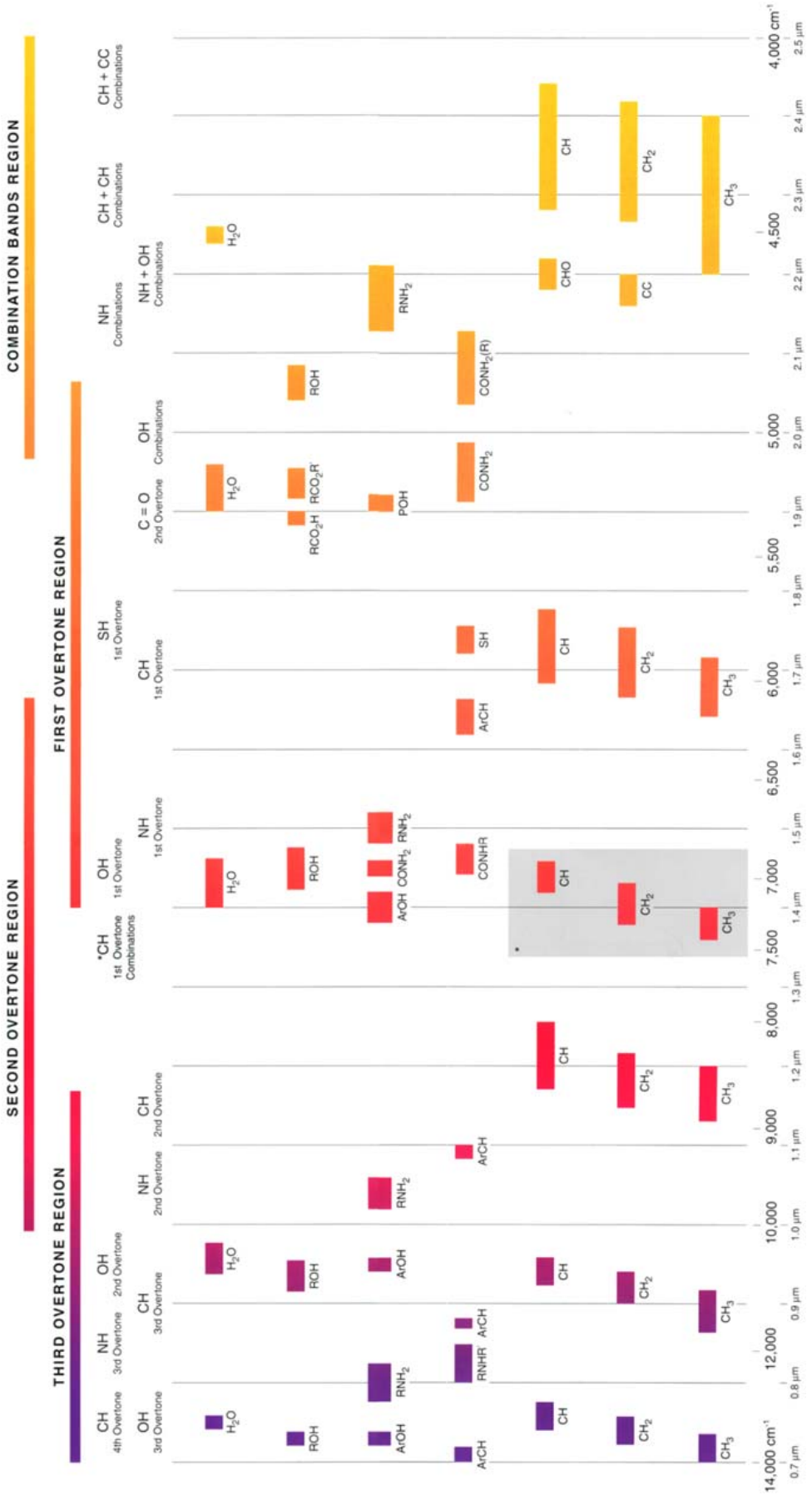

Table 1 - Chemical nature of the NIR absorption bands [Bruker Optics].

I.2.3. Near Infrared Instrumentation

Nowadays, mainly 2 types of NIR spectrometers are available: dispersive and Fourier Transform (FT) NIR spectrometers. Each of them is described separately hereafter. Then the advantages of FT over dispersive instruments are discussed in the following sections.

- *Dispersive NIR spectrometer*

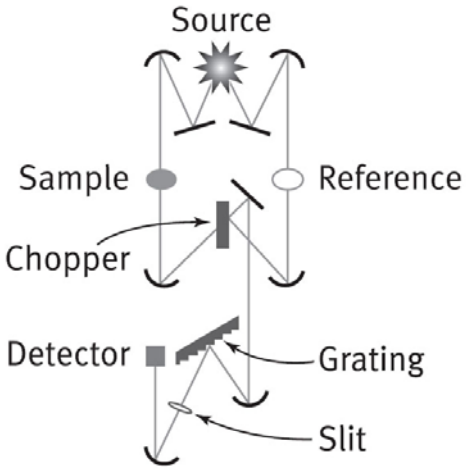

Fig. 6 - Dispersive spectrometer diagram [Thermo scientific].

For dispersive instruments, the NIR beam emitted by the source is separated sequentially into wavelength bandwidths by a moving grating (Figure 6). The grating then directs each wavelength to the detector via a slit. Consequently, each wavelength is analyzed separately and the entire spectrum is measured when the moving grating has selected the entire spectral range [58-59].

- *Fourier Transform NIR spectrometer*

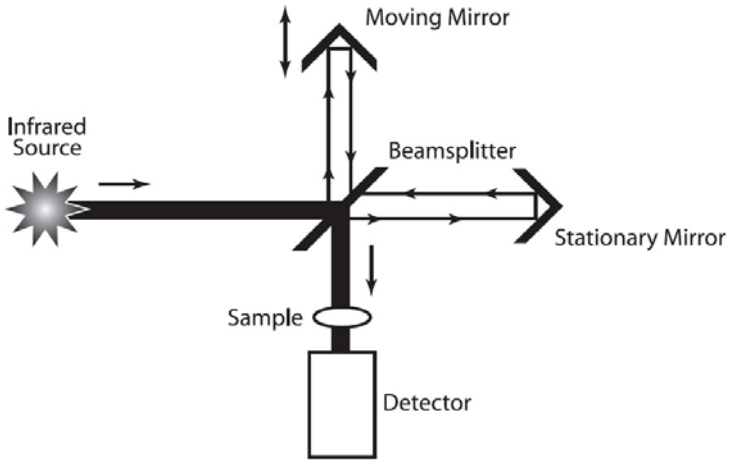

Fig. 7 - FT spectrometer diagram [Thermo scientific].

FT-NIR instruments are based on the Michelson Interferometer system which directs the NIR beam as described in Figure 7: the NIR beam coming from the source is divided into 2 beams by a beamsplitter. One beam is directed on a moving mirror while the other is directed on a fixed mirror. Further, the separated beams are reflected and recombined at the beamsplitter. According to the difference of travel distance happening between the 2 beams, constructive and destructive interference occur, leading to a global interference pattern called the interferogram. The interferogram then goes through the sample. Some of the energy is absorbed, some is transmitted. The transmitted part containing all the spectral range finally goes to the detector. The data are then sent to a computer which converts the interferogram into a spectrum by performing the Fourier Transform algorithm [58-59].

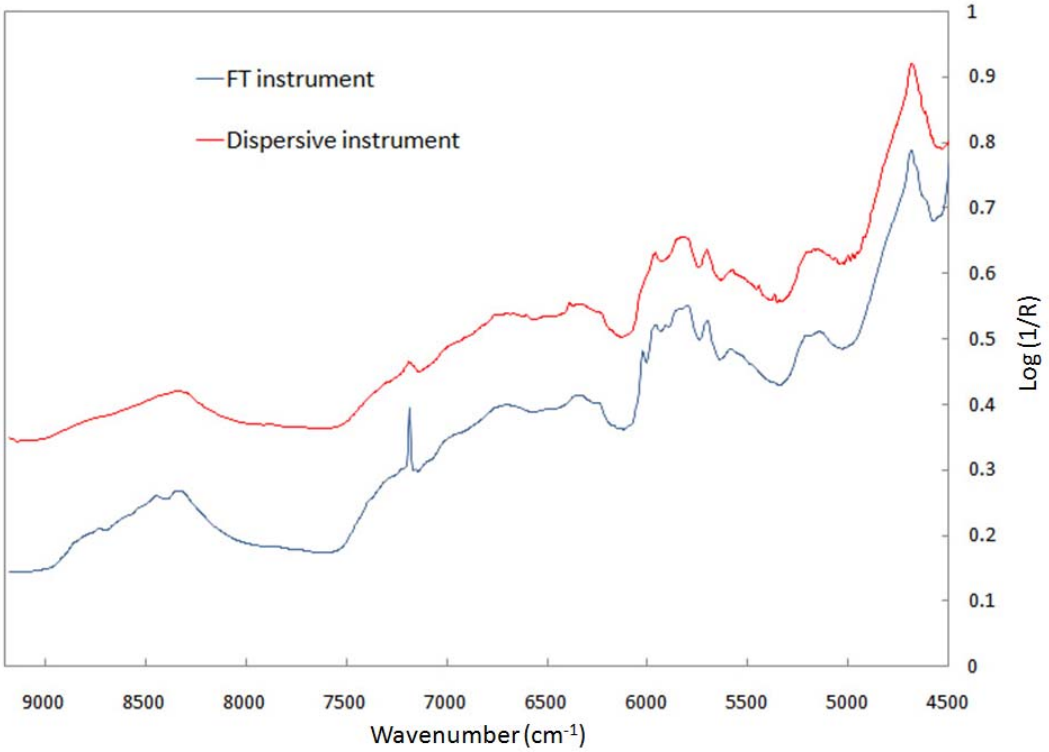

Fig. 8 - FT and dispersive NIR reflectance spectra of pharmaceutical pellets.

The technical differences between dispersive and FT instruments have significant consequences in terms of spectral quality. Figure 8 shows the NIR reflectance spectra of a pharmaceutical pellets sample acquired with both FT and dispersive instruments. From a visual point of view, one can see that the absorption bands look sharper when acquired with a FT instrument.

From a technical and physical point of view, the FT system has the following advantages over the dispersive system [59].

- **Multiplex advantage** (Fellget advantage).

All the wavelengths are measured simultaneously with FT instruments while the measurement is only sequential for dispersive instruments. The previous consideration leads to no discontinuities in FT spectra.

- **Throughput advantage** (Jacquinot advantage).

Due to the absence of gratings and slits in FT instruments, the amount of light reaching the detector is higher than in dispersive instruments. Consequently, a higher signal to noise ratio is obtained with FT instruments which is convenient for NIR spectra with small intensities absorption bands.

- **Connes advantage**.

The velocity of the moving mirror of the FT interferometer is controlled by a HeNe laser whose wavenumber is stable and defined accuratly. It acts like an internal reference for each scan. This type of wavenumber accuracy cannot be achieved with a dispersive spectrometer which does not have such internal reference.

- **Stable resolution**.

The resolution of dispersive instruments is set by modifying the slit width for the acquisition while the resolution does not change during the data collection for FT instruments.

I.2.4. Near Infrared measurement modes

NIR spectroscopy typically follows the energy conservation law: when the NIR beam reaches the matter, the intensity of the incident beam I_0 must be equal to the sum of intensity of the reflected and transmitted beams. Accordingly, depending on the sample type, two different measurement modes are available with NIR spectroscopy: transmission and reflection measurements [58]. These measurement modes as well as optical fibers will be discussed in the following sections.

- *Transmission measurement*

The transmission mode allows to measure the light transmitted through a sample.

Transmittance *T* is defined by the light fraction crossing the entire sample as explained in Figure 9 and equation (8):

$$T = I_T/I_0 \quad (8)$$

Where I_T is the intensity of the transmitted light and I_0 is the intensity of the incident light. I_T is always lower than I_0 as part of the light is absorbed by the sample.

The absorbance is defined by the following equation:

$$A = \log (1/T) = \log (I_0/I_T) \quad (9)$$

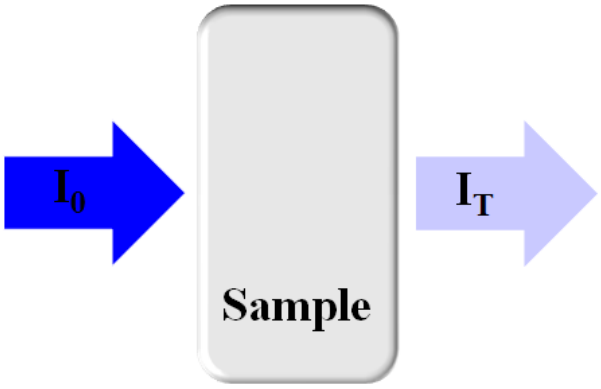

Fig.9 - Representation of a NIR transmission measurement.

The transmission mode has the advantage to analyze the entire sample. This measurement mode is particularly suited for tablets if the sample thickness is not too high. However, as it requires a detector at the opposite side of the measurement point, this measurement mode might not be adequate for in process measurement. Indeed, the use of a transmission compartment might be too invasive, especially for a solid form process monitoring. However, pipe-mounted transmission cells are well accepted for the manufacturing of pharmaceutical liquid forms.

- *Reflection measurement*

A reflection measurement can be explained as follows: when NIR light hits a sample, 2 components are taken into account during the reflection measurement as outlined in Figure 10: specular and diffuse reflection. On one hand, the first reflection component corresponds to the NIR light which is directly reflected at the surface of the sample. It only contains information related to the physical property of the sample. On the other hand, diffuse reflection designates the part of the NIR light that penetrates inside the sample and is subjected to molecular absorption, diffraction, reflection leading to a light scattering. Part of

the light scattered then goes to the detector. Diffuse reflection contains both the physical and chemical features of the sample. The reflected light containing specular and diffuse reflection is analyzed by the detector which is located at the same side as the incident NIR beam.

Reflectance *R* is defined by the following relation:

$$R = I_R / I_0 \quad (10)$$

Where I_R is the intensity of the light reflected by the sample and I_0 is the intensity of the incident NIR light.

The absorbance is defined by the following equation:

$$A = \log (1/R) = \log (I_0/I_R) \quad (11)$$

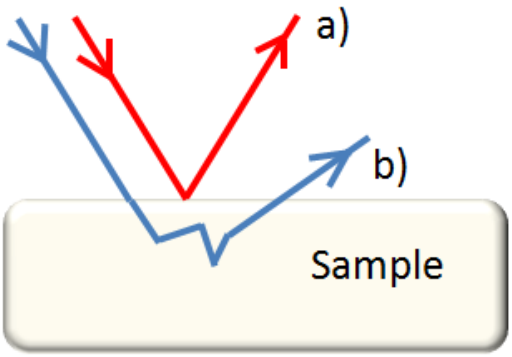

Fig. 10 - Representation of the (a) specular and (b) diffuse reflection phenomena occurring in a reflection measurement.

Compared to the transmission measurement mode, reflection measurement offers much more flexibility for process interfacings as it does not require the detector at the other side of the measurement point. However, the low penetration depth of the NIR beam (5 mm or less depending on the sample density) is the main disadvantage of this measurement mode: in case of high sample thickness and density, this measurement mode can be used only for homogeneous samples. However, other possibilities exist to measure non homogeneous powders. As an example, the use of a rotating cup can be useful to acquire spectra from a non homogeneous sample. In addition, in case of a blending process for example, multiple reflectance probes can be mounted on the blender to better evaluate the blend homogeneity in real-time [60].

o *Optical fibers*

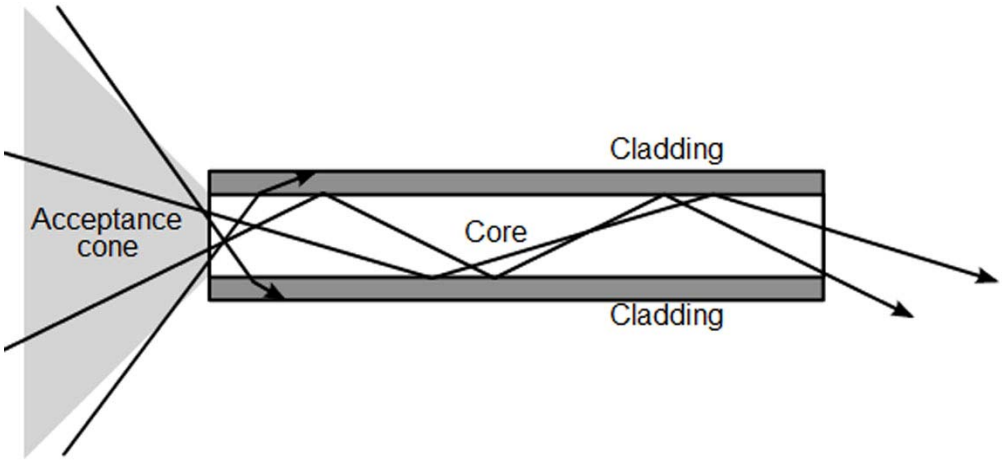

Fig. 11 - Light optical path through an optical fiber.

Optical fibers are used to carry the NIR light towards the measurement site or back to the detector without loss of intensity. As shown in Figure 11, an optical fiber basically consists in 2 different parts with a different refractive index: a core surrounded by a cladding. The cladding has a higher refractive index than the core. If the incident light enters the fiber with an angle greater than the critical angle, then light will be completely reflected by the cladding all the way of the fibre optic. This latter phenomenon is called total internal reflection. The critical angle can be defined based on the refractive index value difference between the core and the cladding. The range of incident angles that meets the total internal reflection is called the acceptance cone of the fiber (see Figure 11) [58].

I.2.5. Near Infrared spectroscopy: advantages and disadvantages

o *Advantages*

- **Minimal sample preparation and no sample destruction.**

As no sample preparation is required, the technique can be used in various environments and directly in the manufacturing area, *at-line*, *on-line* or *in-line*. The non-destructive feature of NIR spectroscopy allows to keep the sample intact in the manufacturing line.

- **From one single spectrum, possibility to evaluate multiple sample critical quality attributes.**

A NIR spectrum contains both chemical and physical information. Therefore, contrary to conventional analytical techniques which need a specific sample preparation per quality attribute testing, the NIR technology allows to assess multiple attributes non-destructively from the same spectral acquisition. For instance, it is possible to evaluate the API content of tablets and also their hardness at the same time.

- **Fast acquisition time.**

NIR measurements and results collection can be performed within seconds. Consequently, NIR as a process analyzer can span a higher amount of the manufacturing process than what is currently achieved during laboratory testing.

- **Various measurement modes are available.**

Although most of the measurements are performed using diffuse reflection. Other acquisition modes such as transmission for solid, transmission for liquids and transflection which is a combination of diffuse reflection and transmission are also available, depending on the NIR spectrometer model.

- **Green and low cost analytical technique.**

Contrary to liquid chromatography which is the most used analytical technique for the quality control of the pharmaceutical products, no solvant is required.

- **Unique calibration for qualitative and quantitative NIR models.**

Once calibration models are developed, recalibration is not needed. However model update may be necessary in case of within specification samples which spectra are drifting away from the calibration set spectra. A change in raw materials provider or in the process parameters could be responsible for this type of spectral deviation.

- **A wide range of NIR instruments is available.**

In the context of a research and development application area, a NIR instrument with multiple sample measurement modules would be the most adequate choice. However, in case of the implementation of one NIR instrument dedicated to one specific process, a specific instrument will always provide the highest reliability.

- **The use of fiber optics probes allows *at-line*, *on-line* and *in-line* measurements.**

According to the interfaced process, a great variety of probes and fiber length are available.

o *Disadvantages*

- **Lack of correlation between a molecule and its spectrum.**

Compared to MIR spectroscopy, structural correlation between a molecule and its spectrum is difficult to establish. It is the previous observation that mainly slowed down the expansion of NIR spectroscopy. However, Chemometrics now enables to extract selectively the chemical and physical information out of the NIR spectra. (see section I.3.).

- **Time consuming calibration phase for quantitative NIR models.**

For the calibration of quantitative NIR models, samples must be analyzed by both NIR and a reference method (Liquid chromatography for API content determination for example). Moreover, the expected sample and environmental (temperature, humidity, ...) variety that the model is likely to meet in routine has to be integrated in the calibration set.

- **In diffuse reflection mode, low penetration depth.**

It is then expected that the sample surface is identical to the sample core in order to make the NIR measurement representative of the sample.

- **NIR is a relative method.**

A reference method is always needed to build a quantitative NIR model.

- **NIR is not an analytical technique fitted for trace analysis.**

Although the sensitivity of NIR spectroscopy may vary from one substance to another, it is generally accepted that NIR will not be able to quantify accurately a substance with a % w/w below 1% making impossible the determination of degradation products for instance.

- **The physical features of a sample are included in the sample spectrum.**

Sometimes the analyst does not wish to analyze the physical features of a sample. Those features may hide or interact with the property of interest NIR absorption bands.

However, Chemometrics makes possible the extraction of specific quality attributes information such as chemical information about the API content for example.

I.3. Introduction to Chemometrics

As discussed in the previous NIR section, there is a need for mathematical and statistical tools to extract relevant information, either chemical or physical, out of the NIR spectra. Indeed, the wide overlapping absorption bands due to poorly specific organic groups make visual spectra interpretation difficult or impossible. Besides, as each spectral wavelength is associated with one absorbance value, the amount of data is huge and as many variables are collinear, there is also a need to reduce the number of variables to the most significant ones regarding the investigated properties of interest.

The use of Chemometrics was born from the previous considerations to meet 3 specific needs. First, during the acquisition of NIR spectra, uncontrolled spectral variations can occur. Many factors could be responsible for these variations: change of optical path length between the samples, moving particles effect during *in-line* process monitoring, probe displacement,… The impact of such uncontrolled parameters on the NIR spectra can be significant as they can hide the relevant spectral features. Therefore, signal pre-processings are used to reduce their impact. Regarding the investigated property of interest, attention must be paid on the selection of the signal pre-processing. One would not want to select a signal pre-processing that reduces the effect of the property of interest in the NIR spectra. Second, classification methods were developed to compress and extract the information contained in the spectra to find out the relation between the samples of the data set. Third, for quantification purpose, algorithms for multivariate regression were programmed to link the spectral data to a numerical value of the property of interest.

I.3.1. Signal pre-processings examples

- *Multiplicative Scatter Correction (MSC)*

Multiplicative Scatter Correction (MSC) is a well known signal pre-processing that reduces the effect of scattered light on diffuse reflectance spectra [61]. On a calibration set for example, MSC performs as follows: first a reference spectrum is selected. Most of the time the reference spectrum consists in the mean spectrum of the calibration set. All the calibration set spectra are then regressed linearly against the reference spectrum. Further, the slope and intercept are calculated. Finally, the spectra are corrected according to the slope and intercept. The extracted information then represents the information that cannot be modeled: the relevant chemical information.

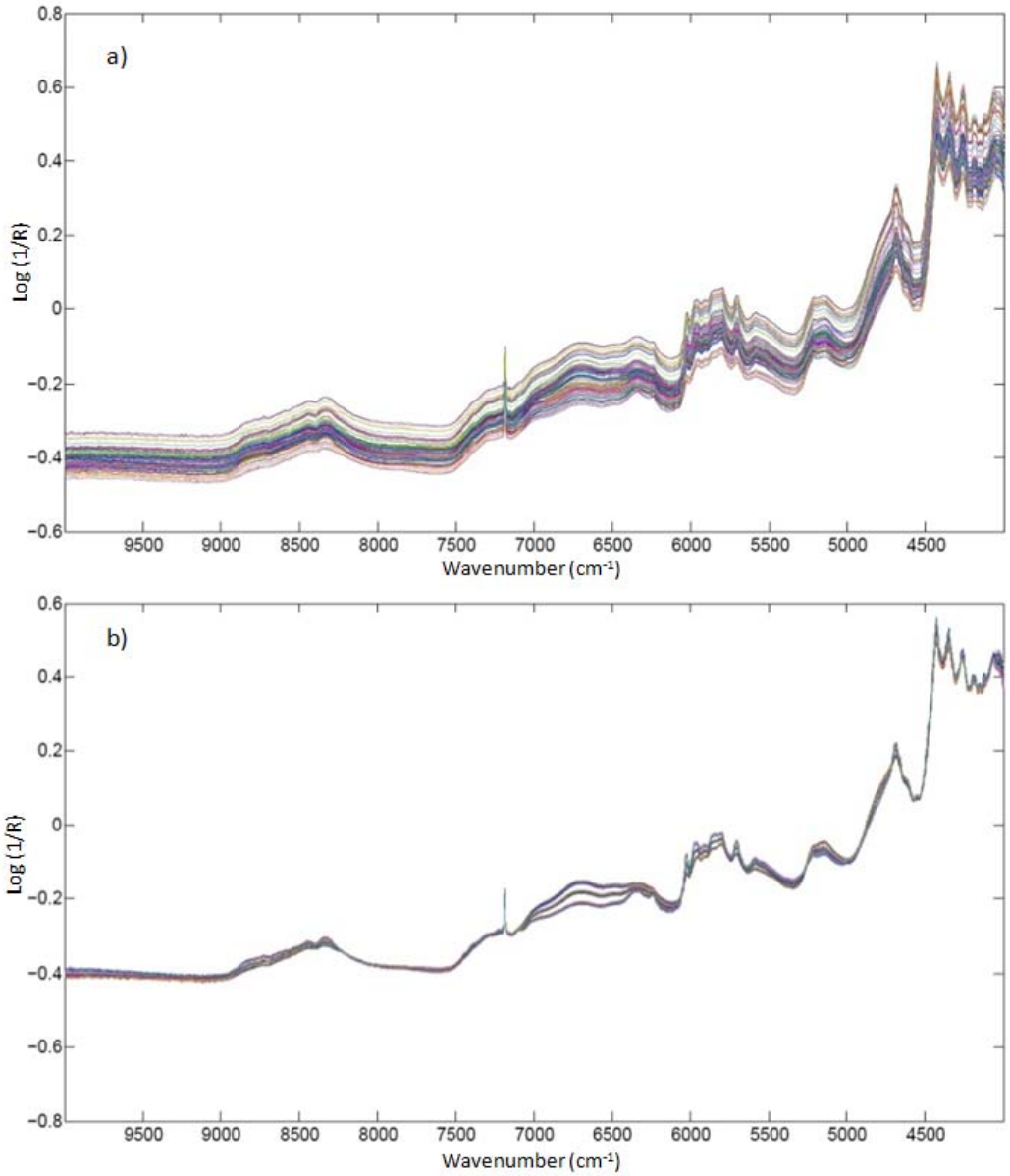

Fig. 12 - Spectra of moving pharmaceutical pellets with different API contents: comparison between NIR spectra (a) before and (b) after MSC signal pre-processing.

Figure 12 shows the spectra of moving pharmaceutical pellets with 3 different API contents before and after MSC signal pre-processing. One can see that MSC highlights the chemical information discriminating the samples: the 3 API levels of the spectral data set.

- *Standard Normale Variate (SNV)*

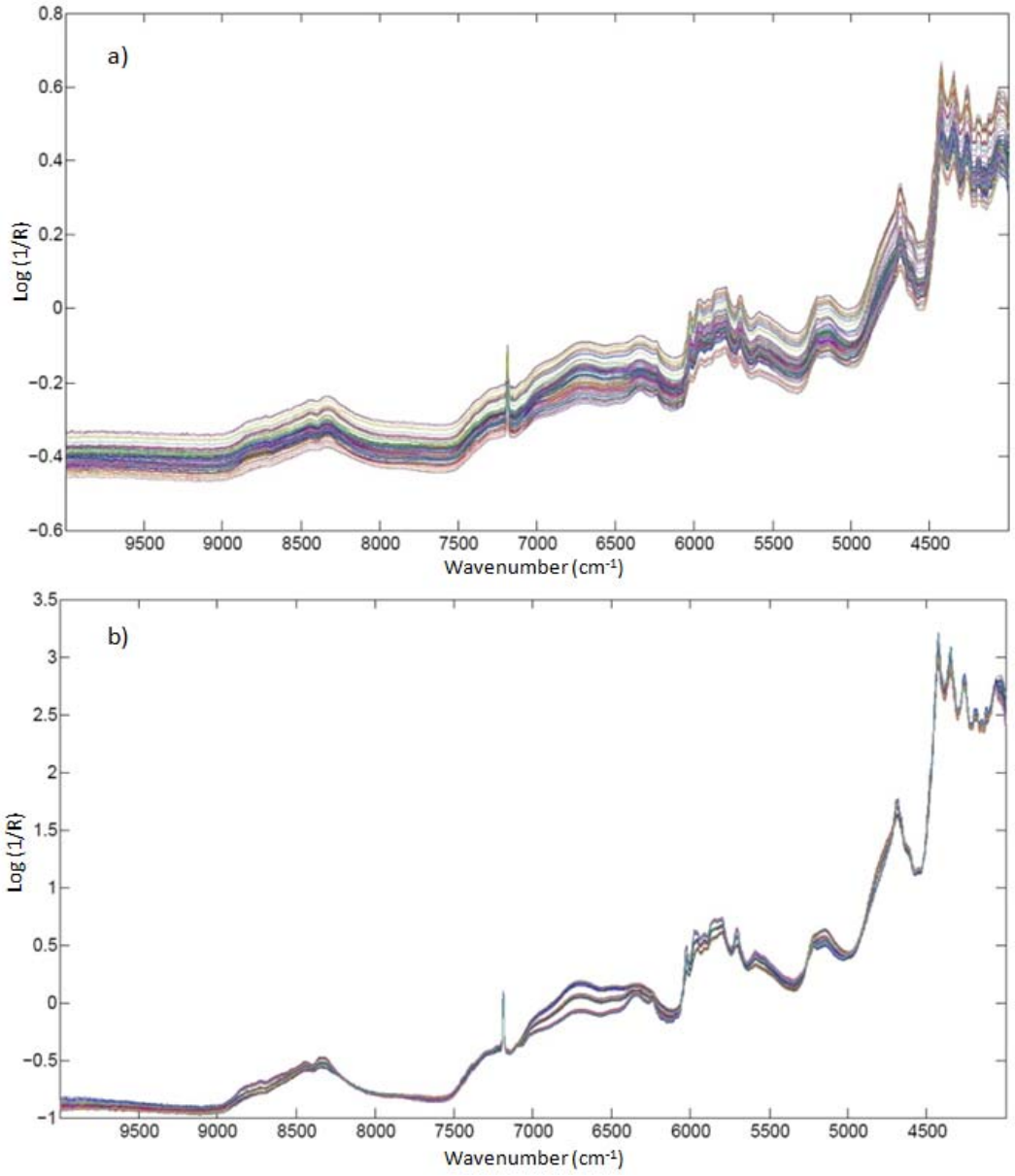

Fig. 13 - Spectra of moving pharmaceutical pellets with different API contents: comparison between NIR spectra (a) before and (b) after SNV signal pre-processing.

Standard Normale Variate (SNV) corrects uncontrolled spectral variations [62]. On a sample spectrum, it performs as follows: each variable absorbance is first corrected by the mean absorbance of the spectrum. The previous result is then divided by the standard deviation of the variables under investigation.

Figure 13 show the spectra of moving pharmaceutical pellets with 3 different API contents before and after SNV signal pre-processing. In the same way as MSC did, SNV allows to highlight the chemical information related to the 3 API levels.

- *Smoothing and derivative signal pre-processings*

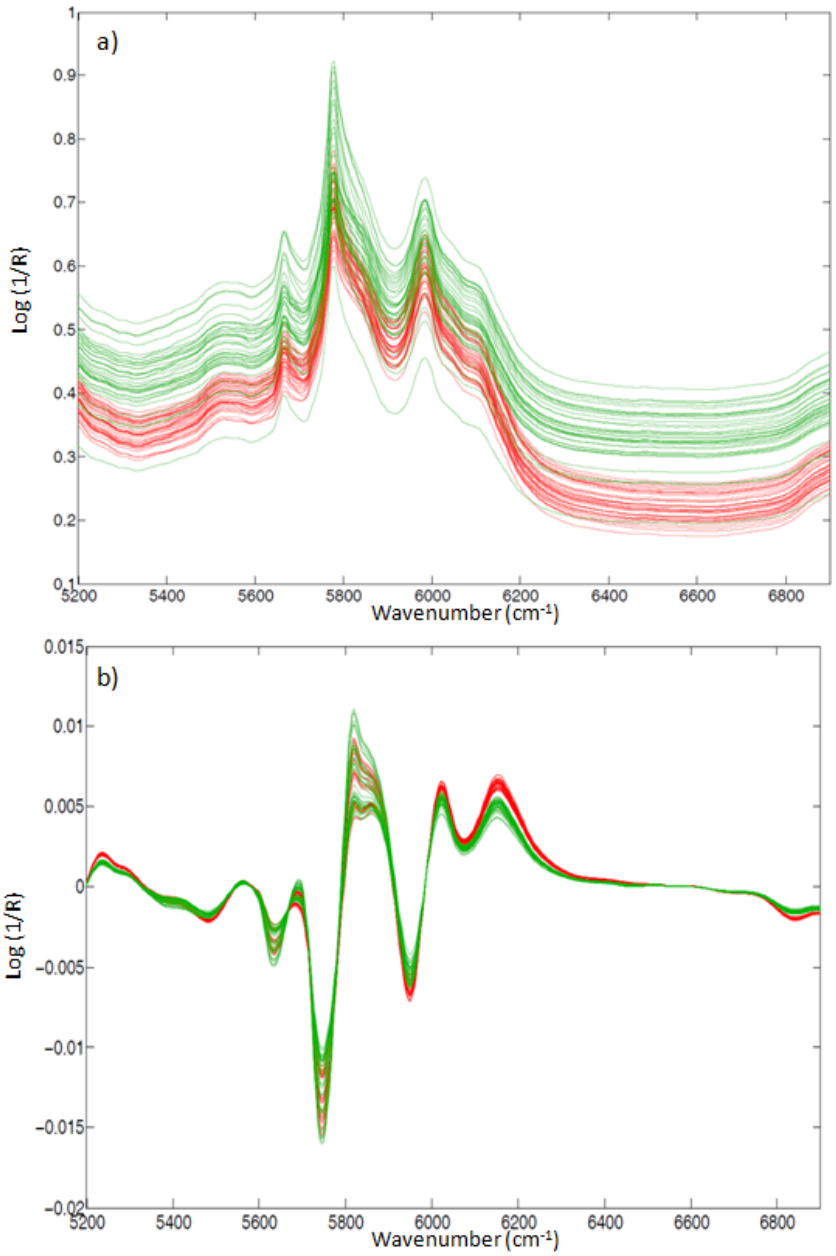

Fig. 14 - Comparison between NIR spectra: Caffeine granules in polyethylene bag (red) and caffeine powder in polyethylene bag (green) (a) before and (b) after first derivative signal pre-processing. The Savitsky-Golay smoothing filter is applied before the first derivative signal pre-processing. The smoothing filter polynomial order is 2 and the filter width is 25 corresponding to 96.25 cm^{-1}.

Smoothing aims to reduce the spectral noise, taking into account that spectral noise can hide the relevant physical or chemical information. The most used smoothing technique is the Savitzky-Golay smoothing filter which basically performs as follows: the spectrum is divided into different spectral windows which all have the same width size. A polynomial regression is then performed on each window allowing to smooth the data [63]. Parameters such as the window size and the polynomial degree can be set in the algorithm knowing that

the larger the window size and the lower the polynomial degree will be, the stronger the smoothing effect will be.

Derivative signal pre-processing can be used to reduce baseline shifts between the spectra in order to extract physical spectral information. Besides, it can also improve the resolution between overlapping absorption bands. However, derivative transformation is highly sensitive to spectral noise which could hide the relevant information. Consequently, the Savitzky-Golay smoothing filter can be performed prior to derivative signal pre-processing.

Figure 14 displays the comparison between the NIR spectra of caffeine granules and caffeine powder before and after the signal preprocessing (Savitzky-Golay [polynomial order:2 and filter width 25] followed by 1st derivative.). From this Figure, it can be seen that the signal pre-processing highlighted the physical difference between the granules and powder at 6180 cm^{-1}.

I.3.2. Classification method example

- *Principal Component Analysis (PCA)*

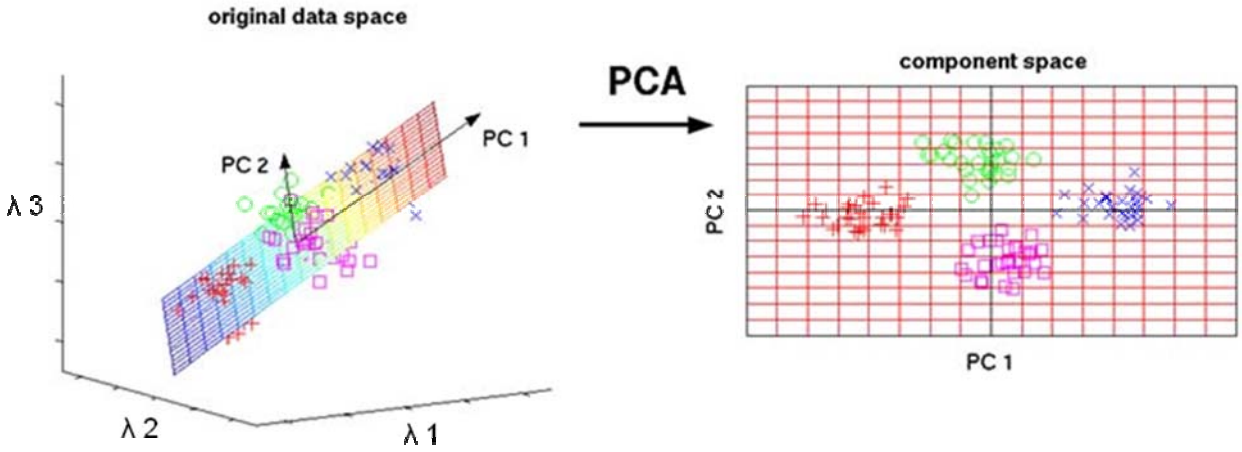

Fig. 15 - Geometric principle of PCA.

Figure 15 geometrically explains the principle of PCA which can be easily understood as follows: given a series of spectra recorded with absorbance values corresponding to 3 wavelengths: λ_1, λ_2 and λ_3, PCA will reduce this 3-dimensional space into the component space, a 2-dimensional space that maximizes the variance between the samples, easing the understanding of the major trends in the data. Even though these major trends in the data are not so difficult to understand when considering data point in a 3-dimensional space, it

becomes obvious that PCA is truly necessary when dealing with datasets having absorbance values for more than 2000 different wavelengths, which is usually the case with NIR spectra.

From a statistical point of view, one can say that PCA finds combinations of variables, or factors that describe major trends in the data. If *X* is a data matrix with *m* rows and *n* columns, and with each variable being a column and each sample a row, PCA decomposes *X* as the sum of *r* t_i and p_i, where *r* is the rank of the matrix *X*:

$$X = t_1p^T_1 + t_2p^T_2 + \dots + t_kp^T_k + \dots + t_rp^T_r \quad (12)$$

Here *r* must be less than equal to smaller dimension of *X*, i.e., $r \leq \min\{m,n\}$. The t_i, p_i pairs are ordered by the amount of variance captured. The t_i vectors are known as scores and contain information on how the samples relate to each other. The p_i vectors are known as loadings and contain information on how the variables relate to each other. Generally the PCA model is truncated after *k* components and the remaining small variance vectors are consolidated into a residual matrix *E*.

$$X = t_1p^T_1 + t_2p^T_2 + \dots + t_kp^T_k + E \quad (13)$$

PCA is one of the mostly used classification method for data exploration [64]. As it describes only the major trends within *X* without maximizing the covariance between *X* and reference measurements, e.g. the active content of each sample row, this classification method is unsupervised. Other Classification methods (supervised or unsupervised) include: Linear Discriminant Analysis (LDA) [65], Soft Independent Modelling of Class Analogy (SIMCA) [66], Partial Least Squares Discriminant Analysis (PLS-DA) [67], K Nearest Neighbours (KNN)[68] ,…

I.3.3. Multivariate regression method example

- *Partial Least Squares (PLS) regression*

The objective of Partial Least Squares (PLS) regression is to combine some reference measurements with their corresponding spectral data in order to create a model that will further only need spectral data to predict some reference measurements. Consequently, two data blocks are needed to perform PLS regression: the *y* block which contains the reference method results and the *X* block containing the corresponding data set. Accordingly, contrary to PCA, PLS is a supervised method.
Reference measurements represent the analytical results obtained with the conventionnal analytical method, in the case of an API content determination method, the reference method could be a HPLC method for instance.

Facing the fact that many variables, many wavelengths, of the NIR spectra are highly collinear, PLS regression selects a subset of a new variables orthogonal to each other, PLS factors which capture the greatest amount of variance in *X* while at the same time maximize the covariance between *X* and *y*. The selected factors are then used as regressors for both *X* and *y* [69].

PLS is the one of the mostly used multivariate regression method, especially in the PAT field. Other multivariate regression methods include Multi-Linear Regression (MLR) [64], Principal Component Regression (PCR) [70], Artificial Neural Networks (ANN) [71], …

I.4. Quantitative NIR model building: methodology

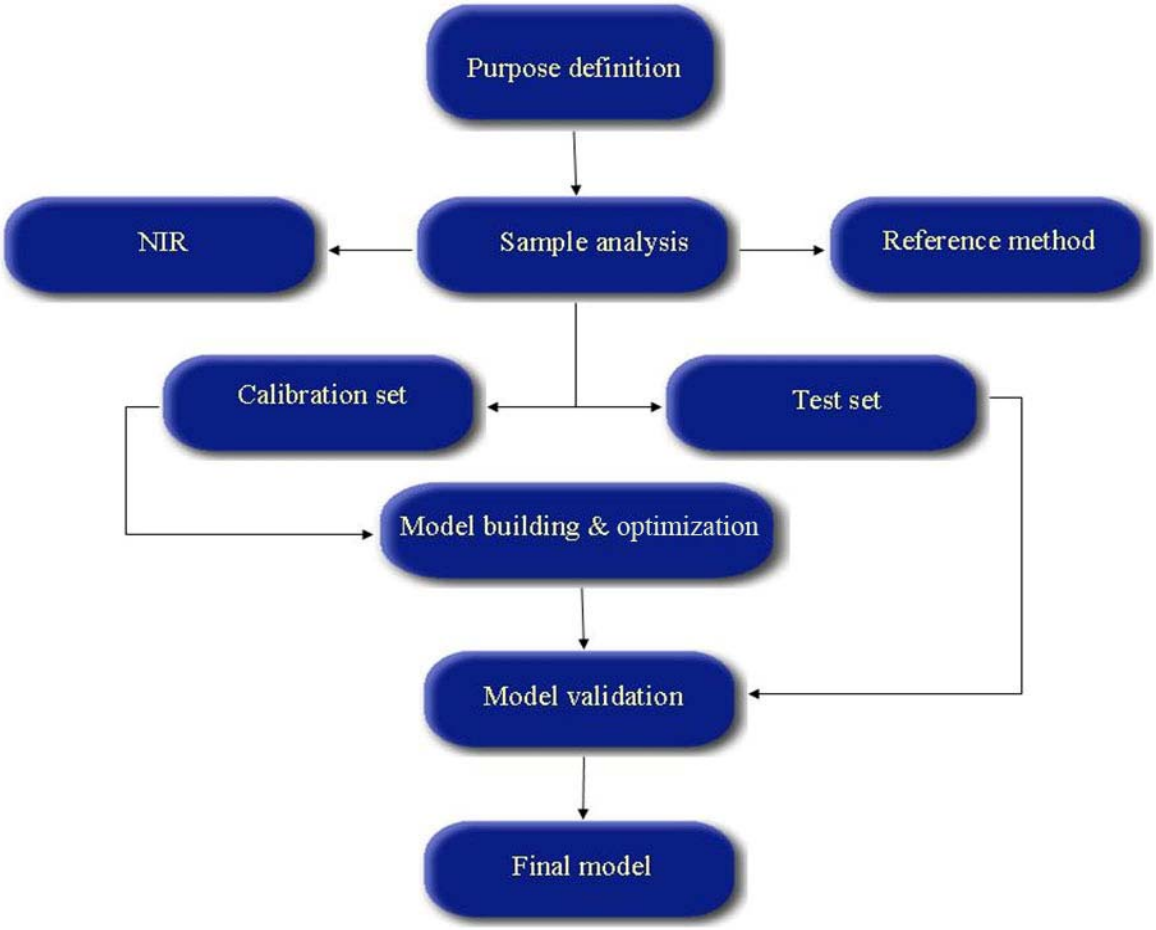

Fig. 16 - Diagram of the methodology followed to create NIR predictive models.

Figure 16 describes the main stages of the methodology to build predictive NIR models as described by the EMA "*guideline on the use of near infrared spectroscopy by the pharmaceutical industry and the data requirements for new submissions and variations*" [72]. Once the purpose of the NIR method has been defined, one has to design a sample set

that will be analyzed by NIR and by another analytical technique designated as the reference method. Indeed, one has to be aware that NIR is a relative analytical technique: it only provides samples spectra. Therefore, there is a need to bind the collected spectra with concentrations of the property of interest to build the NIR model. The developed model will no longer need the reference method to predict a quantitative result. Depending on the nature of the investigated property of interest, a wide range of reference methods exist. When the property of interest is of chemical nature, reference methods such as HPLC, thermogravimetry and dissolution batch testing are commonly used. On the other hand, for the evaluation of tablets hardness for example, a hardness tester will be typically used as the reference method. In addition, one has to be aware that most of the reference methods are sample destructive methods. The NIR spectral acquisition will therefore be performed prior to the reference measurement. Besides, attention must be paid on the sample size analyzed by both NIR and the corresponding reference method: it has to be the same to maximize the agreement between the 2 techniques. The entire sample set is then divided into a calibration and a validation set. The first is used to create the quantitative model while the second is used to test the developed NIR model in an external way.
To obtain a robust NIR model, it is crucial to include in the calibration set the variability that the model is likely to meet in the future. In addition, the same type of variability has also to be included in the validation set to properly evaluate the accuracy and robustness of the model. Depending on the manufacturing process of the studied formulation, many sources of variability can be integrated in the calibration and validation sets. The main sources of variability can include:

- **Concentration levels of the property of interest.**

To Build a NIR predictive model, it is necessary to include the expected concentration range of the property of interest to be quantified in the future.

- **The raw materials.**

Variability in the raw materials must be integrated. This concerns both the API and the excipients. As an example, in case of a NIR model able to determine the API content of a formulation, different batches of API as well as different batches of excipients must be integrated in the calibration and testing sets. Indeed, chemical and physical variability may exist from a batch to another, leading to spectral variations. The latter effect is even more significant when different raw materials providers exist.

- **A batch effect.**

Between the manufacturing of two batches, the manufacturing tools are dismantled, cleaned and then put together again. Afterwards, a new manufacturing starts with the same

targeted manufacturing conditions. However, slight modifications of the manufacturing conditions can occur leading to slight differences between the batches. Besides, a batch effect can also arise from an alteration/modification of manufacturing elements such as compression punches, extrusion screws, extrusion grids, ...

- **A production campaign effect**

This effect is the same as the previous one but to a greater extent.

- **A pilot and industrial batch effect.**

To create a property of interest concentration range, most of the time, pilot batches are manufactured with small scale manufacturing tools. The obtained products are different from the ones manufactured with an industrial manufacturing tool. Therefore, industrial batches must also be integrated in the building and testing sets, at least for the targeted concentration level.

- **Operator effect.**

If operators have been demonstrated to influence the NIR measurement, multiple operators must be integrated as a variability source in the model. For example: in case of the raw material identification, the pressure applied with the handheld probe on the raw material can affect the NIR spectra.

- **Temperature effect.**

Temperature has a significant effect on the NIR spectra collected from liquids. Besides, spectral deviations due to temperature can also occur when measuring the moisture content of solid samples.

- **Day effect.**

From a day to another, the spectral acquisition of the same sample may slightly differ. This can be due to modification of the atmospheric conditions (temperature, humidity, luminosity) or to slight variations in the optics of the NIR spectrometer. Therefore, in the calibration and validation protocols, the same batches are analyzed at different days.

From the calibration set, the model is built based on Partial Least Squares (PLS) regression. The ability of the model to fit the data is then checked with the calculation of the Root Mean Square Error of Calibration (RMSEC) which is calculated as follows:

$$RMSEC = \sqrt{((\sum^{n}_{i=1} (y_{ipred}-y_i)^2)/n)} \quad (14)$$

Where y_{ipred} is the predicted concentration of the sample *i* that is included in the model formation while *y* represent the sample *i* concentration of the property of interest determined by the selected reference method. "*n*" is the total number of objects in the data set.

Model selection and optimization is usually performed by means of cross-validation which is a fast and easy way to obtain a first estimation about the model ability to predict samples that were not included in the model calibration. Cross-validation divides the calibration set into one smaller building set and one test set. The procedure is extended until every spectrum from the entire calibration set has been extracted at least on time as a test set. The model quantitative performance is then evaluated with the Root Mean Square Error of Cross Validation (RMSECV) which is calculated with the same equation as RMSEC except that y_{ipred} is the estimated concentration of the samples by cross-validation (where the value for each sample *i* is predicted using a model that was built using a set of samples that does not include sample *i*). If only one test spectrum is extracted per cross validation loop, the procedure is called leave-one-out cross validation. The latter procedure is particularly suited for small calibration sets. Indeed, with a high sample number, the extraction of only one sample will not have a significant impact on the model construction which will therefore provide optimistic and unrealistic RMSECV values. Depending on the test sample selection scheme, other cross-validation procedures exist: this includes venetian blinds, contiguous blocks, and random sub sets [73]. The selection of the model number of PLS factor is evaluated with the plot: RMSECV versus the number of PLS factors. The optimal number of PLS factors is selected from the moment the RMSECV is low and stable. A selection of higher number of PLS would result in overfitting the model, meaning that its prediction accuracy would be very good for the calibration set but would decrease if the model was tested with new samples.

Besides, the model spectral area has to be selected according to the property of interest. This can be done by comparing the spectrum of the property of interest with the final formulation spectrum. Further, from the loadings factors of the chosen PLS factors, one should also check the level of contribution of the data variance arising from the net signal of the analyte of interest [73].

Once the model has been optimized, it is validated with the external validation set. This leads to the calculation of the Root Mean Square Error of Prediction (RMSEP) which is computed the same way as RMSEC except that y_{ipred} refers to samples that were never included in the calibration set. Compared to RMSECV and RMSEC, the RMSEP is true performance indicator of the model as it is calculated with samples that were never included in the calibration set.

If the RMSEP and RMSEC are both low and close to each other, it means that the model is accurate and robust enough. However, if the RMSEP is too high, further optimization is necessary. If the RMSEP is still high after the optimization, one has to investigate the presence of outliers and if enough variability was introduced in the calibration set.

In addition to RMSEP, an accuracy profile can be calculated with the validation results to visualize the accuracy of the NIR model over the investigated concentration range. Further considerations about the accuracy profile for analytical method validation will be described in the following section.

I.5. Analytical Method validation

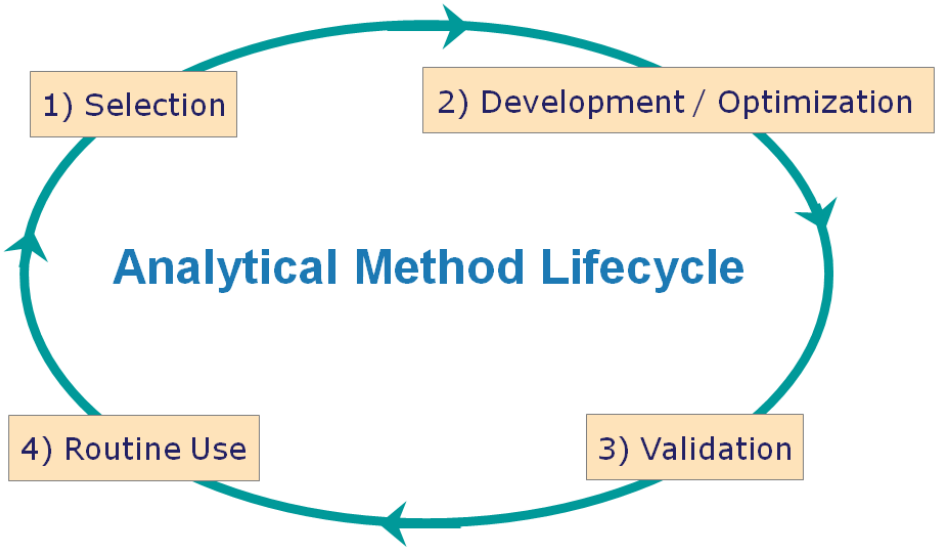

Fig. 17 - Description of the Analytical Method Lifecycle.

Any analytical method lifecycle contains at least 4 major steps connected together as shown in Figure 17.The first step is the selection phase: a suitable analytical technique must be selected to evaluate the property of interest of a defined type of formulation sample. The second step corresponds to the method development and optimisation in order to obtain an analytical tool able to evaluate quantitatively the property of interest. The third step is the analytical method validation enabling to test the suitability of the analytical method regarding its purpose: to quantify accurately the property of interest [74]. Once the accuracy of the analytical method has been demonstrated to be in full accordance regarding its purpose, the analytical method is then ready to be used in routine conditions. However, the previous lifecycle illustration is dynamic. Any modification of the analytical method parameters will require its new validation before using it in routine conditions again. If the

method has been developed using the Design Space approach, only changes of the model parameters outside the Design Space will require a new method validation.

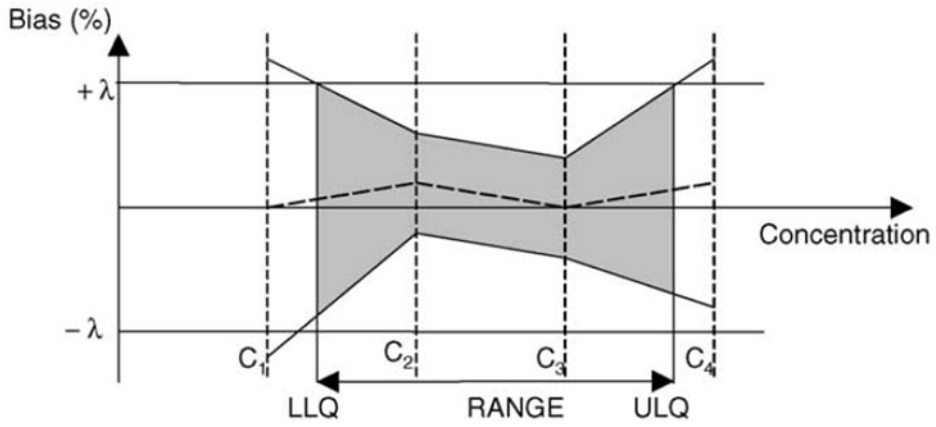

Fig. 18 - Illustration of the accuracy profile as a decision tool. LLQ, lower limit of quantification; ULQ, upper limit of quantification.

In the present thesis, the developed analytical methods were validated using the accuracy profile approach which takes into account the total error in the validation results. Indeed, the tolerance interval computed on the validation results allows a visual representation of the total error which is the sum of the systematic and random errors [75-83].

The use of accuracy profile as a decision tool is illustrated in Figure 18. Accuracy profile plots the bias which corresponds to the relative error (100 X ((NIRprediction-reference method result)/reference method result)) against the range of concentration investigated. The ± λ lines define the acceptance limits of the NIR method, they are defined by the analyst or defined according to the regulatory requirements (e.g. 5 % for the analysis of pharmaceutical formulations and 15 % for bioanalysis purpose). The grey area describes the concentration range in which the analytical method is able to quantify with a relative error lower than ± λ with a defined risk chosen by the analyst.

The grey area corresponds to a tolerance interval computed with the validation results. Compared to confidence interval which only takes into account the existing results, tolerance intervals allow predicting a region of concentration where each future result has a defined probability to fall, this probability is defined by the analyst. As an example, if the selected risk α is equal to 5 %, the calculated tolerance interval will contain on average 95 % of the future results.

Besides, the previous approach is also ICHQ2(R1) compliant as it provides the values of validation criteria such as accuracy, trueness, precision, limits of quantification, range and linearity.

This approach has many advantages compared to the conventional RMSEP approach: while RMSEP represents a global accuracy indicator, the accuracy profile enables to visualize the accuracy of the NIR method all over the property of interest concentration range investigated. For example, if the reason for a poor RMSEP is caused only by the results of one concentration level, one will presume that the overall model accuracy is low while accuracy profile will quickly allow to visually assess the accuracy of the NIR method at every concentration level investigated.

I.6. Raman spectroscopy

Raman spectroscopy was discovered by Indian scientists Raman and Krishman in 1928.

Like infrared spectroscopy, Raman spectroscopy is also part of vibrational spectroscopy as it also provides information on the molecule vibrations [84]. However, contrary to NIR spectroscopy which is based on the absorption and reflection of light, the Raman spectrum arises from a scattering of light by the vibrating molecules. Indeed, when the radiation coming from the laser source hits the sample, two main phenomena occur as depicted in Figure 19:

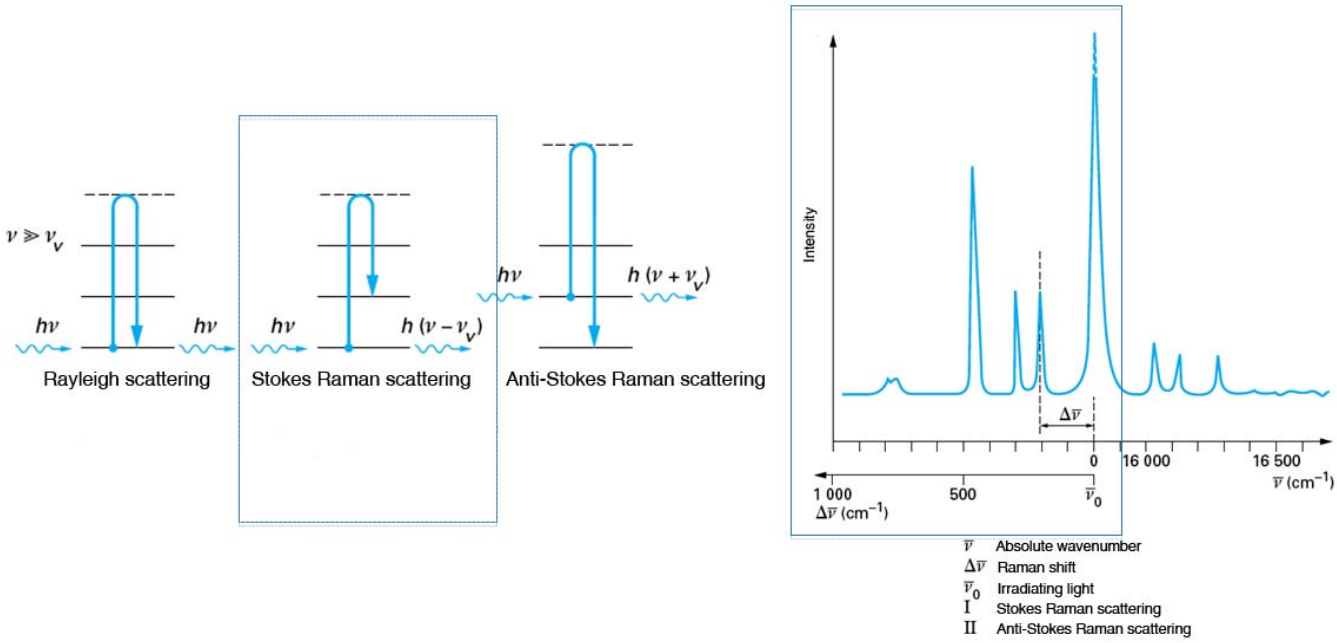

Fig. 19 - The Raman scattering phenomenon [85].

- The Rayleigh scattering in which the photon frequency is not modified, it corresponds to an elastic collision.
- Stokes and anti-Stokes Raman scatterings characterized by a modification of the photon frequency during the scattering. It corresponds to an inelastic collision. The

difference between these 2 scatterings lies in the photon frequency decrease or increase. Regarding the Stokes scattering, the energy of the scattering proton is reduced: the molecule goes from the fundamental to the first excited vibrational state. On the other hand, in the anti-stokes Raman scattering, the energy of the scattering photon is elevated: the energy level of the molecule moves from the first excited to the fundamental vibrational state.

Among the two previous phenomenona, the Rayleigh scattering represents 99.9 % of the Raman activity. In the remaining 0.1 %, the Stokes scattering is dominant as most of the vibrational population is located at the fundamental state.

The Raman spectra are usually presented with the intensity displayed as the Y axis. On the other hand, different possibilities exist for the X axis. The wavelength can be displayed or the absolute wavenumber which is the reciprocal of the wavelength. However, different types of laser wavelength exist. Consequently, the X axis displayed by means of wavelengths or wavenumbers does not allow the harmonization between the spectra collected under different Raman configurations. Accordingly, the X axis is usually expressed as a Raman shift which can be defined as a frequency of the band expressed as a shift from the excitation wavelength, 0 designating the position of the excitation wavelength.

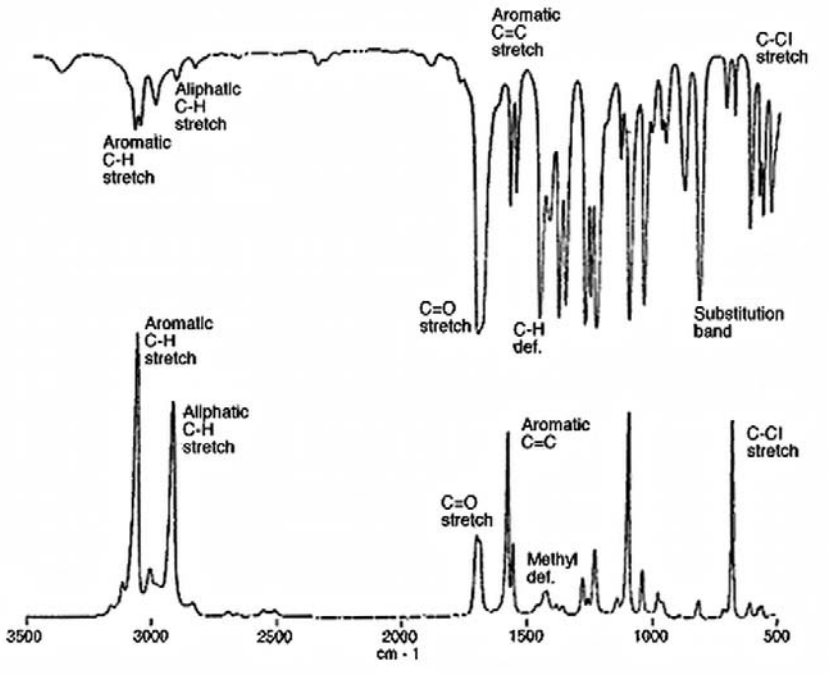

Fig. 20 - Mid-infrared and Raman spectra of 2.5- dichloroacetophenon.

As can be seen from the MIR and Raman spectra of dichloroacetophenon displayed in Figure 20, high intensity Raman bands usually correspond to low intensity MIR bands. This is due to the fact that a variation of the molecule polarizability is required for the molecule to be active in Raman spectroscopy while it is a variation of the dipole moment that is needed

for the molecule to be active in MIR spectroscopy. The fact that these two phenomena cannot possibly occur at the same time leads to the "*exclusion principle*", making MIR and Raman complementary spectroscopic techniques.

Raman spectroscopy sensitivity to polarizability variations leads to significant spectral differences between common atoms such as C-H, C-O or O-H and molecules with benzene rings (many APIs). Indeed, there is often no overlap between the first atoms and benzene rings which have a strong Raman response around 1000 cm^{-1}. Accordingly, the intensity of the API bands will be most of the time stronger than the excipients bands, making Raman spectroscopy an interesting technique for the API evaluation inside a pharmaceutical formulation. One can relativize the previous consideration as many pharmaceutical excipients have complex spectra [86]. However, compared to NIR spectroscopy the sharpness of the Raman bands usually makes possible the monitoring of a non-overlapped API band.

Raman spectroscopy also offers other advantages. Like NIR spectroscopy, it does only require minimal sample preparation and it is compatible with optical fibers accessories making reaction and process monitoring possible. Raman spectroscopy can also be used to analyze substances in various states: in gas, liquid and solid states. Moreover, the technique is particularly suited for solid state evaluation. In addition, the Raman technique is less sensitive to water than NIR allowing the analysis of samples with a high moisture content.

However, this technique also has its specific disadvantages: the Raman spectra, which signal to noise ratio is low, are often partially affected or totally overwhelmed by fluorescence. Besides, this technique was also considered as a destructive analytical technique due to the strong laser light. Nowadays, these issues are significantly reduced by the technological progresses made mainly on the laser sources and on the detector fields.

References

[1] United States Food and Drug Administration (FDA), Guidance for industry PAT-A framework for innovative pharmaceutical manufacturing and quality assurance, FDA, 2004.

[2] United States Food and Drug Administration (FDA), Pharmaceutical CGMPs for the 21st century – a risk-based approach, FDA, 2004.

[3] International Conference on Harmonization (ICH) of technical requirements for registration of pharmaceuticals for human use, Topic Q8(R2): Pharmaceutical Development, Geneva, 2009.

[4] International Conference on Harmonisation (ICH) of technical requirements for registration of pharmaceuticals for human use, Topic Q9: Quality Risk Management, Geneva, 2006.

[5] International Conference on Harmonisation (ICH) of technical requirements for registration of pharmaceuticals for human use, Topic Q10: Pharmaceutical quality system, Geneva, 2008.

[6] Food and Drugs Administration. Applying ICH Q8(R2), Q9, and Q10 Principles to CMC Review. MAPP 5016.1, February 2011.

[7] Y. Sulub, B. Wabuyele, P. Gargiulo, J. Pazdan, J. Cheney, J. Berry, A. Gupta, R. Shah, H. Wu, M. Khan, J. Pharm. Biomed. Anal. 49 (2009) 48.

[8] H. Stenlund, E. Johansson, J. Gottfries, J. Trygg , J. Anal. Chem. 81 (2009) 203.

[9] J. J. Moes, M. M. Ruijken, E. Gout, H. W. Frijlink, M. I. Ugwoke, Int. J. Pharm. 357 (2008) 108.

[10] C. Bodson, W. Dewé, Ph. Hubert, L. Delattre, J. Pharm. Biomed. Anal. 41 (2006) 783.

[11] T.R.M. De Beer, C. Bodson, B. Dejaegher, B. Walczak, P. Vercruysse, A. Burggraeve, A. Lemos, L. Dellatre, Y. Vander Heyden, J.P. Remon, C. Vervaet, W.R.G. Baeyens, J. Pharm. Biomed. Anal. 48 (2008) 772.

[12] J. Rantanen, S. Lehtola, P. Rämet, J.-P. Mannermaa, J. Yliruusi, Powder Technol. 99 (1998) 163.

[13] J. Rantanen, E. Räsänen, J. Tenhunen, M. Känsäkoski, J.-P. Mannermaa, J. Yliruusi, Eur. J. Pharm. Biopharm. 50 (2000) 271.

[14] J. Rantanen, E. Räsänen, O. Antikainen, J.-P. Mannermaa, J. Yliruusi, Chemo. Intel. Lab. Syst. 56 (2001) 51.

[15] A. Miwa, T. Yajima, H. Ikuta, K. Makado, Int. J. Pharm. 352 (2008) 202.

[16] M. Alcala, M. Blanco, M. Bautista, J.M. Gonzales, J. Pharm. Sci. 99 (2010) 336.

[17] S.H. Tabasi, R. Fahmy, D. Bensley, C. O'Brien, S.W. Hoag, J. Pharm. Sci. 97 (2008) 4067.

[18] K. Kamada, S. Yoshimura, M. Murata, H. Murata, H. Nagai, H. Ushio, K. Terada, Int. J. Pharm. 368 (2009) 103.

[19] S.H. Tabasi, R. Fahmy, D. Bensley, C. O'Brien, S.W. Hoag, J. Pharm. Sci. 97 (2008) 4052.

[20] K. Heymann, G. Mirschel, T. Scherzer, Appl. Spectrosc. 64 (2010) 419.

[21] S.H. Tabasi, V. Moolchandani, R. Fahmy, S.W. Hoag, Int. J. Pharm. 382 (2009) 1.

[22] J. Müller, K. Knop, J. Thies, C. Uerpmann, P. Kleinebudde, Drug Dev. Ind. Pharm. 36 (2010) 234.

[23] L. Maurer, H. Leuenberger, Int. J. Pharm. 370 (2009) 8.

[24] J. Märk, M. Karner, M. Andre, J. Rueland, C.W. Huck, Anal. Chem. 82 (2010) 4209.

[25] S.H. Tabasi, R. Fahmy, D. Bensley, C. O'Brien, S.W. Hoag, J. Pharm. Sci. 97 (2008) 4040.

[26] M. Blanco, A.J. Peguero, Pharm. Biomed. Anal. 52 (2010) 59.
[27] C. Bodson, E. Rozet, E. Ziémons, B. Evrard, Ph. Hubert, L. Delattre, J. Pharm. Biomed. Anal. 45 (2007) 356.
[28] M. Ito, T. Suzuki, S. Yada, A. Kusai, H. Nakagami, E. Yonemochi, K. Terada, J. Pharm. Biomed. Anal. 47 (2008) 819.
[29] S. S. Rosa, P. A. Barata, J. M. Martins, J. C. Menezes, Talanta 75 (2008) 725.
[30] W. Li, L. Bagnol, M. Berman, R. A. Chiarella, M. Gerber, Int. J. Pharm. 380 (2009) 49.
[31] M. Blanco, R. Cueva-Mestanza, A. Peguero, J. Pharm. Biomed. Anal. 51 (2010) 797.
[32] A. Eustaquio, M. Blanco, R.D. Jee, A.C. Moffat, Anal. Chim. Acta 383 (1999) 283.
[33] P. Chalus, Y. Roggo, S. Walter, M. Ulmschneider, Talanta 66 (2005) 1294.
[34] E.T.S. Skibsted, J.A. Westerhuis, A.K. Smilde, D.T. Witte, J. Pharm. Biomed. Anal. 43 (2007) 1297.
[35] C. Ravn, E. Skibsted, R. Bro, J. Pharm. Biomed. Anal. 48 (2008) 554.
[36] M. Blanco, M. Alcalá, Anal. Chim. Acta 557 (2006) 353.
[37] N. Sandler, J. Rantanen, J. Heinämäki, M. Römer, M. Marvola, J. Yliruusi, AAPS PharmSciTech 6 (2) (2005) 174.
[38] L. Saerens, L. Dierickx, B. Lenain, C. Vervaet, J.P. Remon, T. De Beer, Eur. J. Pharm. Biopharm. 77 (2011) 158.
[39] Y. Zheng, X. Lai, S. Wrang Bruun, H. Ipsen, J. Nedergaard Larsen, H. Løwenstein, I. Søndergaard, S. Jacobsen, J. Pharm. Biomed. Anal. 46 (2008) 592.
[40] H. Grohganz, M. Fonteyne, E. Skibsted, T. Falck, B. Palmqvist, J. Rantanen,, Eur. J. Pharm. Biopharm. 74 (2010) 406.
[41] T.R.M. De Beer, M. Wiggenhorn, R. Veillon, C. Debacq, Y. Mayeresse, B. Moreau, A. Burggraeve, T. Quinten, W. Friess, G. Winter, C. Vervaet, J.P. Remon, W.R.G. Baeyens, Anal. Chem. 81 (2009) 7639.
[42] H. Grohganz, D. Gildemyn, E. Skibsted, J.M. Flink, J. Rantanen, Anal. Chim. Acta 676 (2010) 34.
[43] T.R.M. De Beer, M. Allesø, W.R.G. Baeyens, Y. Vander Heyden, H. Lopez de Diego, J. Rantanen, C.Vervaet, J.P. Remon, Anal. Chem.79 (2007) 7992.
[44] J. A. Lopes, P. F. Costa, T. P. Alves, J. C. Menezes, Chemom. Intel. Lab. Syst., 74 (2004) 269.
[45] W. Herschel, Philos. Trans. R. Soc. 90 (1800) 255.
[46] W. Abney, E. R. Festing, Philos. Trans. R. Soc. 172 (1881) 887.
[47] W.W. Coblentz, Investigations of Infrared Spectra Part 1. Carnegie Institute of Washington (1905) 35.
[48] F.E. Fowle, Astrophys. J. 35 (1912) 149.
[49] J. Ellis, J. Bath, Journal of Chemical Physics 6 (1938) 723.
[50] J. Moros, S. Garrigues, M. de la Guardia, Trends Analyt. Chem. 29 (2010) 578.
[51] H. Huang, H. Yu, H. Xu, Y. Ying, J. Food Eng. 87 (2008) 303.
[52] Q. Chen, J. Zhao, S. Chaitep, Z. Guo, Food Chem. 113 (2009) 1272.
[53] I. Komorizono de Oliveira, W.F. de Carvalho Rocha, R.J. Poppi, Anal. Chim. Acta 642 (2009) 217.
[54] M. R. Monteiro, A. R. P. Ambrozin, L. M. Liao, A. G. Ferreira, Talanta 77 (2008) 593.
[55] J. Luypaert, D. L. Massart, Y. Vander Heyden, Talanta 72 (2007) 865.
[56] Y. Roggo, P. Chalus, L. Maurer, C. Lema-Martinez, A. Edmond, N. Jent, J. Pharm. Biomed. Anal. 44 (2007) 683.

[57] T. De Beer, A. Burggraeve, M. Fonteyne, L. Saerens, J.P. Remon, C. Vervaet, Int. J. Pharm. (2011), doi:10.1016/j.ijpharm.2010.12.012
[58] D. Bertrand, E. Dufour, La spectroscopie infrarouge et ses applications analytiques, second ed., Lavoisier, Paris, 2006.
[59] D.A. Burns, E.W. Ciurczak, Handbook of Near-Infrared Analysis, third ed., CRC Press, New York, 2008.
[60] A.S. El-Hagrasy, H. Morris, F. D'Amico, R. Lodder, J.K. Drennen, J. Pharm. Sci. 90 (2001) 1298.
[61] P. Geladi, D. MacDougall, H. Martens, Appl. Spectrosc. 39 (1985) 491.
[62] R.J. Barnes, M.S. Dhanoa, S.J. Lister, Appl. Spectrosc. 45 (1989) 772.
[63] A. Savitzky, M.J.E. Golay, Anal. Chem. 36 (1964) 1627.
[64] H. Martens, T. Naes, Multivariate Calibration, JohnWiley&Sons, Chichester, 1996.
[65] D. Coomans, M. Jonckheer, D.L. Massart, I. Broeckaert, P. Blockx, Anal. Chim. Acta 103 (1978) 409.
[66] S. Wold, Pattern Recogn. 8 (1976) 127.
[67] L. Stahle, S. Wold, J. Chemom. 1 (1987) 185.
[68] M.-P. Derde, L. Buydens, C. Guns, D.L. Massart, P.K. Hopke, Anal. Chem. 59 (1987) 1868.
[69] S. Wold, M. Sjöström, L. Eriksson, Chemom. Intel. Lab. Syst. 58 (2001) 109.
[70] T. Naes, T. Isaksson, T. Fearn, A.M.C. Davies, A User-Friendly Guide to Multivariate Calibration and Classification, NIR Publications, Chichester, UK, 2002.
[71] Y. Dou, Y. Sun, Y. Ren, P. Ju, Y. Ren, J. Pharm. Biomed. Anal. 37 (2005) 543.
[72] European Medicines Agency, draft: Guideline on the use of near infrared spectroscopy by the pharmaceutical industry and the data requirements for new submissions and variations, EMEA/CHMP/CVMP/QWP/17760/2009 Rev 1.
[73] http://wiki.eigenvector.com/index.php?title=Using_Cross-Validation (accessed 26/07/11).
[74] International Conference on Harmonization (ICH) of Technical Requirements for registration of Pharmaceuticals for human Use, Topic Q2(R1): Validation of analytical Procedures: Text and Methodology, Geneva, 2005.
[75] Ph. Hubert, P. Chiap, J. Crommen, B. Boulanger, E. Chapuzet, N. Mercier, S. Bervoas-Martin, P. Chevalier, D. Grandjean, P. Lagorce, M. Lallier, M.C. Laparra, M. Laurentie, J.C. Nivet, Anal. Chim. Acta 391 (1999) 135.
[76] Ph. Hubert, J.J. Nguyen-Huu, B. Boulanger, E. Chapuzet, P. Chiap, N. Cohen, P.A. Compagnon, W. Dewé, M. Feinberg, M. Lallier, M. Laurentie, N. Mercier, G. Muzard, C. Nivet, L. Valat, J. Pharm. Biomed. Anal. 36 (2004) 579.
[77] Ph. Hubert, J.J. Nguyen-Huu, B. Boulanger, E. Chapuzet, P. Chiap, N. Cohen, P.A. Compagnon, W. Dewé, M. Feinberg, M. Lallier, M. Laurentie, N. Mercier, G. Muzard, C. Nivet, L. Valat, E. Rozet, J. Pharm. Biomed. Anal. 45 (2007) 70.
[78] Ph. Hubert, J.J. Nguyen-Huu, B. Boulanger, E. Chapuzet, N. Cohen, P.-A. Compagnon, W. Dewé, M. Feinberg, M. Laurentie, N. Mercier, G. Muzard, L. Valat, E. Rozet, J. Pharm. Biomed. Anal. 45 (2007) 82.
[79] E. Rozet, A. Ceccato, C. Hubert, E. Ziémons, R. Oprean, S. Rudaz, B. Boulanger, P. Hubert, J. Chromatogr. A 1158 (2007) 111.
[80] E. Rozet, R. Morello, F. Lecomte, G.B. Martin, P. Chiap, J. Crommen, K.S. Boos, P. Hubert, J. Chromatogr. B 844 (2006) 251.

[81] E. Rozet, V. Wascotte, N. Lecouturier, V. Préat, W. Dewé, B. Boulanger, Ph. Hubert, Anal. Chim. Acta 591 (2007) 239.
[82] Bouabidi, E. Rozet, M. Fillet, E. Ziemons, E. Chapuzet, B. Mertens, R. Klinkenberg, A. Ceccato, M. Talbi, B. Streel, A. Bouklouze, B. Boulanger, Ph. Hubert, Critical analysis of several analytical method validation strategies in the framework of the fit for purpose concept, J. Chrom. A. 1217 (2010) 3180.
[83] R. Rozet, W. Dewe, S. Rudaz, R. Marini Djang'Eing'A, E. Ziemons, B. Boulanger, Ph. Hubert, Trends Analyt. Chem. 30 (2011) 797. http://hdl.handle.net/2268/81653
[84] S. Sasic, Pharmaceutical Applications of Raman Spectroscopy, John Wiley & Sons, New Jersey, 2007.
[85] M. Delhaye, J. Barbillat, F. Fillaux, P. Dhamelincourt, D. Bougeard, G. Buntinx, Techniques de l'Ingénieur (1999) Ref. P2865.
[86] M. de Veij, P. Vandenabeele, T. De Beer, J.P . Remon, L. Moens, J. Raman Spectrosc. 40 (2009) 297.

Chapter II

Objectives

The concept of Process Analytical Technology (PAT) was introduced in 2004 by the FDA. At that time batch release was achieved by means of end product testing. Contrary to post-manufacturing end product testing, which most pharmaceutical companies are still doing nowadays, the goal of the PAT initiative was to enable Real Time Release (RTR), i.e. achieving batch release directly in the end of the production with the analytical data collected throughout the entire manufacturing itself.

In addition to RTR, PAT may also detect the appearance of Out Of Specification (OOS) products at the earliest stages during the manufacturing, giving opportunities for feed-back loops redirecting the formulation towards the defined product performance, or in the very worst case, to stop the manufacturing before the entire process flow sequence is completed. Besides, from the early stages of a pharmaceutical formulation development, the amount of data collected during the manufacturing processes can clearly improve the process knowledge and be part a global Quality by Design approach defining, throughout the complete process, the design space that will provide adequate product performance with a high level of confidence.

Although the combination of advanced process understanding and RTR makes the PAT concept attractive for the Pharmaceutical Industry, the lack of practical documents slowed down its implementation in the manufacturing line. However, recent guidelines on multivariate model calibration and validation as well as the increasing number of PAT applications found in the literature represent facilitating factors for the Pharmaceutical Industry to embrace that concept.

The PAT approach comes together with great expectations but also high requirements in terms of process analyzers. Indeed, monitoring a manufacturing process requires fast, non-invasive and non-destructive analytical means. NIR and Raman spectroscopy match the requirements of the PAT framework. In the present thesis, the emphasis will be mainly put on NIR spectroscopy even though Raman spectroscopy could also be considered.

For any quality control laboratory or pharmaceutical industry to adopt a new analytical method, its validation is mandatory. Nowadays, a major trend in the analytical method development consists in evaluating the risk to obtain future analytical results outside the analytical method acceptance limits. Accordingly, the present study will also investigate whether the accuracy profile methodology could be easily extended to NIR method validation.

In the context of the implementation of PAT, the present thesis mainly focuses on the development of NIR methods, qualitative and quantitative to control critical quality attributes of 3 types of commercially available pharmaceutical formulations: a liquid, solid

and polymeric drug reservoir formulation. In addition, all the developed quantitative methods will be thoroughly validated to evaluate their suitability regarding their purpose.

In the first place, we will focus on a first PAT checkpoint suited for any pharmaceutical process: a NIR identification method will be investigated to identify the API raw materials in a pharmaceutical manufacturing area. In addition, as it is well known that polymorphism influences powder properties and process-ability, a case study of API raw material polymorphism will also be investigated: the interchangeability between NIR spectroscopy and X-Ray powder diffraction for the quantification of pure crystalline form II of fluconazole in binary polymorphic mixtures (From II + III) will be envisaged for that purpose.

In the second place, the ability of NIR to assess the API content in a low dose formulation will be challenged. The chosen model formulation will consist in a 2 % (w/v) acetaminophen syrup. Using a transmission liquid probe accessory, a NIR model able to determine the acetaminophen content will be developed and then fully validated. Finally, the use of the NIR method will be extended to the real time API monitoring of syrups during addition of placebo and non-placebo syrups. The agreement between the NIR predictions and the calculated reference results will be checked and the feasibility of an in-line application will be discussed.

Later on, keeping in mind the concept of real time batch release, we will try to introduce 3 different In Process Control (IPC) steps in the manufacturing of a sustained release pharmaceutical pellets formulation. Following the process flow-chart, an off/at–line NIR method able to determine the API content of the pellets prior to the coating step will be envisaged. Between the coating and final packaging steps, an off/at-line NIR method will also be necessary to determine the moisture content of the coated pellets. Finally, using the coated pellets, different particles movements found in the manufacturing line will be reproduced in a lab-scale. Each motion device will then be non-invasively interfaced with NIR spectroscopy. The effect of sample speed and density on the API content determination will be investigated qualitatively and quantitatively to evaluate the feasibility of in-line methods dedicated to the pellets manufacturing line.

Finally, the emphasis will be put on the use of NIR and Raman spectroscopy as PAT tools for the manufacturing of a polymeric drug reservoir formulation. 3 critical quality attributes of silicone-based drug reservoirs will be studied. First, the crosslinking process will be monitored at different temperatures. Further, the API homogeneity within the drug reservoir will be evaluated with Raman mapping. Eventually, a NIR method able to determine the API content of the drug reservoirs will be developed and validated.

Chapter III

Results and discussion

Part III.1.

NIR as a PAT tool to check the API raw materials

Section III.1.1.

Identification of the API raw materials in the manufacturing area using NIR spectroscopy

J. Mantanus, E. Ziemons, R. Klinkenberg, B. Streel, Ph. Hubert. *(Unpublished results)*

1. Context and aim of the study

Within the framework of the pharmaceutical manufacturing line, the aim of the present study was to develop a near infrared (NIR) method able to identify [1-3] the API processed in standardized polyethylene (PE) bags at SMB's pharmaceutical industry. Indeed, the raw materials selection, weighting and dispatching step is the first critical step of any pharmaceutical manufacturing process having a major impact on the final product performance. A NIR identification method was therefore developed using a handheld NIR probe to analyze the API directly through PE bags as a final checkpoint before the APIs processing in the manufacturing line.

2. Experimental

2.1 Spectral library reference samples

Labscale API samples transferred into PE bags were used as reference samples.

2.2 NIR instrument and software for data acquisition

Labscale API samples in PE bags were analyzed with a Fourier transform NIR spectrometer (Matrix-F duplex, Bruker Optics, Ettlingen, Germany) equipped with a temperature stabilized indium-gallium-arsenic (InGaAs) detector, thermoelectrically cooled. The NIR spectra were collected with a NIR reflectance hand-held probe for solids (probe head length = 80 mm; probe diameter = 10 mm). A background spectrum using a Spectralon® diffuse reflectance standard (Labsphere, North Sutton, USA) was acquired before analyzing a new API sample. The background and sample measurement acquisition were triggered by the hand-held probe. The NIR probe makes contact with the PE bag during the measurement. The NIR spectra were collected with the OPUS Software 6.5 (Bruker Optics). Each spectrum was the average of 32 scans and the resolution was 8 cm^{-1} over the spectral range from 12,500 to 3600 cm^{-1}. The time necessary for a NIR measurement was 15 s.

2.3 Design of the identification spectral library

The identification spectral library was built taking into account the variability sources displayed in Table 1.

Table 1 – Variability sources included in the identification spectral library.

Variability sources
API batches
API pharmaceutical providers
PE bag thickness
Operators
NIR sampling location
NIR measurement time effect

2.4 Identification method external validation

The external validation of the identification method was carried out on full scale API bags processed in SMB's manufacturing area.

2.5 Multivariate data analysis

The collected spectra for the identification library were classified into different groups, each group corresponding to one API. Principal Component Analysis (PCA) was then performed with the IDENT application from the Opus software 6.5 to evaluate if group separation could be achieved.

The distance between the spectra were calculated by means of Mahalanobis distance, enabling the distance calculation in the selected scores domain:

$$D = \sqrt{\sum_i \left(T_{\mathbf{sample},i} - T_{\mathbf{reference},i}\right)^2} \quad (1)$$

Where:

- T_i score of i^{th} factor
- 1, 2 …. i factors used.

The factors selection is supported by the number of group separation achieved.

Compared to geometric distance, the use of Mahalanobis distance to measure distance between the API groups has the advantage to provide weighting of different directions relative to variability present in the spectral library dataset.

To develop the identification method, a distance threshold defining the area where all the corresponding API samples should be located is calculated for each group as follows:

$$D_{threshold} = D_{max} + X \,.\, S_0 \quad (2)$$

Where:

- D_{max} = maximum sample distance within the corresponding API group, it is the worst hit.
- X = individual factor set by default to 0.25 for all the API groups.
- S_0 = standard deviations of sample distances D_i

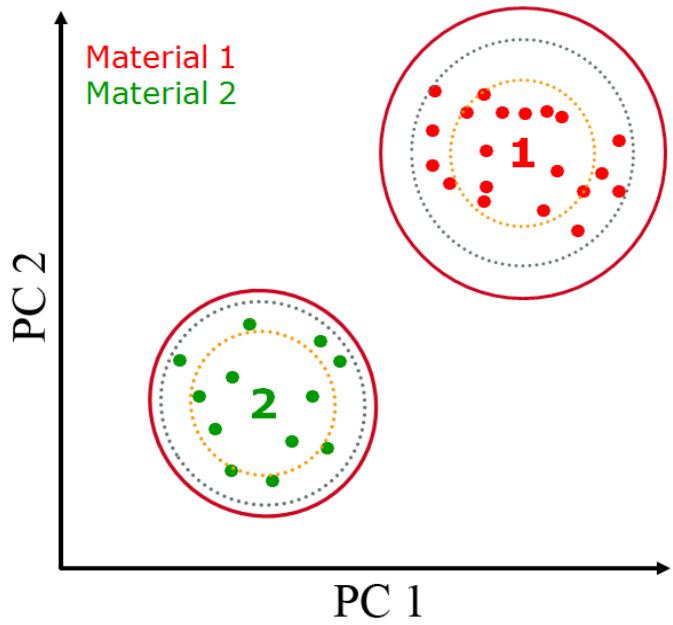

Fig. 1 – Identification method development: definition of threshold for groups material 1 and 2. The pink continuous line represents the group thresholds. The grey discontinuous line represents the D_{max}. The orange discontinuous line represents the group samples mean distance.

The confidence level of the threshold was set to 99 % to take into account the entire variability included in the spectral library.

Afterwards, the identification method is internally validated as follows: each of the original spectra is checked against all mean spectra in the library to verify that there is no overlapping between the established group thresholds.

The proximity between the critical thresholds is indicated by the selectivity which is the ratio of distance *D* between average spectra to sum of threshold values *T1* and *T2* (cluster radii).

$$S = D / (T1 + T2) \quad (3)$$

Accordingly, a selectivity value less than 1 indicates the overlapping of 2 critical groups while a selectivity value greater than 1 indicates that the 2 API groups are well distinguished by the identification method.

Finally, the reliability of the developed identification method is tested with new samples with a known API identity but never included in the reference spectral library. Each new spectrum is checked against all mean spectra in the library. In addition, it is also checked that the dedicated mean spectrum is within threshold and that all other mean spectra are out of threshold.

3. Results and discussion

3.1 Identification method development

To design an identification method fitted for the manufacturing line, 6 variability sources were introduced in the method calibration protocol as described in Table 1. Per API, spectra of different batches have been collected. The batch selection has been carried out in a way that the samples spanned each API shelf-life. In the event multiple providers existed for the same API, all providers were included in the calibration protocol to further be able to identify the samples origin. Besides, as the pharmaceutical industry is using PE bags with 100 and 130 µm thicknesses, the API samples have been packaged and analyzed in both types of bags. As the pressure applied with the handheld probe on the raw material can affect the sample density leading to slight modifications in NIR spectra, 2 operators were integrated in the calibration protocol to add the variability linked to the pressure applied during the measurement. In addition, the samples were analyzed in 3 different locations to include variability related to the sample and to the PE bags. Although this type of application does not require a background spectrum acquisition more than 2 times a day, a new background measurement was carried out per new sample measurement to simulate a time effect in the identification spectral library.

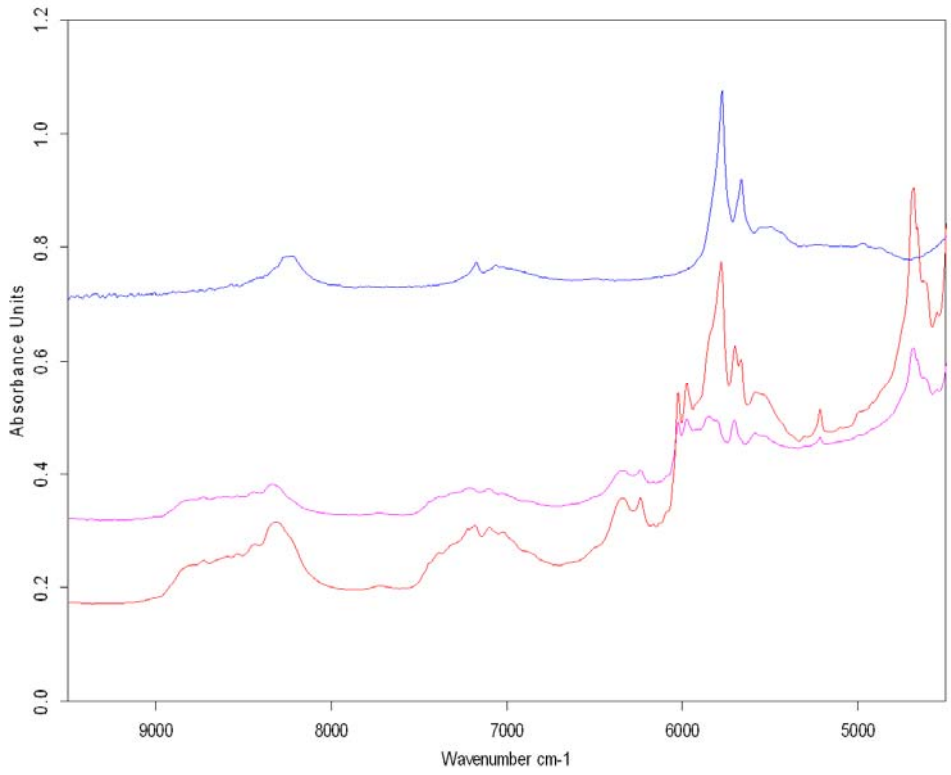

Fig. 2 – PE bag (blue line), tramadol.HCl (pink line) and PE bag containing tramadol.HCl (red line) NIR reflectance spectra.

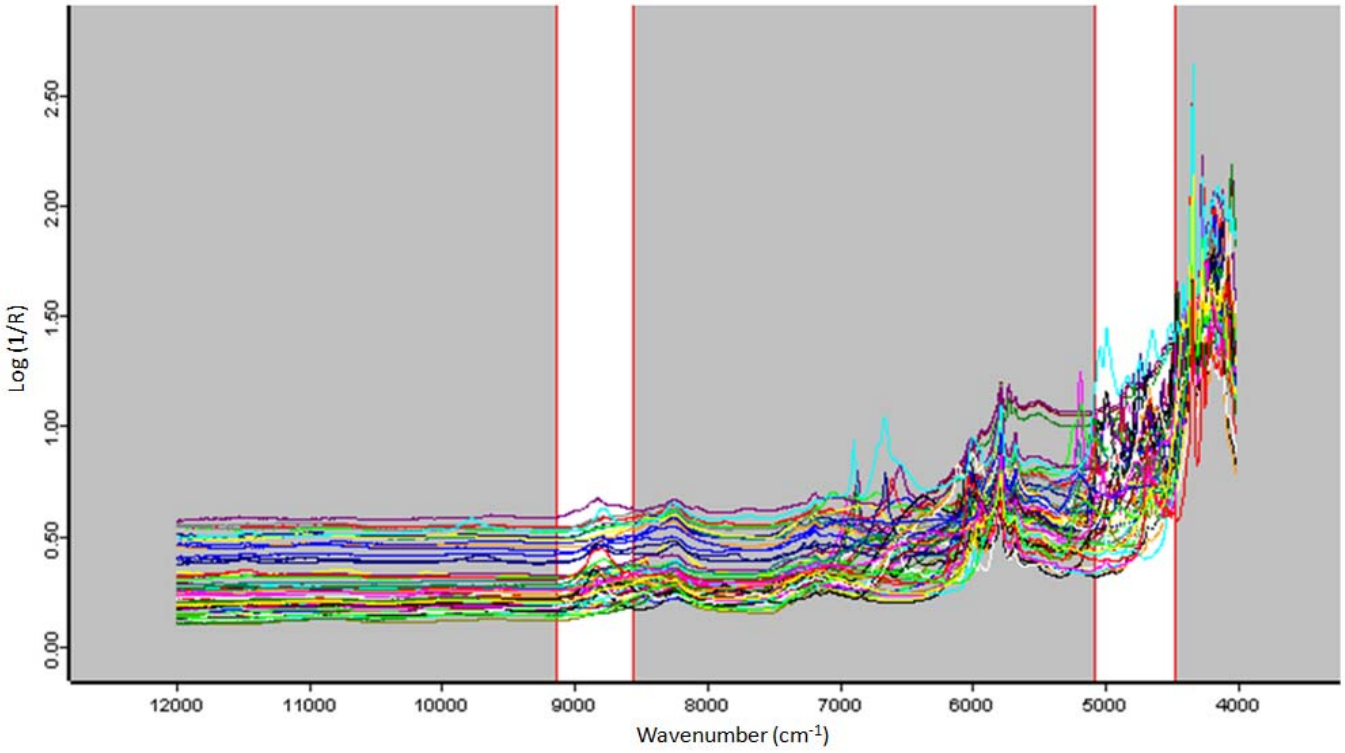

Fig. 3 – APIs NIR reflectance spectra. The white area defines the spectral area selected for the primary identification method.

In order to develop the identification method, a spectral range has first to be selected for the PCA analysis. As can be seen in Figure 2, the NIR spectrum of a PE bag contains major specific absorption bands in the following wavenumber ranges: 8500-8000, 7320-6660 and 6000-5330 cm^{-1}. Accordingly, spectral ranges outside the PE bag absorption bands were chosen for the development of the identification method (cf. Figure 3). Even though 2 types of PE bag were integrated in the calibration protocol, spectral ranges outside the PE bags absorption bands may increase the identification model robustness in case of bag thickness modification for example.

A primary identification method was developed. Indeed, among the API available in the production area, some have multiple grades and/or providers leading to physical and/or chemical differences. Therefore, a first identification method was developed to identify the chemical identity of the samples with no further indication on the grade or provider.

For the primary identification method, SNV was selected as it is able to lower the spectral variations linked the physical variabilities, highlighting the chemical differences between the samples.

The threshold values were calculated for each chemical group of the library and the selectivity was checked to find out if overlaps between groups occurred.

Table 2 – Primary identification method selectivity results.

Group 1	Group 2	Selectivity
Acetylsalicylic acid 80 Mesh	Indometacin micronized	2,98
Fenofibrat	Alprazolam	2,32
Tramadol HCl	Clarithromycin	2,92
Diltiazem HCl	Molsidomin	1,46
Ascorbyl Palmitate	Omeprazol UQUIFA	2,30
Pyridoxin HCl 97%	Thiamin mononitrate 97%	3,17
Omeprazol UQUIFA	Loratadin	1,13
Omeprazol NATCO	Loratadin	1,39
Riboflavin	Amlodipin maleate	1,88
Thiamin mononitrate 97%	Molsidomin	2,07
Allopurinol	Omeprazol UQUIFA	2,87
Codein phosphate	Omeprazol UQUIFA	2,37
Calcium pantothenate	Loratadin	1,73
Chlorhexidin HCl	Alprazolam	2,97
Doxycyclin hyclate	Diltiazem HCl	1,49
Doxycyclin monohydrate	Loperamide HCl	2,30
Fluoxetin HCl	Omeprazol UQUIFA	1,79
Guaifenesin	Clarithromycin	3,05
Ibuprofen	Loratadin	2,00
Dextromethorphan HBr	Piroxicam	2,43
Dextropropoxyphen HCl	Loperamid HCl	1,52
Loperamid HCl	Alprazolam	1,06
Loratadin	Omeprazol UQUIFA	1,13
Nicotinamid 99.5%	Alprazolam	3,75
Molsidomin	Omeprazol UQUIFA	1,42
Epitizid	Clarithromycin	3,56
Amlodipin besilate	Riboflavin	1,97
Amlodipin maleate	Clarithromycin	1,02
Alprazolam	Loperamid HCl	1,06
Folic acid	Omeprazol UQUIFA	1,81
Cetrimid	Clarithromycin	2,52
Clarithromycin	Amlodipin maleate	1,02
Hyamin HCl	Omeprazol UQUIFA	4,23
Indometacin micronized	Omeprazol UQUIFA	2,21
Lormetazepam	Clarithromycin	3,29
Piroxicam	Dextromethorphan HBr	2,43
Nipagine M	Clarithromycin	3,27
Sodium Pravastatin	Amlodipin maleate	1,47
Sodium Benzoate	Alprazolam	1,81
Tocopherol acetate	Loratadin	1,35
Triamteren	Alprazolam	1,99

Verapamil HCl BASF	Clarithromycin	2,53
Ascorbic acid HEBEI	Ascorbic acid TAKEDA	0.49
Thiamine mononitrate 100 %	Thiamine mononitrate 97 %	0.54
Theophyllin monohydrate 100 Mesh	Theophyllin monohydrate 200 Mesh	0.17
Omeprazol NATCO	Omeprazol UQUIFA	0.07
Acetaminophen DC284	Acetaminophen PVP3	0.28
Acetaminophen fine crystals	Acetaminophen dense powder	0.2

As can be seen from Table 2, most of the selectivity between the groups is greater than 1. However, for a minor part of the library, the selectivity is less than 1. This can be explained by 2 main reasons:

Either the difference between the groups is due to physical differences (ascorbic acid, theophylline monohydrate, omeprazol, acetaminophen (fine crystals, dense powder)) or the difference lies on the quantitative chemical content (acetaminophen DC284, acetaminophen PVP3, thiamine mononitrate).

Secondary and ternary identification methods were therefore developed for the identification of the remaining overlapping groups. These methods are parametered with specific signal pre-processing and spectral range. Primary, secondary and ternary identification methods are then combined to provide a global identification method.

A representative example of the use of secondary and ternary identification methods can be found with acetaminophen. Indeed, the pharmaceutical industry processes 2 main acetaminophen grades: acetaminophen for direct compression where a defined amount of povidone is added and pure acetaminophen. Regarding the identification method, the critical specifications of the different grades are displayed in Table 3.

Table 3 – Critical specifications of 4 acetaminophen grades.

Acetaminophen grade	**Critical specification**
Acetaminophen DC284	4 % povidone
Acetaminophen PVP3	3 % povidone
Acetaminophen dense powder	5 % max on 250 µm, 30 to 55 % on 63 µm
Acetaminophen fine crystals	20 % max on 250 µm, 60 to 80 % on 63 µm

Accordingly, a secondary identification method (ID2) was created to distinguish acetaminophen with the presence or absence of povidone.

As can be seen from Figure 4, ternary methods (ID 3) were also developed for 2 purposes:

- From a chemical point of view, to differentiate acetaminophen DC284 from acetaminophen PVP3.
- From a physical point of view, to differentiate dense powder from fine crystals acetaminophen.

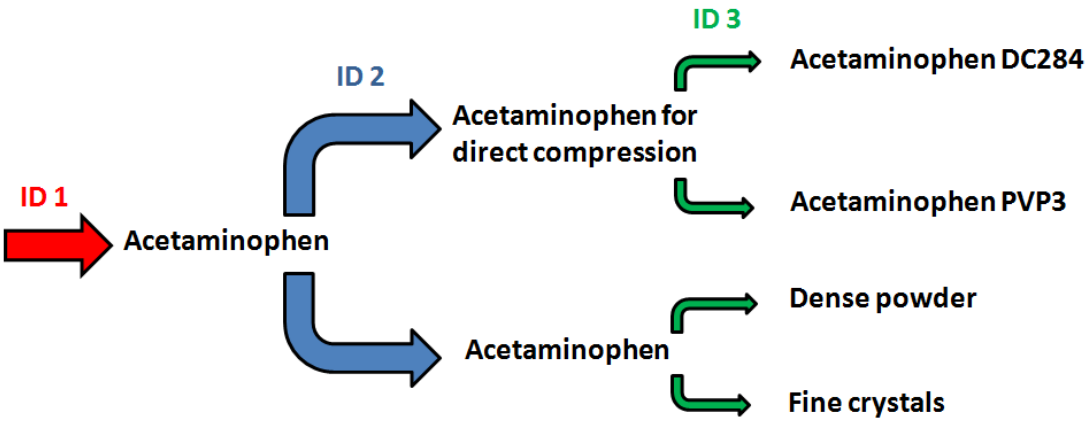

Fig. 4 – Example of secondary and ternary identification methods.

Table 4 illustrates how the use of secondary and ternary methods improved the selectivity between the different acetaminophen grades.

Table 4 – Use of secondary and ternary identification methods for the differentiation of acetaminophen grades: effect on the selectivity.

Group 1	Group 2	Selectivity
Acetaminophen DC 284	Acetaminophen PVP 3	1.55
Acetaminophen fine crystals	Acetaminophen dense powder	1.11

As can be seen in Table 5, the use of secondary and ternary identification methods enabled to increase the selectivity above 1 for all the other critical primary identification method API groups.

Table 5 – Improved selectivity using secondary and ternary identification methods.

Group 1	Group 2	Selectivity
Ascorbic acid HEBEI	Ascorbic acid Takeda	1.12
Thiamine mononitrate 100 %	Thiamine mononitrate 97 %	2.47
Theophyllin monohydrate 100 Mesh	Theophyllin monohydrate 200 Mesh	1.48
Omeprazol NATCO	Omeprazol UQUIFA	2.98

3.2 Identification method external validation

The external validation phase is carried out in the manufacturing area with full scale new samples, with known API identity, never included in the identification method spectral library: the API processed in the manufacturing line. Table 6 shows the validation results obtained so far.

Table 6 – External validation results.

API sample	Validation results
Acetylsalicylic acid 80 Mesh	Positive identification (100%)
Fenofibrate	Positive identification (100%)
Acetaminophen DC 284	Positive identification (100%)
Acetaminophen PVP3	Positive identification (100%)
Clarithromycin	Positive identification (100%)
Verapamil	Positive identification (100%)
Theophylline monohydrate	Positive identification (100%)
Ascorbic acid Hebei	Positive chemical identification (100%) (25 % error between Hebei and Takeda)
Ascorbic acid Takeda	

Table 6 shows that the chemical identification of ascorbic acid is 100 % positive. However, misidentification can occur sometimes between ascorbic acid providers Hebei and Takeda. This can be explained by the fact that there is no grade difference between the 2 raw materials: both chemical and physical specifications are the same.

3.3 Preliminary robustness testing

The developed method was tested with a PE bag containing acetaminophen PVP3 while deliberately doing actions that could alter the NIR measurement and so the reliability of the identification method.

The following robustness testing situations and their influence on the identification result were investigated and summarized in Table 7.

Table 7 – NIR identification method: preliminary robustness testing results.

Robustness test	Identification result
Analysis through PE bags covered with dust	Positive identification
Analysis through the lateral joints of the plastic bag	Positive identification
Analysis through the bottom joint of the plastic bag	No identification
Sample analysis through a triple bag thickness	No identification
Analysis while moving the probe in contact of the plastic bag	Positive identification
Applying a high pressure with the probe during the measurement	Positive identification
During the measurement, the probe is not in close contact with the plastic bag	No identification
Analysis performed by 2 operators with no prior knowledge about the NIR technique	Positive identification
Analysis performed under complete obscurity	Positive identification
Sample measurement through marker pen writings	Positive identification

It is important to clarify the fact that in case of 'no identification' as written in Table 6, the method is not able to identify the sample, there is no misidentification.

4. Conclusions

A NIR method able to identify the API raw materials in a pharmaceutical manufacturing area was developed: the method internal validation demonstrated that not only the API chemical identification was possible, API grade and provider identification can also be achieved.

The method is now being validated at the moment in the manufacturing area. The first validation results look promising in terms of method accuracy and robustness.

Besides, the developed NIR model is a dynamic application: it may be updated with new APIs, API providers or raw materials. In addition, optical probes can be dispatched from the NIR process instrument to various weighting sites.

As a conclusion, the present identification method represents a first PAT checkpoint for any pharmaceutical manufacturing process. It is a checkpoint of major importance as the

raw materials selection, weighting and dispatching towards the right manufacturing line is the first critical step leading to adequate product performance.

References

[1] K. Krämer, S. Ebel, Anal. Chim. Acta 420 (2000) 155.
[2] Y.-C. Feng, X.-B. Zhang, C.-Q. Hu, J. Pharm. Biomed. Anal. 51 (2010) 12.
[3] X.-M. Chong, C.-Q. Hu, Y.-C. Feng, H.-H. Pang, Vib. Spectrosc. 51 (2009) 313.

Section III.1.2.

Determination of binary polymorphic mixtures of fluconazole using near infrared spectroscopy and X-ray powder diffraction: A comparative study based on the pre-validation stage results

E. Ziemons, H. Bourichi, J. Mantanus, E. Rozet, P. Lebrun, E. Essassi, Y. Cherrah, A. Bouklouze, Ph. Hubert, Journal of Pharmaceutical and Biomedical Analysis 55 (2011) 1208.

Summary

The aim of the present study was to develop near infrared (NIR) and X-ray powder diffraction methods (XRPD) able to determine pure crystalline form II of fluconazole in a binary polymorphic mixtures containing form II and III. In order to give a first performance estimation of both methods, these latters were pre-validated using accuracy profiles, a statistical approach based on β-expectation tolerance intervals. Both methods showed a good trueness, precision and accuracy and their β-expectation tolerance intervals were fully included within the acceptance limits.

The comparative study was carried out using statistical analysis based on the work of Bland and Altman. A good agreement between the two methods was demonstrated indicating the interchangeability of NIR method with XRPD method.

1. Introduction

Nowadays, polymorphism determination in pharmaceutical solid drug substance has become a major matter of concern for the Pharmaceutical Industry as a proper knowledge of the crystalline transformations is requested by the regulatory authorities. According to polymorphic form, physical and chemical properties of drug (e.g. melting point, solubility, dissolution rate, chemical reaction and resistance to degradation) may be potentially different and affect its bioavailability, process-ability, and chemical and physical stability. Therefore, it is crucial to identify the optimal polymorphic form during the early R&D stages.

FDA's Process Analytical Technology (PAT) is "a system for designing, analyzing, and controlling manufacturing through timely measurements (i.e., during processing) of critical quality and performance attributes of raw and in-process materials and processes, with the goal of ensuring the final product quality". In a PAT context, regulatory authorities have established the need to control polymorphic forms used as drugs in order to ensure the integrity of the targeted polymorphic form during the manufacturing process and storage [1-5]. Based on its advantages such as suppression of samples preparation and of destruction, fast data acquisition and interfacing with manufacturing processes using probes, NIR spectroscopy matches the requirements of PAT.

Fluconazole (Figure 1) is a synthetic antifungal agent belonging to the group of triazoles. It is effective in the treatment of superficial and systemic mycoses, namely in the treatment of oropharyngeal, oesophageal, and vulvovaginal candidiasis for patients with the acquired immunodeficiency syndrome (AIDS) [6-9].

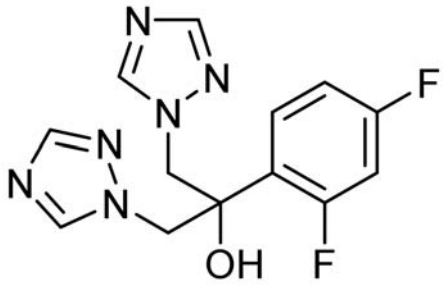

Fig. 1 - Structural formula of fluconazole.

The existence of three polymorphic forms of fluconazole has been reported and designated as forms I, II and III [10]. But the crystalline form of the drug substance marketed by Pfizer corresponds to form III [10]. Alkhamis et al. reported that polymorphic form II is a metastable form that is converted to the more stable form: polymorph III under the effect of compression or during the storage in standard ambience conditions of temperature and humidity [11]. At the moment pure polymorph II and III, blends of form II and III, and monohydrate form can be found on the market [12]. These forms were characterized by X-

ray powder diffraction (XRPD), thermal analysis, FT-mid-infrared and FT-Raman spectroscopy [12-16]. Only XRPD was used as quantitative method for determination of form II in form III in binary mixtures [13]. On the other hand, Bourichi et al. demonstrated the relationship between the presence of specific impurities and polymorphic form [17].

Analytical method pre-validation is the first evaluation step of the method accuracy and it helps the analyst to optimally design the validation experiments. In previous works, accuracy profiles, a statistical approach based on β-expectation tolerance intervals was found to be advantageous to evaluate quantitative method accuracy in pre-validation and validation stages [18-20].

In a full accordance with the PAT framework, using fluconazole as the model raw material, the aims of the present paper are firstly to develop a fast near infrared method (NIR) for the determination of pure crystalline form II in binary polymorphic mixtures containing form II and III and secondly to compare its results with those obtained with an XRPD method in a pre-validation stage.

2. Experimental

2.1 Materials

Polymorphic forms II and III of fluconazole were supplied by Vorin Laboratories Limited (Andrea Pradesh, India) and Pfizer (Dublin, Ireland), respectively. The purity of both forms was greater than 99%. The moisture content of forms II and III were 0.46% and 0.31%, respectively.

All the samples consisted in very fine white powder and were delivered in sealed containers at room temperature. The experimental protocol was carried out under controlled relative humidity and temperature conditions.

2.2 Preparation of calibration mixtures

Laboratory scale samples (150 mg total) containing various amounts of the two polymorphs were obtained by mixing known quantities of pure polymorphs II and III. The form II in form III concentration range was investigated from 0 to 100% (w/w) using samples at 25% intervals. Each sample, which was carried out in triplicate during 3 days, was mixed gently with an agate pestle and a mortar. The mixing was performed until the spectral deviation between two consecutive NIR spectra was below a fixed limit (data not shown). A total of 45 samples were used to build the calibration model.

2.3 Preparation of test mixtures

A set of 12 samples covering a concentration range from 37.5 to 87.5% (37.5, 50, 62.5, 87.5% (w/w)) was used to test the NIR method.

2.4 Reference method

The reference values used for the calibration and test samples were calculated gravimetrically from the actual weights of pure crystalline form II and III of fluconazole in the mixtures.

2.5 Near infrared spectroscopy

NIR spectra of samples put in vials were recorded in reflexion mode using a multipurpose analyzer Fourier transform near infrared spectrometer (MPA, Bruker Optics, Ettlingen, Germany) equipped with a semi-conductor room temperature sulfide lead (RT-PbS) detector. Each spectrum was the average of 32 scans and the resolution was 8 cm^{-1} over the range from 12500 to 4000 cm^{-1}. The spectra were collected with OPUS software 6.5 (Bruker Optics).

2.6 X-ray powder diffraction

The X-ray powder diffractograms of the samples were recorded between 5 and 35° (2θ), at room temperature, using a D8 Advance Bruker AXS spectrometer fitted with an ultrafast detector LynxEye and a copper anticathode (θ = 1.5406 Å, 40 kV, 40 mA). The diffractograms were recorded with a step width of 0.017° (2θ) and a count time of 7,8 s per step.

The quantitative determination was conducted on the integrated intensity of the peak located at about 10° (2θ), which is specific to fluconazole form II [12-13]. The composition of samples containing various percentages of pure polymorphs II and III was determined using the calibration plot of the change in the integrated 10° (2θ) peak area, as a function of polymorph II concentration.

2.7 Multivariate data analysis

PLS regression and pre-processing techniques were performed using OPUS/Quant software 6.5. All the spectral data were mean-centered prior to running the PLS.

The pre-validation of both methods was processed using the e.noval V3.0 (Arlenda, Liège, Belgium).

2.8 Agreement between NIR and XRPD

The agreement between the two methods was evaluated by a statistical analysis based on the work of Bland and Altman [21]. A plot of the relative differences between the two methods results against their average is used to compare the NIR and XRPD techniques. This comparison was performed using three samples for each concentration level corresponding to 25, 50, 75 and 100% of fluconazole during three different runs thus leading to a total of 36 results for each method. The aim of this direct method comparison is used to evaluate whether the two analytical techniques can be interchangeable. A linear mixed model was thus fitted on the results differences versus their average together with its 95% prediction interval. The computations were performed using nlme package of R v2.9.1 (CRAN, http://cran.r-project.org). The maximum relative difference that was defined acceptable between any result of the NIRS and XRPD methods was set at $\pm$5%.

3. Results and discussion

3.1 Quantification by NIR method

The NIR spectra of pure crystalline forms II and III of fluconazole are depicted in Figure 2. These spectra were pre-processed with a Satvisky-Golay first derivative in order to highlight the spectral differences according to the form.

Several calibration models based on PLS regression were built using different spectral ranges and common pre-processing techniques of near infrared spectral data such as spectral derivatives (Savitzky-Golay derivation) and scatter-correction methods (Standard Normal Variate and Multiplicative Scatter Correction) [22]. Based on the number of components in the mixtures, which are present in the calibration set, the number of PLS latent variables of each calibration model was set to 2. Table 1 displays the parameters of the predictive models. The best results were obtained when the spectral data was first derivative prior to MSC leading to RMSEC and RMSEP values of 0.458% and 0.538%, respectively.

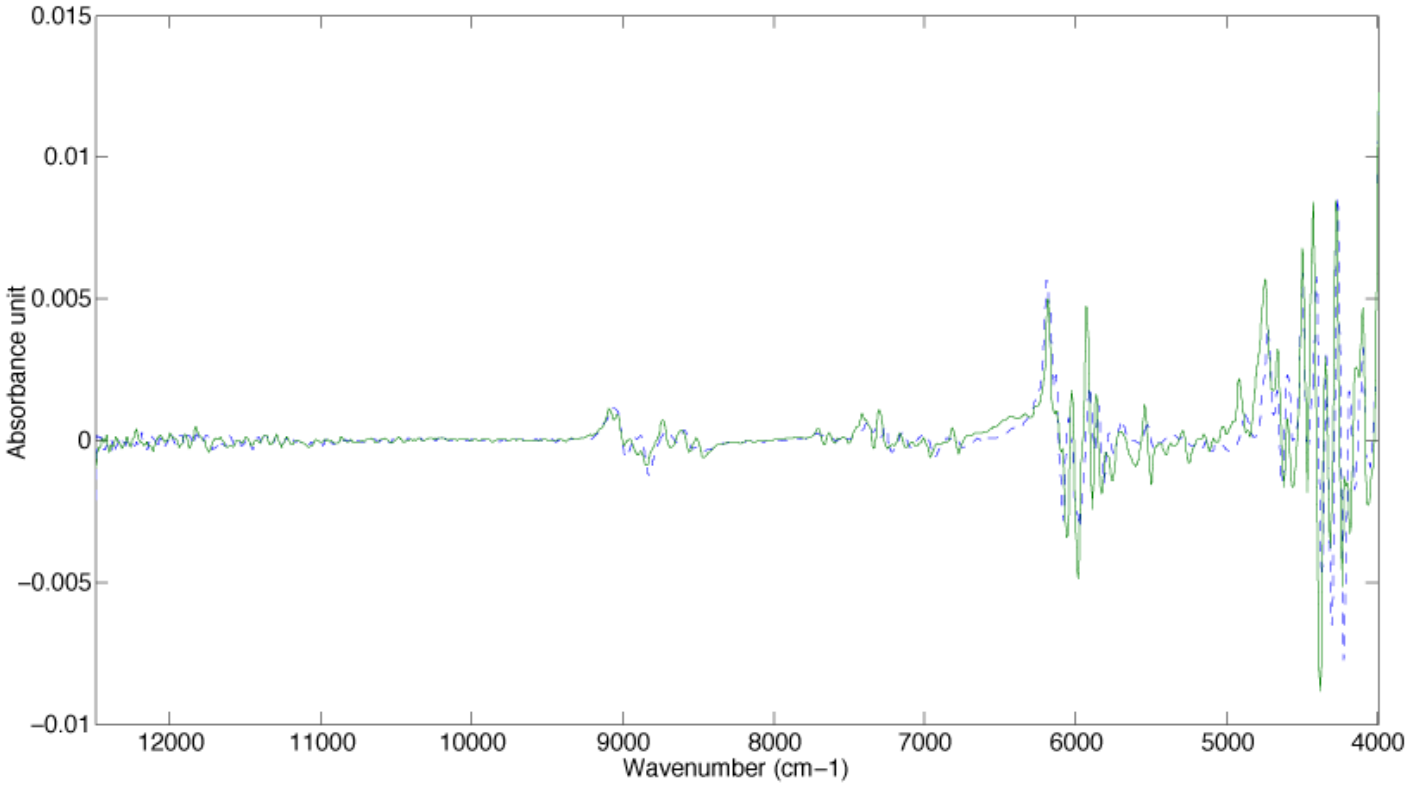

Fig. 2 - NIR spectra of fluconazole: (a) Form II and (b) Form III.

Table 1 - Spectral range, spectral pretreatment, number of latent variables, RMSEC, RMSECV and RMSEP of the NIR models.

Model	Pretreatment	Spectral range (cm^{-1})	Latent variables	RMSEC (%)	RMSECV (%)	RMSEP (%)
(a)	Raw data	9200-6500 5930-4000	2	3.77	3.99	3.48
(b)	MSC	9200-6500 5930-4000	2	1.07	1.18	0.966
(c)	First derivative + MSC	9200-6500	2	0.458	0.578	0.538
(d)	SNV	8005-4915	2	0.729	0.750	0.800
(e)	First derivative + SNV	8005-5930	2	0.828	0.847	0.697

3.2 Quantification by XRPD method

The X-ray diffraction patterns are shown in Figure 3 between 5 and 35° (2θ). The main diffraction peaks of crystalline form III are observed at 2θ = 11.6°, 14.7°, 17.3°, 18.4°, 19.7°, 24.3° and 26.8°. Those of form II are observed at 2θ =10.0°, 15.0°, 16.0°, 16.6°, 20.0° and 25.6°. Comparison of pure form II and III diffractograms showed that form II has a specific diffraction peak at 10° (2θ) and thus, this last one was used for the quantification of form II in the samples of fluconazole.

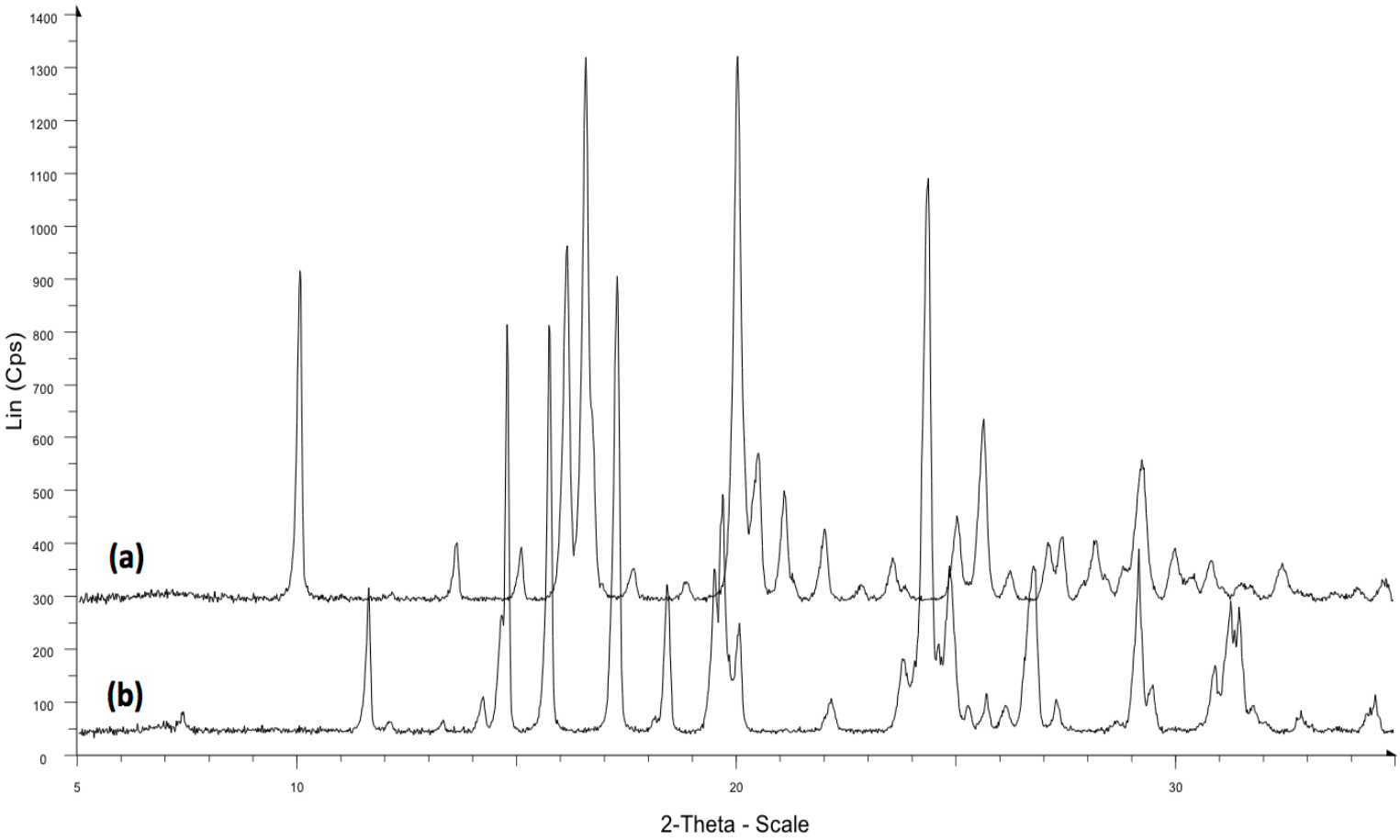

Fig. 3 - RX spectra of fluconazole: (a) Form II and (b) Form III.

3.3 Pre-validation of both methods

In this study, pre-validation experiments were carried out exclusively with the calibration set in order to give a first estimation of the performance of both methods regarding their purpose. Figure 4 shows accuracy profiles obtained with NIR and XRPD using the calibration model (C) and a linear regression model, respectively. Due to the objective of both methods, the acceptance limits were set at ± 5% and the maximum risk (1-β) of having a future result outside these acceptance limits was set at 5%. NIRS and XRPD accuracy

profiles were built based on results obtained from the leave-one-out cross-validation of the predictive model (C) and based on back-calculated results of the linear regression model, respectively. Table 2 shows the pre-validation results of both methods according to the ICH Q2(R1) validation criteria. The trueness and the precision of both methods are very satisfactory irrespective of the concentration levels and never exceed 1% and 2%, respectively.

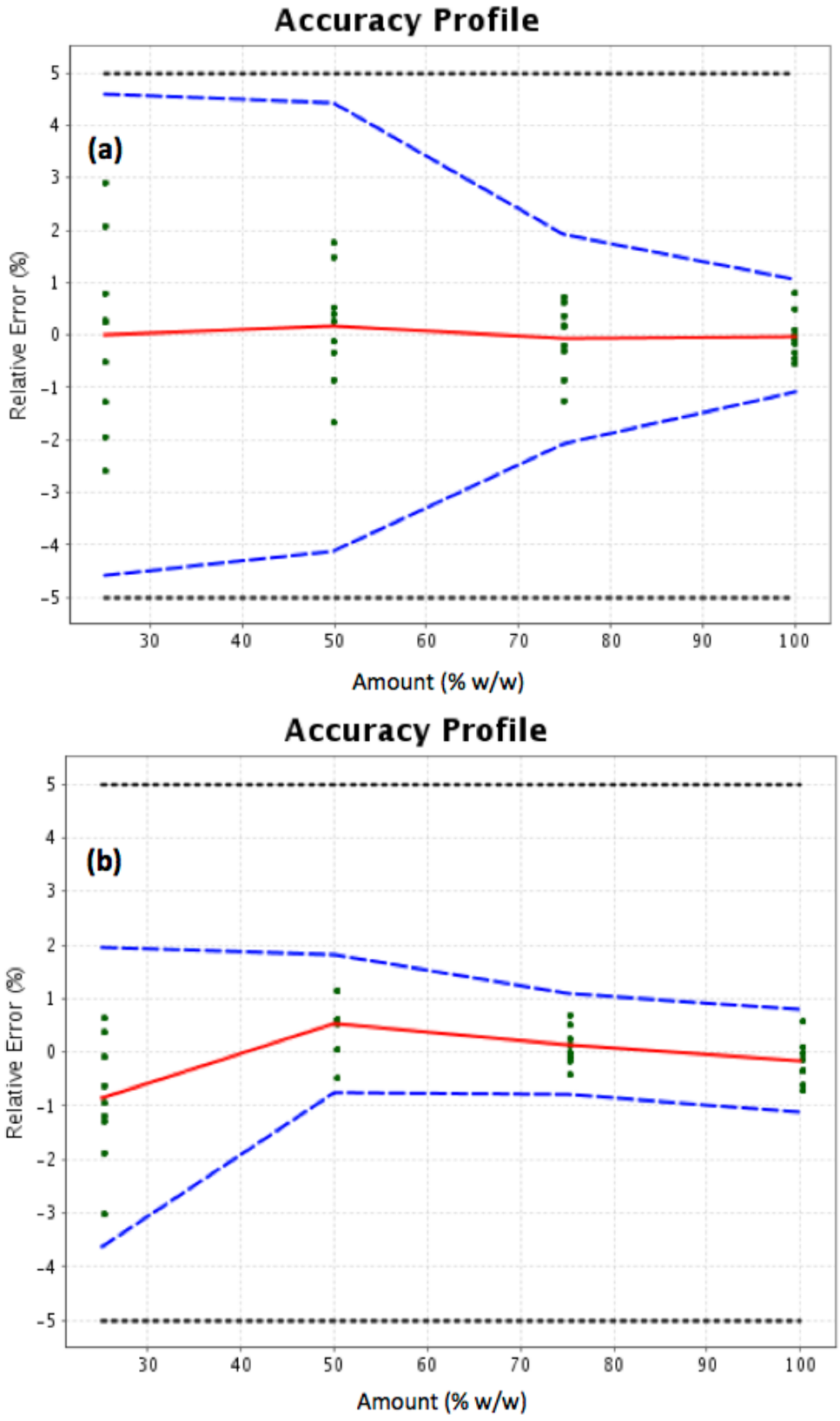

Fig. 4 - Accuracy profile of fluconazole (form II) using (a) cross-validated data of the NIR PLS model (c) and (b) the XRPD method prevalidation results. The plain line is the relative bias, the dashed lines are the β-expectations tolerance limits (β =95%) and the dotted lines represent the acceptance limits (±5%).

Table 2 - ICH Q2(R1) validation criteria of NIR and XRPD methods.

Trueness	Concentration level (% of Fluconazole II)	Relative bias (%)			
		NIR		XRPD	
	25	0		-0.8	
	50	0.2		0.5	
	75	-0.1		-0.1	
	100	0		-0.2	
Precision	Concentration level (% of Fluconazole II)	Repeatability (RSD %)		Intermediate precision (RSD %)	
		NIR	XRPD	NIR	XRPD
	25	1.7	1.1	1.8	1.1
	50	0.6	0.5	1.2	0.5
	75	0.5	0.3	0.7	0.4
	100	0.4	0.4	0.4	0.4
Accuracy	Concentration level (% of Fluconazole II)	Relative β-Expectation tolerance limits (%)			
		NIR		XRPD	
	25	[-4.6 , 4.6]		[-3.6 , 2.0]	
	50	[-4.1 , 4.4]		[-0.8 , 1.8]	
	75	[-2.1 , 1.9]		[-0.8 , 1.1]	
	100	[-1.1 , 1.1]		[-1.1 , 0.8]	
Limits of quantification (LOQ)	Lower LOQ (% of Fluconazole II)			Upper LOQ (% of Fluconazole II)	
	NIR	XRPD		NIR	XRPD
	25			100	

From Figure 4, it can be observed that β-expectation tolerance intervals of both methods are fully included within the acceptance limits of ± 5%. These results gives a first guarantee that the methods should be able to achieve their objective prior running a formally validation process which is usually time-consuming regarding the use of a reference method to determine the form II/III ratio of real samples.

3.4 Agreement between NIR and XRPD methods

The agreement between the two techniques was evaluated to know if the NIR could replace the XRPD using a methodology adapted from Bland and Altman [21]. The difference plot is shown in Figure 5. This plot represents the relative differences of the two methods results against their average and displays their agreement. The prediction interval limits delimits the area containing 95% of the difference values obtained. As these limits are confined inside the ±5% acceptance limits, the two methods agree sufficiently for the NIRS to replace safely the XRPD method and vice versa. Additionally it can be seen in Figure 5 that on average the results obtained by both methods agree extremely well except for the smallest concentration level (25%) where the XRPD results under estimates systematically those of the NIRS method. However, as shown in Figure 5, this does not impair the excellent agreement of both methods results.

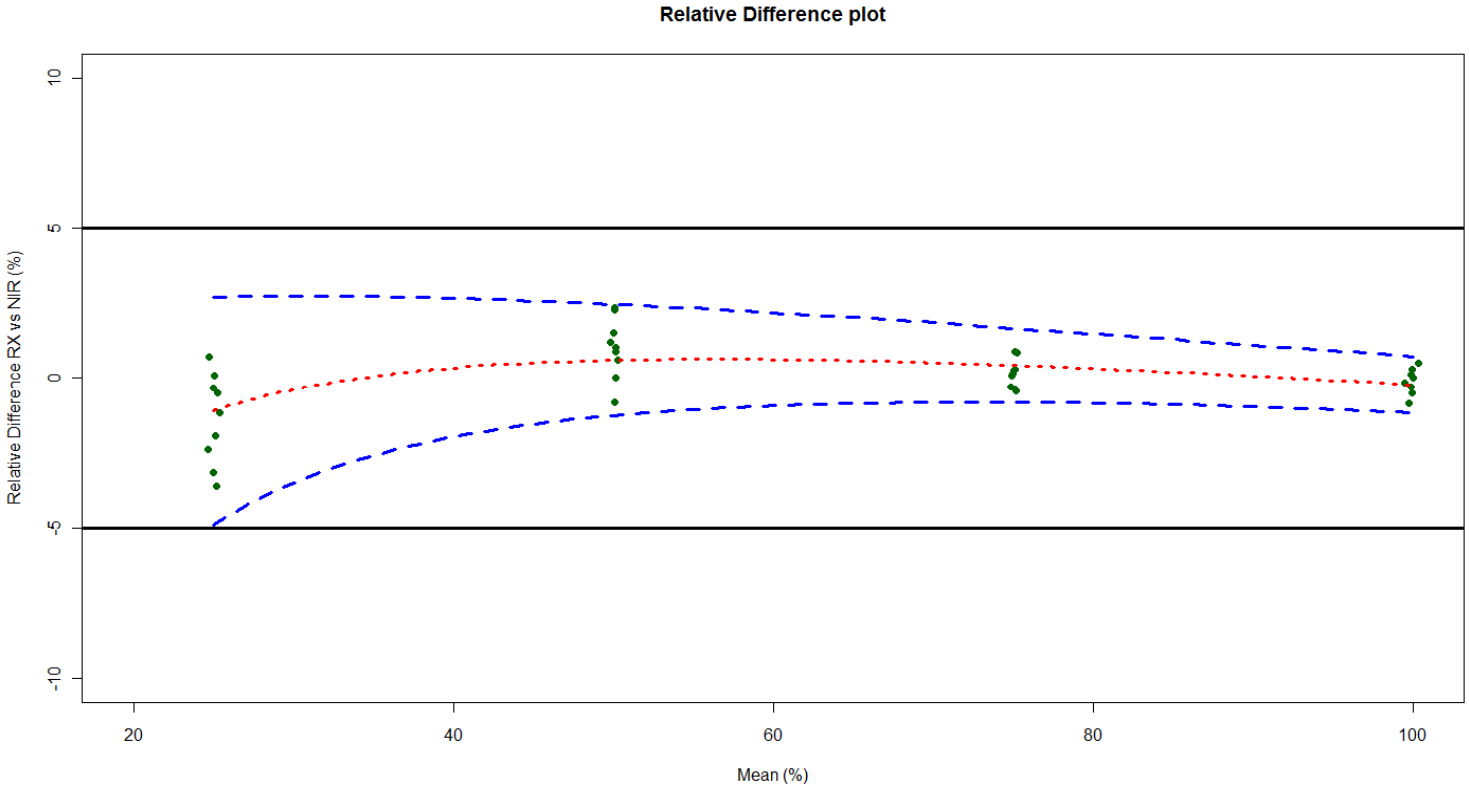

Fig. 5 – Relative difference of the XRPD and NIR methods results versus their average. The dashed red line is the relative bias, the dashed blue lines are the β-expectations tolerance limits (β =95%) and the continuous black lines represent the acceptance limits (±5%).

4. Conclusion

NIR and XRPD methods were developed for determination of pure crystalline form II of fluconazole in binary polymorphic mixture containing form II and form III. Both methods were successfully pre-validated and showed a good trueness, precision and accuracy for the determination of compound of interest irrespective of the concentration levels confirming their potential in this topic.

The agreement between both methods demonstrated that NIR could replace safely XRPD method and vice versa allowing the analyst to choose the method taking into account the advantages and drawbacks of each one.

References

[1] Polymorphism, European Pharmacopoeia 6th Edition, Strasbourg 2010, p 649.
[2] D.J.W. Grant, S.R. Byrn, A timely re-examination of drug polymorphism in pharmaceutical development and regulation, Adv. Drug Deliver Rev. 56 (2004) 237–239.
[3] A.S. Raw, M.S. Furness, D.S. Gill, R.C. Adams, F.O. Holcombe Jr., L.X. Yu, Regulatory considerations of pharmaceutical solid polymorphism in abbreviated new drug applications (ANDAs), Adv. Drug Deliver. Rev. 56 (2004) 397- 414.
[4] International Conference on Harmonisation (ICH) of technical requirements for registration of pharmaceutical for human use, Topic Q6A: Specifications: Test Procedures and acceptance criteria for new drug substances and new drug products, Geneva, 1999.
[5] D.A. Snider, W. Addicks, W. Owens, Polymorphism in generic drug product development. Adv. Drug Deliver. Rev. 56 (2004) 391-395.
[6] R. Musiol, J. Jampilek, V. Buchta, L. Silva, H. Niedbala, B. Podeszwa, A. Palka, K. Majerz-Maniecka, B. Oleksyn, J. Polanski, Antifungal properties of new series of quinoline derivatives, Bioorgan. Med. Chem. 14 (2006) 3592–3598.
[7] Q.Y. Sun, W.N. Zhang, J.M. Xu, Y.B. Cao, Q.Y Wu, D.Z. Zhang, C.M. Liu, S.C. Yu, Y.Y. Jiang, Synthesis and evaluation of novel 1-(1H-1,2,4-triazol-1-yl)-2-(2,4-difluorophenyl)-3-[(4-substitutedphenyl)- piperazin-1-yl]-propan-2-ols as antifungal agents, Eur. J. Med. Chem. 42 (2007) 1151-1157.
[8] M. Zervos, F. Meunier, Fluconazole (Diflucan®): a review, Int. J. Antimicrob. Ag. 3 (1993) 147-170.
[9] D.J. Sheehan, C.A. Hitchcock, C.M. Sibley, Current and emerging azole antifungal agents, Clin. Microbiol. Rev. 12 (1999) 40-79.
[10] A.K. Dash, W.F. Elmquist, Fluconazole, in: H. G. Brittain (Eds.), Analytical profiles of drug substances and excipients, Academic Press, Milford, 2002, pp. 67-113.
[11] K. A. Alkhamis, A. A. Obaidat, A. F. Nuseirat, Solid-state characterization of fluconazole, Pharm. Dev. Technol. 7 (2002) 491-503.

[12] H. Bourichi, Y.Brik, E. Essassi, A. Bouklouze, Y. Cherrah, Solid-state characterization of fluconazole, STP Pharma Pratiques 17 (2007) 49-57.
[13] X.J. Gu, W. Jiang, Characterization of polymorphic forms of fluconazole using Fourier-transform Raman spectroscopy, J. Pharm. Sci-US. 84 (1995) 1438-1441.
[14] M.R. Caira, K.A. Alkhamis, R.M. Obaidat, Preparation and crystal characterisation of a polymorph a monohydrate and an ethyl acetate solvate of the antifungal fluconazole, J. Pharm. Sci-US. 93 (2004) 601-611.
[15] S.R. Desai, M.M. Shaikh, S.R. Dharwadkar. Thermoanalytical study of polymorphic transformation in fluconazole drug. Thermochim. Acta 399 (2003) 81-89.
[16] T.D. Cyr, B.A. Dawson, G.A. Neville, H.F. Shurvell, Spectral characterization of fluconazole, J. Pharm. Biomed. Anal. 14 (1996) 247-255.
[17] H. Bourichi, Y. Brik, E. Essassi, A. Bouklouze, Y. Cherrah, Quality control of impurities in fluconazole active raw material by HPLC-UV, STP Pharma pratiques 18 (2008) 285-291.
[18] C. Bodson, E. Rozet, E. Ziemons, B. Evrard, Ph. Hubert, L. Delattre, Validation of manufacturing process of Diltiazem HCl tablets by NIR spectrophotometry (NIRS), J. Pharma. Biomed. Anal. 45 (2007) 356-361. http://hdl.handle.net/2268/1642
[19] A. Bouabidi, E. Rozet, M. Fillet, E. Ziemons, E. Chapuzet, B. Mertens, R. Klinkenberg, A. Ceccato, M. Talbi, B. streel, A. Bouklouze, B. Boulanger, Ph. Hubert, Critical analysis of several analytical method validation strategies in the framework of the fit for purpose concept, J. Chrom. A 1217 (2010) 3180-3192. http://hdl.handle.net/2268/29471
[20] J. Mantanus, E. Ziemons, P. Lebrun, E. Rozet, R. Klinkerberg, B. Streel, B. Evrard, Ph. Hubert, Moisture content détermination of pharmaceutical pellets by near infrared spectroscopy : method development and validation, Ana. Chim. Acta 642 (2009) 186-192. http:/hdl.handle.net/2268/18780
[21] J. M. Bland and D. G. Altman, Statistical methods for assessing agreement between two methods of clinical measurement, Lancet 1 (1986) 307-310.
[22] A. Rinnan, F. van den Berg, S. Balling Engelsen, Review of the most common pre-processing techniques for near-infrared spectra, Trends Anal. Chem. 10 (2009) 1201-1222.

Part III.2.

NIR as a PAT tool to control pharmaceutical formulations

Section III.2.1.

Liquid formulation: Acetaminophen determination in low-dose pharmaceutical syrup by NIR spectroscopy

J. Mantanus, E. Ziemons, P. Lebrun, E. Rozet, B. Evrard, Ph. Hubert, J. Pharm. Biomed. Anal. 53 (2010) 510.

Summary

The aim of the present study was first to develop a robust near infrared (NIR) calibration model able to determine the acetaminophen content of a low-dose syrup formulation (2 % (w/v)). Therefore, variability sources such as production campaigns, batches, API concentration, syrup basis, operators and sample temperatures were introduced in the calibration set. A prediction model was then built using Partial Least Square (PLS) regression. First derivative followed by Standard Normal Variate (SNV) were chosen as signal pre-processing. Based on the random subsets cross validation, 4 PLS factors were selected for the prediction model. The method was then validated for an API concentration ranging from 16 to 24 mg/mL (1.6-2.4 % (w/v)) using an external validation set. The 0.26 mg/mL RMSEP suggested the global accuracy of the model. The accuracy profile obtained from the validation results, based on tolerance intervals, confirmed the adequate accuracy of the results generated by the method all over the investigated API concentration range. Finally, the NIR model was used to monitor in real time the API concentration while mixing syrups containing various amounts of API, a good agreement was found between the NIR method and the theoretical concentrations.

1. Introduction

FDA's Process Analytical Technology (PAT) focuses on the real time monitoring of pharmaceutical manufacturing processes [1]. While time consuming laboratory testings still nowadays slow down the batch release step, the data collected during the manufacturing could reduce the batch release time and eventually enable real time batch release. A real time monitoring system such as PAT requires a high data acquisition speed and has to be compatible with probes for on-line and in-line analysis.

Near infrared (NIR) spectroscopy is a well-established vibrational spectroscopic technique [2-4]. In the covered wavelength region (between 14000 and 4000 cm^{-1}), relatively wide bands related to overtones and combination of fundamental vibration of chemical groups with hydrogen, such as C-H, N-H, O-H and S-H are observed. Such vibrations lead to overlapping bands which contain both physical and chemical information. Consequently, chemometric tools such as spectral pretreatments and regression methods are needed to extract the significant information.

NIR spectroscopy has many advantages: fast spectral acquisition, minimization of sample preparation and/ or destruction and the use of probes allowing at-line, on-line and in-line measurements. Based on those advantages, NIR spectroscopy matches the PAT requirements. It has been part of PAT applications to monitor critical process attributes such as blend homogeneity, the coating level, the moisture content and the active content [3-13].

The acetaminophen determination in solid dosage forms by near infrared spectroscopy has already been investigated in previous studies [14-16].

As one of the main drawbacks of NIR spectroscopy is its relatively low sensibility, few NIR quantitative applications have been performed on low dosage forms [17-18]. Therefore the challenge still remains to quantify low dosage pharmaceutical forms.

In full accordance with the PAT concept, the acetaminophen content of low-dose syrups could be determined by NIR spectroscopy. The NIR measurements could be performed off-line, at-line, on-line or in-line to check the conformity of the pharmaceutical syrups during the manufacturing and/or before the final packaging stage. Such a NIR method could then be the first step towards a real time release quality-based system.

Validation is a crucial and mandatory step in the lifecycle of an analytical method [19]. Based on β-expectation tolerance intervals, the accuracy profile makes possible a visual and reliable representation of the actual and future performances of the analytical method. It enables a better risk management [20]. Besides, it fully complies with the ICH Q2(R1)

regulatory documents as it integrates all the useful required validation criteria such as accuracy, trueness, precision, limits of quantification, range and linearity [21-23].

The aim of the present study was first to develop a reliable near infrared method able to determine the active content of a low-dose acetaminophen syrup. The second aim was to fully validate the method for an active content ranging from 16 to 24 mg/mL. Finally, the ability of the validated NIR method to monitor in real time changes in API concentration was tested.

2. Materials and methods

2.1 Syrups preparation

Laboratory scale syrups containing an acetaminophen concentration between 16 and 24 mg/mL (1.6-2.4 % (w/v)) were manufactured. An accurately weight amount of acetaminophen (between 400 and 600 mg) was dissolved into 20 mL of syrup basis in a 25 mL volumetric flask using a sonic bath Branson 2510 (Branson Ultrasonics Corporation, Danbury, USA). After complete acetaminophen dissolution, syrup basis was added to 25 mL. The syrup basis is prepared using 60 mL of glycerol (Fagron, Certa), 10 mL of ethanol (Merck), 5 mL of water and syrup conservans (Fagron, Certa) was added to 100 mL.

2.2 Calibration samples

3 syrups production campaigns were included in the calibration of the NIR method. 16, 20 and 24 mg/mL (1.6, 2.0 and 2.4 % (w/v)) API syrups were manufactured for each production campaign, 3 syrups per concentration level.

2.3 External validation samples

3 new syrups production campaigns were used for the validation set. The validation set was built in the same way as the calibration set except that 18 and 22 mg/mL (1.8 and 2.2 % (w/v)) API syrups were also manufactured.

2.4 FT-NIR equipment and software

The syrups samples were analyzed with a multipurpose analyzer Fourier transform near infrared spectrometer (MPA, Bruker Optics, Ettlingen, Germany) equipped with a semiconductor room temperature sulfide lead (RT-PbS) detector. A transmittance probe for

liquids with a fixed optical pathlength of 2 mm was used to collect the NIR spectra. The probe was directly in contact with the syrups. A background spectrum with the empty probe was acquired before each series of measurements. Between each measurement, the probe was cleaned with water and dryed with a nitrogen flow. The spectra were collected with the Opus Software 6.5 (Bruker Optics). Each spectrum was the average of 32 scans and the resolution was 8 cm^{-1} over the range from 12500 to 3600 cm^{-1}. The time necessary for a NIR measurement was 15 seconds. The NIR spectrum of acetaminophen was collected using the integrating sphere module of the spectrometer allowing a reflectance measurement.

2.5 Reference method

The reference method used for the API determination was the HPLC assay recommended by the USP 32 for acetaminophen capsules [24]. The HPLC method was performed in a LaChrom HPLC system (Hitachi High-Tech, Tokyo, Japan). One determination was made for each sample and was used as the reference value.

2.6 Near infrared method: calibration and validation protocols

Variability sources such as production campaigns, batches, API levels, syrup basis, operators and temperatures were introduced in the calibration and validation protocols. The NIR spectra of the samples were first recorded before performing the reference measurements.

2.7 Multivariate data analysis

Partial Least Squares (PLS) regression, first derivative (order: 2, window: 15 points, corresponding to 57.75 cm^{-1}) and Standard Normal Variate (SNV) were carried out with PLS Toolbox 5.0 for Matlab version 7.6. PLS regression using cross-validation random subsets was performed on the calibration set to build the prediction model [25]. The random subsets cross-validation is performed as follows: if *s* is the number of data splits, *n* the total number of samples and *r* the number of iterations, *s* different test sets are determined through random selection of *n*/*s* objects in the data set, such that no single object is in more than one test set. This procedure is repeated *r* times [26].

The model ability to predict the API content was further tested with the external validation set.

The calculation of the accuracy profile based on the external validation set results were performed with e.noval V3.0 (Arlenda, Liège, Belgium).

3. Results and discussion

3.1 Calibration

Table 1 – Variability sources included in the calibration and validation sets.

	Calibration set	Validation set
Variability sources	Amount of variability	
Production campaigns	3	
Batches per production campaign	9	15
API levels	3 (16, 20 and 24 mg/mL)	5 (16, 18, 20, 22 and 24 mg/mL)
Basis of excipients	2 brands of glycerol and syrup conservans, 1 batch per brand.	2 brands of glycerol and syrup conservans, 1 new batch per brand
Operators	2	1
Sample temperature during the NIR acquisition	2 (25 and 30 °C)	

To build a robust NIR model, the calibration set has to contain the future expected variability that the model will meet in the routine environment. Therefore, 6 sources of variability were integrated in the calibration set, these are cited in Table 1. First of all, 3 different syrup production campaigns were manufactured. Indeed, during the lifecycle of an analytical method, many production campaigns will be analyzed. It is then necessary to include different production campaigns in the calibration set. In full accordance with the previous consideration, 9 independent batches were manufactured per production campaign, 3 batches per API level. In order to cover a large part of the acetaminophen concentration range, each syrup was manufactured around the targeted concentration levels (between 16 and 24 mg/mL ± 5 %) by weighing various amounts of API. Besides, from one production campaign to another, variability was also introduced in the syrup basis: 2 brands of glycerol and syrup conservans were used, 1 batch per brand. They were combined randomly to manufacture 3 syrup basis per production campaign. Also, as an analytical method is not dedicated to only one operator, the calibration set was designed with 2 operators. Operator (a) manufactured the first syrup production campaign and performed the corresponding HPLC and NIR analyses. Operator (b) worked on the remaining production campaigns of the calibration set. Finally, as liquid samples are analyzed in the present study,

temperature changes can induce spectral variations leading to increased Mahalanobis distances. With increasing temperatures, the water absorption bands are moving to higher wavenumbers and there is an increase in signal height [2]. Therefore samples were scanned while thermostated at 25 °C and 30 °C. The samples were then analyzed once by the HPLC reference method. Per production campaign, 18 NIR spectra were recorded and 9 reference measurements were carried out. As 3 different production campaigns were manufactured, the entire calibration set contains a total of 54 NIR spectra and 27 reference measurements.

3.2 External Validation

New batches were manufactured for the external validation set. As can be seen from Table 1, the introduced variability sources were the same as for the calibration set except that only operator (b) designed the external validation set. In order to demonstrate that 3 API concentration levels were sufficient to built a robust calibration set and to fully validate the model, 5 API concentration levels were integrated in the external validation set.

Per production campaign, 30 NIR spectra were recorded and 15 reference measurements were carried out. As 3 different production campaigns were manufactured, the entire validation set contains a total of 90 NIR spectra and 45 reference measurements.

3.3 Validation results of the NIR method

Figure 1 displays the 20 mg/mL acetaminophen syrup formulation transmittance spectrum and the acetaminophen reflectance spectrum. From this figure, absorption bands coming from the syrup basis can be observed in the 3900-5300 and 6000-7200 cm^{-1} spectral areas. Besides, the reflectance spectrum of acetaminophen shows absorption bands from 4000 to 9000 cm^{-1}. Table 2 displays the conventional parameters of the NIR model. It can be seen that the 5955-7212 cm^{-1} spectral region was selected to build the quantitative model as it contains information about the API. PLS regression was performed with the calibration set. Cross-validation based on random subsets was carried out to select the model number of PLS factors. For the random subsets cross-validation, 9 splits and 10 iterations were selected.

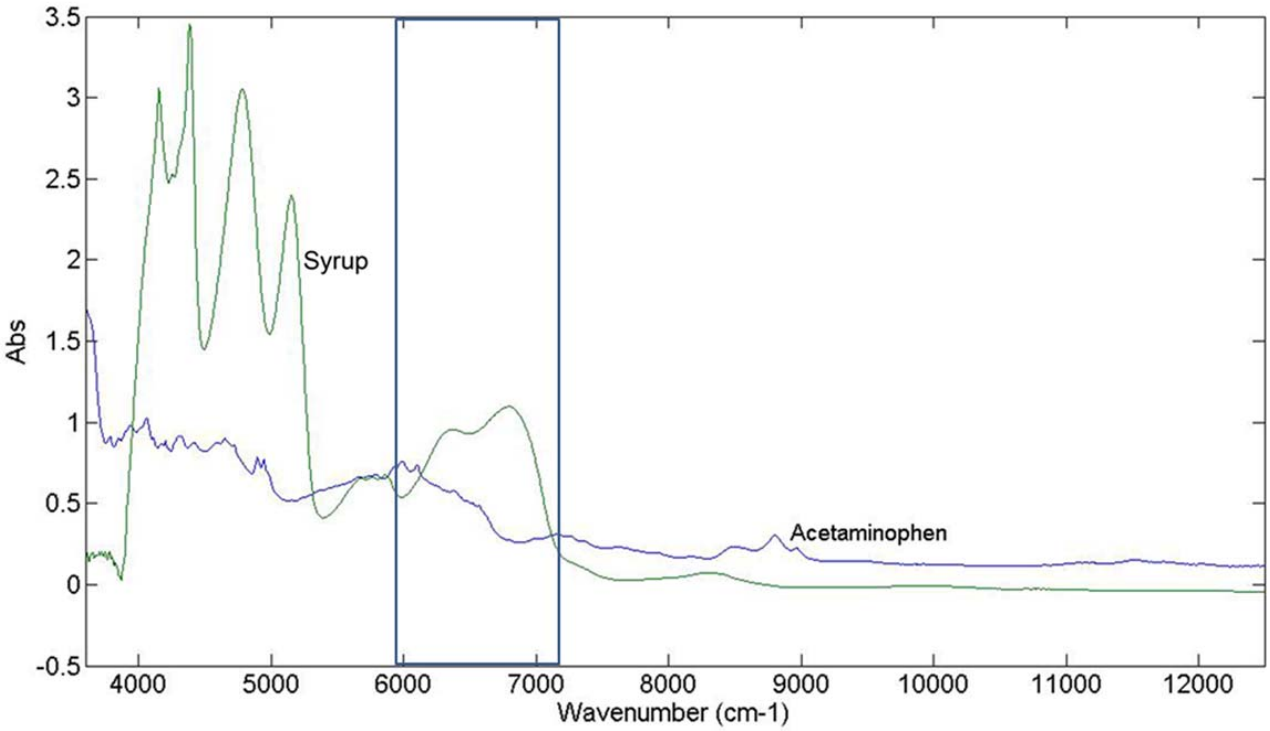

Fig. 1 – Syrup transmittance and acetaminophen reflectance spectra. The highlighted area defines the selected spectral range for the NIR model.

Table 2 – Spectral range, spectral pre-treatment, number of PLS factors, R^2 of validation, RMSEC, RMSECV and RMSEP of the NIR model.

NIR model	Selected parameter
Spectral range selected (cm^{-1})	5955-7212
Spectral pre-treatment	1^{st} derivative + SNV
Number of PLS factors	4
R^2 Val	0.993
RMSEC (mg/mL)	0.34
RMSECV (mg/mL)	0.39
RMSEP (mg/mL)	0.26

About the number of PLS factors, Figure 2 shows the evolution of the RMSECV according to the number of PLS factors. Based on this Figure, 4 PLS factors were selected as the RMSECV value is minimal from 4 PLS factors.

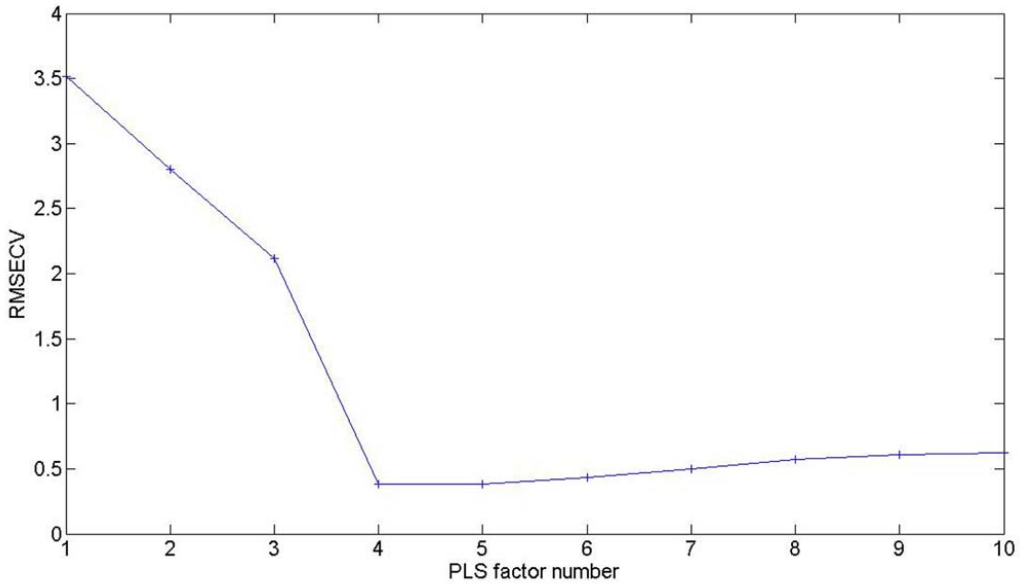

Fig. 2 – RMSECV according to the PLS factor number.

Figure 3 shows a good agreement between the NIR predictions and the HPLC reference method results for both the calibration and validation sets.

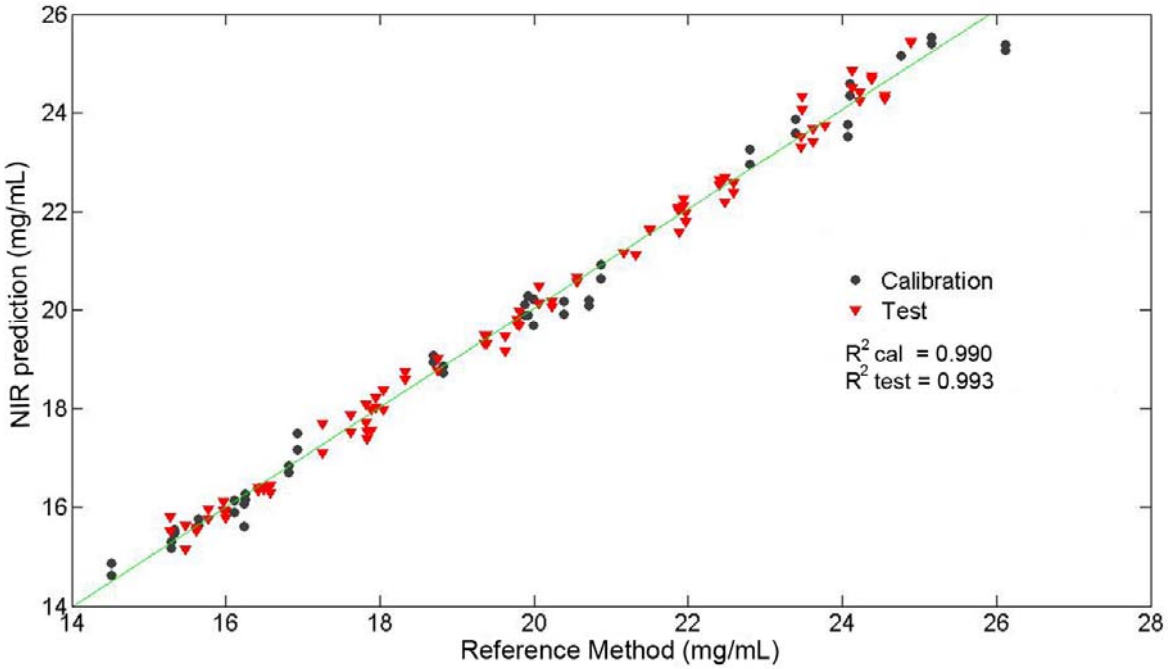

Fig. 3 – API NIR predictions versus the Reference Method results. The black dots and the red triangles represent the results of the calibration and the external validation sets respectively.

The RMSEC, RMSECV and RMSEP values are low. However, those criteria do not allow the assessment of the model ability to quantify accurately over the entire API range.

Therefore, the model predictive performance was evaluated with accuracy profiles computed on the external validation results. This innovative approach uses tolerance intervals as statistical methodology that allows predicting a region of concentration where each future result has a defined probability to fall. This probability is defined by the analyst.

Facing the confusion found between accuracy and trueness in the ICH document, it seems important to remind that accuracy represents the total error concept which is the sum of the trueness (systematic error) and precision (random error). In this aspect, the accuracy profile takes into account the total error [21-22].

As the focus of the present study is the determination of an API in a pharmaceutical formulation, the acceptance limits were set at ± 5 % for the validation of the NIR method while the probability to obtain results within the tolerance interval was set at 95 %.

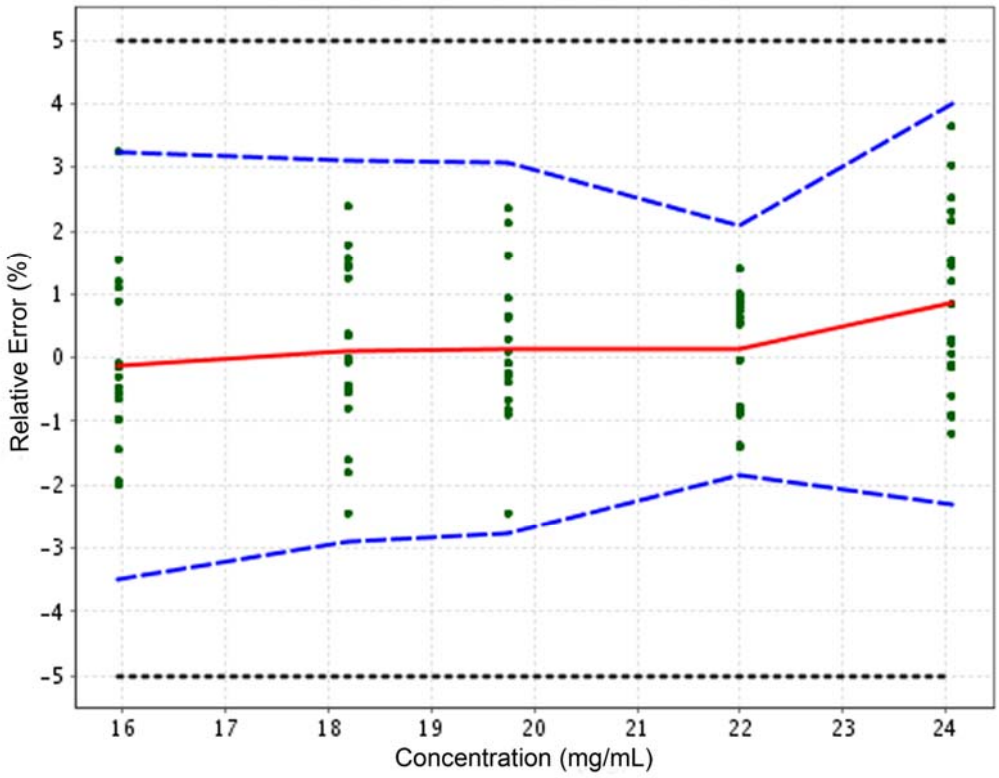

Fig. 4 – Accuracy profile based on the validation results of the NIR model. The plain line is the relative bias, the dashed lines are the β-expectations tolerance limits (β = 95 %) and the dotted lines represent the acceptance limits (±5 %).

The lower and upper limits of quantification (LLOQ and ULOQ) define the range where an analytical method is able to quantify accurately. They are respectively the smallest and

highest concentration levels where the β-expectation tolerance intervals are included within the acceptance limits. If the β-expectation tolerance interval never crosses the acceptance limits, then the LLOQ and ULOQ are located at the beginning and at the end of the active content range investigated.

Figure 4 displays the accuracy profile computed with the external validation set results. It can be seen from this figure that the validation results concentrations are different from the ones displayed in Figure 3. For the accuracy profile calculation, it was necessary to perform an alignment on the mean concentration obtained by the reference method per API concentration level to compute repeatability and intermediate precision variance estimates [22]. It can be observed that the β-expectations tolerance limits are fully included within the ± 5 % acceptance limits. Therefore, each future result has at least 95 % probability to fall within the ± 5 % acceptance limits. Besides, it can be seen that the developed NIR model quantifies with the same level of accuracy API levels not included in the calibration set: 18 and 22 mg/mL API syrups.

Table 3 shows the ICH Q2(R1) validation criteria of the developed method. As seen in the accuracy profile, the bias is close to zero from 16 to 22 mg/mL. It is equal to 0.9 % for the 24 mg/mL concentration level.

The precision of the method was estimated by measuring repeatability and intermediate precision at the 5 concentration levels investigated. As can be seen from Figure 4, the dispersion of the results is the lowest for the 22 mg/mL concentration level, leading to the best repeatability and intermediate precision values. However, the other concentration levels repeatability and intermediate precision values are still very satisfactory and never exceed 1.4 % as shown in Table 3.

Table 3 – ICH Q2(R1) validation criteria of the NIR method.

	Concentration level (mg/mL)	Mean introduced concentration (mg/mL)	Relative bias (%)	
Trueness	16	15.9	-0.1	
	18	18.2	0.1	
	20	19.7	0.1	
	22	22.0	0.1	
	24	24.1	0.9	
	Concentration level (mg/mL)	Mean introduced concentration (mg/mL)	Repeatability (RSD %)	Intermediate precision (RSD %)
Precision	16	15.9	1.1	1.4
	18	18.2	1.3	1.3
	20	19.7	1.0	1.2
	22	22.0	0.9	0.9
	24	24.1	1.4	1.4
	Concentration level (mg/mL)	Mean introduced concentration (mg/mL)	Relative β-Expectation tolerance limits (%)	
Accuracy	16	15.9	[-3.5 , 3.2]	
	18	18.2	[-2.9 , 3.1]	
	20	19.7	[-2.8 , 3.1]	
	22	22.0	[-1.8 , 2.1]	
	24	24.1	[-2.3 , 4.0]	
Limits of quantification (LOQ)		Lower LOQ (mg/mL)	Upper LOQ (mg/mL)	
		15.9	24.1	

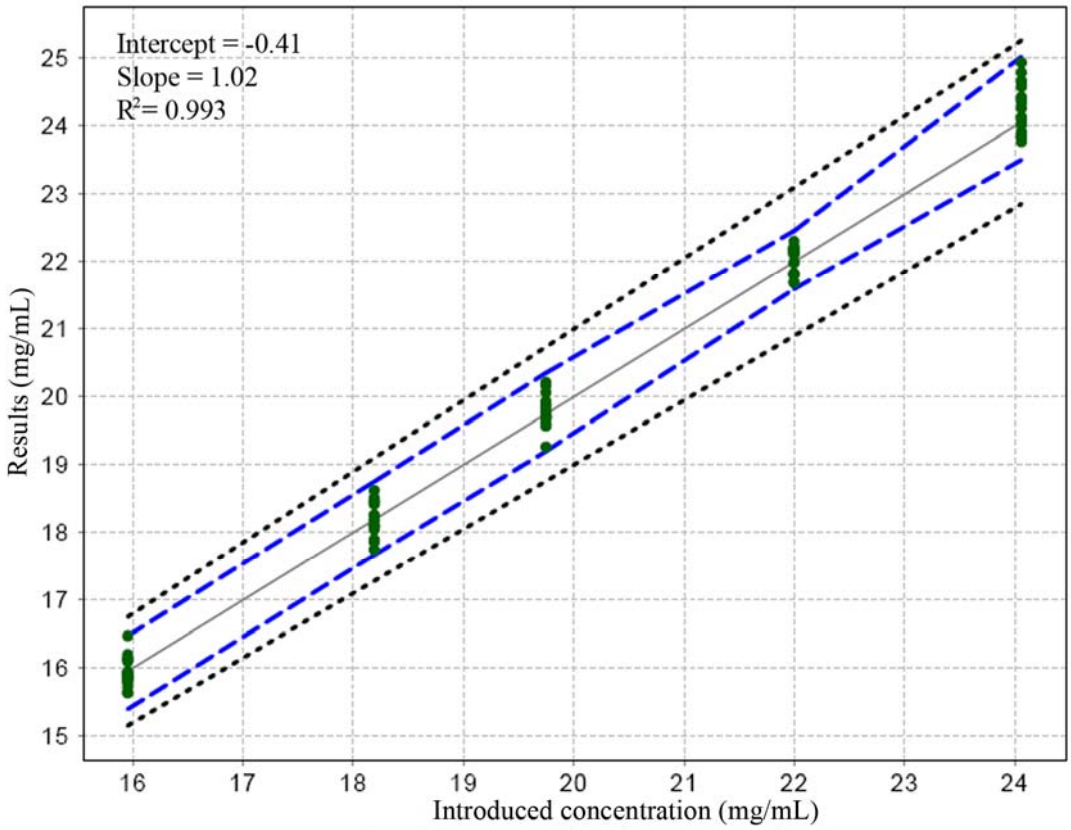

Fig. 5 – Linear profile of the NIR model. The dashed limits on this graph correspond to the accuracy profile, i.e. the β-expectation tolerance limits expressed in absolute values. The dotted curves represent the acceptance limits at ±5 % expressed in the concentration unit. The continuous line is the identity line y = x.

The linear profile of the prediction model is shown in Figure 5. A linear model was fitted on the calculated concentrations of the validation standards for all series as a function of the introduced concentration. The intercept, the slope and the R^2 values are also presented in Figure 5. The slope and intercept are close to 1 and 0 respectively confirming the absence of proportional and constant systematic error of the model. The linearity of the results obtained by the NIR method for the 16-24 mg/mL concentration levels is demonstrated since the β-expectation tolerance limits were included in the absolute acceptance limits.

3.4 Uncertainty assessment of the NIR method

The uncertainty characterizes the dispersion of the values that could reasonably be attributed to the measurand [27,28]. Several uncertainty results were generated and are present in Table 4: the uncertainty of bias of the method at each concentration level of the validation standard, the uncertainty which combines the uncertainty of the bias with the uncertainty of the method obtained during the validation step, ie. the intermediate precision standard deviation, and the expanded uncertainty which equals to the uncertainty

multiplied by a coverage factor *k* = 2 representing an interval around the results where the unknown true value can be observed with a confidence level of 95 % [29,30]. In addition, the relative expanded uncertainties with the corresponding introduced concentrations are not higher than 3 %, which means that with a confidence level of 95 %, the unknown true value is located at a maximum of ± 3 % around the measured results.

Table 4 – NIR method: estimates of measurements uncertainties related to the acetaminophen concentration in the syrups at each concentration level investigated.

Concentration level (mg/mL)	Mean introduced concentration (mg/mL)	Uncertainty of the bias (mg/mL)	Uncertainty (mg/mL)	Expanded uncertainty (mg/mL)	Relative expanded uncertainty (%)
16	15.9	0.08	0.23	0.47	2.9
18	18.2	0.07	0.26	0.51	2.8
20	19.7	0.09	0.25	0.51	2.6
22	22.0	0.05	0.20	0.41	1.9
24	24.1	0.08	0.36	0.72	3.0

3.5 NIR monitoring of API concentration changes in syrups

The ability of the validated NIR method to monitor changes in API concentration was tested with 2 mixing experiments. The syrups used all belonged to the external validation set. First, 5 mL fractions of a 24 mg/mL syrup were added to a 15 mg/mL syrup to manufacture a 20 mg/mL syrup. The mixture was all the time under magnetic agitation. A NIR spectrum was acquired after each fraction addition. Secondly, the same type of experiment was performed except that 2 mL fractions of the syrup basis were added to a 24 mg/mL syrup to manufacture a 15 mg/mL syrup. Theoretical syrup concentrations were calculated to compare them with the NIR predictions.

From Figure 6, it can be observed that the NIR predictions agree quite well with the theoretical concentration calculations, taking into account the uncertainty of the NIR method.

The above experiments clearly show that the monitoring ability of such NIR method could be used to prevent the risk to obtain out of specification products. Even though the present study was performed in a laboratory scale, the authors believe that the present methodology could be transposed in a real manufacturing environment while taking care of

additional challenges such as the interfacing and advanced probe cleaning procedures. Applied before the final packaging steps, such method could be the first step towards a real time release quality-based system.

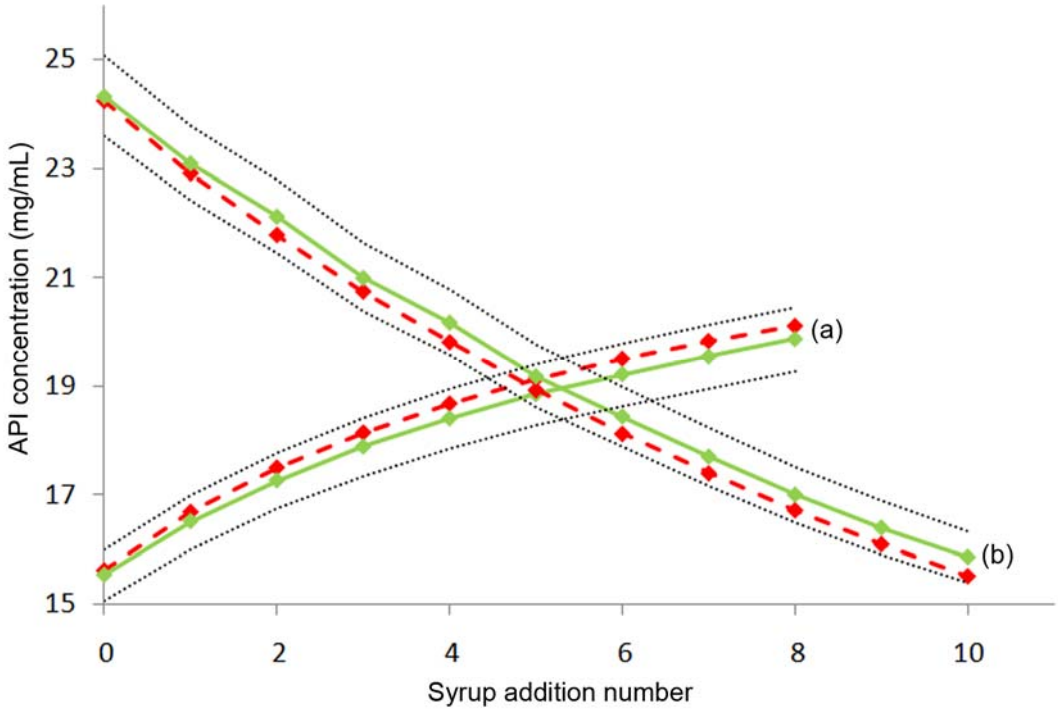

Fig. 6 – Theoretical and NIR monitoring of the API content of (a) a 15 mg/mL API syrup, (b) a 24 mg/mL API syrup while addition of (a) a 24 mg/mL syrup and (b) the syrup basis. The green continuous lines and the red discontinuous lines represent respectively the NIR and the theoretical results. The dotted lines represent the ± 3 % uncertainty of the NIR method.

4. Conclusions

A robust NIR model able to quantify acetaminophen in a low-dose pharmaceutical syrup formulation (2 % (w/v)) was developed.

The model was successfully validated for an active content ranging from 16 to 24 mg/mL using an external validation set. The RMSEP value of the model suggested the overall model accuracy. The accuracy profile on the validation results demonstrated the good accuracy of the results generated by the model all over the investigated API range. Indeed, based on the calculated tolerance interval, each future result will be included within the ±5 % acceptance limits with a probability of at least 95 %.

Finally, it was shown that the developed method is able to monitor in real time the API content of laboratory scale pharmaceutical syrups. Consequently, the present method

transposed in the manufacturing line could be used to monitor the syrups API concentrations. The information provided by this monitoring system may eventually reduce the risk to obtain out of specification products. Applied to the manufacturing line, such method could be one key element towards a real-time release quality system-based.

References

[1] United States Food and Drug Administration (FDA), Guidance for Industry PAT-A Framework for Innovative Pharmaceutical Manufacturing and Quality Assurance, FDA, 2004.

[2] D.A. Burns, E.W. Ciurczak, Handbook of Near-Infrared Analysis, vol. 35, 3rd ed., CRC Press, New York, 2008.

[3] J. Luypaert, D.L. Massart, Y. Vander Heyden, Near-infrared spectroscopy applications in pharmaceutical analysis, Talanta 72 (2007) 865-883.

[4] Y. Roggo, P. Chalus, L. Maurer, C. Lema-Martinez, A. Edmond, N. Jent, A review of near infrared spectroscopy and chemometrics in pharmaceutical technologies, J. Pharm. Biomed. Anal. 44 (2007) 683-700.

[5] C. Bodson, W. Dewé, Ph. Hubert, L. Delattre, Comparison of FT-NIR Transmission and UV-vis spectrophotometry to follow the mixing kinetics and to assay low-dose tablets containing riboflavin, J. Pharm. Biomed. Anal. 41 (2006) 783-790.

[6] J.J. Moes, M.M. Ruijken, E. Gout, H.W. Frijlink, M.I. Ugwoke, Application of process analytical technology in tablet process development using NIR spectroscopy: Blend uniformity, content uniformity and coating thickness measurements, Int. J. Pharm. 357 (2008) 108-118.

[7] S.H. Tabasi, V. Moolchandani, R. Fahmy, S.W. Hoag, Sustained release dosage forms dissolution behavior prediction: a study of matrix tablets using NIR spectroscopy, Int. J. Pharm. 382 (2009) 1-6.

[8] W. Li, L. Bagnol, M. Berman, R. A. Chiarella, M. Gerber, Applications of NIR in early stage formulation development. Part II. Content uniformity evaluation of low dose tablets by principal component analysis, Int. J. Pharm. 380 (2009) 49-54.

[9] S.S. Rosa, P.A. Barata, J.M. Martins, J.C. Menezes, Development and validation of a method for active drug identification and content determination of ranitidine in pharmaceutical products using near-infrared reflectance spectroscopy: A parametric release approach, Talanta 75 (2008) 725-733.

[10] J. Mantanus, E. Ziémons, P. Lebrun, E. Rozet, R. Klinkenberg, B. Streel, B. Evrard, Ph. Hubert, Active content determination of non-coated pharmaceutical pellets by near infrared spectroscopy: Method development, validation and reliability evaluation, Talanta 80 (2010) 1750-1757.

[11] J. Mantanus, E. Ziémons, P. Lebrun, E. Rozet, R. Klinkenberg, B. Streel, B. Evrard, Ph. Hubert, Moisture content determination of pharmaceutical pellets by near infrared spectroscopy: Method development, validation and reliability evaluation, Anal. Chim. Acta 642 (2009) 186-192.

[12] J. Rantanen, E. Räsänen, O. Antikainen, J.-P. Mannermaa, J. Yliruusi, In-line moisture measurement during granulation with a four-wavelength near-infrared sensor: an

evaluation of process-related variables and a development of non-linear calibration model, Chemo. Intel. Lab. Syst. 56 (2001) 51-58.

[13] N. Sandler, J. Rantanen, J. Heinämäki, M. Römer, M. Marvola, J. Yliruusi, Pellet manufacturing by extrusion-spheronization using Process Analytical Technology, AAPS PharmSciTech. 6 (2) (2005) Article 26.

[14] M. Blanco, R. Cueva-Mestanza, A. Peguero, Controlling individual steps in the production process of paracetamol tablets by use of NIR spectroscopy, J. Pharm. Biomed. Anal. 51 (2010) 797-804.

[15] A. Eustaquio, M. Blanco, R.D. Jee, A.C. Moffat, Determination of paracetamol in intact tablets by use of near infrared transmittance spectroscopy, Anal. Chim. Acta 383 (1999) 283-290.

[16] M. Ito, T. Suzuki, S. Yada, H. Nakagami, H. Teramoto, E. Yonemochi, K. Terada, Development of a method for nondestructive NIR transmittance spectroscopic analysis of acetaminophen and caffeine anhydrate in intact bilayer tablets, J. Pharm. Biomed. Anal. (2008), doi : 10.1016/j.jpba.2010.04.029

[17] M. Blanco, M. Castillo, A. Peinado, R. Beneyto, Determination of low analyte concentrations by near-infrared spectroscopy: Effect of spectral pretreatments and estimation of multivariate detection limits, Anal. Chim. Acta 581 (2007) 318-323.

[18] P. Chalus, Y. Roggo, S. Walter, M. Ulmschneider, Near-infrared determination of active substance content in intact low-dosage tablets, Talanta 66 (2005) 1294-1302.

[19] International Conference on Harmonization (ICH) of Technical Requirements for registration of Pharmaceuticals for human Use, Topic Q2 (R1): Validation of analytical Procedures: Text and Methodology, Geneva, 2005.

[20] International Conference on Harmonisation (ICH) of technical requirements for registration of pharmaceuticals for human use, Topic Q9: Quality risk management, Geneva, 2005.

[21] Ph. Hubert, J.J. Nguyen-Huu, B. Boulanger, E. Chapuzet, P. Chiap, N. Cohen, P.A. Compagnon, W. Dewé, M. Feinberg, M. Lallier, M. Laurentie, N. Mercier, G. Muzard, C. Nivet, L. Valat, Harmonization of strategies for the validation of quantitative analytical procedures: A SFSTP proposal-part I, J. Pharm. Biomed. Anal. 36 (2004) 579-586.

[22] Ph. Hubert, J.J. Nguyen-Huu, B. Boulanger, E. Chapuzet, P. Chiap, N. Cohen, P.A. Compagnon, W. Dewé, M. Feinberg, M. Lallier, M. Laurentie, N. Mercier, G. Muzard, C. Nivet, L. Valat, E. Rozet, Harmonization of strategies for the validation of quantitative analytical procedures: A SFSTP proposal-part II, J. Pharm. Biomed. Anal. 45 (2007) 70-81.

[23] A. Bouabidi, E. Rozet, M. Fillet, E. Ziemons, E. Chapuzet, B. Mertens, R. Klinkenberg, A. Ceccato, M. Talbi, B. Streel, A. Bouklouze, B. Boulanger, Ph. Hubert, Critical analysis of several analytical method validation strategies in the framework of the fit for purpose concept, J. Chrom. A. 1217 (2010) 3180-3192.

[24] Acetaminophen Capsules, United States Pharmacopoeia USP32NF27, The United States Pharmacopeial Convention, Rockville, 2009, 1389.

[25] European Medicines Agency, draft: Guideline on the use of near infrared spectroscopy by the pharmaceutical industry and the data requirements for new submissions and variations, EMEA/CHMP/CVMP/QWP/17760/2009 Rev 1.

[26] http://wiki.eigenvector.com/index.php?title=Using_Cross-Validation (26/02/10).

[27] Analytical Methods Committee, Uncertainty of measurement: implication of its use in the Analytical Science, Analyst 120 (1995) 2303-2308.

[28] Eurachem/Citac guide Quantifying the uncertainty in analytical measurement, second ed., 2000.
[29] CB EA-4/16, EA Guidelines on the Expression of Uncertainty in Quantitative Testing, 2004, http://www.european-accreditation.org.
[30] R.D. Marini, P. Chiap, B. Boulanger, S. Rudaz, E. Rozet, J. Crommen, Ph. Hubert, LC method for the determination of R-timolol in a S-timolol maleate : Validation of its ability to quantify and uncertainty assessment, Talanta 68 (2006) 1166-1175.

Section III.2.2.

Solid formulation: Building the quality into pellet manufacturing environment

Section III.2.2.1.

Active content determination of non-coated pharmaceutical pellets by near infrared spectroscopy: Method development, validation and reliability evaluation

J. Mantanus, E. Ziemons, P. Lebrun, E. Rozet, R. Klinkenberg, B. Streel, B. Evrard, Ph. Hubert, Talanta 80 (2010) 1750.

Summary

A robust near infrared (NIR) method able to quantify the active content of pilot non-coated pharmaceutical pellets was developed. A protocol of calibration was followed, involving 2 operators, independent pilot batches of non-coated pharmaceutical pellets and two different NIR acquisition temperatures. Prediction models based on Partial Least Squares (PLS) regression were then carried out. Afterwards, the NIR method was fully validated for an active content ranging from 80 to 120 % of the usual active content using new independent pilot batches to evaluate the adequacy of the method to its final purpose. Conventional criteria such as the R^2, the Root Mean Square Error of Calibration (RMSEC), the Root Mean Square Error of Prediction (RMSEP) and the number of PLS factors enabled the selection of models with good predictive potential. However, such criteria sometimes fail to choose the most fitted for purpose model. Therefore, a novel approach based on accuracy profiles of the validation results was used, providing a visual representation of the actual and future performances of the models. Following this approach, the prediction model using signal pre-treatment Multiplicative Scatter Correction (MSC) was chosen as it showed the best ability to quantify accurately the active content over the 80-120 % active content range. The reliability of the NIR method was tested with new pilot batches of non-coated pharmaceutical pellets containing 90 and 110 % of the usual active content, with blends of validation batches and industrial batches. All those batches were also analyzed by the HPLC reference method and relative errors were calculated: the results showed low relative errors in full accordance with the results obtained during the validation of the method, indicating the reliability of the NIR method and its interchangeability with the HPLC reference method.

1. Introduction

Near infrared (NIR) spectroscopy belongs to vibrational spectroscopy and covers a region between 14000 and 4000 cm^{-1}. Vibrations like overtones and combination of fundamental vibration of hydrogen bonds such as C-H, N-H, O-H and S-H give birth to the NIR spectrum. Such vibrations lead to large overlapping bands which contain both physical and chemical information. Therefore, chemo-metrical tools such as mathematical pretreatments and regression methods are required to extract the significant information [1-3].

FDA's Process Analytical Technology (PAT) is an analytical concept which focuses on the real time monitoring of each critical step of a manufacturing process leading to a better understanding of the process itself. Consequently, as the process understanding improves, PAT gives the opportunity to detect the endpoints inherent in a process and so to optimize it in order to lower the risk of losing batches. PAT may also reduce the batch release time as most of the conformity analyses are realized during the manufacturing process itself [4-5].

An analytical tool such as PAT requires analyzers able to perform fast data acquisition without any sample preparation and compatible with the use of optical fibers. Thanks to its own features, NIR spectroscopy matches the PAT requirements: it has already been used many times in this concept [6-10]. Indeed, once you overcome the calibration phase which takes into account a reference method as well as environmental constrains, near infrared spectroscopy offers many advantages such as suppression of sample preparation and/or destruction and the use of optical fibres allows online analyses [1-3]. Moreover, the calibration set does not need to be updated or rebuilt as long as there is an agreement between the validation results and the Quality Controls (QCs) results.

The more complex is a manufacturing process, the more interesting becomes the PAT approach. An example of a complex manufacturing process associated with PAT can be found in the pellets manufacturing field [11-12]. Indeed, pellets fabrication can be split into plenty of crucial steps, including successively: weighting, blending, extrusion, spheronization, drying, coating, and a last drying step. For such a complex process, it would be interesting to evaluate the active content of the non-coated pellets before beginning the coating and final drying steps. The active determination is usually performed using time consuming and sample destructive HPLC methods. NIR spectroscopy can replace those tedious methods: it has already been used in different fields such as the pharmaceutical [9; 13-15], the food [16-17] and the fuel industries [18].

To give laboratories guarantees about the accuracy of a new method, validation must be carried out, as defined by the ICH Q2(R1) regulatory documents [19]. Based on β-expectation tolerance intervals, the accuracy profile makes possible a visual and reliable

representation of the actual and future performances of the analytical method [20-22]. This novel approach facilitates the analytical interpretation and enables a better risk management [23-29]. In addition, the accuracy profile integrates all the useful required validation criteria, such as accuracy, trueness, precision, quantitative limits and linearity [20-22].

The aim of the present study was first to develop a reliable near infrared method able to determine the active content of non-coated pilot pharmaceutical pellets. The second aim was to fully validate the method for an active content ranging from 80 to 120 % of the usual active content. The final aim was to test the method reliability with new pilot batches containing 90 and 110 % of the usual active content, blends of pilot batches used for the validation and industrial batches.

2. Materials and methods

2.1. Chemicals

2.1.1 Calibration samples

Pilot batches of non-coated pharmaceutical pellets were manufactured at Galephar Research Center M/F. The usual targeted formulation contains 57 % w/w of Active Pharmaceutical Ingredient (API) T200999, this formulation will be further considered as the 100 % active content formulation. For the calibration set, pilot batches containing 46 and 69 % w/w of API were also manufactured (80 and 120 % API formulations). Three independent batches were manufactured per formulation type.

2.1.2 External validation samples

New pilot batches of non-coated pharmaceutical pellets were manufactured at Galephar Research Center M/F. The same formulations as for the calibration samples were manufactured: 80, 100 and 120 % API formulations, three batches per formulation type.

2.1.3 Reliability evaluation samples

To evaluate the reliability of the developed NIR method, new pilot batches containing 52 and 63 % w/w of API were also manufactured at Galephar Research Center M/F (90 and 110 % API formulations, 3 batches per formulation type). Industrials batches of non-coated pellets were also provided by Galephar. Besides, blends of batches belonging to the validation sets were made to obtain active content formulations between 80 and 120 %.

2.2. FT-NIR equipment and software

Non-coated pharmaceutical pellets were analyzed with a multipurpose analyzer Fourier transform near infrared spectrometer (MPA, Bruker Optics, Ettlingen, Germany) equipped with a semi-conductor room temperature sulfide lead (RT-PbS) detector. The NIR spectra of the samples put in vials were acquired using the integrating sphere module of the spectrometer which allows reflectance measurement of a 18 mm diameter sample area. An internal computer-controlled reference wheel enables an automatic background spectrum acquisition without the need to remove the sample from the integrating sphere window. The spectra were collected with the Opus software 6.5 (Bruker Optics). Each spectrum was the average of 32 scans and the resolution was 8 cm^{-1} over the range from 12500 to 3600 cm^{-1}.

2.3. Reference method

A confidential HPLC method previously developed and validated by Galephar was used to determine the amount of API in batches of non-coated pharmaceutical pellets.

2.4. Near infrared method: calibration and validation protocol

An experimental protocol was followed for the calibration and validation steps to develop and to validate a robust near infrared model. This protocol included batches, operators, days and temperature conditions as sources of variability for the calibration as well as for the validation steps. Three concentration levels of active ingredients were evaluated.

NIR spectra of the pellets samples were first recorded before performing one active content measurement per vial using the reference method. Three different NIR measurements (i.e. replicates) of the same sample were performed. After each NIR acquisition, the vial was gently shaken to completely evaluate the sample.

2.5. Data treatment

The Opus software 6.5 (Bruker Optics) has been used to carry out the signal processing of the near infrared spectra.

Using the QUANT package of the Opus 6.5 software, prediction models based on PLS (Partial Least Squares) regression using stratified cross-validation were carried out with the calibration set and tested with the validation set. Each cross-validation fold contains the six spectra associated with a sample.

In PLS methods the regressions are computed with least squares algorithms. The goal of the PLS is to establish a linear link between two matrices, the spectral data X and the reference values Y (which can be of dimension above one). This technique works both on X and Y in order to find out the variables in the X matrix that will best describe the Y matrix through linear combinations of wavelengths, called factors, which describe best the studied properties [2].

Cross-validation is a classical way of building a model [30]. The first step consists in removing a group of samples from the calibration set. If the group of samples contains only one sample, the cross-validation is called leave-one-out cross-validation. Based on the remaining samples, a model is then built and tested with the removed samples. Afterwards, the removed samples are put back in the calibration set while a new group of samples is removed. A new model is then calculated and tested. The operations described above are repeated until all the samples from the calibration set have been removed once [3].

Two different types of data pretreatment were used in our study: Standard Normal Variate (SNV) and Multiplicative Scatter Correction (MSC) pre-treatments. The first reduces mathematically the differences between the baselines of the spectra and then normalizes them while the second reduces the effect of scattered light on diffuse reflection NIR spectra [3].

The calculation of the accuracy profiles based on the validation set results were realized with e.noval V2.1 (Arlenda, Liège, Belgium).

3. Results and discussion

3.1 Calibration

In order to meet the requirements of routine analyses and to guarantee the robustness of the NIR method, the calibration was designed focusing on different parameters. First, prediction models were built using independent pilot batches of non-coated pharmaceutical pellets. Indeed, once a batch of pharmaceutical pellets was manufactured, the mixer-extruder and the spheronizer were successively dismantled, cleaned and put together again before the manufacturing of a new batch. As it is difficult to restore the exact manufacturing conditions of the previous batch, each batch is an independent batch. Secondly, as different operators are likely to use the NIR method, the calibration protocol was designed for two operators. In addition, as temperature changes can induce variations in the spectral response, samples were scanned under two different temperature conditions (25 and 35 °C).

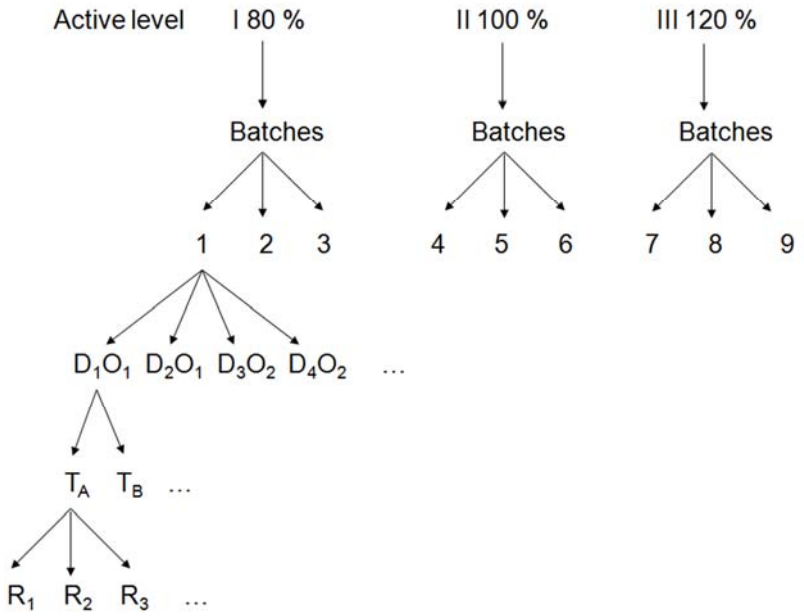

Fig. 1 – Schematic illustration of the calibration protocol. D means *day*, O means *operator*. T_A: the sample is measured under ambient temperature conditions (25°C). T_B: the sample is measured under high temperature conditions (35°C). R_1, R_2 and R_3 represent different NIR measurements of the same sample.

As shown in Figure 1, the calibration was designed using three different active content formulations: 80, 100 and 120 % formulations. There are 3 independent pilot batches of non-coated pharmaceutical pellets per formulation type. All the calibration batches were analyzed by NIR spectroscopy and the reference method by the two operators two times: operator 1 and 2 made their own series on day 1, day 2 and day 3, day 4 respectively. The NIR measurements were realized under two different temperature conditions (25 and 35 °C) and in triplicate. For example, on day 1, operator 1 took a sample from the 9 batches of non-coated pharmaceutical belonging to the calibration set. Those samples were analyzed two times in triplicate by NIR spectroscopy: one first triple measurement when the sample was thermostated at 25 °C and one second triple measurement when the sample was the sample was thermostated at 35 °C. Afterwards, all the samples were analyzed once by the HPLC reference method. For one series, a total number of 54 NIR spectra were recorded and 9 reference measurements were carried out. As the calibration is built with 4 independent series of measurements, the entire calibration set contains a total of 216 NIR spectra and 36 reference measurements.

3.2 Validation

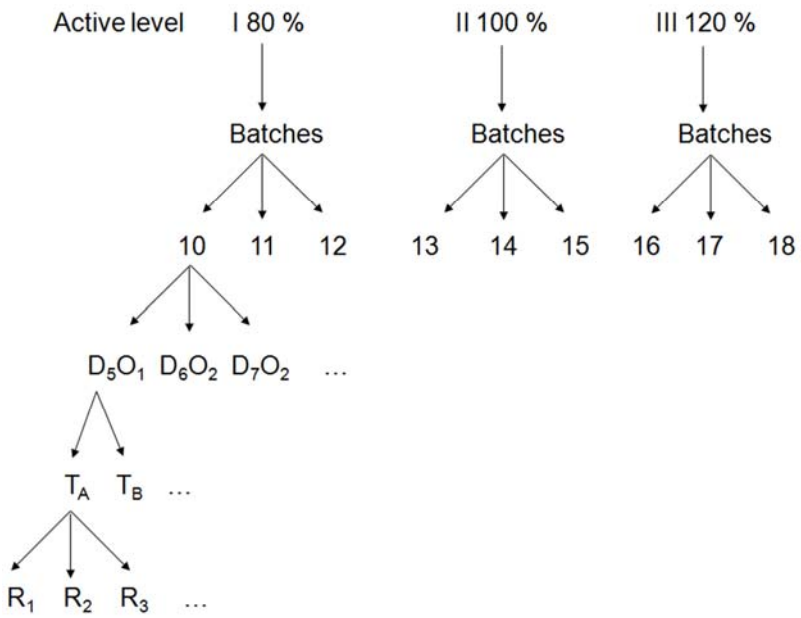

Fig. 2 – Schematic illustration of the validation protocol. D means *day*, O means *operator*. T_A: the sample is measured under ambient temperature conditions (25°C). T_B: the sample is measured under high temperature conditions (35°C). R_1, R_2 and R_3 represent different NIR measurements of the same sample.

Figure 2 illustrates the validation protocol that comprises the same type of formulations as in the calibration protocol: 80, 100 and 120 % active content formulations. There are also 3 independent batches of non-coated pharmaceutical pellets per formulation type. All the validation batches were analyzed by NIR spectroscopy and the reference method by the two operators: one time by operator 1 on day 5 and 2 times by operator 2 on day 6 and day 7. The NIR measurements were realized under two different temperature conditions (25 and 35 °C) and in triplicate. For example, on day 5, operator 1 took a sample from the 9 batches of non-coated pharmaceutical belonging to the validation set. In the same way as for the calibration set, those samples were analyzed two times in triplicate by NIR spectroscopy: one first triple measurement when the sample was thermostated at 25 °C and one second triple measurement when the sample was the sample was thermostated at 35 °C. Afterwards, all the samples were analyzed one time by the HPLC reference method. For one series, a total of 54 NIR spectra were recorded and 9 reference measurements were taken. Consequently, as the validation is built with 3 series of measurements, the entire validation set contains a total of 162 NIR spectra and 27 reference measurements.

3.3 Validation results of the NIR method

Depending on the type of mathematical pre-treatment applied, the spectral range selected and the number of PLS factors chosen, a large amount of models can be generated. Classically, the models with the biggest predictive potential can be selected according to conventional criteria such as the R^2, the number of PLS factors, the Root Mean Square Error of Calibration (RMSEC) and the Root Mean Square Error of Prediction (RMSEP). Table 1 shows the conventional parameters of three potentially interesting models.

Table 1 – Type of spectral pre-treatment, R^2, spectral range selected, number of PLS factors, RMSEC and RMSEP of different models.

Model	(a)	(b)	(c)
Pre-treatment	None	SNV	MSC
R^2	0.991	0.994	0.994
Spectral range selected (cm^{-1})	7502.2-6098.2 5450.2-4597.7	12493.3-7498.3 6102-5774.2 4601.6-4246.7	12493.3-7494.5 6102-5774.2 4917.9-4543.7
Number of PLS factors	7	4	3
RMSEC (%)	1.18	0.95	1.02
RMSEP (%)	2.15	1.37	1.28

As the R^2 of the three models are very close, it does not allow any clear differentiation between the models.

Concerning the spectral regions selected, it can be seen from Figure 3 that the spectral regions selected for the 3 models are related to the pellets active content.

Regarding the number of PLS factors, the bigger the number of PLS factors selected is, the more important is the risk to overfit the model. Hence, the (a) model seems to use too many factors to predict the active content with a good robustness.

Considering RMSEC and RMSEP, the (b) and (c) model seem to be slightly better than the (a) model: their RMSEC and RMSEP are the smallest. However, it is impossible to select the model which is the most fitted for purpose. Moreover, those criteria do not allow the assessment of the model ability to quantify accurately over the investigated active content range.

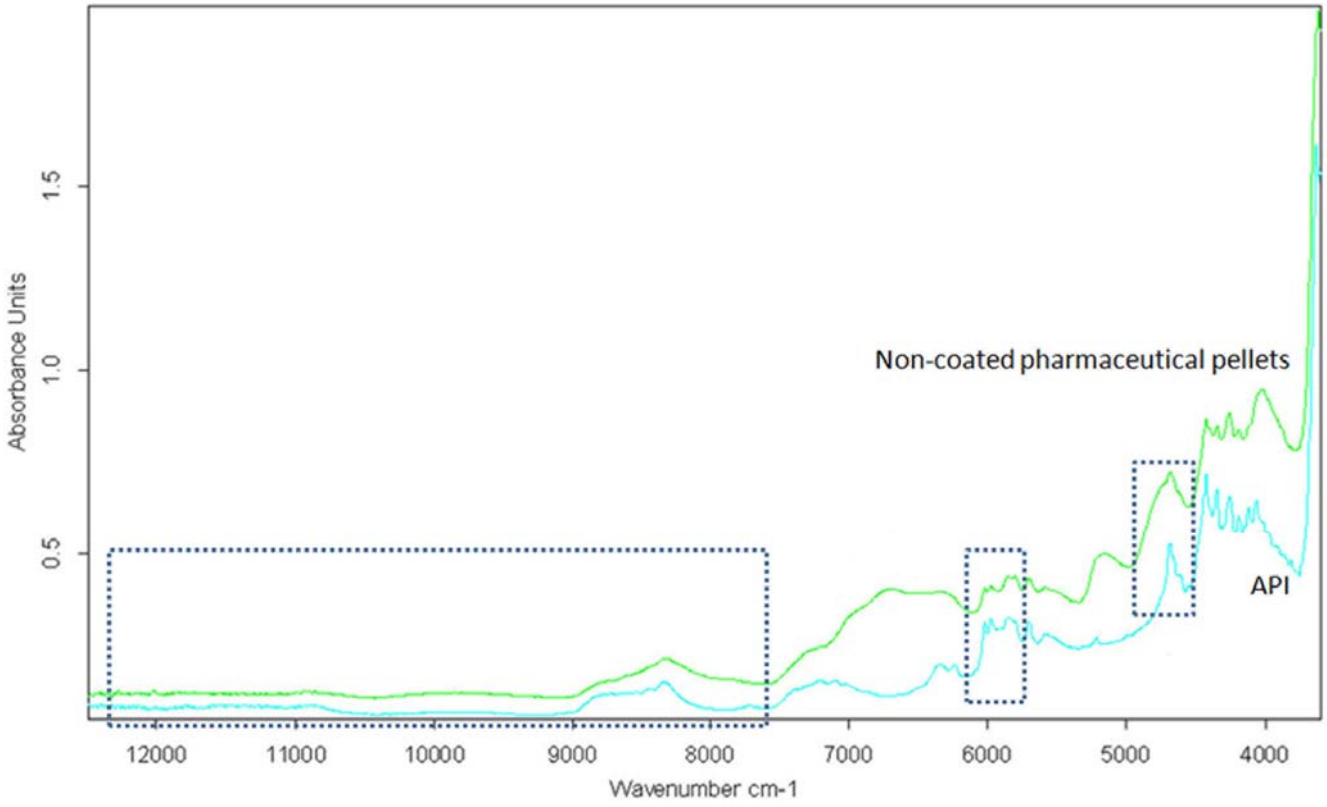

Fig. 3 – NIR spectra of the non-coated pharmaceutical pellets and the API. The spectral areas selected for the (c) model are highlighted.

Consequently, accuracy profiles based on tolerance intervals were used as a complementary decision tool to evaluate the models predictive performances. Tolerance intervals have the advantage to convey a predictive ability to the accuracy profile: for example, 95 % of the future results will be included within a 95 % tolerance interval. In opposition to a confidence interval which only takes into consideration the existing results but does not guarantee that the future results (routine results for example) will be situated within the interval.

Hubert et al. [20-22] showed that the accuracy profile which uses the total error concept meets the ICH Q2(R1) guideline requirements. Facing the confusion found between accuracy and trueness in the ICH document, it seems important to remind that accuracy represents the total error concept which is the sum of the trueness (systematic error) and precision (random error).

Figure 4 shows accuracy profiles based on the validation results obtained with the (a), (b) and (c) model respectively. From this Figure, it can be observed that the active content of validation samples belonging to the same concentration level is identical: it is caused by the alignment on the mean concentration, which is necessary to calculate a variance (for repeatability and intermediate precision estimates).

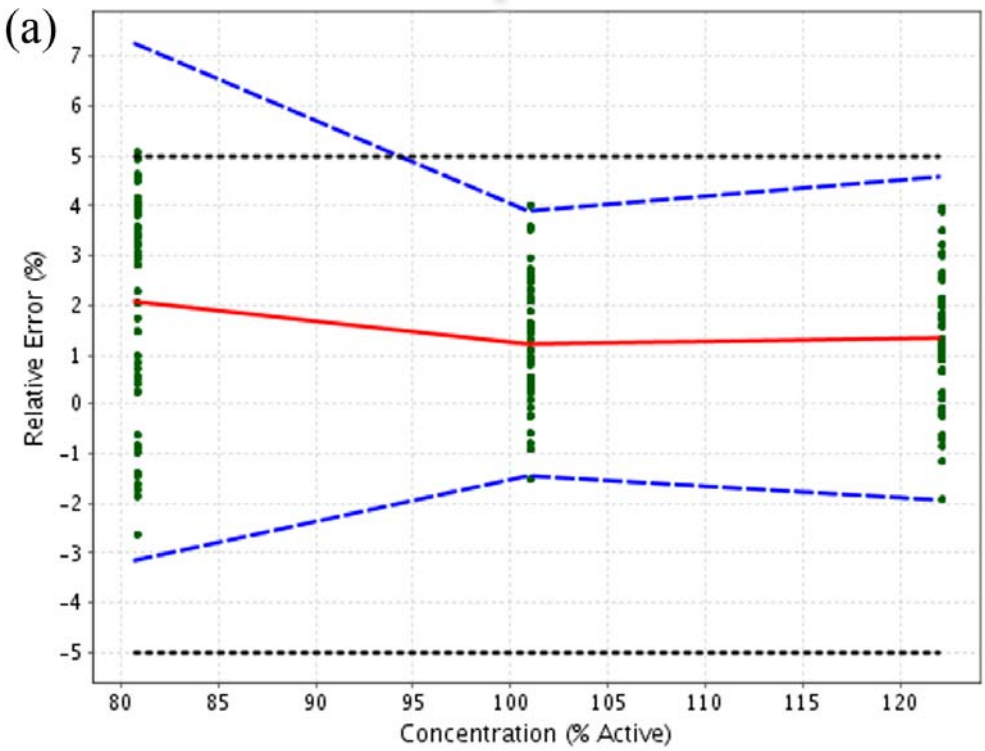
(a)
Relative Error (%)
7
6
5
4
3
2
1
0
-1
-2
-3
-4
-5
80
85
90
95
100
105
110
115
120
Concentration (% Active)

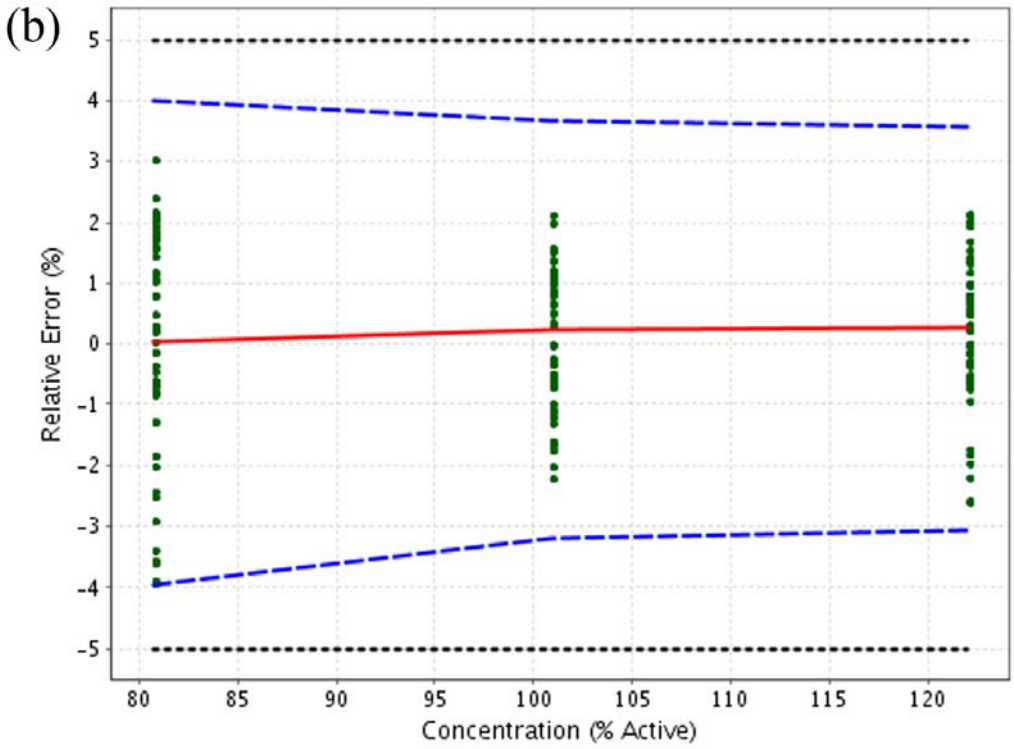
(b)
Relative Error (%)
5
4
3
2
1
0
-1
-2
-3
-4
-5
80
85
90
95
100
105
110
115
120
Concentration (% Active)

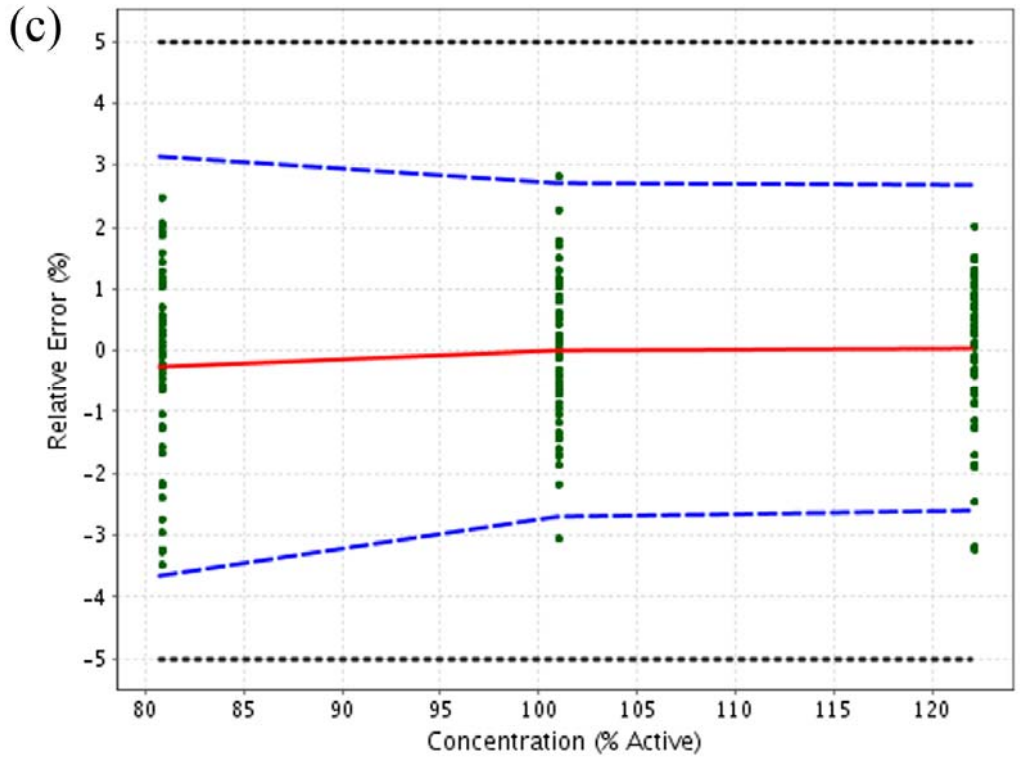

Fig. 4 – (a), (b) and (c) - Accuracy profiles based on the validation results of the (a), (b) and (c) models. The plain line is the relative bias, the dashed lines are the β-expectations tolerance limits (β=95%) and the dotted lines represent the acceptance limits (± 5%).

As this study focuses on the determination of the active content in a pharmaceutical formulation, the acceptance limits were set at ± 5% for the validation of the NIR method while the maximum risk (1-β) to obtain results outside these acceptance limits was set at 5%.

The lower and upper limits of quantification (LLOQ and ULOQ) define the range where an analytical method is able to quantify accurately. They are located where the β-expectation tolerance interval is included within the acceptance limits. If the β-expectation tolerance interval never crosses the acceptance limits, then the LLOQ and ULOQ are located at the beginning and at the end of the active content range investigated.

As can be seen in Figure 4, the (b) and (c) models are able to quantify accurately over all the chosen active content range [80-122 %]. However, the (a) model has a LLOQ of 95 % making this model inaccurate for the 80 % active content level. Moreover, of the 3 models, the (a) model has the most important bias.

Regarding the (b) and (c) models, although 95 % of the future results will be included within the β-expectation tolerance interval which fall in the acceptance limits over the entire active content range, the (c) model is the best fitted for purpose. Indeed, the (b) model β-expectations tolerance limits are closer to the acceptance limits over the entire active

content range than those of the (c) model. Consequently, the NIR method will use the (c) model to determine the active content of the non-coated pharmaceutical pellets.

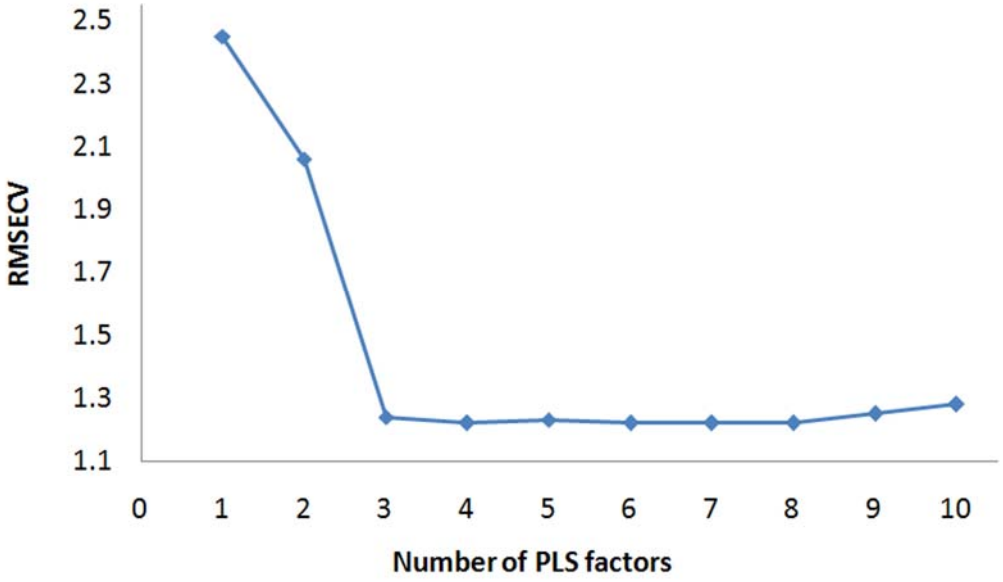

Fig. 5 - (c) model: RMSECV versus the number of PLS factors.

Figure 5 shows the evolution of the (c) model RMSECV according to the number of PLS factors chosen: as there is no significant change of the RMSECV value from 3 PLS factors, this number of PLS factors was selected for the (c) model.

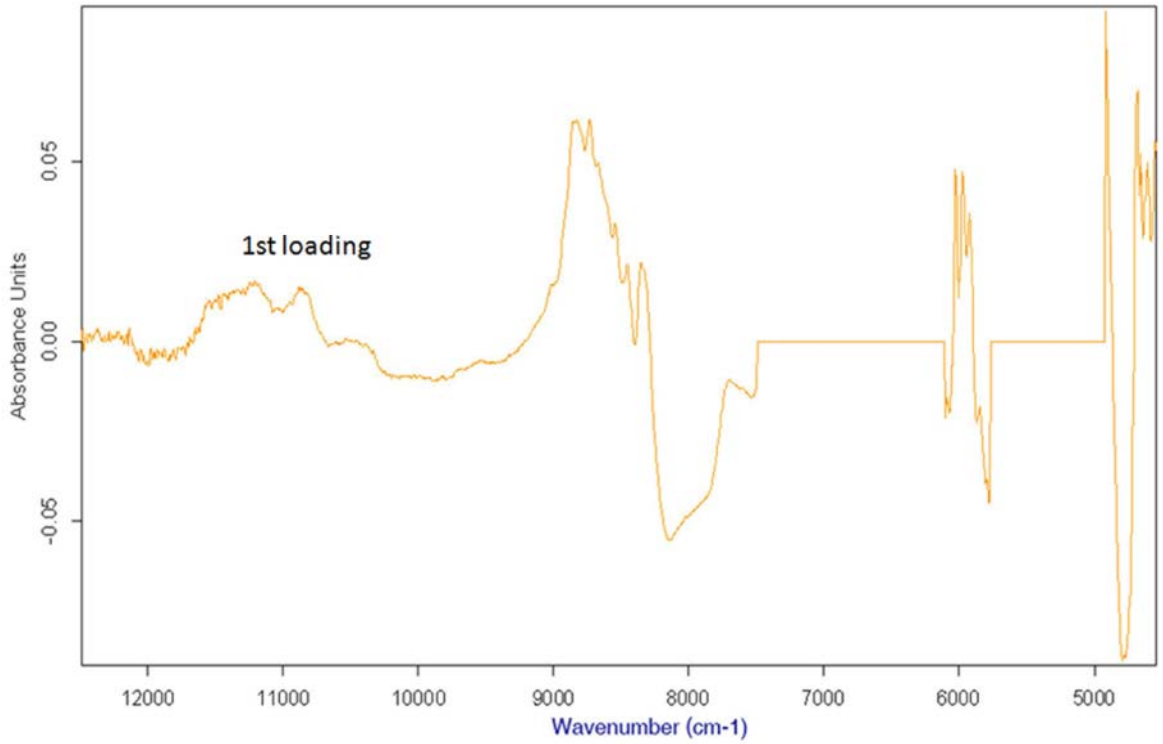

Fig. 6 – (c) model: first loading factor.

The comparison of Figure 3 and the first loadings of the (c) model displayed on Figure 6 confirmed that the spectral area selected were relevant for the determination of the active content.

Table 2 – ICH Q2(R1) validation criteria of the (c) model.

Trueness	Concentration level (% active)	Mean introduced concentration (% active)	Relative bias (%)	
	80 100 120	80.7 100.9 122.0	-0.25 0.00 0.05	
Precision	Concentration level (% active)	Mean introduced concentration (% active)	Repeatability (RSD %)	Intermediate precision (RSD %)
	80 100 120	80.7 100.9 122.0	1.4 1.0 1.0	1.6 1.2 1.2
Accuracy	Concentration level (% active)	Mean introduced concentration (% active)	Relative β-Expectation tolerance limits (%)	
	80 100 120	80.7 100.9 122.0	[-3.65 , 3.14] [-2.70 , 2.71] [-2.59 , 2.68]	
Limits of quantification (LOQ)		Lower LOQ (% active)	Upper LOQ (% active)	
		80.7	122.0	

Table 2 shows the ICH Q2(R1) validation criteria of the (c) model. As seen in the accuracy profile, the bias is stable and points towards zero: the relative bias does not exceed [-0.25%, 0.05%].

The precision of the method was estimated by measuring repeatability and intermediate precision at the three active content levels shown in the validation protocol. The repeatability and intermediate precision are both good for the three levels of active content. As can be observed in the accuracy profile, the 80 % active content level is the worst level for the repeatability and the intermediate precision but this is still very satisfactory.

As shown with the accuracy profile, the accuracy is very good for the entire active content range as the values of the relative β-expectation tolerance limit never exceed [-3.65%, 3.14%].

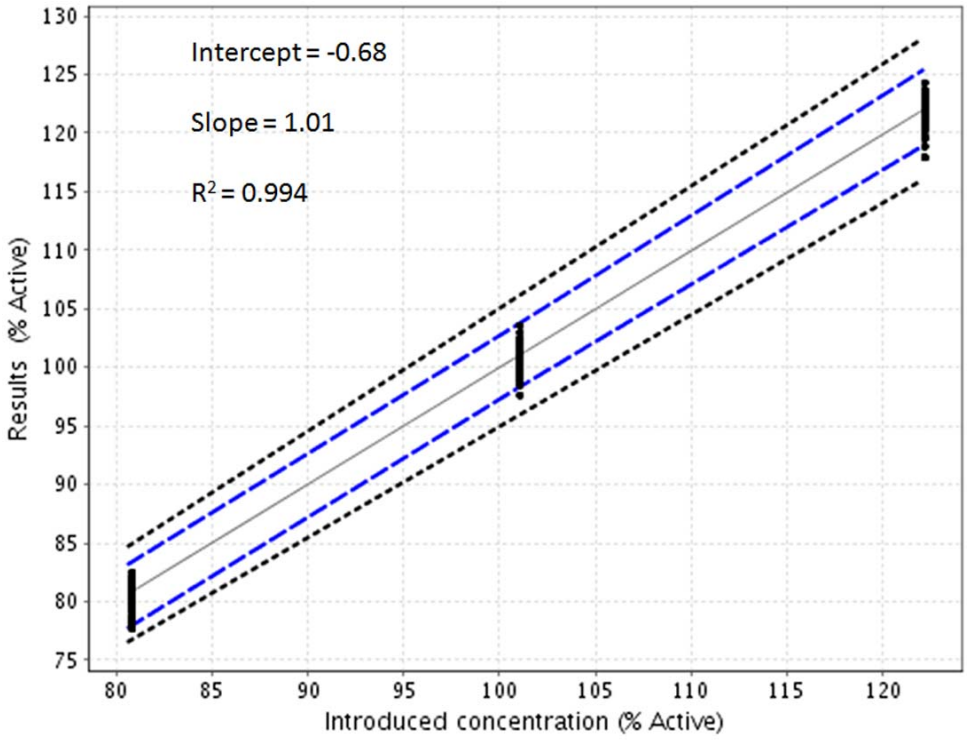

Fig. 7 – Linear profile of the (c) model. The dashed limits on this graph correspond to the accuracy profile, i.e. the β-expectation tolerance limits expressed in absolute values. The dotted curves represent the acceptance limits at ± 5 % expressed in the concentration unit. The continuous line is the identity line y = x.

Figure 7 is showing the linear profile of the (c) model. A linear model was fitted on the calculated concentrations of the validation standards for all series as a function of the introduced concentrations. The intercept, the slope and the R^2 values are also presented in Figure 7. The slope and intercept are close to 1 and 0 respectively confirming the absence of proportional and constant systematic error of the (c) model. The linearity of the method for

the 80-120 % active content range is demonstrated since the β-expectation tolerance limits were included in the absolute acceptance limits. Further, the (c) model reliability was tested with 90 and 110 % active content formulations, providing two additional active content levels to evaluate the NIR method linearity. As can be seen from Figure 8, the linearity was confirmed as the slope and intercept are still close to 1 and 0 respectively.

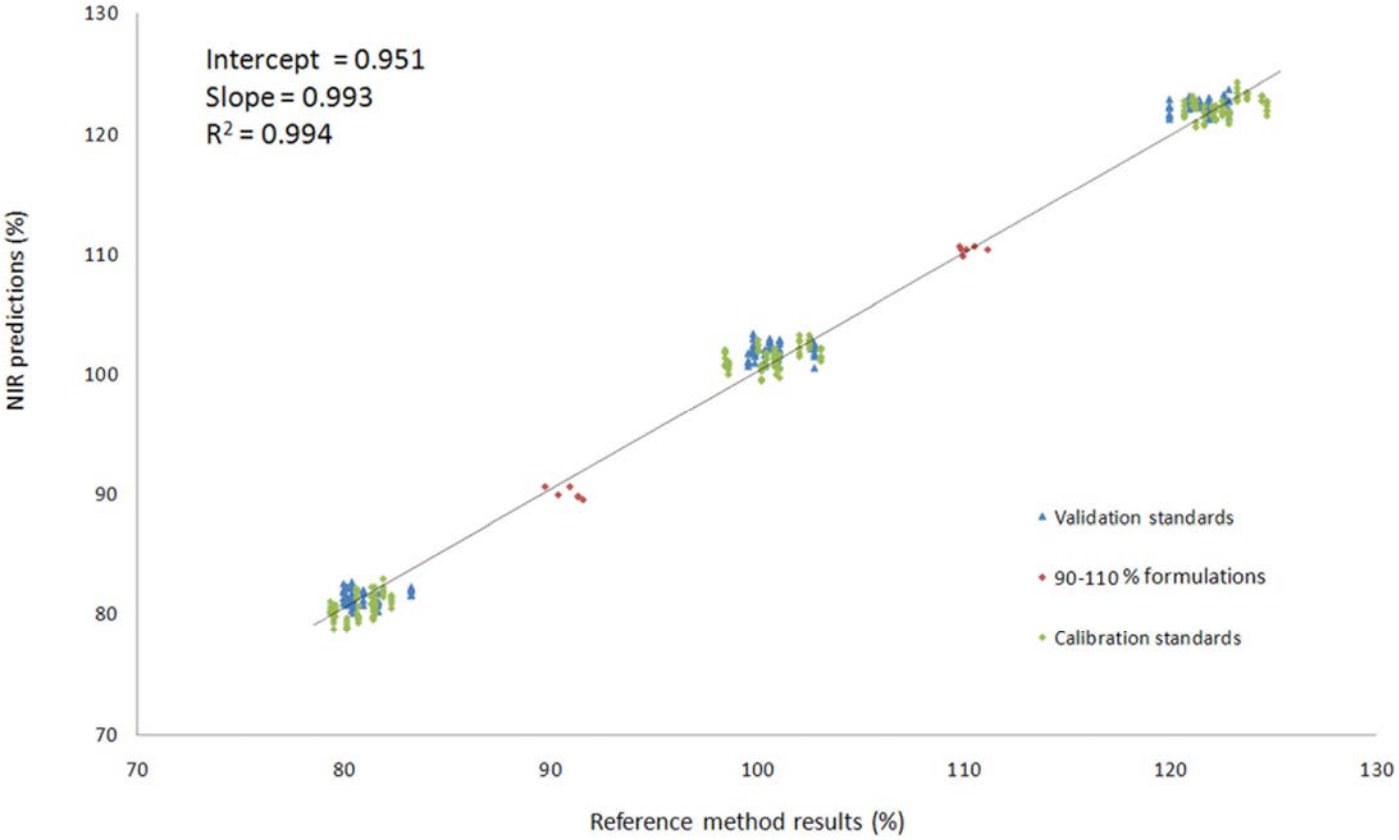

Fig. 8 – (c) model: calibration set, validation set and 90/110 % formulations NIR predictions versus the reference method predictions.

3.5 Uncertainty assessment of the NIR method (c model)

The uncertainty characterizes the dispersion of the values that could reasonably be attributed to the measurand [31-32]. Several uncertainty results were generated and are presented in Table 3: the uncertainty of bias of the method at each concentration level of the validation standard, the uncertainty which combines the uncertainty of the bias with the uncertainty of the method obtained during the validation step, i.e. the intermediate precision standard deviation, and the expanded uncertainty which equals to the uncertainty multiplied by a coverage factor k=2 representing an interval around the results where the unknown true value can be observed with a confidence level of 95% [33-34]. In addition, the relative expanded uncertainties (%) for active content obtained by dividing the corresponding expanded uncertainties with the corresponding introduced concentrations

(Table 3) are not higher than 3.3 %, which means that with a confidence level of 95%, the unknown true value is located at a maximum of ± 3.3 % around the measured result.

Table 3 – Uncertainty of measurements of the (c) model.

Concentration level (% active)	Mean introduced concentration (% active)	Uncertainty of the bias (% active)	Uncertainty (% active)	Expanded uncertainty (% active)	Relative expanded uncertainty (%)
80	80.7	0.35	1.33	2.7	3.3
100	100.9	0.40	1.30	2.6	2.6
120	122.0	0.46	1.53	3.1	2.5

3.6 Reliability evaluation of the NIR method

Method validation is the first step to evaluate the fitness of purpose and the reliability of a newly developed analytical method. In order to increase and further guarantee the reliability of the NIR method (c model), a three steps additional reliability evaluation of the analytical method was performed. The aim of this evaluation is to check the robustness of the NIR method and to ensure its interchangeability with its HPLC reference method.

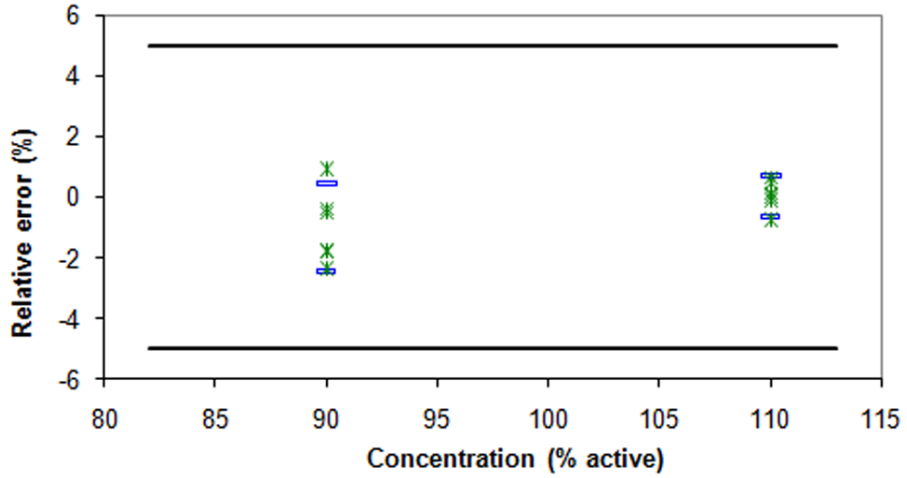

Fig. 9 – Relative errors ($100 \times \left(\frac{NIR - HPLC}{HPLC} \right)$) versus the active content level of batches containing 90 and 110 % of the usual active content. The continuous lines are the ± 5 % acceptance limits. The boxes define the 95% prediction interval limits.

First, 90 and 110 % active content formulations were manufactured. Those batches were analyzed by two operators using both the HPLC reference method and the NIR method (c model), relative errors were calculated. The aim was here to verify that the predictions of

the accuracy profile at concentration levels not investigated during the validation step were reliable. Figure 9 plots the relative error versus the active content level, 95% prediction intervals limits were defined for each level of active content. These prediction intervals define the area containing 95% of the relative errors. Regarding the 90% active content level, 95% of the future results are likely to show a relative error not exceeding [-2.44%, 0.44%]. Besides, 95% of the future results are expected to have a relative error within [-0.62%, 0.72%] for the 110% active content level. All those results indicate that the NIR method is able to quantify accurately 90 and 110 % active content formulations. Figure 8 summarizes the predictions of the (c) model versus the references measurements of the calibration and validation sets as well as for the 90 and 110 % active content batches.

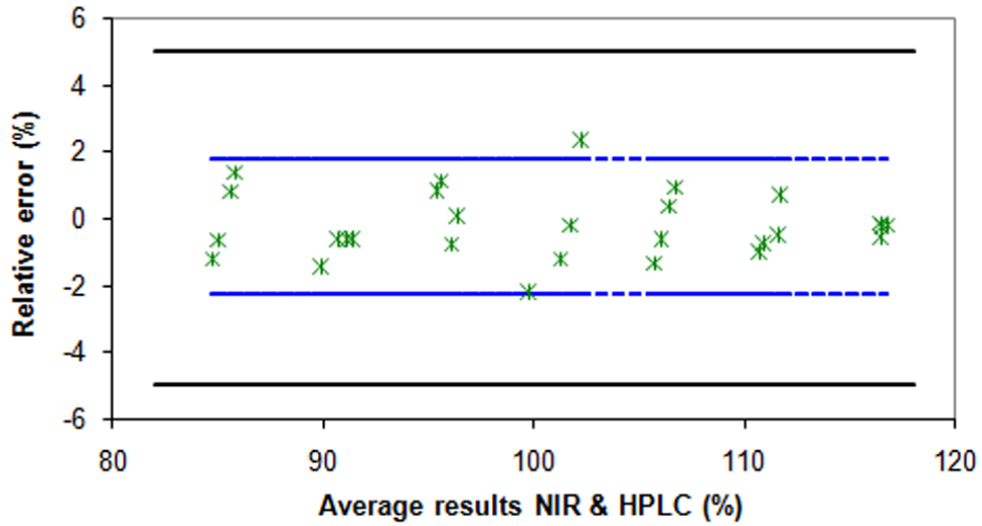

Fig. 10 – Blends of batches of pharmaceutical pellets belonging to the validation set: Bland and Altman's plot: Relative errors ($100 \times \left(\frac{NIR - HPLC}{HPLC} \right)$) against mean ($\frac{NIR + HPLC}{2}$) for different concentration levels. The continuous lines are the ± 5 acceptance limits. The dashed lines define the 95% tolerance interval limits.

Secondly, using batches belonging to the validation set, blends containing different amounts of active content were realized by two operators to obtain between 80-120 % active content formulations. The results of the reference HPLC method were used to calculate a theoretical active content for each blend. The average between the NIR results (c model) and the HPLC reference results and relative errors were calculated. A Bland and Altman plot is shown in Figure 10. This plot represents the relative errors against mean (*NIR* + *HPLC*)/2 results. Regarding this plot, 95% of the relative errors between the two methods do not exceed [-2.25%, 1.74%].

Finally, the NIR method (c model) was also tested with 10 industrial batches of non-coated pharmaceutical pellets (100 % active content formulations) belonging to 2 different production campaigns. Those batches were analyzed by the two operators. The average between the NIR results (c model) and the HPLC reference results and relative errors were

calculated. Figure 11 shows a Bland Altman plot of those results: 95% of the relative errors between the two methods are expected to have relative errors within [-2.32%, 3.40%].

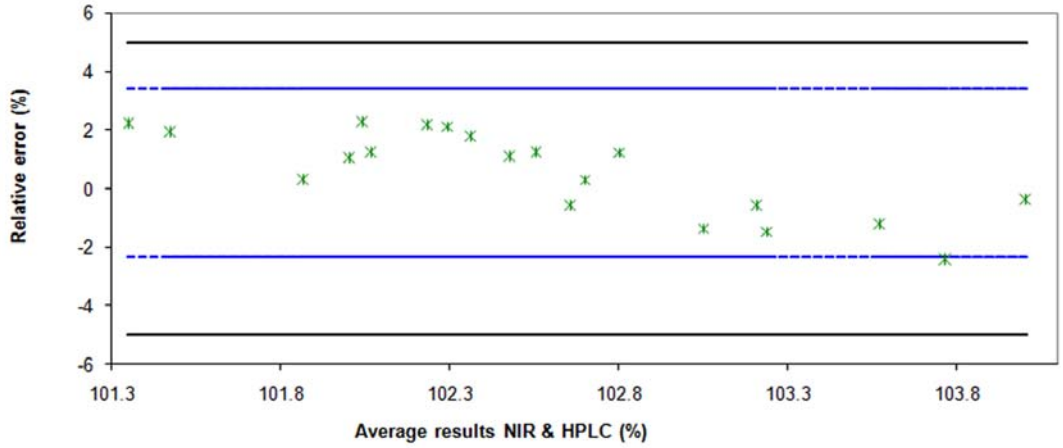

Fig. 11 – Industrial batches of pharmaceutical pellets: Bland and Altman's plot: Relative errors $(100 \times \left(\frac{NIR - HPLC}{HPLC} \right))$ against mean $(\frac{NIR + HPLC}{2})$ for different concentration levels. The continuous lines are the ± 5 acceptance limits. The dashed lines define the 95% tolerance interval limits.

As the results shown in this section are all in full accordance with the validation results, it can be concluded that the NIR method using (c) model was reliable and robust enough to quantify with good accuracy samples with an active content not included in the calibration set (90 and 110 % active content formulations). Therefore, it was not necessary to include those levels of active content in the calibration set. Besides, the (c) model also gave accurate predictions for blends of validation batches, which were independent from the model calibration batches. Further, the predictive ability of the (c) model was also adequate to quantify the active content of 100 % formulation industrial batches of non-coated pharmaceutical. Therefore, the NIR method can replace the HPLC reference method for the accurate quantification of the API in non-coated pharmaceutical pellets.

4. Conclusion

A near infrared method was developed for the determination of the active content of non-coated pharmaceutical pellets. The method was fully validated and showed very good precision, trueness and accuracy for the determination of an active content ranging from 80 % to 120 % of the usual active content confirming the potential of near infrared spectroscopy in the PAT concept.

As the conventional criteria failed to select the most accurate model because of a lack of interpretation, a novel approach based on accuracy profiles was chosen, which translates the results of the validation set in an effective visual manner, showing the models ability to

quantify the active content over the chosen active content range. As it is based on β-expectation tolerance interval, the accuracy profile also gives a representation of the future performances of the analytical method. Consequently, this approach has finally enabled to choose the best model in full accordance with the very final goal of the developed near infrared method: to quantify accurately an active content of non-coated pharmaceutical pellets ranging from 80 to 120 %.

The validated near infrared method was successfully tested with pilot batches of non-coated pharmaceutical pellets containing 90 and 110 % of the usual active content, with blends of validation batches and industrial batches of non-coated pharmaceutical pellets. The results were in full accordance with the validation results, demonstrating the reliability of the NIR method and its interchangeability with the HPLC reference method.

Acknowledgements

Thanks are due to the Walloon region and Galéphar research center M/F for a research grant provided to Jérôme Mantanus. A research grant from the Belgium National Fund for Scientific Research (FRS-FNRS) to E. Rozet is also gratefully acknowledged.

References

[1] J. Luypaert, D. L. Massart, Y. Vander Heyden, Talanta, 72 (2007) 865.
[2] Y. Roggo, P. Chalus, L. Maurer, C. Lema-Martinez, A. Edmond, N. Jent, J. Pharm. Biomed. Anal., 44 (2007) 683.
[3] D. A. Burns, E. W. Ciurczak, Handbook of Near-Infrared Analysis, 3 rd edn., Vol. 35, CRC Press, New York, 2008.
[4] American Food and Drug Administration (FDA), Guidance for Industry PAT-A Framework for Innovative Pharmaceutical Manufacturing and Quality Assurance, FDA, 2004.
[5] International Conference on Harmonisation (ICH) of technical requirements for registration of pharmaceuticals for human use, Topic Q8: Pharmaceutical development, Geneva, 2005.
[6] J. A. Lopes, P. F. Costa, T. P. Alves, J. C. Menezes, Chemo. Intel. Lab. Syst., 74 (2004) 269.
[7] J. J. Moes, M. M. Ruijken, E. Gout, H. W. Frijlink, M. I. Ugwoke, Int. J. Pharm., 357 (2008) 108.
[8] C. Bodson, W. Dewé, Ph. Hubert, L. Delattre, J. Pharm. Biomed. Anal., 41 (2006) 783.
[9] C. Bodson, E. Rozet, E. Ziémons, B. Evrard, Ph. Hubert, L. Delattre, J. Pharm. Biomed. Anal., 45 (2007) 356.

[10] J. Mantanus, et al., Moisture content determination of pharmaceutical pellets by near infrared spectroscopy: Method development and validation, Anal. Chim. Acta (2008), doi:10.1016/j.aca.2008.12.031
[11] J. Rantanen, E. Räsänen, O. Antikainen, J.-P. Mannermaa, J. Yliruusi, Chemo. Intel. Lab. Syst., 56 (2001) 51.
[12] N. Sandler, J. Rantanen, J. Heinämäki, M. Römer, M. Marvola and J. Yliruusi, AAPS PharmSciTech., 6 (2) Article 26.
[13] M. Ito, T. Suzuki, S. Yada, A. Kusai, H. Nakagami, E. Yonemochi, K. Terada, J. Pharm. Biomed. Anal., 47 (2008) 819.
[14] L. O. Rodrigues, J. P. Cardoso, J. C. Menezes, Talanta, 75 (2008) 1203.
[15] S. S. Rosa, P. A. Barata, J. M. Martins, J. C. Menezes, Talanta 75 (2008) 725.
[16] H. Huang, H. Yu, H. Xu, Y. Ying, Journal of Food Engineering, 87 (2008) 303.
[17] Q. Chen, J. Zhao, S. Chaitep, Z. Guo, Food Chemistry 113 (2009) 1272.
[18] M. R. Monteiro, A. R. P. Ambrozin, L. M. Liao, A. G. Ferreira, Talanta, 77 (2008) 593.
[19] International Conference on Harmonization (ICH) of Technical Requirements for registration of Pharmaceuticals for human Use, Topic Q2 (R1): Validation of analytical Procedures: Text and Methodology, Geneva, 2005.
[20] Ph. Hubert, J.J. Nguyen-Huu, B. Boulanger, E. Chapuzet, P. Chiap, N. Cohen, P.A. Compagnon, W. Dewé, M. Feinberg, M. Lallier, M. Laurentie, N. Mercier, G. Muzard, C. Nivet, L. Valat, J. Pharm. Biomed. Anal., 36 (2004) 579.
[21] Ph. Hubert, J.J. Nguyen-Huu, B. Boulanger, E. Chapuzet, P. Chiap, N. Cohen, P.A. Compagnon, W. Dewé, M. Feinberg, M. Lallier, M. Laurentie, N. Mercier, G. Muzard, C. Nivet, L. Valat, E. Rozet, J. Pharm. Biomed. Anal., 45 (2007) 70.
[22] Ph. Hubert, J.J. Nguyen-Huu, B. Boulanger, E. Chapuzet, N. Cohen, P.-A. Compagnon, W. Dewé, M. Feinberg, M. Laurentie, N. Mercier, G. Muzard, L. Valat, E. Rozet, J. Pharm. Biomed. Anal., 45 (2007) 82.
[23] Ph. Hubert, P. Chiap, J. Crommen, B. Boulanger, E. Chapuzet, N. Mercier, S. Bervoas-Martin, P. Chevalier, D. Grandjean, P. Lagorce, M. Lallier, M.C. Laparra, M. Laurentie, J.C. Nivet, Anal. Chim. Acta, 391 (1999) 135.
[24] E. Rozet, A. Ceccato, C. Hubert, E. Ziémons, R. Oprean, S. Rudaz, B. Boulanger, P. Hubert, J. Chromatogr. A, 1158 (2007) 111.
[25] E. Rozet, R. Morello, F. Lecomte, G.B. Martin, P. Chiap, J. Crommen, K.S. Boos, P. Hubert, J. Chromatogr. B, 844 (2006) 251.
[26] E. Rozet, V. Wascotte, N. Lecouturier, V. Préat, W. Dewé, B. Boulanger, Ph. Hubert, Anal. Chim. Acta, 591 (2007) 239.
[27] E. Rozet, C. Hubert, A. Ceccato, W. Dewé, E. Ziemons, F. Moonen, K. Michail, R. Wintersteiger, B. Streel, B. Boulanger, Ph. Hubert, J. Chromatogr. A, 1158 (2007) 126.
[28] M. Feinberg, B. Boulanger, W. Dewé, Ph. Hubert, Anal. Bioanal. Chem., 380 (2004) 502.
[29] International Conference on Harmonisation (ICH) of technical requirements for registration of pharmaceuticals for human use, Topic Q9: Quality Risk Management, Geneva, 2005.
[30] European Medicines Agency, draft: Guideline on the use of near infrared spectroscopy by the pharmaceutical industry and the data requirements for new submissions and variations, EMEA/CHMP/CVMP/QWP/17760/2009 Rev 1.
[31] Analytical Methods Committee, Analyst, 120 (1995) 2303.
[32] Eurachem/Citac guide Quantifying the uncertainty in analytical measurement, second ed., 2000.

[33] CB EA-4/16, EA Guidelines on the Expression of Uncertainty in Quantitative Testing, 2004, http://www.european-accreditation.org.
[34] R.D. Marini, P. Chiap, B. Boulanger, S. Rudaz, E. Rozet, J. Crommen, Ph. Hubert, Talanta, 68 (2006) 1166.

Section III.2.2.2

Moisture content determination of pharmaceutical pellets by near infrared spectroscopy: Method development and validation

J. Mantanus, E. Ziemons, P. Lebrun, E. Rozet, R. Klinkenberg, B. Streel, B. Evrard, Ph. Hubert, Anal. Chim. Acta 642 (2009) 186.

Summary

The aim of the present study was to develop and validate a near infrared method able to accurately determine a moisture content of pharmaceutical pellets ranging from 1 to 8 % in order to check their moisture content conformity. A calibration and validation set were designed for the conception and evaluation of the method adequacy. An experimental protocol was then followed, involving two operators, independent production campaign batches and different temperatures for data acquisition On the basis of this protocol, prediction models based on Partial Least Squares (PLS) regression were then carried out. Conventional criteria such as the R^2, the Root Mean Square Errors of Calibration and Prediction (RMSEC and RMSEP) as well as the number of PLS factors enabled the selection of three preliminary models. However, such criteria did not clearly demonstrate the model's ability to give accurate predictions over the whole analyzed water content range. Consequently, a novel approach based on accuracy profiles which allow the selection of the most fitted model for purpose was used. According to this novel approach, the model using Multiplicative Scatter Correction (MSC) pre-treatment was obviously the most suitable. Indeed, the resulting accuracy profile clearly showed that this model was able to determine moisture content over the range of 1-8% with a very acceptable accuracy.

The present study confirmed that NIR spectroscopy could be used in the PAT concept as a non invasive, non destructive and fast technique for moisture content determination in pharmaceutical pellets. In addition, facing the limit of the classical and commonly used criteria, the use of accuracy profiles proved to be useful as a powerful decision tool to demonstrate the suitability of the proposed analytical method.

1. Introduction

Near infrared (NIR) spectroscopy belongs to vibrational spectroscopy. This analytical technique offers many advantages such as suppression of sample preparation and/or of destruction and fast data acquisition. Besides, the calibration set does not need to be updated or rebuilt as long as there is an agreement between the validation results and the Quality Controls (QCs) results. The use of optical fibres also allows "*at-line*", "*on-line*" or "*in-line*" analyses. Moreover, NIR spectra contain both physical (e.g. granulometry, particle shape, polymorphism...) and chemical information (e.g. the active pharmaceutical ingredient, moisture...). However, each technique has its drawbacks: the NIR system must be carefully calibrated and this calibration phase is a time consuming task since the model creation takes into account the use of a reference method as well as different environmental constrains. Moreover, given that great quantity of physical and chemical information are found in the NIR spectra, visual spectra interpretation is rendered difficult. Indeed, only a small piece of information is relevant with respect to the objective investigated. Therefore chemometrical tools are widely used to extract the significant information arising from the physical and chemical data [1-3]. Two well-known chemometrical tools for spectral analyses are mathematical pre-treatments and regression methods. The first consists in suppressing the biggest part of the information that is not relevant, i.e. not directly linked to the chemical nature of the sample. Examples of mathematical pre-treatments include the Savitzky-Golay smoothing filter, Standard Normale Variate (SNV) and Multiplicative Scatter Correction (MSC) [3-4]. The second links a spectrum to a given concentration allowing the creation of a mathematical model. Examples of regression methods include Multiple-Linear Regression (MLR), Partial Least Squares (PLS) regression and Artificial Neuronal Network (ANN) [3].

In the pharmaceutical field, conformity analyses realized between batch production and batch release can be time consuming if most of them are performed after the manufacturing process. From this statement is born FDA's Process Analytical Technology (PAT) which is also defined in the ICH Q8 documents [5-6]. Indeed, the PAT approach focuses on the monitoring of each critical step of the fabrication in real time reducing the batch release time. PAT also gives the opportunity to tune manufacturing parameters, avoiding the loss of potential batches. Regarding the non-invasive, non-destructive and fast data acquisition character of NIR spectroscopy, it is increasingly associated with the PAT concept [7-10].

Pellets preparation is a complex process which is divided into different operations such as blending, granulation, extrusion, spheronization and drying. The PAT approach is particularly indicated to control such a complex process [11-12]. Moisture determination to control the drying phase of the granulation process is often performed with time consuming and/or sample destructive techniques such as thermo-gravimetric or Karl-Fisher methods.

These techniques could be replaced by NIR spectroscopy. Indeed, the NIR spectrum of water contains two major absorption bands at 5155 cm^{-1} and 6895 cm^{-1} making this technique selective enough to allow a sensitive determination of moisture content [3]. NIR spectroscopy has already been used in different fields such as the pharmaceutical [13-18], the food [19] and the fuel industry [20] to determine moisture content. In the pharmaceutical field, Rantanen et al. [18] described the in-line drying monitoring of a pellet formulation. However their quantitative approach was not fully validated.

After the development of an analytical method, it is crucial and mandatory to validate it in order to guarantee that the laboratory will obtain accurate results in routine analysis [21]. The accuracy profile is used to facilitate the analytical interpretation. It also integrates all the useful required statistics, such as accuracy, trueness, precision, quantitative limits, risk and linearity [22-24]. In addition, the accuracy profile, using β-expectation tolerance intervals, enables a visual and reliable representation of the future performances of the analytical method [25-30].

The aim of the present study was first to develop a robust near infrared model able to determine the moisture content of pharmaceutical pellets. The second aim was to fully validate the method for a moisture content ranging from 1 to 8 % by use of the accuracy profile as decision tool. The final aim was to demonstrate the ability of the proposed method to accurately determine a moisture content below 4% which allows conform liberation of the pharmaceutical pellets.

2. Materials and methods

2.2. Chemicals

Independent batches from 3 different production campaigns of pharmaceutical pellets with Active Pharmaceutical Ingredient (API) T200999 were obtained from Galéphar M/F (Marche en Famenne, Belgium). The pellets analyzed are complex pharmaceutical matrices. Indeed, the pharmaceutical pellets contain two coating layers: the first coating is a subcoating layer while the second layer enables the sustained release of the API during 24 hours.

2.2. FT-NIR equipment

Pharmaceutical pellets were analysed by reflexion mode with a multipurpose analyzer Fourier transform near infrared spectrometer (MPA, Bruker Optics, Ettlingen, Germany)

equipped with a semi-conductor room temperature sulfide lead (RT-PbS) detector. The spectra were collected with the Opus software 6.5 (Bruker Optics).

2.3. Thermogravimetric method

A Thermogravimetric balance (HB43S Halogen balance, Mettler Toledo, Greifensee, Switzerland) was used as reference method. Pellets samples of approximately 2 g were heated at a 105°C desiccation temperature that remained constant during the analysis. The measurement stopped as soon as the mean weight loss per 90 seconds was lower than 1 mg. The thermogravimetric method precision is $\pm$ 0.1% of moisture.

2.4. Validation protocol

An experimental protocol was created for the calibration and validation steps in order to obtain a robust model.

Pellets samples were disposed on sieves in a cold room to reach the targeted moisture levels. As the cold room was saturated with humidity, the more the pellets samples stayed in the cold room, the more moisture content they retained. The sieves were agitated every 30 minutes to obtain homogeneous moisture content. Samples were first scanned with the NIR spectrometer before measuring the moisture content with the reference method which is a destructive method. As pellets are not perfect spherical structures, three different NIR measurements (i.e. replicates) of the same sample were taken to catch its physical state variability.

2.5. Data treatment

The statistical language R 2.7.1 for Windows [31] has been used to implement the signal processing of the near infrared spectra. The following packages have been imported into R: signal, pls and nlme. Each spectrum was the average of 32 scans and the resolution was 8 cm^{-1} over the range from 12500 to 3600 cm^{-1}. The validation results were given by e.noval V2.0 (Arlenda, Liège, Belgium).

3. Results and discussion

3.1. Calibration

As samples analyzed in routine will not all belong to the same production batch or production campaign, the prediction models were built using independent batches of pharmaceutical pellets from three different production campaigns (C1 to C3). It seems important here to define the difference between a batch effect and a production campaign effect: The first effect incorporates batch to batch variations due to fluctuating manufacturing conditions. Indeed, once a batch is manufactured, all the production tools are dismantled, cleaned and put together again leading to possible changes in the manufacturing conditions. Besides, different batches of raw materials are likely to be used inside the same production campaign. The second effect also includes fluctuating manufacturing conditions due to the use of the instruments for the production of another pharmaceutical formulation. Consequently, when a new production campaign of pharmaceutical pellets begins, all the manufacturing parameters have to be restored, causing possible fluctuations in the manufacturing conditions. Again, to match the routine conditions, this protocol was designed for two operators. In addition, as temperature changes can induce variations in the spectral response, especially for the absorption bands of water, samples were scanned under two different temperature conditions (5°C and 25°C). Indeed, with increasing temperatures, the water absorption bands are moving to higher wavenumbers and there is an increase in signal height [3].

As shown in Figure 1, the calibration protocol covered six different moisture levels: 0.5%, 1%, 2%, 4%, 8% and 10%. The entire calibration is realized within 2 days, each operator making his own series per day. Batches belonging to 3 different production campaigns (C1, C2 and C3) were chosen. Each sample was measured with the NIR spectrometer in triplicate under two different temperature conditions. Condition A corresponds to the temperature of the cold room (5°C) whereas condition B corresponds to ambient temperature (25°C).

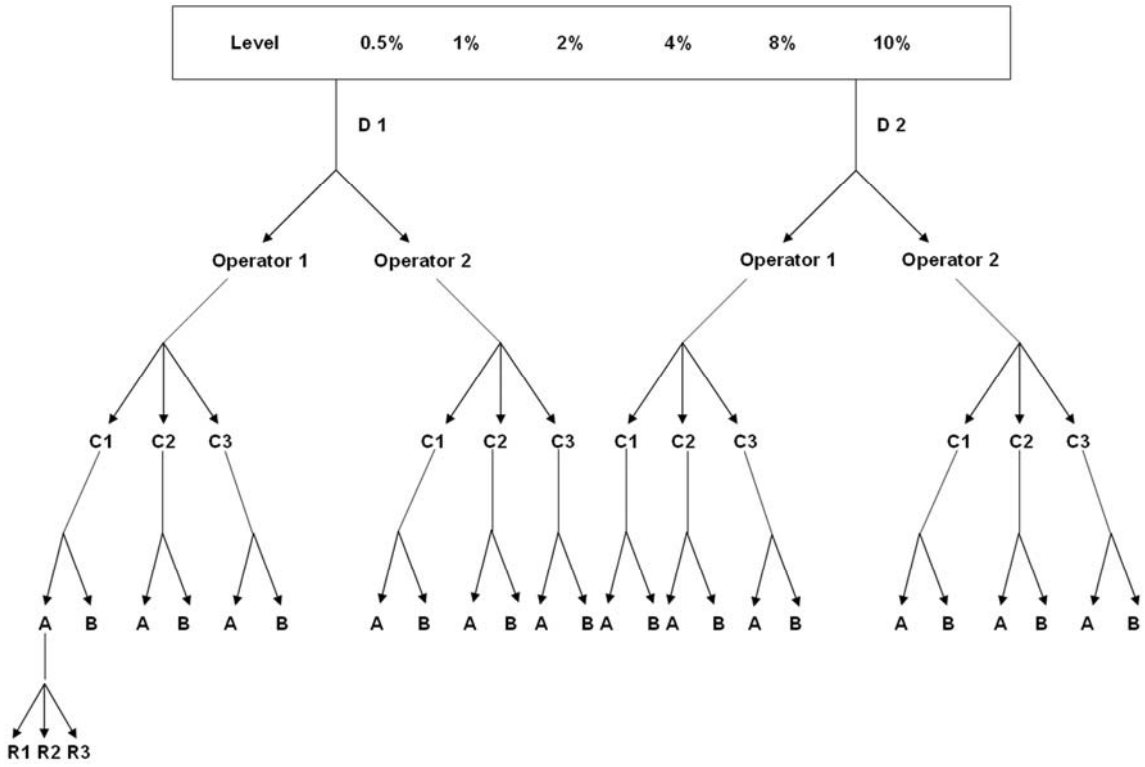

Fig. 1 - Schematic illustration of the calibration protocol. D means day. C1, C2 and C3 represent independent batches from production campaign 1, 2 and 3 respectively. A means that the sample is measured with NIR spectroscopy under low temperature conditions (5°C) whereas B means that the sample is measured with NIR spectroscopy under ambient temperature conditions (25°C). R1, R2 and R3 represent different NIR measurements of the same sample (repetitions).

3.2. Validation

Figure 2 illustrates the validation protocol which covered five different moisture levels: 0.5%, 1%, 2%, 4% and 8%. The entire validation followed the calibration and was realized within three days: operator 1 made one series on days 3 and 5 while operator 2 made one series on day 4. For the validation protocol, three new batches from production campaign 1 were chosen. All samples were measured in triplicate under the same two temperature conditions as in the calibration protocol: condition A and condition B (5°C and 25°C respectively).

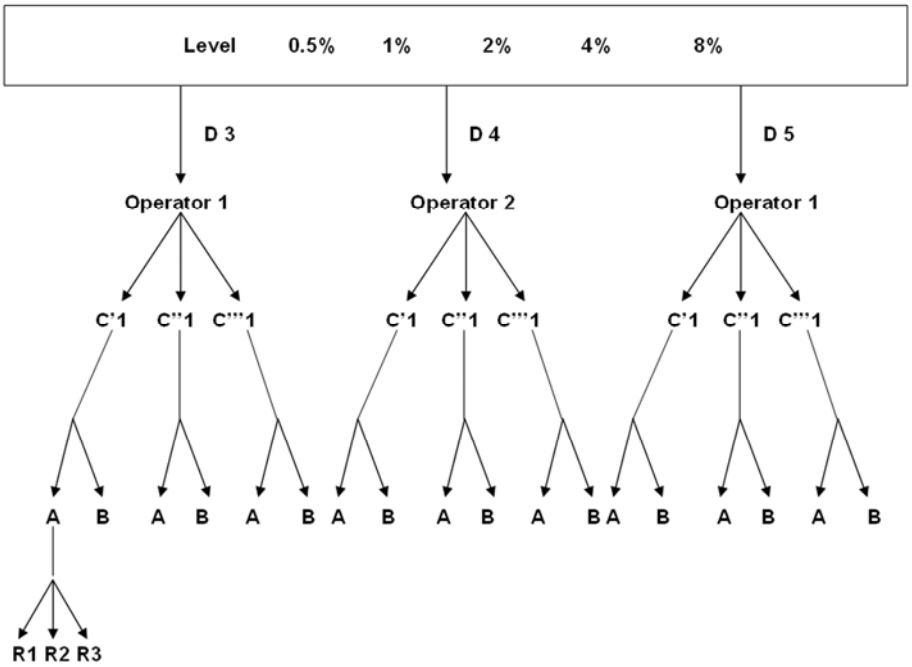

Fig. 2 - Schematic illustration of the validation protocol. D means day. C'1, C''1 and C'''1 represent independent batches from production campaign 1 which are different from the batches used in the calibration protocol. A means that the sample is measured with NIR spectroscopy under low temperature conditions (5°C) whereas B means that the sample is measured with NIR spectroscopy under ambient temperature conditions (25°C). R1, R2 and R3 represent different NIR measurements of the same sample (repetitions).

3.3. Data treatment

Prediction models based on PLS regression were carried out. In PLS [2] method the regressions are computed with least squares algorithms. The goal of the PLS is to establish a linear link between two matrices, the spectral data X and the reference values Y (which can be of dimension above one). This technique works both on X and Y in order to find out the variables in the X matrix that will best describe the Y matrix through linear combinations of wavelengths, called factors, which describe best the studied properties.

The spectra acquired during the calibration were integrated in the calibration set while those acquired during the validation phase were in the test set. In our study, two different types of data pre-treatment were used: first derivative and MSC pre-treatments. The first derivative pre-treatment firstly smoothes the spectra using the Savitzky-Golay smoothing filter and then performs the first derivative transformation on the smoothed spectra [4]. On the other hand, the MSC pre-treatment reduces the effect of scattered light on diffuse reflection NIR spectra [3].

3.4. Validation results

According to the type of data pre-treatment and region selected, plenty of models can be generated. Conventional criteria such as the R^2, the Root Mean Square Error of Calibration (RMSEC), the Root Mean Square Error of Prediction (RMSEP) and the number of PLS factors were used to suppress the model candidates with the less predictive potential. Accuracy profiles were then used to finally evaluate the quantitative performances of the retained models in order to select the most adequate one.

Concerning the selected spectral regions (see Figures 3 and 4), it is obvious that two regions are water content sensitive (7575-6117 cm^{-1}; 5404-4926 cm^{-1}). In fact, these zones correspond to the location of the water bands as told in the introduction. Either one or both of these regions were included in the potential models.

Table 1 shows the conventional parameters of three potentially interesting models. Regarding the number of PLS factors, it is important to choose a model with a small number of factors in order to avoid overfitting the model. Hence, model (a) seems to use too many factors to predict the water content with good robustness. However, neither R^2 of calibration nor R^2 of validation allow the differentiation between the three models as they are very close.

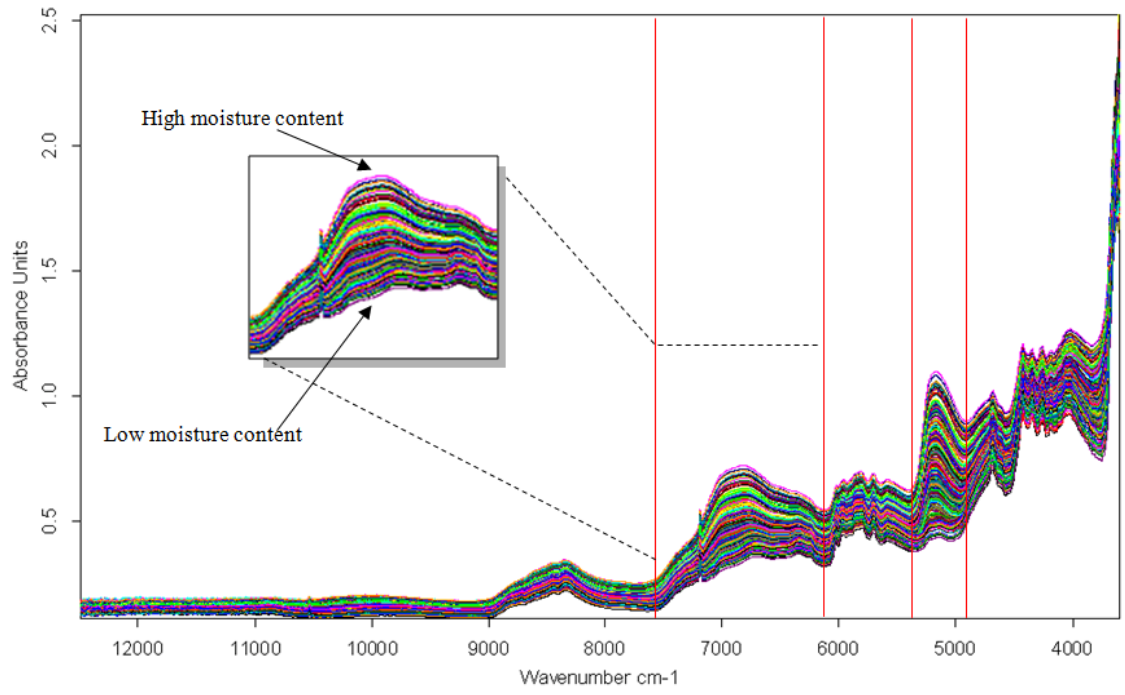

Fig. 3 - NIR spectra used for the calibration set.

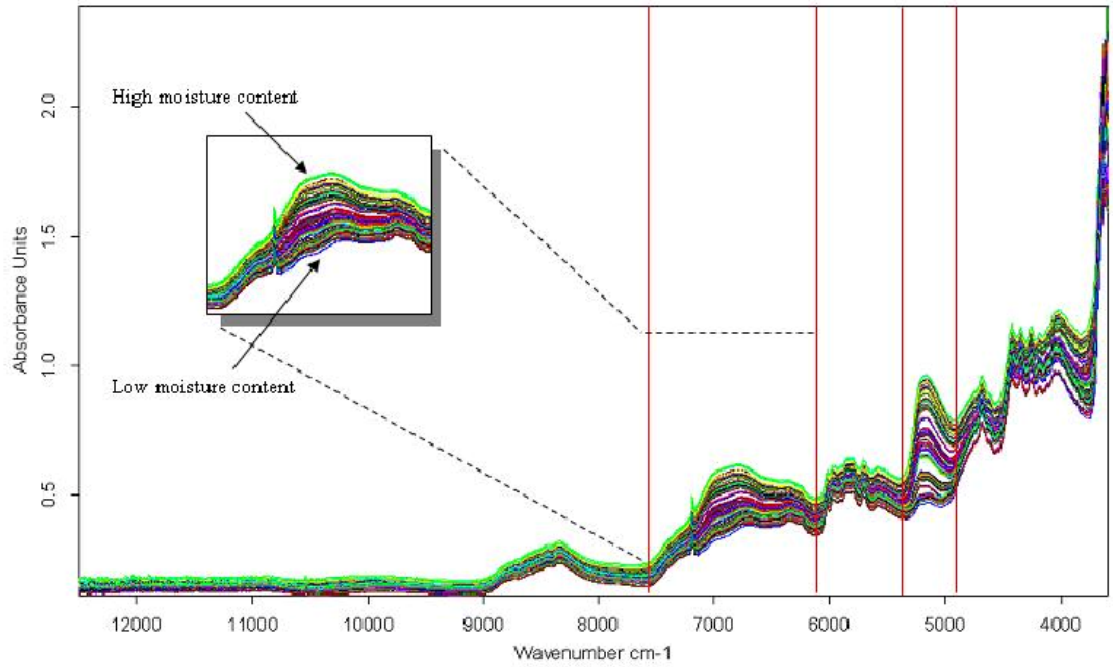

Fig. 4 - NIR spectra used for the validation set.

Table 1 - Type of spectral pre-treatment, R^2 calibration, R^2 validation, number of PLS factors, RMSEP, RMSEC and region selected of different models.

Model	**(a)**	**(b)**	**(c)**
Pre-treatment	None	First derivative	MSC
R^2 calibration	0.998	0.996	0.998
R^2 validation	0.995	0.995	0.997
PLS factors	9	5	5
RMSEC (%)	0.175	0.212	0.163
RMSEP (%)	0.193	0.195	0.167
Region (cm^{-1})	7575-6117 5404-4926	7575-6117 5404-4926	6102-4247

Considering RMSEC and RMSEP, model (c) has the smallest values and the difference between its RMSEP and RMSEC values is smaller than those of other models indicating the good robustness of this model. According to the above criteria, model (c) seems to be slightly better than the two others. However, those criteria do not allow the assessment of

the model ability to quantify accurately over the analyzed water content range. Consequently, accuracy profiles were used as final decision tool to select the most appropriate model. Hubert et al. [22-24] showed that the accuracy profile which uses the total error concept meets the ICH Q2(R1) guideline requirements [21]. Due to the confusion found between accuracy and trueness in the ICH document, it seems therefore important to remind that accuracy represents the total error which is the sum of the trueness (systematic error) and precision (random error) [22-24].

Figure 5 shows accuracy profiles obtained with models (a), (b) and (c) respectively. The acceptance limits were set at ± 20% while the maximum risk (1-β) to obtain results outside these acceptance limits was set at 5%. As mentioned before, the thermogravimetric method precision is ± 0.1% of moisture, which means for example that, the method can give a result of 0.9% for an amount of moisture content of 1 %, representing a 10% error. 95% of the results obtained with this reference method are thus expected to be included into the interval of ± 20% obtained using 2 as coverage factor. This ± 20% interval was finally selected as acceptance limits for the validation of the NIR method.

As can be seen in Figure 5, model (c) has the smallest Lower Limit Of Quantification (LLOQ). Indeed its β-expectation tolerance limits cross the acceptance limits when the moisture content is lower than 1 % (Figure 5).

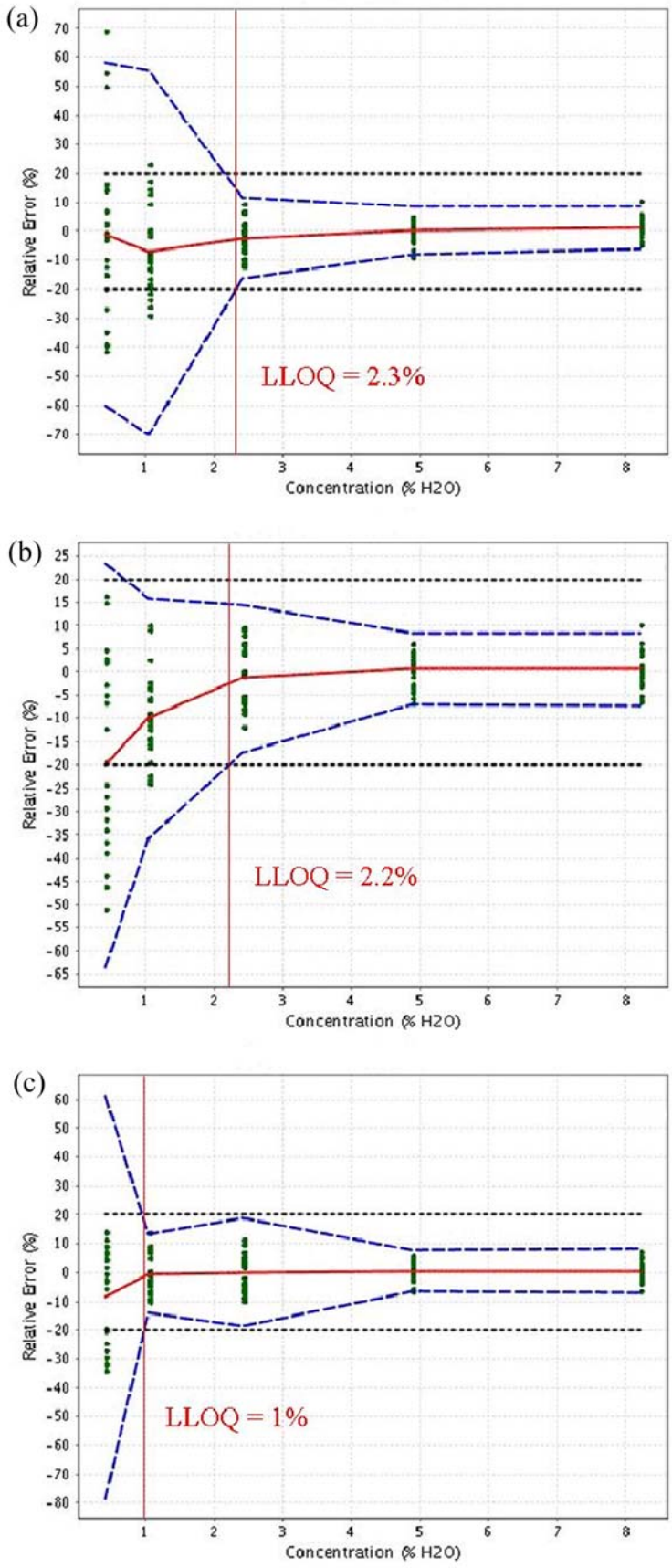

Fig. 5 - Accuracy profiles of models (a), (b) and (c). The plain line is the relative bias, the dashed lines are the β-expectations tolerance limits (β=95%) and the dotted lines represent the acceptance limits (± 20%).

Table 2 - ICH Q2(R1) validation criteria of the model (c).

Trueness	Concentration level (% H_2O)	Relative bias (%)	
	0.5	-8.5	
	1.0	-0.3	
	2.0	0.1	
	4.0	0.6	
	8.0	0.5	
Precision	Concentration level (% H_2O)	Repeatability (RSD %)	Intermediate precision (RSD %)
	0.5	9.2	19.8
	1.0	6.2	6.4
	2.0	4.6	6.8
	4.0	3.5	3.5
	8.0	2.9	3.3
Accuracy	Concentration level (% H_2O)	Relative β-Expectation tolerance limits (%)	
	0.5	[-78.4 , 61.4]	
	1.0	[-13.8 , 13.1]	
	2.0	[-18.7 , 18.8]	
	4.0	[-6.7 , 7.9]	
	8.0	[-7.0 , 8.1]	
Limits of quantification (LOQ)	Lower LOQ (% H_2O)	Upper LOQ (% H_2O)	
	1.0	8.0	

Moreover, model (c) clearly shows the smallest bias: it is stable and points towards zero from a moisture content ranging from 1% to 8%. Under a moisture content of 1%, the bias of the 3 models becomes more important.

Model (c) is thus the most adequate one regarding our objective as it guarantees, on average, that at least 95% of the future results obtained using the developed method will be included within the acceptance limits over the 1-8% moisture content range. However, as the bias becomes more important and the β-expectation tolerance intervals fall outside the acceptance limits for a moisture content below 1%, model (c) should not be used to predict a moisture content below 1%.

Furthermore, considering all the models, model (c) is based on the lowest number of PLS factors: five. This relatively high value can be explained by the complexity of the sample matrix. Moreover, all the loadings were checked: even the fifth loading did not show significant noise.

Table 2 shows the ICH Q2(R1) validation criteria of the model (c). As seen in the accuracy profile, the bias is low and stable: the relative bias does not exceed ± 0.6% over the 1.0-8.0% moisture content range but becomes more important below 1%.

The precision of the method was estimated by measuring repeatability and intermediate precision at the five concentration levels shown in the validation protocol. The repeatability and intermediate precision improve with growing moisture content but are still satisfactory from the 1% moisture content level. Under this level, the repeatability in RSD% increases as well as the intermediate precision in RSD% which increases even more indicating a general lack of precision for the 0.5% moisture content level.

As shown with the accuracy profile, the accuracy is good for the 1.0-8.0% moisture content range as the values of the relative β-expectation tolerance limit never exceed ± 20%: the worst case being the 2% moisture content level where the relative β-expectation tolerance limit is [-18.7 , 18.8]%. Moreover, the accuracy is the best for the 4% moisture content level, the level that is the most important to guarantee the pharmaceutical pellets conformity.

Again, as noticed by the observation of the accuracy profile, the LLOQ is 1.0% while the Upper Limit Of Quantification (ULOQ) is 8.0%.

Figure 6 is showing the linear profile of the model (c). A linear model was fitted on the calculated concentrations of the validation standards for all series as a function of the introduced concentrations. The intercept, the slope and the R^2 values are also presented in Figure 6. The slope and intercept are close to 1 and 0 respectively confirming the absence of proportional and constant systematic error of the model (c). The linearity of the method for the 1.0-8.0% moisture content range is demonstrated since the β-expectation tolerance limits were included in the absolute acceptance limits.

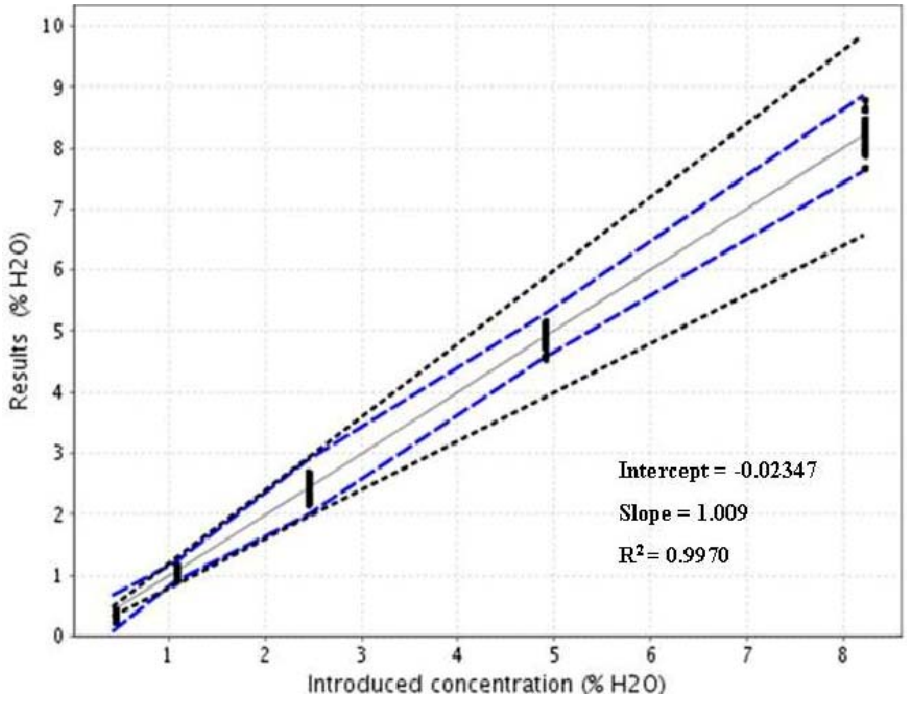

Fig. 6 - Linear Profile of the model (c). The dashed limits on this graph correspond to the accuracy profile, i.e. the β-expectation tolerance limits expressed in absolute values. The dotted curves represent the acceptance limit at ± 20% expressed in the concentration unit. The continuous line is the identity line y = x.

3.5. Uncertainty assessment

The uncertainty characterizes the dispersion of the values that could reasonably be attributed to the measurand [32-33]. Several uncertainty results of the model (c) were generated and are presented in Table 3: the uncertainty of bias of the method at each concentration level of the validation standard, the uncertainty which combines the uncertainty of the bias with the uncertainty of the method obtained during the validation step, i.e. the intermediate precision standard deviation, and the expanded uncertainty which equals to the uncertainty multiplied by a coverage factor k=2 representing an interval around the results where the unknown true value can be observed with a confidence level of 95% [32-36]. In addition, the relative expanded uncertainties (%) for moisture content obtained by dividing the corresponding expanded uncertainties with the corresponding introduced concentrations (Table 3) are not higher than 15%, which means that with a confidence level of 95%, the unknown true value is located at a maximum of ±15% around the measured result. Only for the first concentration level of moisture content in pellets (0.5%) is the relative expended uncertainty extremely high, about 45%.

Table 3 – Model (c): estimates of measurement uncertainties related to moisture content results in pellets at each concentration level investigated.

Concentration level (% H_2O)	Uncertainty of the bias (% H_2O)	Uncertainty (% H_2O)	Expanded Uncertainty (% H_2O)	Relative Expanded Uncertainty (%)
0.5	0.0	0.1	0.2	44.5
1.0	0.0	0.1	0.1	13.0
2.0	0.1	0.2	0.4	14.9
4.0	0.0	0.2	0.3	7.1
8.0	0.1	0.3	0.6	7.0

4. Conclusions

Our study has confirmed that near infrared spectroscopy can be used in the PAT concept as a non invasive, non destructive method to determine moisture content in pharmaceutical pellets. A model was selected, evaluated and then the method was fully validated to guarantee its ability to predict a moisture content ranging from 1% to 8% with very acceptable precision, trueness and accuracy enabling the evaluation of the pellets moisture content conformity: a moisture content below 4%.

Besides, this study also showed that the R^2, the RMSEC and RMSEP were not the most relevant indicators of the accuracy of the NIR models. Therefore, a novel approach based on accuracy profiles was followed, which truly assesses the model ability to quantify accurately over the chosen moisture content range. Moreover, the accuracy profile also gives a reliable representation of the future performances of the analytical method as it is based on β-expectations tolerance intervals. Consequently, this approach has finally enabled to choose the best model in an effective visual manner in full accordance with the very final goal of the developed near infrared method: to quantify accurately a moisture content ranging from 1 to 8 %.

Acknowledgements

Thanks are due to the Walloon region and Galéphar Research center M/F for a research grant provided to Jérôme Mantanus.

References

[1] J. Luypaert, D. L. Massart, Y. Vander Heyden, Talanta, 72 (2007) 865.

[2] Y. Roggo, P. Chalus, L. Maurer, C. Lema-Martinez, A. Edmond, N. Jent, J. Pharm. Biomed. Anal., 44 (2007) 683.

[3] D.A. Burns, E.W. Ciurczak, Handbook of Near-Infrared Analysis. Practical Spectroscopy Series Volume 27, Marcel Dekker: New York, NY, 2001.

[4] A. Savitzky, M. J.E. Golay, Anal. Chem. 36 (1964) 1627.

[5] American Food and Drug Administration (FDA), Guidance for Industry PAT-A Framework for Innovative Pharmaceutical Manufacturing and Quality Assurance, FDA, 2004.

[6] International Conference on Harmonisation (ICH) of technical requirements for registration of pharmaceuticals for human use, Topic Q8: Pharmaceutical development, Geneva, 2005.

[7] J. A. Lopes, P. F. Costa, T. P. Alves, J. C. Menezes, Chemo. Intel. Lab. Syst., 74 (2004) 269.

[8] J. J. Moes, M. M. Ruijken, E. Gout, H. W. Frijlink, M. I. Ugwoke, Int. J. Pharm., 357 (2008) 108.

[9] C. Bodson, W. Dewé, Ph. Hubert, L. Delattre, J. Pharm. Biomed. Anal., 41 (2006) 783.

[10] C. Bodson, E. Rozet, E. Ziémons, B. Evrard, Ph. Hubert, L. Delattre, J. Pharm. Biomed. Anal., 45 (2007) 356.

[11] J. Rantanen, E. Räsänen, O. Antikainen, J.-P. Mannermaa, J. Yliruusi, Chemo. Intel. Lab. Syst., 56 (2001) 51.

[12] N. Sandler, J. Rantanen, J. Heinämäki, M. Römer, M. Marvola and J. Yliruusi, AAPS PharmSciTech., 6 (2) Article 26.

[13] Y. Zheng, X. Lai, S. Wrang Bruun, H. Ipsen, J. Nedergaard Larsen, H. Løwenstein, I. Søndergaard, S. Jacobsen, J. Pharm. Biomed. Anal., 46 (2008) 592.

[14] X. Zhou, P. Hines, M.W. Borer, J. Pharm. Biomed. Anal., 17 (1998) 219.

[15] A. Dunko, A. Dovletoglou, J. Pharm. Biomed. Anal., 28 (2002) 145.

[16] A. Miwa, T. Yajima, H. Ikuta, K. Makado, Int. J. Pharm., 352 (2008) 202.

[17] J. Rantanen, E. Räsänen, J. Tenhunen, M. Känsäkoski, J.-P. Mannermaa, J. Yliruusi, Eur. J. Pharm. Biopharm., 50 (2000) 271.

[18] J. Rantanen, S. Lehtola, P. Rämet, J.-P. Mannermaa, J. Yliruusi, Powder Technol. 99 (1998) 163.

[19] J. De Temmerman, W. Saeys, B. Nicolaï, H. Ramon, Biosystems Eng., 97 (2007) 313.

[20] P. Daugbjerg Jensen, H. Hartmann, T. Böhm, M. Temmerman, F. Rabier, M. Morsing, Biomass and Bioenergy, 30 (2006) 935.

[21] International Conference on Harmonization (ICH) of Technical Requirements for registration of Pharmaceuticals for human Use, Topic Q2 (R1): Validation of analytical Procedures: Text and Methodology, Geneva, 2005.

[22] Ph. Hubert, J.J. Nguyen-Huu, B. Boulanger, E. Chapuzet, P. Chiap, N. Cohen, P.A. Compagnon, W. Dewé, M. Feinberg, M. Lallier, M. Laurentie, N. Mercier, G. Muzard, C. Nivet, L. Valat, J. Pharm. Biomed. Anal., 36 (2004) 579.

[23] Ph. Hubert, J.J. Nguyen-Huu, B. Boulanger, E. Chapuzet, P. Chiap, N. Cohen, P.A. Compagnon, W. Dewé, M. Feinberg, M. Lallier, M. Laurentie, N. Mercier, G. Muzard, C. Nivet, L. Valat, E. Rozet, J. Pharm. Biomed. Anal., 45 (2007) 70.

[24] Ph. Hubert, J.J. Nguyen-Huu, B. Boulanger, E. Chapuzet, N. Cohen, P.-A. Compagnon, W. Dewé, M. Feinberg, M. Laurentie, N. Mercier, G. Muzard, L. Valat, E. Rozet, J. Pharm. Biomed. Anal., 45 (2007) 82.
[25] Ph. Hubert, P. Chiap, J. Crommen, B. Boulanger, E. Chapuzet, N. Mercier, S. Bervoas-Martin, P. Chevalier, D. Grandjean, P. Lagorce, M. Lallier, M.C. Laparra, M. Laurentie, J.C. Nivet, Anal. Chim. Acta, 391 (1999) 135.
[26] E. Rozet, A. Ceccato, C. Hubert, E. Ziémons, R. Oprean, S. Rudaz, B. Boulanger, P. Hubert, J. Chromatogr. A, 1158 (2007) 111.
[27] E. Rozet, R. Morello, F. Lecomte, G.B. Martin, P. Chiap, J. Crommen, K.S. Boos, P. Hubert, J. Chromatogr. B, 844 (2006) 251.
[28] E. Rozet, V. Wascotte, N. Lecouturier, V. Préat, W. Dewé, B. Boulanger, Ph. Hubert, Anal. Chim. Acta, 591 (2007) 239.
[29] E. Rozet, C. Hubert, A. Ceccato, W. Dewé, E. Ziemons, F. Moonen, K. Michail, R. Wintersteiger, B. Streel, B. Boulanger, Ph. Hubert, J. Chromatogr. A, 1158 (2007) 126.
[30] M. Feinberg, B. Boulanger, W. Dewé, Ph. Hubert, Anal. Bioanal. Chem., 380 (2004) 502.
[31] R Development Core Team (2006). R: A Language and Environment for Statistical Computing. Vienna: R Foundation for Statistical Computing. http://www.R-project.org
[32] Analytical Methods Committee, Analyst 120 (1995) 2303.
[33] Eurachem/Citac guide Quantifying the uncertainty in analytical measurement, second ed., 2000.
[34] CB EA-4/16, EA Guidelines on the Expression of Uncertainty in Quantitative Testing, 2004, http://www.european-accreditation.org.
[35] M. Feinberg, B. Boulanger, W. Dewe, Ph. Hubert, Anal. Bioanal. Chem. , 380 (2004) 502.
[36] R.D. Marini, P. Chiap, B. Boulanger, S. Rudaz, E. Rozet, J. Crommen, Ph. Hubert, Talanta 68 (2006) 1166.

Section III.2.2.3.

Building the quality into pellet manufacturing environment – Feasibility study and validation of an in-line quantitative near infrared (NIR) method

J. Mantanus, E. Ziemons, E. Rozet, B. Streel, R. Klinkenberg, B. Evrard, J. Rantanen, Ph. Hubert, Talanta 83 (2010) 305.

Summary

The present study focuses on the implementation of an in-line quantitative near infrared (NIR) spectroscopic method for determining the active content of pharmaceutical pellets. The first aim was to non-invasively interface a dispersive NIR spectrometer with four realistic particle streams existing in the pellets manufacturing environment. Regardless of the particle stream characteristics investigated, NIR together with principal component analysis (PCA) was able to classify the samples according to their active content. Further, one of these particle stream interfaces was non-invasively investigated with a FT-NIR spectrometer. A predictive model based on Partial Least Squares (PLS) regression was able to determine the active content of pharmaceutical pellets. The NIR method was finally validated with an external validation set for an API concentration range from 80 to 120 % of the targeted active content. The prediction error of 0.9 % (Root Mean Square Error of Prediction, RMSEP) was low, indicating the accuracy of the NIR method. The accuracy profile on the validation results, an innovative approach based on tolerance intervals, demonstrated the actual and future performance of the in-line NIR method. Accordingly, the present approach paves the way for real-time release-based quality system.

1. Introduction

FDA's Process Analytical Technology (PAT) aims at "*improving the pharmaceutical development, manufacturing and quality assurance through innovation in product and process development, process analysis and process control*" [1]. According to the PAT framework, the process analysis side should include at least the following two steps. First, the critical process steps relating to the final product quality should be identified using appropriate risk assignment approach [2]. Considering the pellet manufacturing process, the processing steps such as blending, granulation, spheronization, drying and coating phases are critical to ensure the final product quality. Second, a proper process measurement system must be chosen to collect at-line, on-line or in-line process information from the identified critical steps of the manufacturing. This information may eventually provide a better understanding of the manufacturing process, giving opportunities for process control strategies to prevent or mitigate the risk of producing out of specification products. Moreover, the data gathered during the production may enable the real time release of the product, reducing the batch release time which is still dependent on time consuming laboratory tests. The challenge still remains to interface the selected process analytical approach to the real environment and to develop quantitative methods fitted for a real time release quality-based system.

Near infrared (NIR) spectroscopy is a well-established vibrational spectroscopic technique. In the covered wavelength region (between 800 and 2500 nm), relatively wide bands related to overtones and combination of fundamental vibration of chemical groups with hydrogen, such as C-H, N-H, O-H and S-H, are observed. Such vibrations lead to overlapping bands which contain both physical and chemical information. Consequently, chemometric tools are used to extract the significant information [3-4].

NIR spectroscopy has several advantages, such as fast spectral acquisition, minimization of sample preparation and/ or destruction and the use of probes allowing at-line, on-line and in-line analysis. Considering those advantages, NIR spectroscopy matches the process measurement system requirements of the PAT framework. NIR spectroscopy has already been part of PAT applications to monitor critical process attributes such as the blend homogeneity, the coating level, the moisture content, and the active content [5-19].

Validation is a crucial and mandatory step in the lifecycle of an analytical method [20]. Based on β-expectation tolerance intervals, the accuracy profile makes possible a visual and reliable representation of the actual and future performances of the analytical method and thus enables a better risk management. It fully complies with the ICH Q2(R1) regulatory documents as it integrates all the useful required validation criteria such as accuracy, trueness, precision, limits of quantification, range and linearity [21-23].

In a previous work [12], a NIR method able to quantify the API in non-coated pharmaceutical pellets was successfully developed and validated. Using the commercially available formulation, coated pharmaceutical pellets as model particles, the feasibility of a quantitative in-line method was evaluated. The first aim was, for qualitative purpose, to interface a dispersive NIR spectrometer with four realistic particle streams found in the pellets manufacturing line. Second, for quantitative purpose, to interface one of the previous particle stream with a FT-NIR spectrometer. Finally, based on the previous interfacing, to develop and to validate a NIR method able to determine the API content of the pellets.

2. Materials and methods

2.1. Materials

2.1.1 Pharmaceutical pellets

Table 1 – API and main excipient percentage w/w in the 80, 100 and 120 % API formulations.

API formulation	API (% w/w)	Main excipient (% w/w)
80 %	36	38
100 %	45	30
120 %	54	22

For this work, pellets were used as model particles. 18 batches of pharmaceutical pellets were manufactured via extrusion spheronization followed by two coating steps. In the standard pellet formulation, which will later on be called 100 % Active Pharmaceutical Ingredient (API) formulation, the API is 45 % (w/w) of the formulation whereas the formulation main excipient represents 30 % (w/w) of the formulation. As shown in Table 1, the ratio of raw materials was modified in order to manufacture batches containing 80 and 120 % API formulations (6 batches per API level). Moreover, the coating levels were kept the same to provide the same sustained release behavior for all the batches. All the batches were sieved after the manufacturing, the fractions between 800 and 1600 µm were kept for the experiments.

2.1.2. Qualitative study samples

For the qualitative study, 9 batches of pharmaceutical pellets were analyzed, 3 batches per API level.

2.1.3 Quantitative study samples

For the quantitative study, 18 batches of pharmaceutical pellets were analyzed, 6 batches per API level.

2.2. Methods

2.2.1. NIR analysis

For qualitative purpose, a dispersive NIR spectrometer NIR-256L-2.2T2 (Control Development Inc., South Bend, IN, USA) having a thermoelectrically cooled 256 element InGaAs array detector, a tungsten light source and a fiber optic reflectance probe (six illuminating fibres around one collecting fibre) was used. The spectra were collected between 1090 and 2220 nm with a 10 ms integration time. The spectral range used in the data analysis was 1340-1640 nm.

For quantitative purpose, a Bomen FTLA 2000 series FT-NIR spectrometer (ABB Bomen, Quebec, Canada) was used. Samples were measured in the 1000-2500 nm range with a resolution of 8 cm^{-1}.

The number of scans selected for the off-line and the in-line measurements will be described in the following sections.

2.2.2 Off-line measurements

For the dispersive NIR spectrometer, off-line measurements were performed with the reflectance probe directly through the side of glass vials. For the FT-NIR spectrometer, samples in vials were analyzed on the reflectance sample stage. For both systems, each spectrum was the average of 32 scans.

2.2.3. Process interfaces for the dispersive NIR spectrometer

2.2.3.1 Fluidization interface

150 g of pellets sample were introduced in a Mini-Glatt (Glatt GMbH, Germany) fluid bed coater. The system was working in drying mode and no heat was applied while fluidizing the particles. The fluidizing air pressure was 1.75 bars. As can be seen from Figure 1a), the NIR probe was placed outside the coater, directly against the acrylic glass housing of the

fluid bed coater. A background of the acrylic glass housing was taken before each measurement. The spectra were collected by averaging 16 scans. One spectrum was acquired every 3 seconds. Ten spectra per batch were kept for the data analysis.

2.2.3.2 Slow particle flow velocity device

For this interface, pellets slide down through a homemade sample holder. For 100 g of pellets, the average time for the particles to flow through the sample holder was 20 seconds, leading to a particle mean flow rate of 5 g/s. Figure 1b) shows how the particles flow was interfaced in a non-invasive way with the NIR probe. The spectra were collected by averaging 4 scans. One spectrum was acquired every second. Ten spectra per batch were kept for the data analysis.

2.2.3.3 Fast particle flow velocity device

For the fast particle flow device, pellets were freely flowing through a funnel. In this case, the particle mean flow rate was higher (7 g/s) as the samples were falling in the air. As can be seen from Figure 1c), the NIR interfacing was done perpendicularly to the particles flow without disturbing the flow. The spectra were collected by averaging 4 scans. One spectrum was acquired every second. Ten spectra per batch were kept for the data analysis.

2.2.3.4 Interface for compacts

Using a hydraulic press, a pressure of 50 MPa was applied to 1.6 g of pellets samples. The obtained tablets were then analyzed with the NIR probe while rotating on a sample stage as displayed in Figure 1d). The rotating speed was set at 10 rpm. The spectra were collected by averaging 16 scans. One spectrum was acquired every 3 seconds. Ten spectra per batch were kept for the data analysis.

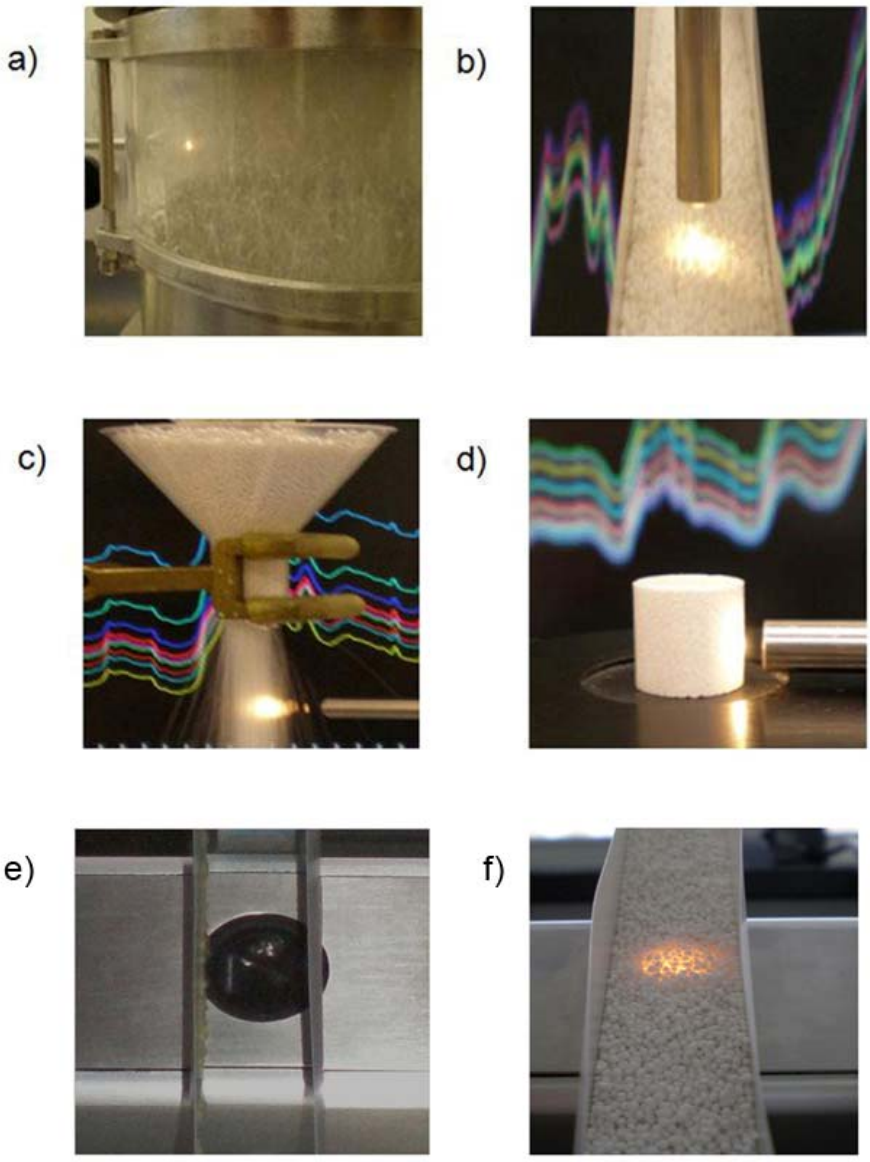

Fig. 1 – Process interfaces for the dispersive NIR spectrometer: a) fluidization interface; b) slow particle flow velocity device; c) fast particle flow velocity device and d) interface for compacts. Process interface for the FT-NIR spectrometer: e) without particles and f) with particles.

2.2.4. Process interface for the FT-NIR spectrometer

The particle flow velocity device was the same as the slow particle flow velocity device developed for the dispersive NIR spectrometer. However, as can be seen from Figure 1e) and 1f), the interfacing with the FT-NIR spectrometer was performed via the reflectance sample stage, through the glass bottom of the sample holder. The spectra were collected while averaging 16 scans.

2.2.5. Multivariate data analysis

Principal Components Analysis (PCA), Partial Least Squares (PLS) regression and Multiplicative Signal Correction (MSC) were carried out with PLS Toolbox 5.0 for Matlab version 7.6. The data were mean-centered before performing PCA or PLS. Cross-validation was performed based on contiguous blocks. Using contiguous blocks, each test set is determined by selecting contiguous blocks of *n*/*s* objects in the data set, starting at object number 1 where *n* is the total number of objects and *s* the number of data splits specified in the cross-validation procedure [24].

2.2.6. Near infrared quantitative method: calibration and validation protocols

Sources of variability such as batches, API levels and days were introduced in the calibration and validation sets.

2.2.7. Reference method

A confidential HPLC reference method previously developed and validated by Galephar Research Center M/F was used to determine the amount of API in the batches of pharmaceutical pellets. Per batch, three HPLC determinations were performed. The average API content was used as the reference value for each batch.

3. Results and discussion

3.1 Qualitative study

The NIR spectra of the 100 % Active Pharmaceutical Ingredient (API) formulation, the API and the main excipient are shown in Figure 2.

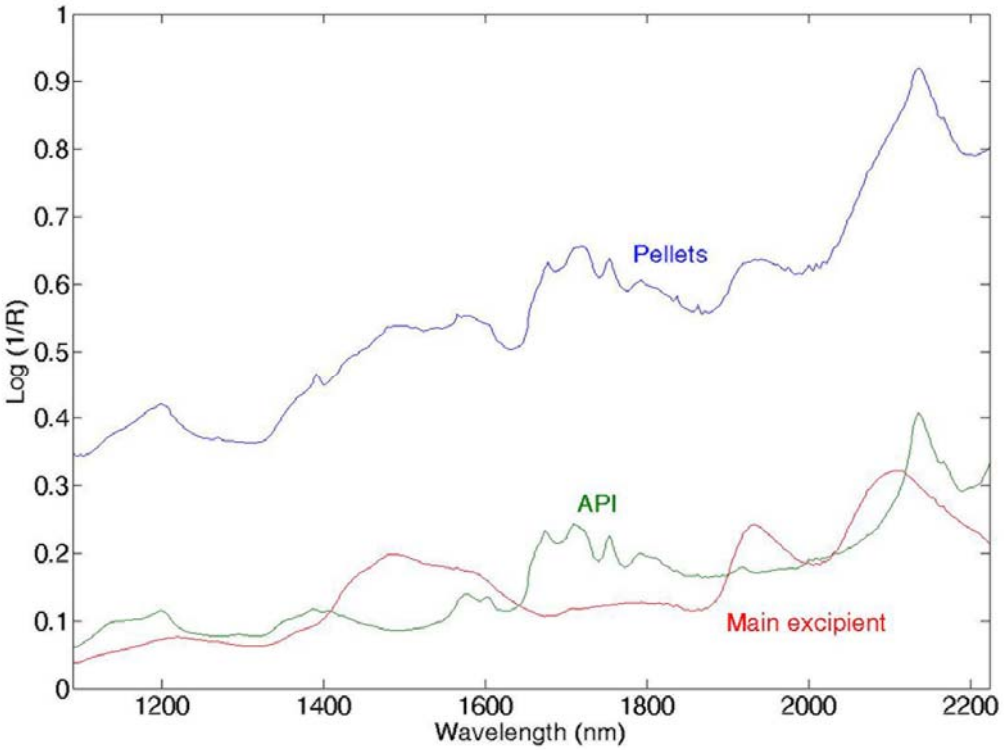

Fig. 2 – 100 % Active Pharmaceutical Ingredient (API) formulation, API and main excipient off-line NIR spectra (dispersive NIR spectrometer).

It can be observed that a major part of the pharmaceutical pellets spectrum belongs to the API regarding its amount in the formulation. The main excipient which represents 30 % (w/w) of the 100 % API formulation seems to influence the spectrum of the final product in the 1415-1555 and in the 2000-2200 nm areas.

In the present study, the four process interfaces were developed based on real life pharmaceutical process streams - especially particle streams which can be found in the pellets manufacturing. As fluidization is a critical step in the manufacturing of sustained release formulations, fluidization interfacing can be used to monitor the coating and drying steps. In the production line, feeding lines lead the pharmaceutical product towards the packaging site or inject the raw materials in a blending process for example. The slow velocity flow motion device was developed to mimic the typical motion observed in those feeding lines. Moreover, the objective of the high velocity flow motion device was to simulate the capsule filling stage which is also critical to guarantee the final product conformity. Finally, as formulations using compacted pellets are also available on the market, rotating compacted pellets were interfaced, simulating the real time monitoring of tablets transferred towards the packaging line.

Given the moving particles density and speed, a defined number of scans was chosen for each spectral acquisition interface. The sample density being the lowest for the fluidizing particles, 16 scans were necessary to collect representative NIR spectra of the samples. As

the samples density and speed were higher for the low and high velocity devices, 4 scans were selected for those setups. Although the compacts density was the highest, 16 scans were selected to collect a general overview of the samples during a low speed rotational movement.

A spectral range containing the API contribution and compatible with the 4 spectral acquisition systems was chosen. As the spectral interferences coming from the polyacrylic glass housing of the fluidbed coater were minimal in the 1340-1640 nm region, this spectral range was selected. Figure 3 (top) shows the spectra obtained with each setup after MSC signal pre-processing on the chosen spectral area. Regardless of the acquisition system, it is possible to distinguish the 3 API formulations. The selected spectral range reflects the increase of the API content and the simultaneous relative decrease of the main excipient content. The API and the main excipient have a strong signal and it is the ratio between both ingredients that mainly defines the three different API content formulations. The main spectral feature that differentiates the 4 acquisition interfaces is the noise affecting each type of particle movement. When comparing the high velocity flow device to the slow velocity flow device which both share the same NIR acquisition settings, the slower particle movement resulted in less noise. In the case of the interface for compacts, the dense particulate system had a smoothing effect on the spectra. The spectral noise obtained with the fluidization interface may be caused by the polyacrylic glass housing of the fluid bed coater or a combination between the housing interferences and the interfaced particles movement. Moreover, because of the different speeds, densities, numbers of scans, the effective sampling volume varies between each spectral acquisition interface. All the previous considerations consequently lead to spectral noise variations between the four spectral acquisition interfaces.

PCA was performed with the spectra collected with each spectral acquisition interface. The data were pre-processed with MSC. Figure 3 (bottom) shows the PCA plots of the corresponding spectral acquisition interfaces. A clustering given the type of API formulation can be observed for each spectral acquisition interface. Most of the variance is explained by PC1 which discriminates the samples according to their active content. A minor part of the variance is represented by PC2 which may modelize batch-to-batch variations and/or moisture contents. For the fluidization interfacing, PC2 is also affected by the spectral interferences caused by the acrylic glass housing of the fluid bed: it separates the different batch measurements, especially for the 80 and 120 % active content levels. The loadings on PC1 and PC2 were checked to confirm the previous observations. As the loadings on PC1 and PC2 look the same for all the spectral acquisition interfaces, Figure 4 only displays the loadings of the PCA performed with the slow particle flow velocity device. The loadings on PC1 contain information about the API at the 1390 and 1590 nm areas whereas the region between the two previous ones is related to the main excipient. PC1 then discriminates the samples according to their active content as it contains information about the ratio API/main

excipient. PCA was performed over a wider spectral range to determine whether PC2 was responding to batch-to-batch moisture or to other batch-to-batch differences. The corresponding loadings highlighted moisture content sensitive spectral regions (1320-1635 and 1850-2030 nm).

The quality of spectral acquisition is suitable for all the different set-ups as they all allowed discriminating the batches of pharmaceutical pellets according to their active content. Therefore, the first part of the study confirmed that qualitative real time process monitoring with NIR spectroscopy can be achieved in various process streams.

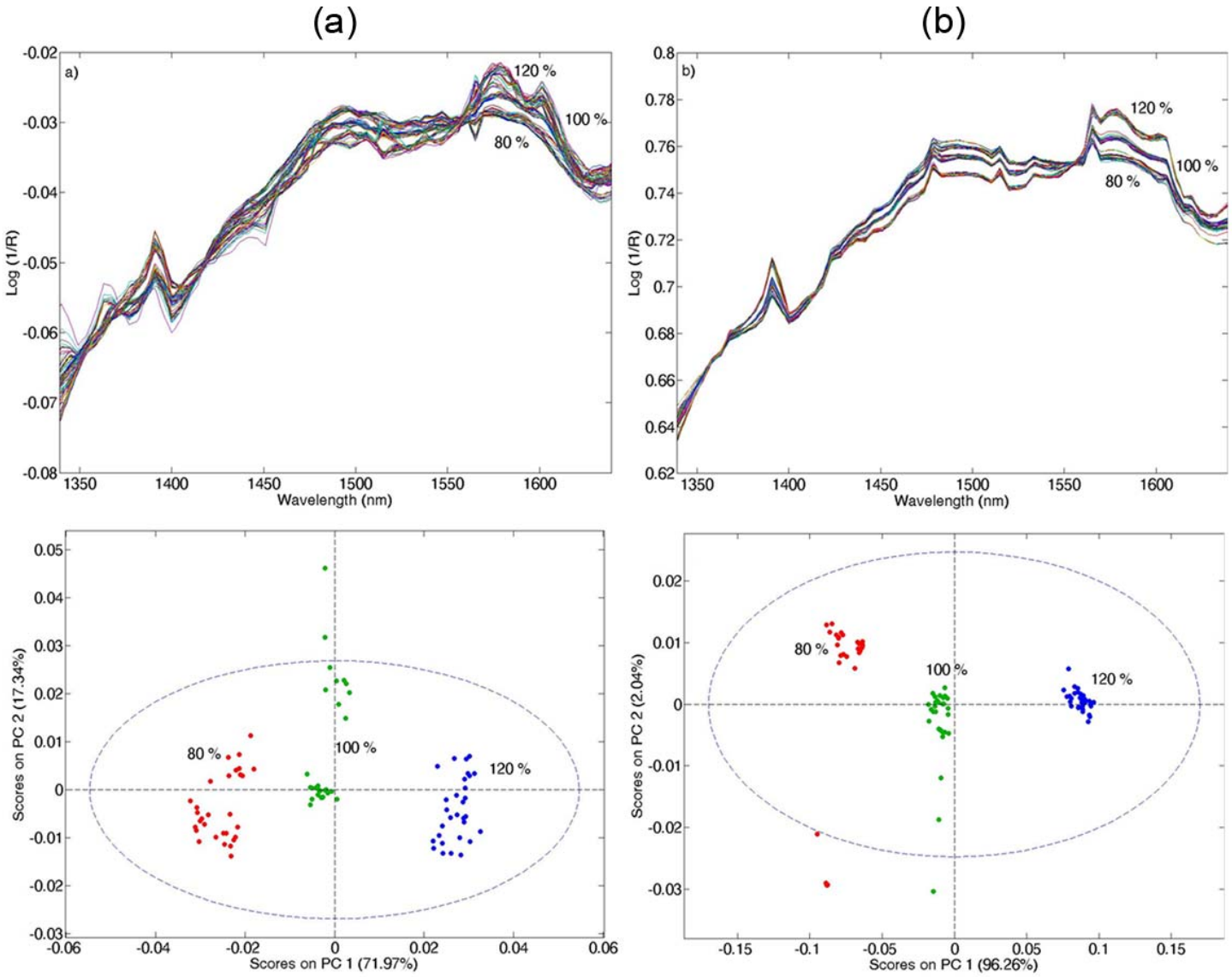

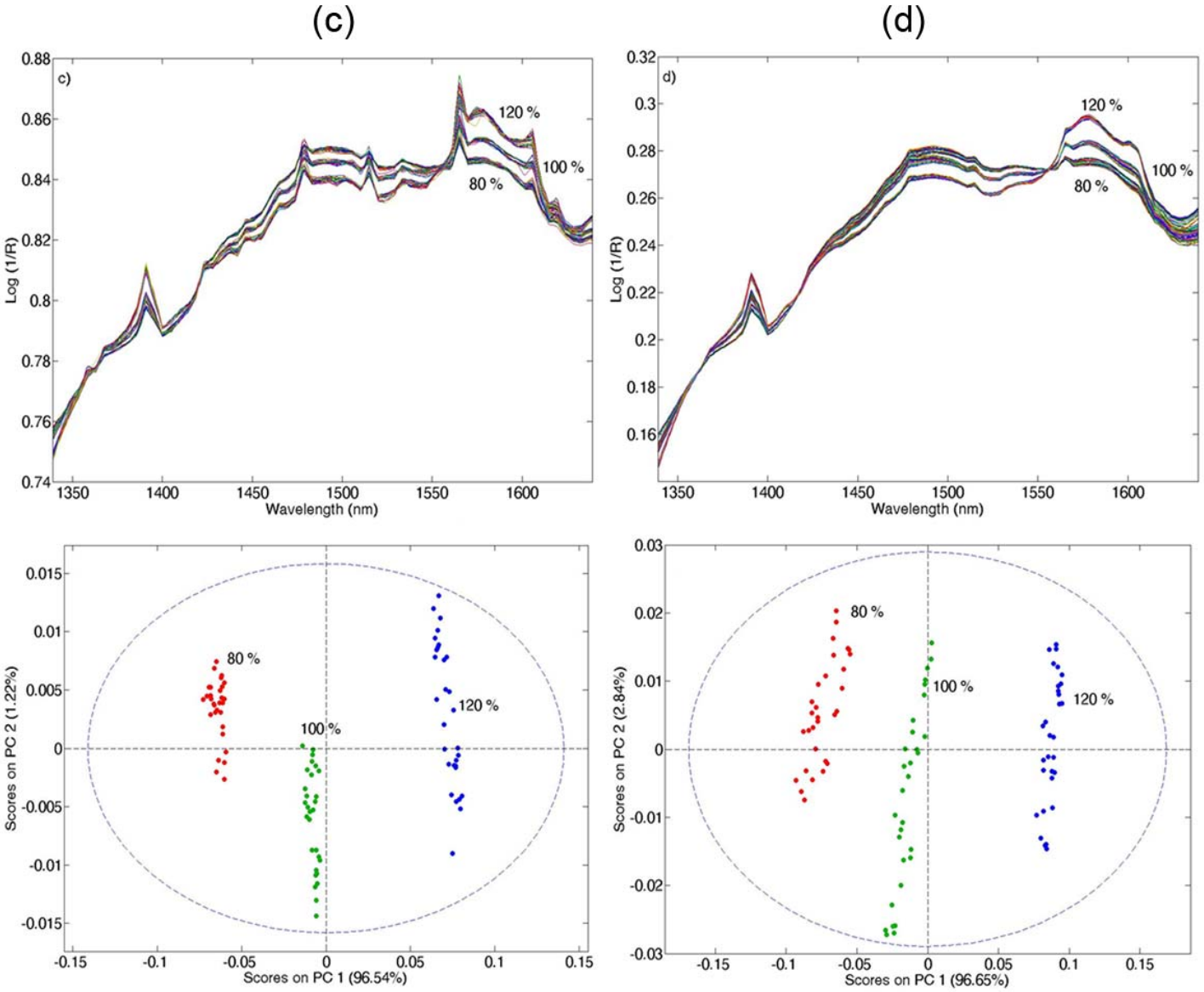

Fig. 3 – Top: MSC corrected NIR spectra in the 1340-1640 nm region collected while interfacing (a) the fluidization,(b) the slow particle flow velocity device, (c) the fast particle flow velocity device and (d) the compacts. Bottom: Corresponding PCA score plots .The NIR spectra were pre-processed with MSC.

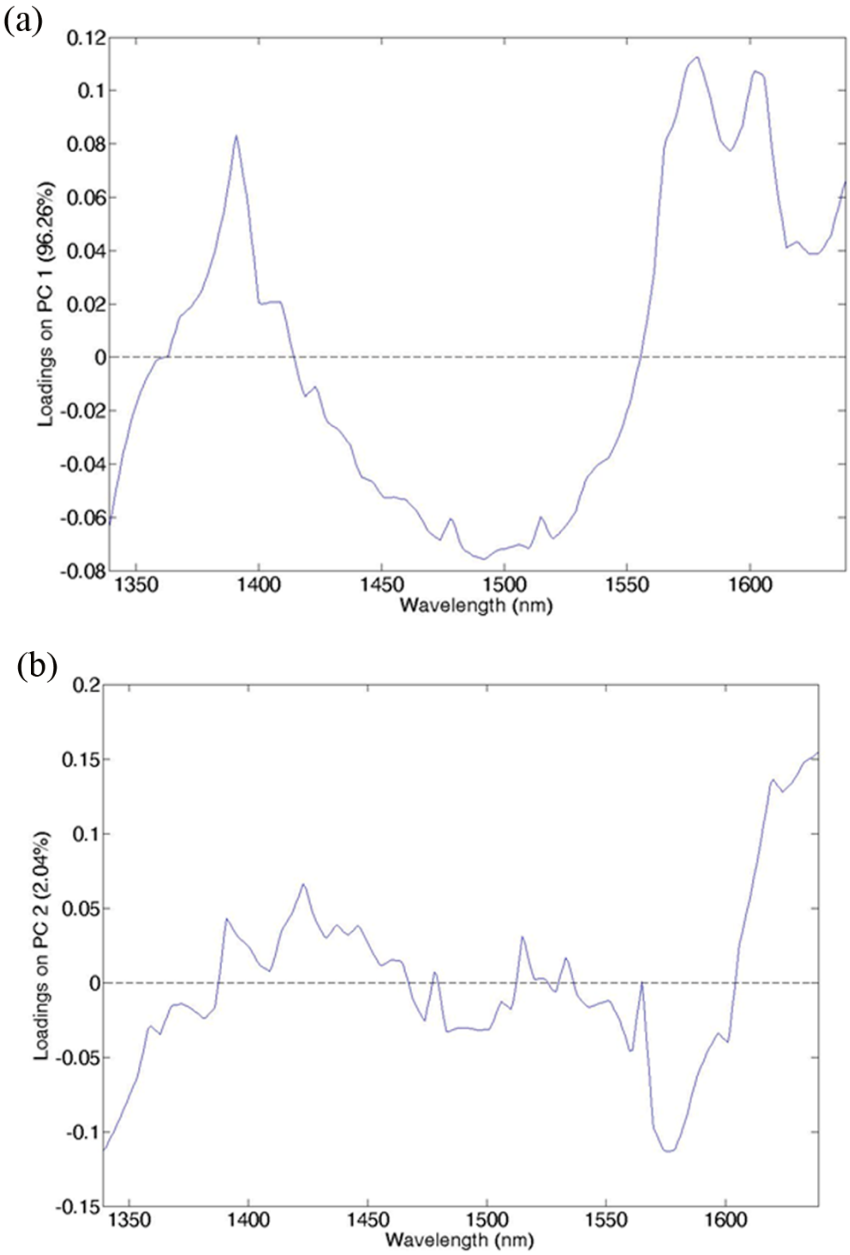

Fig. 4 – PCA loadings plot computed with the NIR spectra acquired while interfacing the slow particle flow velocity device.

3.2 Quantitative study

As shown in the qualitative study and as demonstrated by Andersson et al. [25], spectral artifacts appear in NIR spectra when conducting measurements on moving solids by a dispersive NIR spectrometer. For quantitative purpose, the slow particle flow velocity was therefore interfaced with a FT-NIR spectrometer. At the sample velocity investigated, artifacts appeared outside the NIR wavelength region. Based on the samples average flow rate and the time necessary for the NIR acquisition (4.5 seconds), the average effective sampling volume was around 22 g of pharmaceutical pellets. This volume was selected

taking into account that in the manufacturing line, it would be interesting to detect small API level changes within kilograms of moving particles. Table 2 displays the variability sources included in the calibration and validation sets. As this study focuses on the feasibility of an in-line NIR method, the expected sample variety that the model will meet in the manufacturing environment was introduced in the calibration set. 9 different pellets batches were manufactured, including 80, 100 and 120 % API levels, 3 batches per API levels. Moreover, 3 series of measurements were integrated in the calibration set, one series of measurements was performed per day. Each sample was analyzed in triplicate by NIR spectroscopy. Per series of measurements, a total number of 27 NIR spectra were recorded. As the calibration is built with 3 independent series of measurements, the entire calibration set contains a total of 81 NIR spectra. The accuracy and the robustness of the NIR model were further tested with an external validation set containing the same sources of variability as the calibration set. The validation set protocol is the same as the calibration protocol, a total of 81 NIR spectra were recorded.

Table 2 – Quantitative NIR method: variability sources included in the calibration and validation sets.

	Calibration set	Validation set
Variability sources	Amount of variability	
Independent batches	9	9
API levels	3 (80, 100 and 120 % API)	3 (80, 100 and 120 % API)
Number of batches per API levels	3	3
Series of measurements	3	3

Table 3 shows the selected parameters for the NIR model. As can be seen from Figure 5, the selected spectral area is related to the API content of the sample. It was further confirmed by the first loading factor of the PLS model.

Table 3 – Conventional criteria of the NIR method.

NIR model	Selected parameter
Spectral area (nm)	1320-1040, 2090-2200
Spectral pre-processing	MSC
Number of PLS factors	4
RMSEC (%)	0.7
RMSECV	1.1
RMSEP	0.9

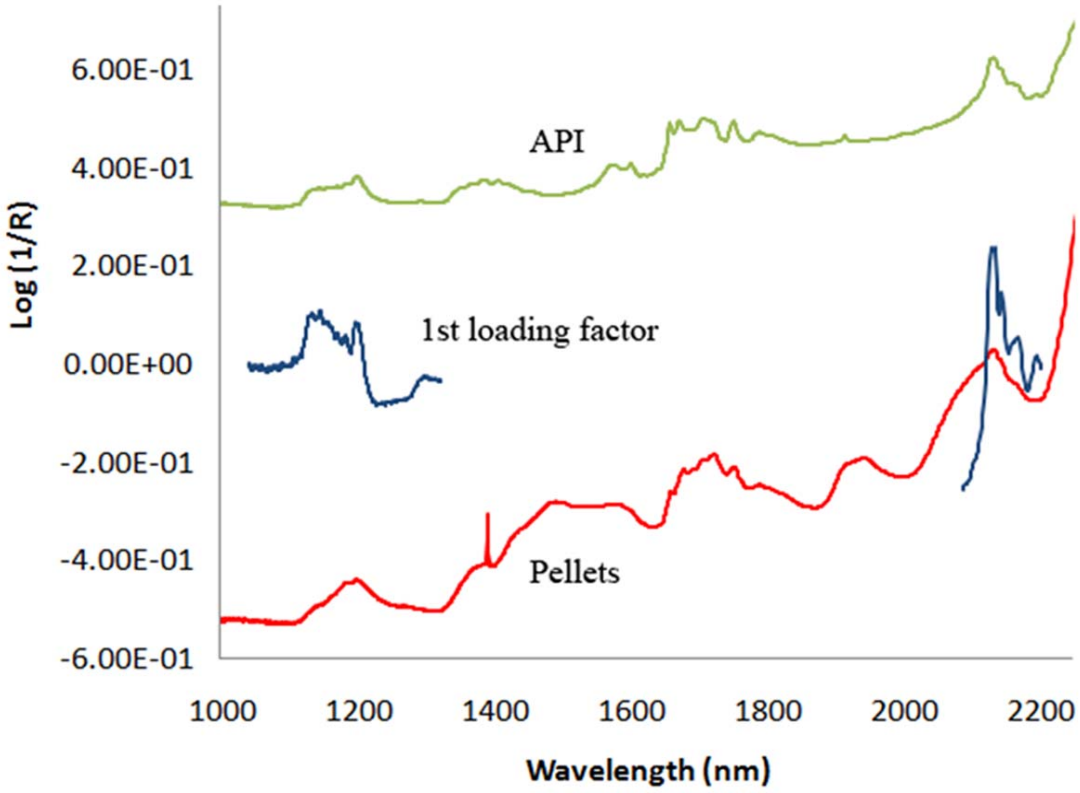

Fig. 5 – FT-NIR spectra of the API, the pharmaceutical pellets and the first loading factor.

MSC was selected as signal pre-processing taking into account that this signal pre-processing reduces the effect of scattered light on diffuse reflection NIR spectra.

Contiguous blocks cross-validation was carried out with the calibration set, the number of data splits was 3, defining each calibration series of measurements as a test set.

4 PLS factors were selected for the NIR model as the RMSECV was the lowest from this number of PLS factors (data not shown).

Considering the RMSEC, RMSECV and RMSEP values, the RMSECV and RMSEP are both low and close to the RMSEC indicating the robustness and the global accuracy of the NIR model. Figure 6(a) shows the agreement observed between the NIR predictions and the reference method results for both the calibration and external validation sets. However, those criteria do not assess the ability of the NIR method to predict the API content of new samples. Therefore, the model predictive performance was evaluated with accuracy profiles computed on the validation results. This innovative approach uses tolerance intervals as statistical methodology that allows predicting a region of concentration where each future result has a defined probability to fall [21-23]. This probability is defined by the analyst. As the focus of the present study is the determination of an API in a pharmaceutical formulation, the acceptance limits were set at ± 5 % for the validation of the NIR method while the probability to obtain results within the tolerance interval was set at 95 %.

The lower and upper limits of quantification (LLOQ and ULOQ) define the range where an analytical method is able to quantify accurately. They are respectively the smallest and highest concentration levels where the β-expectation tolerance intervals are included within the acceptance limits. If the β-expectation tolerance interval never crosses the acceptance limits, then the LLOQ and ULOQ are located at the beginning and at the end of the active content range investigated.

Figure 6(b) displays the accuracy profile computed with the external validation set results. It can be seen from this figure that the validation results concentrations are different from the ones displayed in Figure 6(a). Indeed, for the accuracy profile calculation, it was necessary to perform an alignment on the mean concentration obtained by the reference method per API concentration level to compute repeatability and intermediate precision variance estimates. From this figure, it can be observed that the tolerance interval is narrow and fully included within the ± 5 % acceptance limits. Therefore, each future result has at least 95 % probability to fall within the ± 5 % acceptance limits.

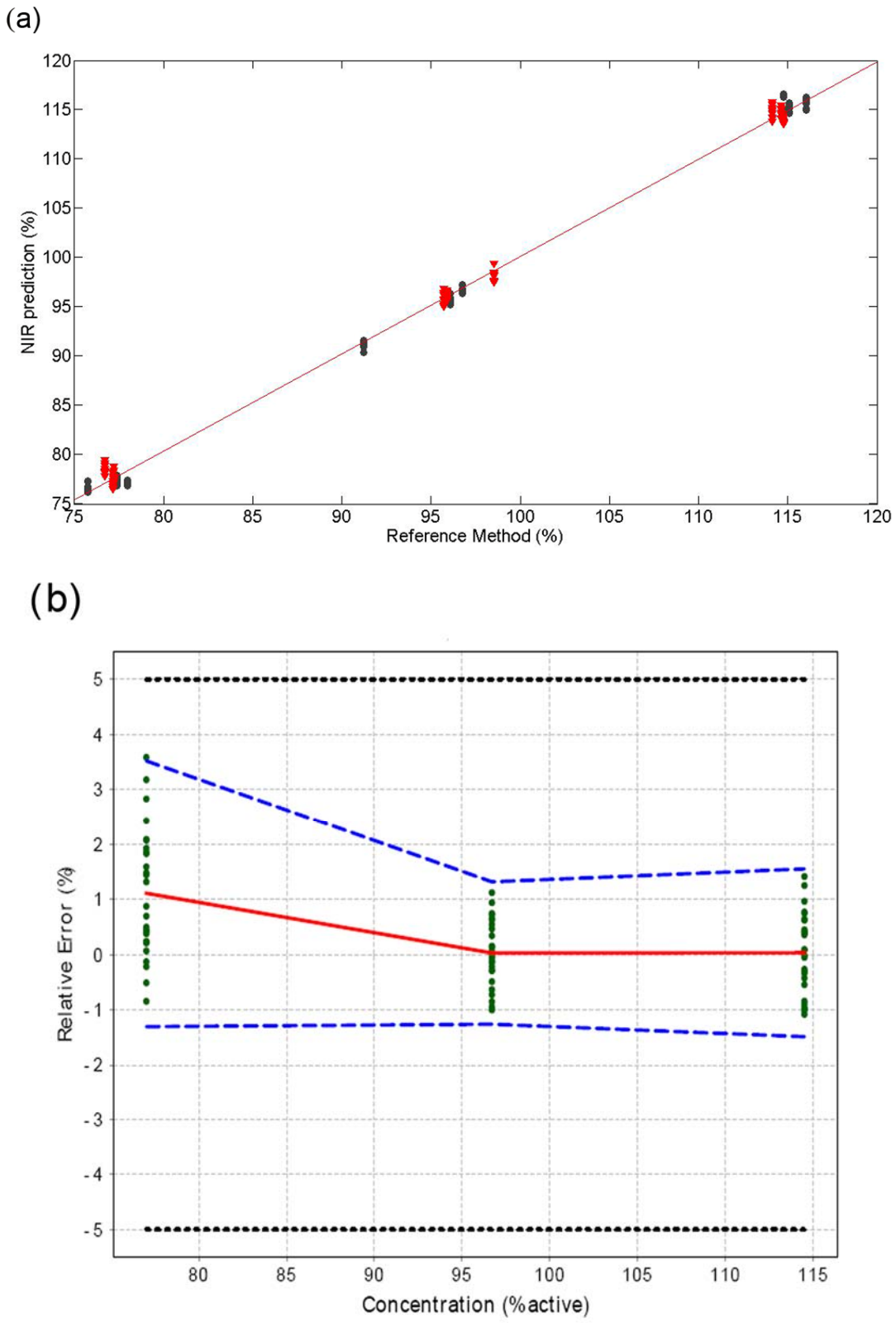

Fig. 6 – NIR method: (a) API NIR predictions versus the Reference Method results. The black dots and the red triangles represent the results of the calibration and validation sets respectively; (b) Accuracy profile based on the validation results of the NIR method. The plain line is the relative bias, the dashed lines are the β-expectations tolerance limits (β = 95 %) and the dotted lines represent the acceptance limits (±5 %).

Table 4 shows the ICH Q2(R1) validation criteria of the developed method. As can be seen from the accuracy profile, the bias is 0 for the 100 and 120 % API levels whereas it is 1.1 % for the 80 % API level. The precision of the method was estimated by measuring repeatability and intermediate precision at the 3 concentration levels investigated. The dispersion of the results observed in the accuracy profile is small for the concentration levels investigated. Consequently, repeatability and intermediate precision are both very satisfactory and never exceed 1.1% as shown in Table 4.

Table 4 – ICH Q2(R1) validation criteria of the NIR method.

Trueness	Concentration level (% API)	Relative bias (%)	
	77.0	1.1	
	96.7	0.0	
	114.5	0.0	
Precision	Concentration level (% API)	Repeatability (RSD %)	Intermediate precision (RSD %)
	77.0	1.1	1.1
	96.7	0.5	0.6
	114.5	0.7	0.7
Accuracy	Concentration level (% API)	β-Expectation tolerance limits (% API)	
	77.0	[76.0 , 79.7]	
	96.7	[95.5 , 98.0]	
	114.5	[112.8 , 116.3]	
LOQ	Lower LOQ (% API)	Upper LOQ (% API)	
	77.0	114.5	
Linearity of results	Intercept	Slope	R^2
	2.43	0.98	0.997

Concerning the linearity of the NIR method, the intercept, and the slope are close to 0 and 1 respectively confirming the absence of proportional and constant systematic error of the model.

The uncertainty characterizes the dispersion of the values that could reasonably be attributed to the measurand [26-27]. Several uncertainty results were generated and are present in Table 5: the uncertainty of bias of the method at each concentration level of the validation standard, the uncertainty which combines the uncertainty of the bias with the uncertainty of the method obtained during the validation step, ie. the intermediate precision standard deviation, and the expanded uncertainty which equals to the uncertainty multiplied by a coverage factor k=2 representing an interval around the results where the unknown true value can be observed with a confidence level of 95% [28-29]. In addition, the relative expanded uncertainties with the corresponding introduced concentrations are not higher than 2.3 %, which means that with a confidence level of 95 %, the unknown true value is located at a maximum of ± 2.3 % around the measured results.

Table 5 – NIR method: estimates of measurements uncertainties related to the API content at each concentration level investigated.

Concentration level (% API)	Uncertainty of the bias (% API)	Uncertainty (% API)	Expanded Uncertainty (% API)	Relative Expanded Uncertainty (% API)
77.0	0.2	0.9	1.8	2.3
96.7	0.2	0.6	1.2	1.2
114.5	0.2	0.8	1.7	1.5

Based on the present feasibility study, accurate quantitative real time monitoring of a pharmaceutical pellet formulation can be achieved with NIR spectroscopy. The present quantitative method is now being transposed in the real manufacturing environment before the capsule filling stage in order to reduce the post-manufacturing laboratory analysis, paving the way for product real time release.

4. Conclusions

The present study confirmed that NIR spectroscopy can be interfaced with a great variety of particle streams to provide reliable real-time qualitative data. Regardless of the particle stream investigated, PCA was able to classify the samples according to their active content, indicating the quality of each interfacing.

The developed quantitative NIR method also revealed that accurate quantitative measurements from moving particles could be achieved with NIR spectroscopy. The validation results in terms of RMSEP indicated the good performance of the model. However, such performance indicator is only related to past results while the main issue is to know how accurate the future results will be. Therefore, the accuracy profile based on tolerance intervals was used to generate a complete validation report. It guaranteed that the future results will be included within the acceptance limits with a defined probability chosen by the analyst. Consequently, such NIR method enables the real time monitoring of products directly from the production line, giving the opportunity to ensure the final product conformity at the end of the manufacturing process itself and thus enabling real-time release (RTR) of the batches.

Acknowledgements

Thanks are due to the Walloon region and Galephar research center M/F for a research grant provided to Jérôme Mantanus and Eric Ziémons. Also, special thanks go to the Fonds Leon Fredericq for a travel grant provided to Jérôme Mantanus. Novo Nordisk A/S is acknowledged for the donation of Bomem FT-NIR spectrometer.

References

[1] United States Food and Drug Administration (FDA), Guidance for industry PAT-A framework for innovative pharmaceutical manufacturing and quality assurance, FDA, 2004.

[2] International Conference on Harmonisation (ICH) of technical requirements for registration of pharmaceuticals for human use, Topic Q9: Quality risk management, Geneva, 2005.

[3] D.A. Burns, E.W., Ciurczak, Handbook of Near-Infrared Analysis, 3rd ed., CRC Press, New York, 2008.

[4] J. Luypaert, D.L. Massart, Y. Vander Heyden, Talanta 72 (2007) 865-883.

[5] C. Bodson, E. Rozet, E. Ziemons, B. Evrard, Ph. Hubert, L. Delattre, J. Pharm. Biomed. Anal. 45 (2007) 356-361. http://hdl.handle.net/2268/1642

[6] J.J. Moes, M.M. Ruijken, E. Gout, H.W. Frijlink, M.I. Ugwoke, Int. J. Pharm. 357 (2008) 108-118.

[7] E.T.S. Skibsted, J.A. Westerhuis, A.K. Smilde, D.T. Witte, J. Pharm. Biomed. Anal. 43 (2007) 1297-1305.

[8] W. Li, L. Bagnol, M. Berman, R.A. Chiarella, M. Gerber, Int. J. Pharm. 380 (2009) 49-54.

[9] H. Grohganz, M. Fonteyne, E. Skibsted, T. Falck, B. Palmqvist, J. Rantanen,, Eur. J. Pharm. Biopharm. 74 (2010) 406-412.

[10] S.S. Rosa, P.A. Barata, J.M. Martins, J.C. Menezes, Talanta 75 (2008) 725-733.

[11] J. Mantanus, E. Ziémons, P. Lebrun, E. Rozet, R. Klinkenberg, B. Streel, B. Evrard, Ph. Hubert, Anal. Chim. Acta 642 (2009) 186-192. http://hdl.handle.net/2268/18780

[12] J. Mantanus, E. Ziémons, P. Lebrun, E. Rozet, R. Klinkenberg, B. Streel, B. Evrard, Ph. Hubert, Talanta 80 (2010) 1750-1757. http://hdl.handle.net/2268/26616

[13] J. Rantanen, S. Lehtola, P. Rämet, J.P. Mannermaa, J. Yliruusi, Powder Technol. 99 (1998) 163-170.

[14] J. Rantanen, E. Räsänen, O. Antikainen, J.P. Mannermaa, J. Yliruusi, Chemom. Intel. Lab. Syst. 56 (2001) 51-58.

[15] N. Sandler, J. Rantanen, J. Heinämäki, M. Römer, M. Marvola, J. Yliruusi, AAPS PharmSciTech 6 (2) (2005) 174-183.

[16] S.H. Tabasi, V. Moolchandani, R. Fahmy, S.W. Hoag, Int. J. Pharm. 382 (2009) 1-6.

[17] L. Maurer, H. Leuenberger, Int. J. Pharm. 370 (2009) 8-16.

[18] C. Ravn, E. Skibsted, R. Bro, J. Pharm. Biomed. Anal. 48 (2008) 554-561.

[19] M. Blanco, M. Alcalá, M. Bautista, Eur. J. Pharm. Sci. 33 (2008) 409-414.

[20] International Conference on Harmonization (ICH) of Technical requirements for registration of pharmaceuticals for human use, Topic Q2 (R1): Validation of analytical Procedures: Text and Methodology, Geneva, 2005.

[21] Ph. Hubert., J.J. Nguyen-Huu, B. Boulanger, E. Chapuzet, P. Chiap, N. Cohen, P.A. Compagnon, W. Dewé, M. Feinberg, M. Lallier, M. Laurentie, N. Mercier, G. Muzard, C. Nivet, L. Valat, J. Pharm. Biomed. Anal. 36 (2004) 579-586. http://hdl.handle.net/2268/6169

[22] Ph. Hubert, J.J Nguyen-Huu, B. Boulanger, E. Chapuzet, P. Chiap, N. Cohen, P.A. Compagnon, W. Dewé, M. Feinberg, M. Lallier, M. Laurentie, N. Mercier, G. Muzard, C. Nivet, L. Valat, E. Rozet, J. Pharm. Biomed. Anal. 45 (2007) 70-81. http://hdl.handle.net/2268/6170

[23] A. Bouabidi, E. Rozet, M. Fillet, E. Ziémons, E. Chapuzet, B. Mertens, R. Klinkenberg, A. Ceccato, M. Talbi, B. Streel, A. Bouklouze, B. Boulanger, Ph. Hubert, J. Chrom. A. 1217 (2010) 3180-3192. http://hdl.handle.net/2268/29471
[24] http://wiki.eigenvector.com/index.php?title=Using_Cross-Validation (accessed 26/02/10).
[25] M. Andersson, O. Svensson, S. Folestad, M. Josefson, K.-G. Wahlund, Chemom. Intel. Lab. Syst. 75 (2005) 1-11.
[26] Analytical Methods Committee, Uncertainty of measurement: implication of its use in the Analytical Science, Analyst 120 (1995) 2303-2308.
[27] Eurachem/Citac guide, Quantifying the uncertainty in analytical measurement, second ed., 2000.
[28] CB EA-4/16, EA guidelines on the expression of uncertainty in quantitative testing, http://www.european-accreditation.org (2004)
[29] R.D. Marini, P. Chiap, B. Boulanger, S. Rudaz, E. Rozet, J. Crommen, Ph. Hubert, Talanta 68 (2006) 1166-1175. http://hdl.handle.net/2268/18790

Section III.2.3.

Polymeric formulation: Near infrared and Raman spectroscopy as Process Analytical Technology tools for the manufacturing of silicone-based drug reservoirs

J. Mantanus, E. Rozet, K. Van Butsele, C. De Bleye, A. Ceccato, B. Evrard, Ph. Hubert, E. Ziemons, Anal. Chim. Acta 699 (2011) 96.

Summary

Using Near Infrared (NIR) and Raman spectroscopy as PAT tools, 3 critical quality attributes of a silicone-based drug reservoir were studied. First, the Active Pharmaceutical Ingredient (API) homogeneity in the reservoir was evaluated using Raman spectroscopy (mapping): the API distribution within the industrial drug reservoirs was found to be homogeneous while API aggregates were detected in laboratory scale samples manufactured with a non optimal mixing process. Second, the crosslinking process of the reservoirs was monitored at different temperatures with NIR spectroscopy. Conformity tests and Principal Component Analysis (PCA) were performed on the collected data to find out the relation between the temperature and the time necessary to reach the crosslinking endpoints. An agreement was found between the conformity test results and the PCA results. Compared to the conformity test method, PCA had the advantage to discriminate the heating effect from the crosslinking effect occurring together during the monitored process. Therefore the 2 approaches were found to be complementary. Third, based on the HPLC reference method, a NIR model able to quantify the API in the drug reservoir was developed and thoroughly validated. Partial Least Squares (PLS) regression on the calibration set was performed to build prediction models of which the ability to quantify accurately was tested with the external validation set. The 1.2 % RMSEP of the NIR model indicated the global accuracy of the model. The accuracy profile based on tolerance intervals was used to generate a complete validation report. The 95 % tolerance interval calculated on the validation results indicated that each future result will have a relative error below ±5 % with a probability of at least 95 %. In conclusion, 3 critical quality attributes of silicone-based drug reservoirs were quickly and efficiently evaluated by NIR and Raman spectroscopy.

1. Introduction

Quality by Design (QbD) is a scientific, risk-based, holistic and proactive approach to the Pharmaceutical Development [1] based on the fact that quality should not be tested into products, but it should rather be built in or integrated by design [2]. The additional knowledge provided by such a scientific approach may then support the Pharmaceutical Quality System (PQS) [3].

Silicone polymers are one of the mostly used synthetic and non-degradable polymers. Biocompatibility, minimal tissue reaction, biological inertness, chemical and thermal stability, mechanical properties and easy processability are some of the reasons justifying their widespread use in medical and pharmaceutical applications [4-6]. Due to their excellent diffusion properties, they allow drugs to be delivered in a therapeutic amount that might have not been possible with other polymeric systems. The present study formulation consists in silicone-based long-term implant products containing one active substance.

FDA's Process Analytical Technology (PAT) is part of the QbD concept, it focuses on "*improving the pharmaceutical development, manufacturing and quality assurance through innovation in product and process development, process analysis and process control*" [7].

According to the PAT framework, the critical manufacturing steps related to the final product quality have first to be identified [7]. Concerning the long-term implant manufacturing, the raw materials mixing is the first critical step: the crosslinking uniformity is dependent on the homogeneity of the raw materials. Besides, the API has to be uniformly distributed inside the excipient matrix to always provide the same release profile. The second critical step is the crosslinking step which completion time is influenced by the temperature. Moreover, the rate of drug diffusion in the polymer directly relies on the crosslinking status of the drug reservoir [8]. Secondly, proper process measurement systems must be selected. The information given by those systems may eventually provide a better understanding of the manufacturing process, giving opportunities for process control strategies to prevent or mitigate the risk of producing a poor quality product [9]. The challenge still remains to interface process analytical analyzers with a polymeric pharmaceutical formulation.

Near infrared (NIR) and Raman spectroscopy belong to vibrational spectroscopy [10-12]. Both techniques share several advantages, such as fast spectral acquisition, minimization of sample preparation and/ or destruction and the use of probes allowing at-line, on-line and in-line analysis [10-13].

Raman spectrum has the advantage of revealing raw materials specific peaks, making this technique a very powerful tool for identification purposes. Contrary to Raman spectroscopy, the vibrations observed in the near infrared spectral range lead to overlapping bands which contain both physical and chemical information. Consequently, more chemometrics are needed to extract the significant information out of NIR spectra [10, 12, 14].

Based on those advantages, NIR and Raman spectroscopy matches the process measurement system requirements of the PAT framework. They have indeed already been part of PAT applications to monitor critical process attributes such as blend homogeneity, polymorphism, coating level, moisture content, and active content, at-line or in-line [15-33].

Saerens et al [34] demonstrated the potentiality of Raman spectroscopy as a PAT-tool for in-line determination of the API concentration and the polymer-drug solid state during pharmaceutical holt-melt extrusion. Within the framework of the optimisation of a silicone-based drug reservoir manufacturing process, 3 critical quality attributes of the formulation were first identified: the API homogeneity within the reservoir, the crosslinking state of the drug reservoir and the API content of the reservoir. In addition, there was also a need for process analyzers able to accurately assess these critical quality attributes. Accordingly, the aim of the present study was to take advantage of NIR and Raman spectroscopy as PAT tools for the control of the 3 identified critical quality attributes. First, using Raman spectroscopy (mapping), the homogeneity of the drug reservoirs was checked. Second, using NIR spectroscopy, the influence of the temperature in the crosslinking process was studied to evaluate the appropriate working temperature during the manufacturing process. Further, the ability of NIR spectroscopy to predict the crosslinking status of new samples was evaluated. Finally, for an In Process Control (IPC) purpose, a NIR method able to predict the API content in the reservoirs was developed and validated. The present study is one of the first applications of NIR and Raman spectroscopy for the evaluation of a polymeric pharmaceutical formulation.

2. Experimental

2.1. Long-term implant samples

The studied implant formulation consists in a 50/50 (w/w) mixture between the API and poly(dimethylsiloxane) (PDMS).

This formulation will later on be called 100 % API formulation. The ratio of the raw materials was modified in order to also manufacture 80, 90, 110 and 120 % API formulations.

The industrial implant samples are manufactured as follows. A PDMS mixture is prepared by mixing 3 components: the silicone base (hydroxyterminated PDMS), a crosslinker and a catalyst. Next, the previous blend is mixed together with the API. This final mixture is then injected into thermostating moulds for the crosslinking process. At the end of the crosslinking step, the implants are removed from the moulds. The final product then goes to the packaging steps. The industrial implants look like pierced cylinders.

2.2. Raman equipment

Raman spectra were collected with a dispersive spectrometer, the RamanStation 400F (Perkin Elmer, Massachusetts, USA) equipped with a two-dimensional CCD detector (1024 * 256 pixel sensor).The laser excitation wavelength used was 785 nm. The spectral coverage was 250-3400 cm^{-1} and the spectral resolution was equal to 2 cm^{-1}. One accumulation with a 1 second exposure time was performed per sample mapping point. A cosmic ray filter was applied. The distance between 2 consecutives mapping measurements was 0.2 mm. During the mapping spectral acquisition, one background spectrum was collected every 20 minutes. The spectra were collected with the Spectrum software version 6.3.2.0151 (Perkin Elmer) while the mapping data were treated with the Spectrum IMAGE software version R1.6.2.0378 (Perkin Elmer).

2.3. Sample preparation for Raman mapping

Raman mapping was performed with implants transverse and longitudinal sections as shown in Figure 1(a). Because of the shape of the implants, a home-made sample holder providing a flat surface and constant sample thickness was used. As can be seen in Figure 1(b), it consists in a transmission cell equipped with quartz windows. The optical path length is defined by a Teflon spacer with a constant 0.5 mm thickness.

The typical number of spectra collected for the mapping of longitudinal and transverse section is 1150 and 850, respectively.

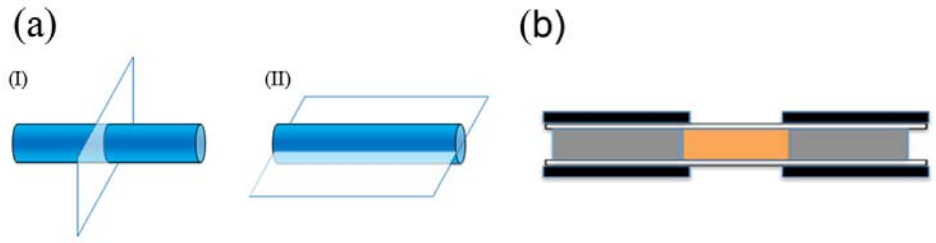

Fig. 1 – (a) Transverse (I) and longitudinal (II) sections of silicone-based drug reservoirs. (b) Home-made transmission cell used for the Raman mapping sample preparation. The white boxes, the grey boxes and the orange box represent the quartz windows, the Teflon spacer and the sample, respectively.

2.4. FT-NIR equipment

The samples were analyzed with a multipurpose analyzer Fourier transform near infrared spectrometer (MPA, Bruker Optics, Ettlingen, Germany) equipped with a semiconductor room temperature sulfide lead (RT-PbS) detector. For the crosslinking study, the NIR spectra were collected with a NIR reflectance probe for solids (probe head length = 80 mm; probe diameter = 10 mm). A background spectrum using a Spectralon® diffuse reflectance standard (Labsphere, North Sutton, USA) was acquired before each series of measurements. For quantitative purpose, the drug reservoirs were analyzed with the integrating sphere module of the spectrometer which allows reflectance measurement of an 18 mm sample area. An internal computer-controlled reference wheel enables an automatic background spectrum acquisition without the need to remove the sample from the integrating sphere window.

The spectra were collected with the Opus Software 6.5 (Bruker Optics). Each spectrum was the average of 32 scans and the resolution was 8 cm^{-1} over the range from 12500 to 3600 cm^{-1}. The time necessary for a NIR measurement was 6 seconds.

2.5. Sample preparation for the crosslinking study

Labscale raw materials mixtures were prepared. Instead of injecting them into the thermostating moulds, aliquots were transferred into vial caps and thermostated during the crosslinking step at different temperatures. The thermostating system consists in a thermostating bath filled with silicone-oil. In the present study, each sample is manufactured independently.

2.6. Crosslinking NIR interfacing

The samples were non-invasively interfaced with a NIR reflectance probe during the crosslinking process. The distance between the probe and the samples was 2 mm. One NIR spectrum was acquired every 30 or 60 seconds according to the crosslinking speed.

2.7. API NIR determination in the drug reservoirs: sample presentation

In order to present the sample to the NIR spectrometer, the drug reservoir shape was imprinted in modelling material oven hardening making a sample holder fitted to the reflection window. However, when placed in the sample holder, only one side of the sample was scanned. Therefore, the two sides of each sample were measured and the average of the two spectra was derived as the experimental result.

2.8. API NIR determination in the drug reservoirs: calibration and validation protocols

An experimental protocol was followed for the calibration and validation steps to develop and validate a robust near infrared model. Sources of variability such as industrial batches, pilot batches, manufacturing, API concentration levels and days were introduced in the calibration and validation protocols. The NIR spectra were first recorded before performing the API determination with the HPLC reference method.

2.9. Multivariate data analysis

Conformity tests were performed with the Opus software 6.5 (Bruker Optics). For each sample conformity test calculation, reference spectra, i.e. spectra of the fully crosslinked sample, are first selected. The average and the standard deviation *(σ)* of the absorbance values for each of the *i*th wavelength selected of the reference spectra are then calculated. Based on those values, a Conformity Index (CI) limit can be calculated or selected, defining which amount of variations on each selected spectral wavelength is acceptable for a particular product.

Second, the closeness of agreement between the test sample, i.e. spectrum of the sample acquired during the crosslinking process, and the reference spectra is checked. The difference between this sample and the average of the reference samples is calculated on each selected wavelength *i*. This absolute deviation is now weighted by the corresponding standard deviation σ on the respective wavelength, which results in a relative deviation referred to as Conformity Index (CI).

$$CI = (A_{reference,i} - A_{sample,i}) / \sigma_{reference,i}$$

Where, for wavelength *i*, $A_{reference}$ is the absorbance of the reference spectra, A_{sample} is the absorbance of a test spectrum and $\sigma_{reference}$ is the standard deviation between the reference spectra.

Considering a sample spectrum collected at a defined test time, the corresponding CI test result is generated using the following two steps procedure. First, the sum of spectral data points exceeding the CI limit is calculated. Second, the previous sum is divided by the total number of data points within the frequency range selected, this last value being the CI test result.

First derivative (order: 2, window: 15 points, corresponding to 57.75 cm^{-1}) and Standard Normal Variate (SNV) were used as signal pre-processings. Principal Component

Analysis (PCA) [35] and Partial Least Squares regression (PLS regression) [36] using random subsets cross-validation were carried out with PLS Toolbox 5.0 for Matlab version 7.6 (Eigenvector Research Inc, Wenatchee, USA).

For the random subsets cross-validation, *s* different test sets are determined through random selection of *n/s* objects in the data set (n being the total number of objects), such that no single object is more than one test set. This procedure is repeated *r* times, where *r* is the number of iterations [37].

3. Results and discussion

3.1. Raman spectroscopy (mapping) results

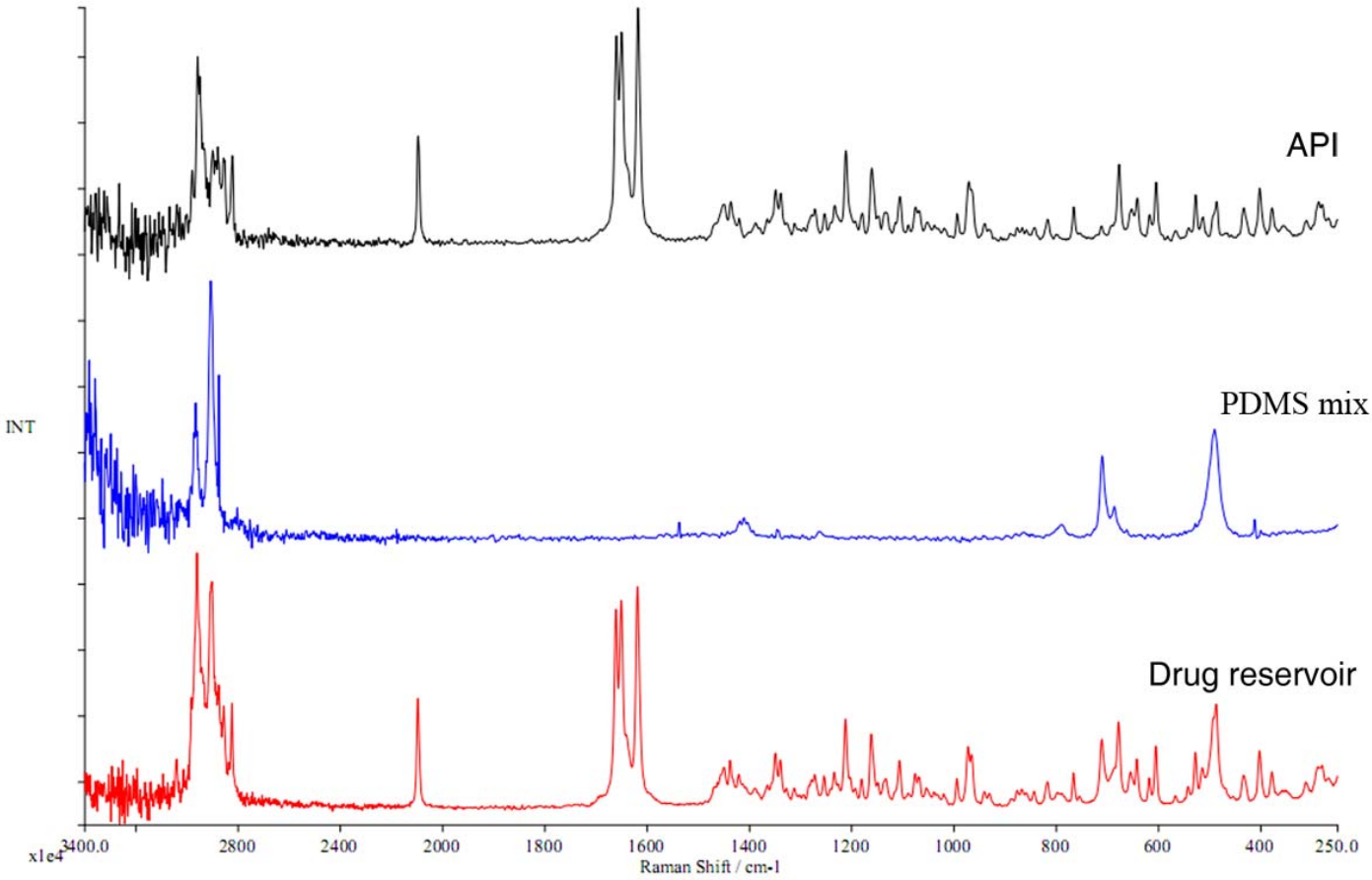

Fig. 2- API (black), PDMS mixture (blue) and drug reservoir (red) Raman spectra.

Based on the Raman spectra displayed in Figure 2, it can be seen that the API has a major specific peak at 2090 cm^{-1}. On the other hand, the polymer has also 2 specific absorption bands at 700 and 500 cm^{-1}. In order to compare the spectra collected during the Raman mapping acquisition, the Normalization function of the Spectrum IMAGE software (Perkin Elmer) was used. A common peak linked to the polymer was first selected: the 700 cm^{-1} polymer peak (start 698 cm^{-1}, end 726 cm^{-1}). The Zero Point at which the baseline was

corrected was 740 cm^{-1}. Based on these settings, the 700 cm^{-1} polymer peak was set to the same ordinate limit in all the spectra. Other peaks in the collected spectra could then be compared. For the evaluation of the API homogeneity within the reservoir matrix, the spectral area variations of the 2090 cm^{-1} API peak were derived as the mapping test result.

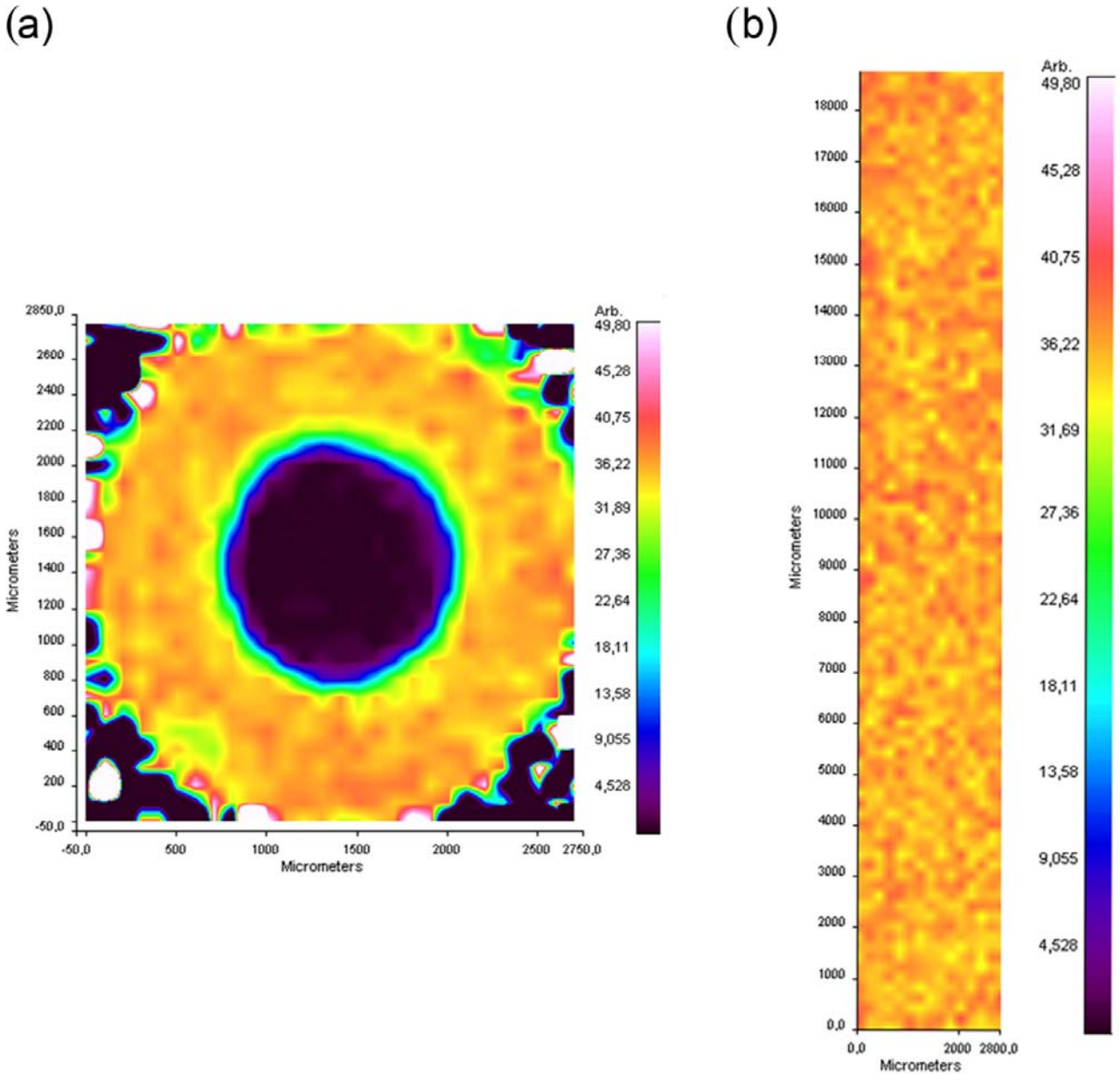

Fig. 3 – Raman mapping of an industrial implant sample (a) transverse and (b) longitudinal section.

Figure 3a) and 3b) show the mapping results of a transverse and longitudinal section of an industrial implant. The color homogeneity displayed in Figure 3 indicates that the API distribution within the drug reservoirs is homogeneous. This was confirmed by the 4.58 % RSD of the 2090 cm^{-1} API peak area.

Further, the ability of Raman mapping to detect poor API distribution within the drug reservoir was challenged. Lab scale pilot samples with a non optimal mixing process were manufactured.

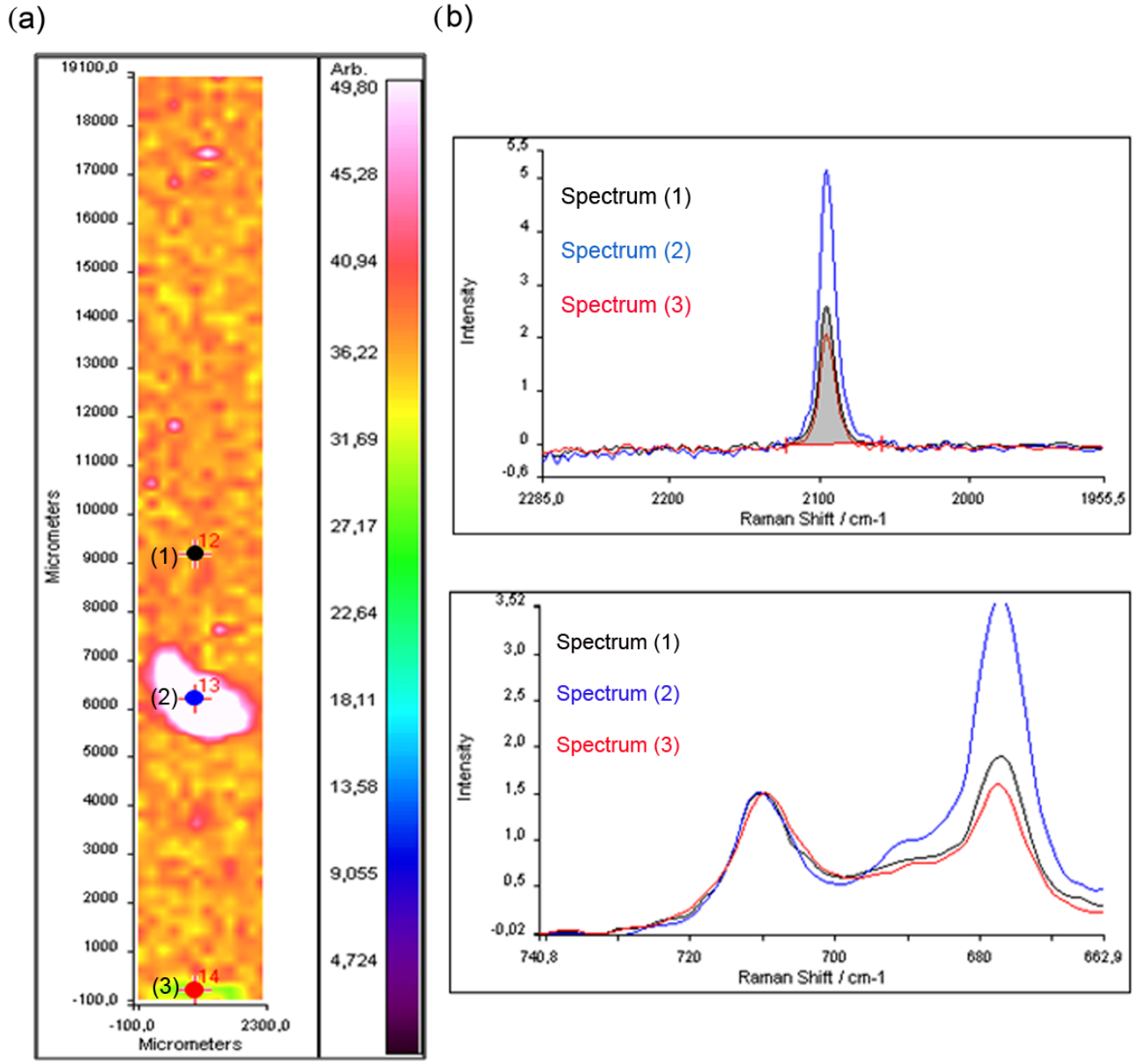

Fig. 4 – Raman mapping result of a laboratory scale drug reservoir with poor API homogeneity and the spectra associated with mapping locations (1), (2) and (3).

Figure 4 displays the Raman mapping results of a laboratory scale drug reservoir longitudinal section and the spectra corresponding to 3 mapping locations. The mapping results visually indicate that mapping locations (1), (2) and (3) correspond to 3 different API concentration areas. The previous consideration was confirmed by the corresponding spectra: the peak area, expressed in arbitrary unit, of the 2090 cm^{-1} API peak is 37 for measurement (1) while it 75 and 30 for measurement (2) and (3) respectively. The same observations can be obtained if considering the API peak at 680 cm^{-1}.

Consequently, Raman mapping was able to detect poor and good product performance related to the API distribution.

3.2. Crosslinking study

To study the crosslinking process at the earliest stages, thermostated samples were interfaced with NIR spectroscopy directly after the raw materials mixing. Samples were thermostated at temperatures ranging from 20 to 80 °C to investigate the influence of the temperature on the crosslinking process.

First, the spectra of the PDMS mixture, the API and the implant were checked to select a spectral range linked to the crosslinking process. As can be seen from Figure 5, the PDMS mixture spectrum has a significant impact on most of the absorption bands of the final product, especially the 8929.3-4493.6 cm^{-1} spectral range. This spectral range was therefore selected for the calculation of the conformity tests. 1st derivative was selected as the signal pre-processing as it reduces the baseline off-set occurring between the collected spectra.

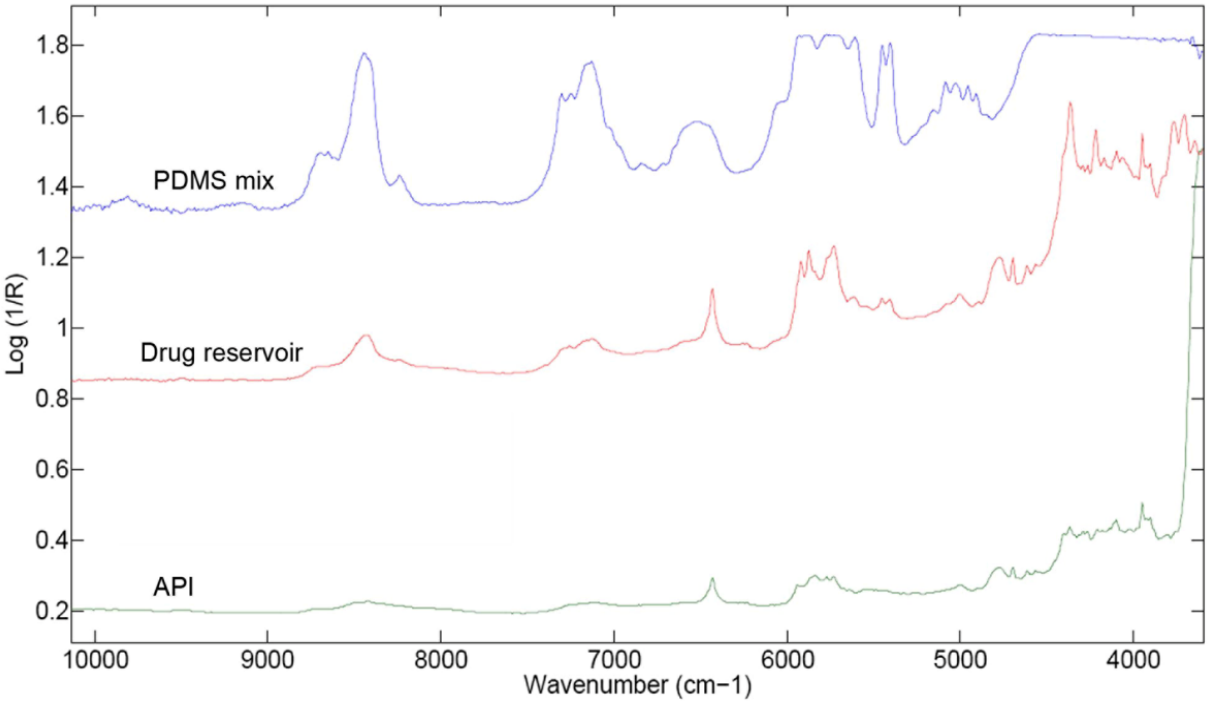

Fig. 5 – PDMS mixture, API and drug reservoir NIR reflectance raw spectra. The 8929.3-4493.6 cm^{-1} spectral region was selected for the conformity tests. The 8837-8181, 7679-6715, 6367-5981, 5364-4823 and 4708-4495 cm^{-1} spectral ranges were selected for the PCA. The 7224-6495 and 6360-4500 cm^{-1} spectral ranges were selected for the PLS model.

Reference spectra, i.e. spectra of the fully crosslinked corresponding sample, were selected for the conformity test calculation. As the time necessary for crosslinking completion was unknown, a long NIR monitoring was set. In order to determine the number of reference spectra the following methodology was followed. First a 3 parameters logistic

function was fitted on the observed data (Sum over CI vs Time) and the residual error of the fit was computed. Then the last half of the number of spectra not exceeding 2 times the residual error was defined as the number of reference spectra. The last half was only selected for reference spectra in order to further ensure the completion of the crosslinking kinetic. Based on this methodology the number of reference spectra was defined as 16 spectra. The CI limit was determined by monitoring a fully crosslinked sample at ambient temperature (24 °C). When test spectra had a [Sum over CI > Limit (/N total)] below 0.1, meaning that those tests spectra were identical to the reference spectra, it was concluded that the monitored sample was fully crosslinked.

(a)

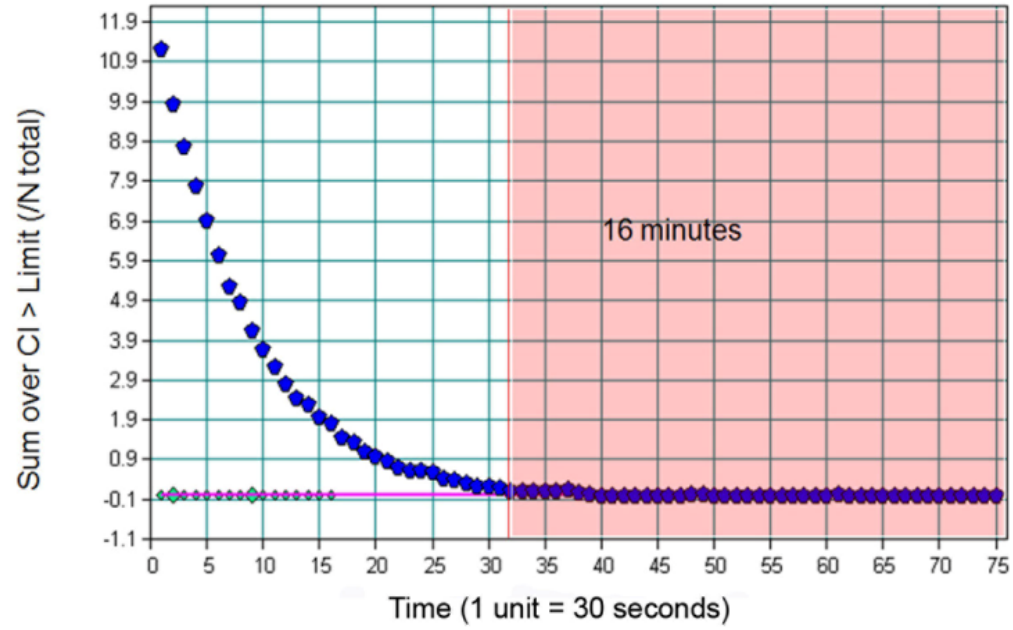

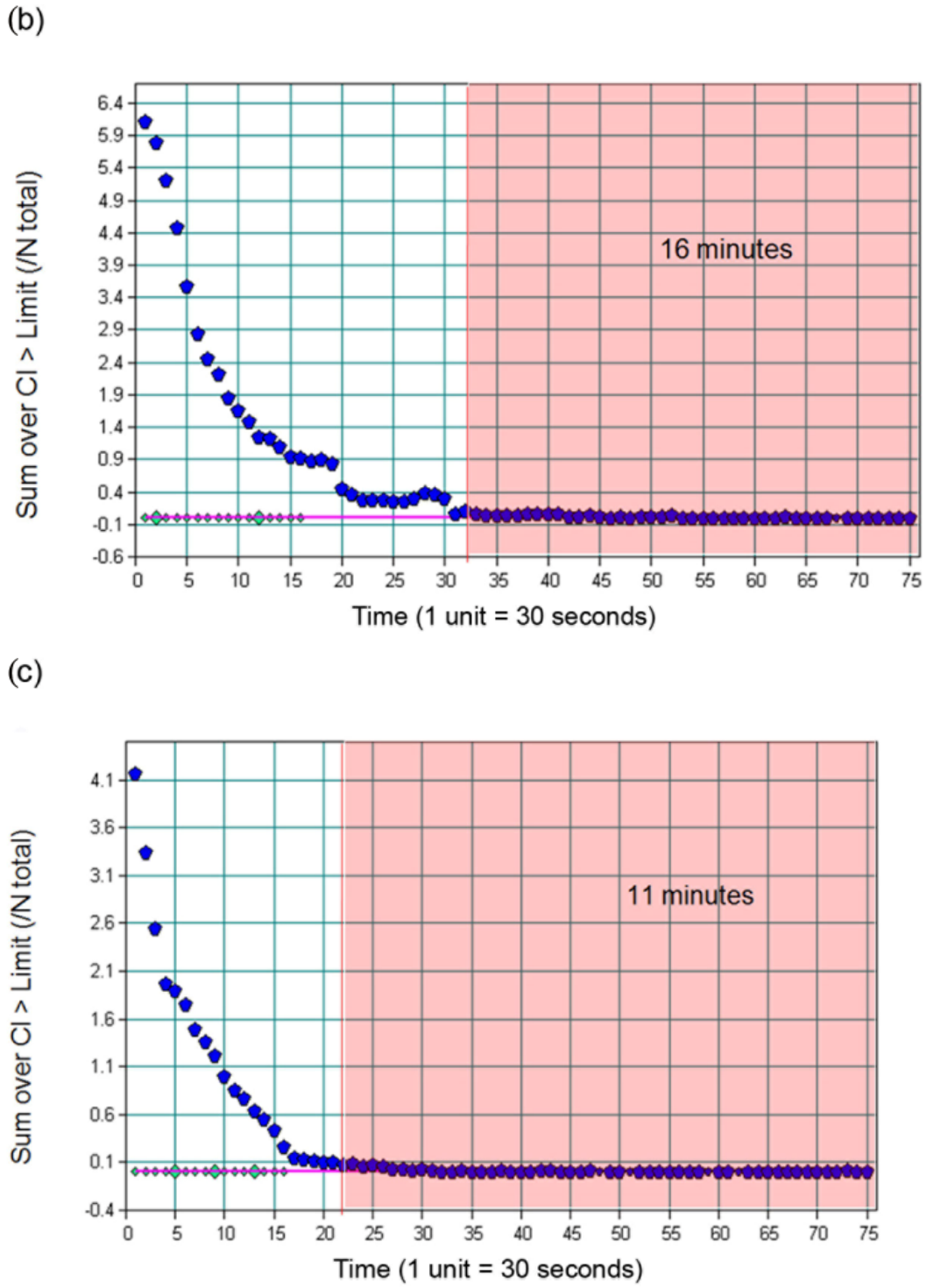

Figu. 6 – Spectral deviations observed while NIR monitoring samples thermostated at 80 °C. (a) Crosslinking kinetic of a sample monitored directly after the raw materials mixing. (b) Crosslinking kinetic of a sample that was previously stored at – 20 °C during 24 hours to avoid the start of the crosslinking process. (c) A fully crosslinked sample is monitored.

Figure 6(a) displays the crosslinking kinetic of a sample thermostated at 80 °C. As the crosslinking process at that temperature was expected to be fast, one NIR spectrum was collected every 30 seconds. As shown in Figure 6(a), the CI test result of the NIR spectra was

below 0.1 from spectrum number 32, meaning that the crosslinking completion time was reached after 16 minutes.

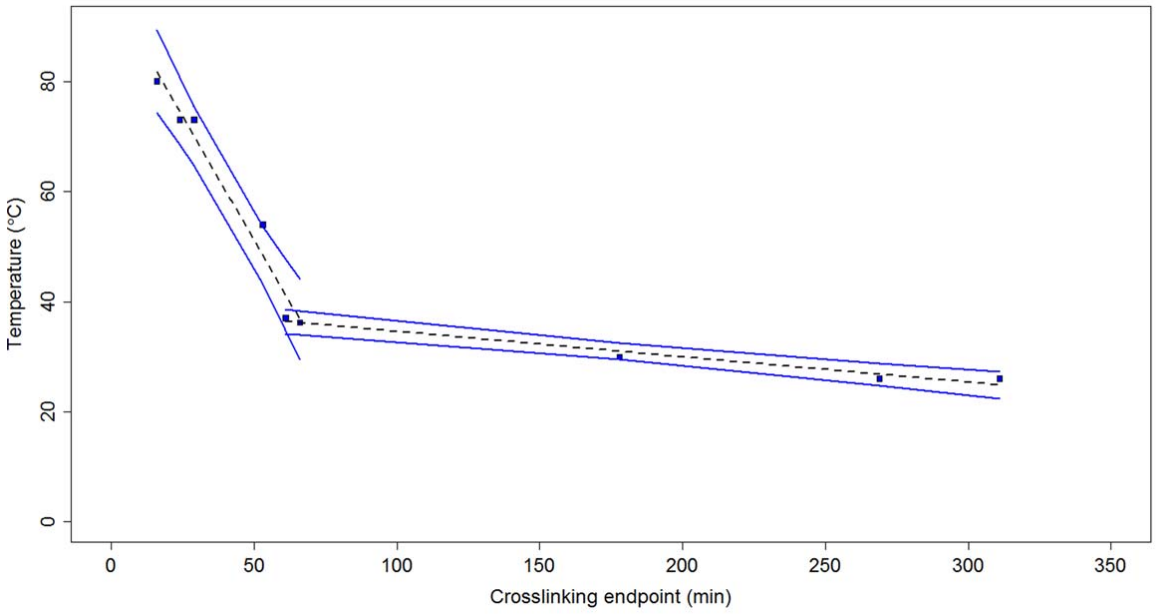

Fig. 7 – Relation between the temperature and the crosslinking endpoint. The blue lines represent the 95 % confidence intervals.

8 other independent crosslinking experiments were planned to find out the relation between the temperature and the time necessary to reach the crosslinking completion time. The results are summarized in Figure 7. It can be seen that the higher the temperature is, the sooner the crosslinking completion time is reached. However, the relation between these 2 factors is not linear and clearly shows 2 different kinetics: below 35 °C, the value of the crosslinking endpoint increases dramatically. On the other hand, from 70-80 °C, the crosslinking endpoint is the lowest and might not decrease significantly with higher temperatures. In addition, if the second slope of relationship between the temperature and the crosslinking endpoint is extrapolated to – 20 °C, Figure 7 shows that a very important time period would be required before observing a change in the crosslinking state. Based on this observation, it can be reasonably assumed that sample storage at – 20 °C during 24 hours could avoid the start of the crosslinking process.

To learn more about the influence of the storage conditions on the crosslinking process, part of the raw materials mix used for the 80 °C crosslinking experiment was stored at – 20 °C during 24 hours. Figure 6(b) shows the crosslinking kinetic of that sample. The calculated endpoint was the same as the one calculated with the storage free experiment: 16 minutes. Consequently, samples storage at -20 °C during 24 hours seems appropriate to prevent the crosslinking process. Hence, the raw materials do not necessarily need to go through the crosslinking step directly after the raw materials mixing. Some of them may be

stored at low temperature during a defined period of time and still provide the adequate final product performance.

Based on the previous experiments, conformity tests seem to be adequate method to monitor the crosslinking process. However, it is unclear whether the spectral deviations highlighted by the conformity test are solely caused by the crosslinking process. Hence, a fully crosslinked sample was thermostated at 80 °C. The entire thermostating process was interfaced with NIR spectroscopy. Although the sample crosslinking status was constant during the experiment Figure 6(c) shows that another process with a different type of kinetic was also monitored. The calculated process endpoint is 11 minutes. This result may suggest that the thermostating process is also monitored when calculating conformity tests. However, it seems that the thermostating process takes less time than the crosslinking process. One can then presume that the crosslinking endpoints of the previous experiments were not influenced by the thermostating process.

Facing the previous observations, PCA was then performed on the collected data to confirm the reliability of the conformity test results.

First, a PCA model based on crosslinking experiments performed between 24 and 74 °C was built, the scores of PC 3 against PC 2 are plotted in Figure 8. In order to increase the percentage of variance explained by those PCs, the spectral range selected for the conformity tests was optimized. PC 3 classifies the spectra according to the reservoirs crosslinking status. Non-crosslinked and fully crosslinked spectra are located respectively at the top and at the bottom of PC 3. Besides, an agreement was found between the conformity test results and the PCA results: the crosslinking endpoints determined by the conformity tests, the black triangles surrounded by red, correspond to the end of the crosslinking process highlighted by the PCA. The 95 % confidence interval computed with the crosslinking endpoints defined by the conformity tests contains the crosslinking endpoints of the calibration data. Furthermore, it can be seen that PC 2 classifies the samples according to their respective thermostating temperature. When the thermostating temperature is close to the ambient temperature, no deviations are observed according to PC 2, meaning that those samples are already close to the thermostating temperature. On the other hand, when a sample is thermostated at 74 °C for example (sample Cal T74 represented by green crosses), it undergoes trough a heating period before reaching its thermostating temperature. The heating period of that sample is clearly visible in Figure 8 when the green crosses are projected on the PC 2 axis.

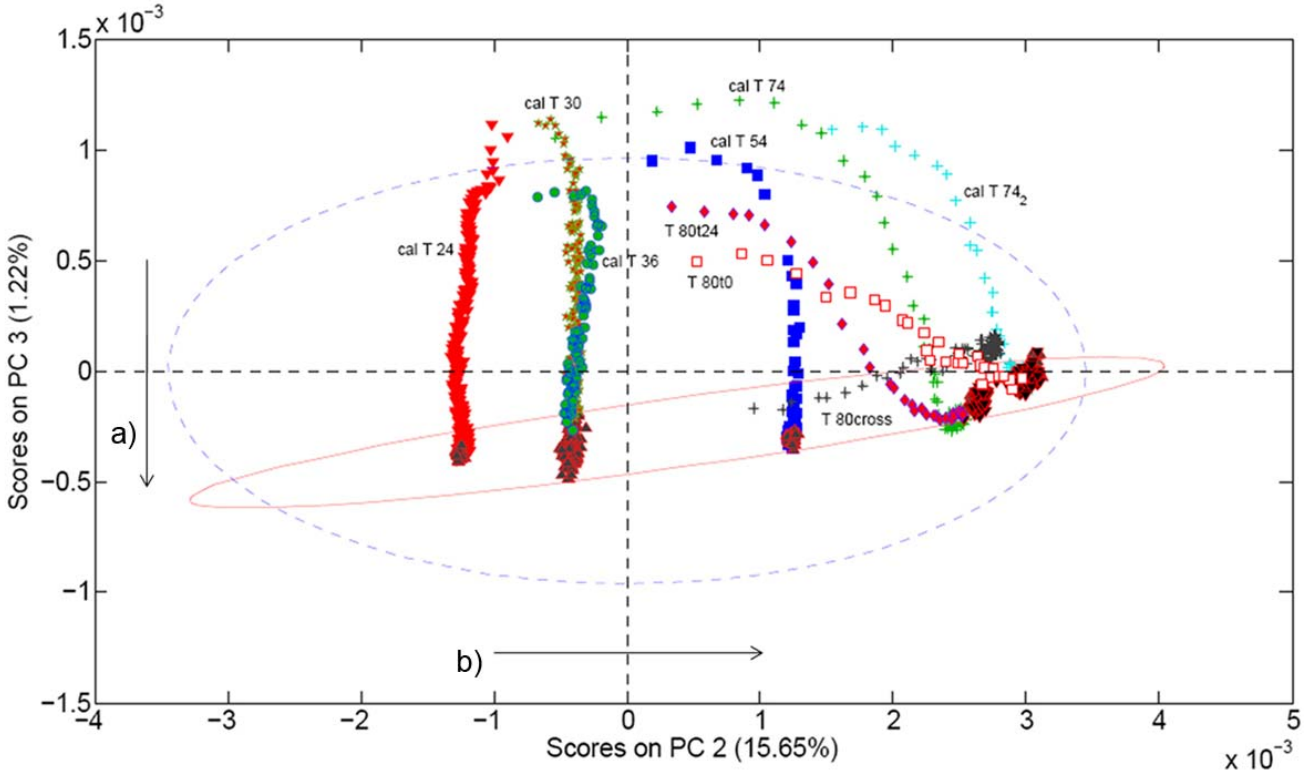

Fig. 8 – NIR PCA model calculated with drug reservoirs thermostated at 24, 30, 36, 54 and 74 °C [cal T 24 (red triangles), cal T 30 (red stars surrounded by green), cal T 36 (green circles surrounded by blue), cal T 54 (blue squares), and cal T 74 (green crosses) and cal T 74_2 (blue crosses)] while crosslinking. The black triangles surrounded by red correspond to the crosslinking completion times determined by the CI method. T 80t0 (white squares surrounded by red), T 80t24 (pink diamonds surrounded by blue) represent respectively test samples thermostated at 80 °C after the raw materials mixing and after 24 hours storage at -20 °C. T 80cross (black crosses) is a fully crosslinked sample that was thermostated at 80 °C. The a) and b) arrows represent the crosslinking and thermostating status of the samples, respectively. The dashed blue ellipse is the 95 % confidence interval calculated on the the calibration data. The red continuous ellipse represents the 95 % confidence interval calculated with the black triangles surrounded by red (crosslinking completion times determined by the CI method).

The developed PCA model was then tested with spectra collected during crosslinking experiments performed at 80 °C. Regarding the 2 uncrosslinked samples thermostated at 80 °C, the PCA results suggest that the 24 hours sample storage at – 20 °C did not influence significantly the crosslinking process: The 2 crosslinking processes when projected on PC 3, the PC axis that models the crosslinking process, end at the same level. Besides, the PCA prediction agreed with the CI method for those samples.

PCA also revealed that the spectral deviations highlighted by the CI method for the crosslinked sample were caused by the temperature. Concerning this particular sample, which crosslinking status was constant, only the results projected on PC 2 varies significantly. Indeed, the only process monitored here was the heating process. Hence, for this last sample, the endpoint determined by the conformity test was the heating endpoint.

Consequently, a conformity test can be useful for process endpoint determination but one has to be aware that this is not a discriminating technique: the test will take into account any factor that induces spectral variation regardless of the monitored process. Therefore, the discriminating ability of PCA must be used to check the relevance of the conformity test results.

3.3. NIR results: API determination in the drug reservoirs

Table 1 – Calibration and validation protocols.

Introduced sources of variability	Calibration set	Validation set
Batch type	- 2 industrial batches (100 % API level) - 13 pilot batches	- 1 industrial batch (100 % API level) - 8 pilot batches
Manufacturing	- 3 Production campaigns - Manufacturing tool effect - Raw material effect - Manufacturing operator effect	
API concentration levels (%)	80, 90, 100, 110 and 120	80, 100 and 120
Series of measurements	3	

In order to obtain a robust NIR model, it was important to build but also to test the model with the future routine expected variability. As shown in Table 1, the expected future sources of variability were introduced in both the calibration and validation sets. Although the same sources of variability were introduced in both sets, they are independent. The 100 % API level being the targeted formulation, pilot batches and industrial batches were analyzed. Manufacturing sources of variability were also integrated. The first consisted in a manufacturing tool effect: for example, for the crosslinking process, the raw materials mixes were injected in 3 different crosslinking moulds. Furthermore, different batches of the same type of raw materials were used for the manufacturing. Besides, the manufacturing was carried out with 3 operators. To guarantee the NIR model robustness 5 API levels were integrated in the calibration set while the validation set contained 3 API levels. Finally, a day

effect was also present in the protocols: the batches were analyzed 3 times, making 3 independent series of measurements. The samples spectra were collected prior to the destructive reference HPLC analysis. From the 15 batches of the calibration set, 30 NIR spectra were collected. As the 2 spectra from the same sample were averaged, 15 NIR spectra were kept for the data analysis. As 3 series of measurement were performed, one series par day, the set contain a total number of 45 NIR spectra associated with 45 reference HPLC measurements. From the 9 batches of the validation set, 18 NIR spectra were collected. Since the 2 spectra from the same sample were averaged, 9 NIR spectra were kept for the data analysis. As 3 series of measurement were performed, one series par day, the set contain a total number of 27 NIR spectra associated with 27 reference HPLC measurements.

Table 2 – Conventional criteria of the NIR model.

NIR model	Selected parameter
Spectral range selected (cm^{-1})	7224-6495 6360-4500
Spectral pre-treatment	SNV
Number of PLS factors	4
R^2 Val	0.996
RMSEC (% API)	1.0
RMSEP (% API)	1.3

As can be seen from Table 2, a spectral range linked to the API was manually selected for the calibration of the NIR model. To check its adequacy, the model first loading factor plotted in Figure 9 was compared with the raw materials spectra displayed in Figure 5. It was found that the first loading factor highlighted spectral bands belonging to both the API and the PDMS mix. For example, the negative bands between 6000 and 5350 cm^{-1} are linked to the PMDS mixture while the positive bands located at 4700 cm^{-1} are related to the API. Indeed, it is the ratio between both ingredients that mainly defines the 3 different API content formulations. Consequently, the selected spectral range was found to be adequate regarding the purpose of the NIR model: to quantify accurately the API content of the drug reservoir.

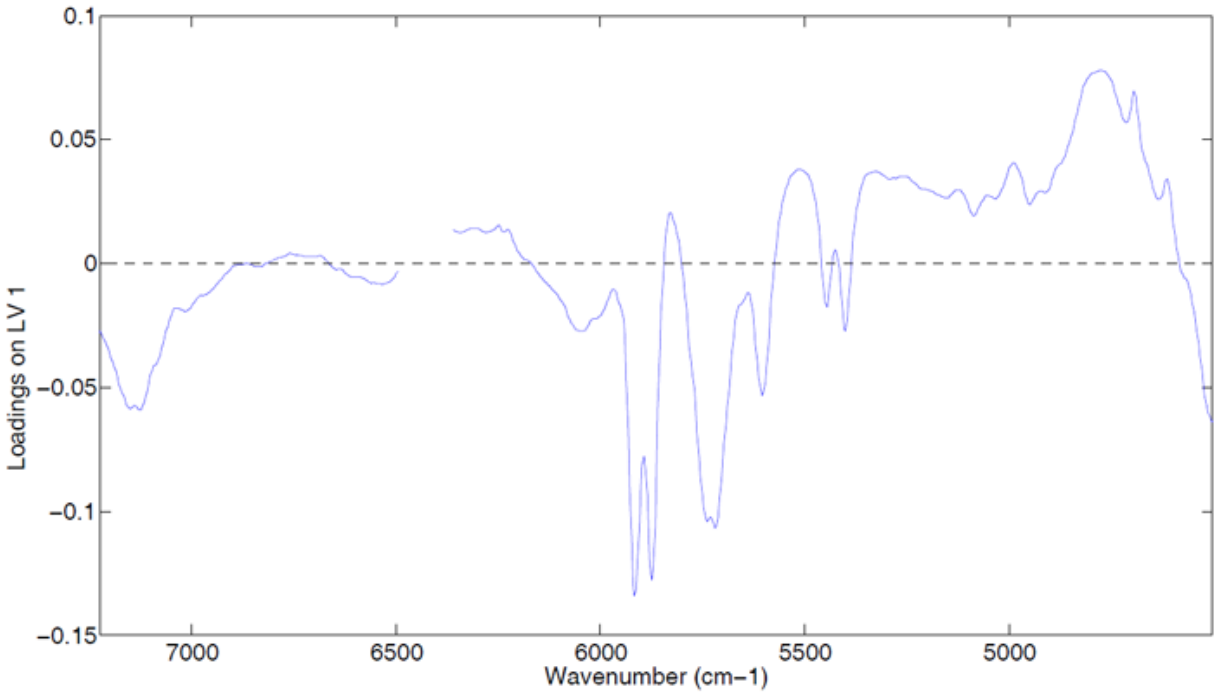

Fig. 9 – NIR PLS model for the API determination in the drug reservoirs: First loading factor.

Cross-validation based on random subsets was carried out to select the optimal number of PLS factors. For the random subsets cross-validation, 10 random splits and 15 iterations were selected.

4 PLS factors were selected for the NIR model as the RMSECV was the lowest from this number of factors (data not shown).

SNV was used as the signal pre-processing as it is well known to reduce the physical influence on the spectrum. This spectral filter is calculated based on the average and standard deviation of each single spectrum. Therefore, this correction is less sensitive to outliers in a data set, compared to filters that are calculated on an average spectrum of a sample set such as Multiplicative Signal Correction (MSC).

Considering the Root Mean Squared Error of Calibration (RMSEC) and the Root Mean Squared Error of Prediction (RMSEP) of the NIR model, their values are both close indicating the robustness and the global accuracy of the NIR model. Figure 10(a) shows the agreement observed between the NIR predictions and the reference method results for both the calibration and validation sets.

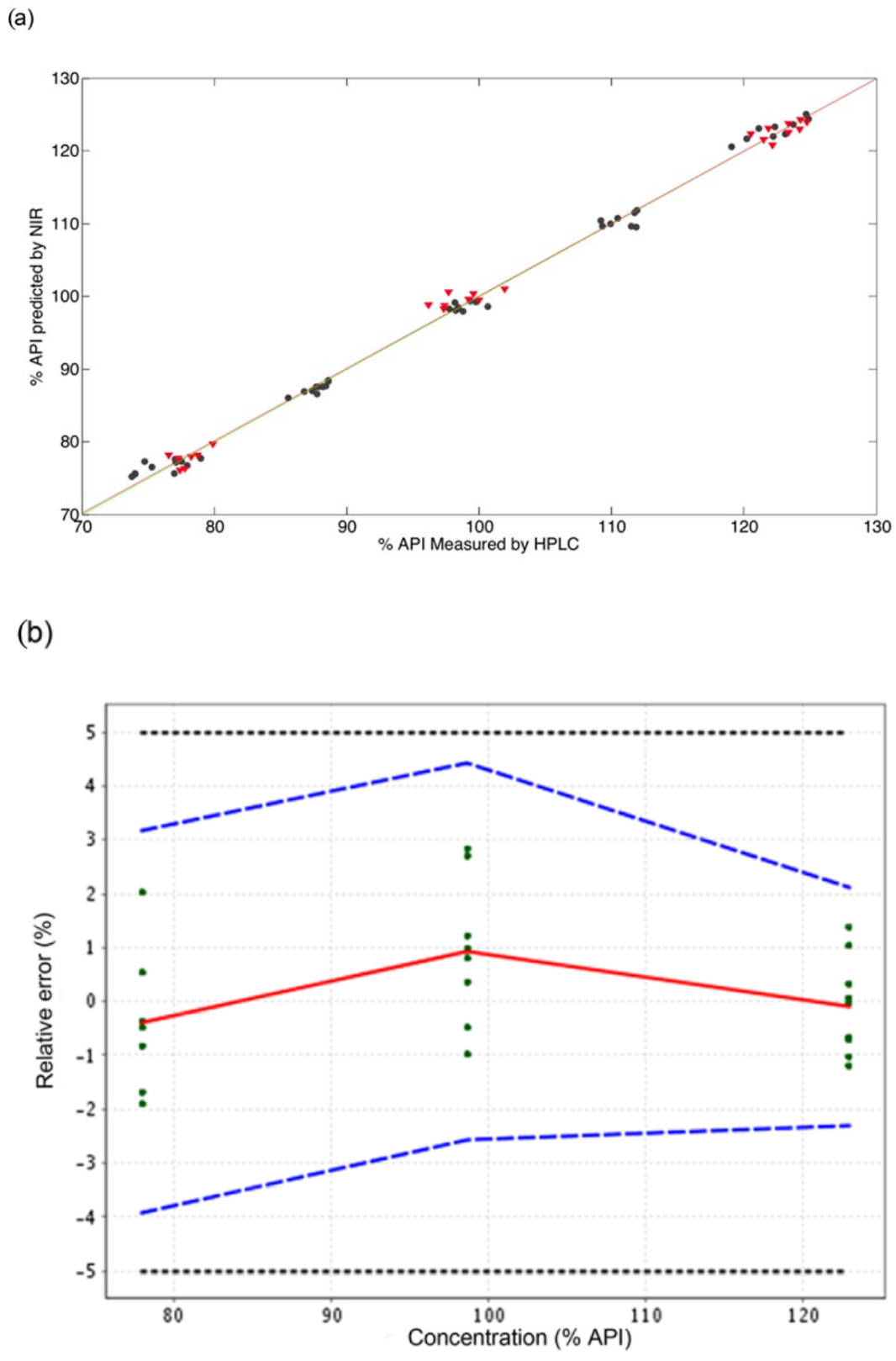

Fig. 10 – NIR model: (a) API content predicted by the NIR method versus the API content measured by HPLC for the calibration (black dots) and validation set (red triangles).(b) Accuracy profile based on the validation results of the NIR method. The plain line is the relative bias, the dashed lines are the β-expectations tolerance limits (β = 95 %) and the dotted lines represent the acceptance limits (±5 %).

Further, the model predictive performance was evaluated with accuracy profiles computed on the validation results [38-39]. This approach uses tolerance intervals as statistical methodology that allows predicting a region of concentration where each future result has a defined probability to fall. The present study focusing on the API determination in a pharmaceutical formulation, the probability to obtain results within the tolerance interval was set at 95 % while the acceptance limits were set at ± 5 % for the validation of the NIR method.

The lower and upper limits of quantification (LLOQ and ULOQ) define the range where an analytical method is able to quantify accurately. They are respectively the smallest and highest concentration levels where the β-expectation tolerance intervals are fully included within the acceptance limits. The LLOQ and ULOQ are here located at the beginning and at the end of the active content range investigated.

Figure 10(b) displays the accuracy profile obtained with the validations results. It can be seen from this figure that the validation results concentrations are different from the ones displayed in Figure 10(a). For the accuracy profile calculation, it was necessary to perform an alignment on the mean concentration obtained by the reference method per API concentration level to compute repeatability and intermediate precision variance estimates. As can be seen from the accuracy profile, the bias and dispersion of the validation results are both low for the entire concentration range investigated in the present study. It can therefore be observed that the 95 % tolerance interval is situated within the ±5 % acceptance limits which means that the future results will at least have a 95 % probability to be situated within the ±5 % acceptance limits. Based on the previous considerations, the NIR method accuracy is then suitable for routine analysis.

Table 3 shows the ICH Q2 (R1) validation criteria of the developed method. As can be seen from the accuracy profile, the trueness results are very acceptable: the bias is close to 1 for the 100 % while it is close to 0 for the 80 and 120 % API levels. The precision of the method was estimated by measuring repeatability and intermediate precision at the 3 concentration levels investigated. As observed in the accuracy profile, the dispersion of the validation results was small. Hence, repeatability and intermediate precision are both very satisfactory and never exceed 1.4 % as shown in Table 3.

Table 3 – ICH Q2 (R1) validation criteria of the NIR method.

Trueness	Concentration level (% API)	Mean introduced concentration (% API)	Relative bias (%)	
	80	78.0	-0.4	
	100	98.7	0.9	
	120	122.9	-0.1	
Precision	Concentration level (% API)	Mean introduced concentration (% API)	Repeatability (RSD %)	Intermediate precision (RSD %)
	80	78.0	1.3	1.3
	100	98.7	1.3	1.4
	120	122.9	0.9	0.9
Accuracy	Concentration level (% API)	Mean introduced concentration (% API)	Relative β-Expectation tolerance limits (%)	
	80	78.0	[-3.9 , 3.2]	
	100	98.7	[-2.6 , 4.4]	
	120	122.9	[-2.3 , 2.1]	
Limits of quantification (LOQ)		Lower LOQ (%)	Upper LOQ (%)	
		78.0	122.9	

Concerning the linearity of the NIR method, the intercept and the slope are close to 0 and 1 respectively confirming the absence of proportional and constant systematic error of the model.

Table 4 – NIR method: estimates of measurements uncertainties related to the API concentration in the drug reservoirs at each concentration level investigated.

Concentration level (% API)	Mean introduced concentration (% API)	Uncertainty of the bias (% API)	Uncertainty (% API)	Expanded uncertainty (% API)	Relative expanded uncertainty (%)
80	78.0	0.4	1.1	2.2	2.9
100	98.7	0.5	1.4	2.9	2.9
120	122.9	0.4	1.2	2.3	1.9

The uncertainty characterizes the dispersion of the values that could reasonably be attributed to the measurand [40-41]. Several uncertainty results were estimated and are present in Table 4: the uncertainty of the bias of the method at each concentration level of the validation standard, the uncertainty which combines the uncertainty of the bias with the uncertainty of the method obtained during the validation step, i.e. the intermediate precision standard deviation, and the expanded uncertainty with equals to the uncertainty multiplied by a coverage factor k=2 representing an interval around the results where the unknown true value can be observed with a confidence level of 95 % [42-44]. In addition, the relative expanded uncertainties with the corresponding introduced concentrations are not higher than 2.9 % which means that with a confidence level of 95 %, the unknown true value of the API content is located at a maximum of ± 2.9 % around the measured results.

Consequently, the method validation results clearly show that the developed NIR method can replace the conventional reference HPLC method. Furthermore, compared to the HPLC method, which takes hours because of the tedious and time consuming extraction step prior to the HPLC analysis, the added value of the NIR method is significant: it is non-invasive, non-destructive, only few seconds are needed to collect an accurate quantitative result and it can be used as an IPC in the manufacturing line.

4. Conclusions

Three critical quality attributes were checked using vibrational spectroscopy. First, Raman mapping was found to be a suitable technique to evaluate the API homogeneity within the drug reservoir. Second, the NIR spectral deviations linked to the crosslinking

process were successfully tracked by conformity tests and PCA. Compared to the conformity test analysis, PCA had the advantage to discriminate the crosslinking process from the heating process. The relation between the temperature and the time necessary to reach the crosslinking endpoint was highlighted. Finally, a NIR method able to determine the API content of the drug reservoirs was developed and successfully validated. The accuracy profile calculated on the validation results demonstrated that the NIR method could efficiently and reliably replace the actual time consuming HPLC reference analysis. As a conclusion, 3 main critical quality attributes of the silicone based drug reservoirs can be assessed, the authors believe that the developed PAT tools can advantageously be used for process optimisation leading to the definition of process Design Space or represent the first steps towards a Real Time Release quality based system.

Supplemental data

Crosslinking NIR interfacing: supplemental data

Figure S1 a) displays an aliquot of the raw materials mixture transferred into a vial cap. The latter is put at the bottom of a beaker which is thermostated by heated silicone oil.

Figure S1 b) shows the vials cap interfaced the NIR reflectance probe. The distance between the probe and the cap was 2 mm. The top of the beaker was covered with a pierced polystyrene plate to avoid the heat loss during the thermostating process.

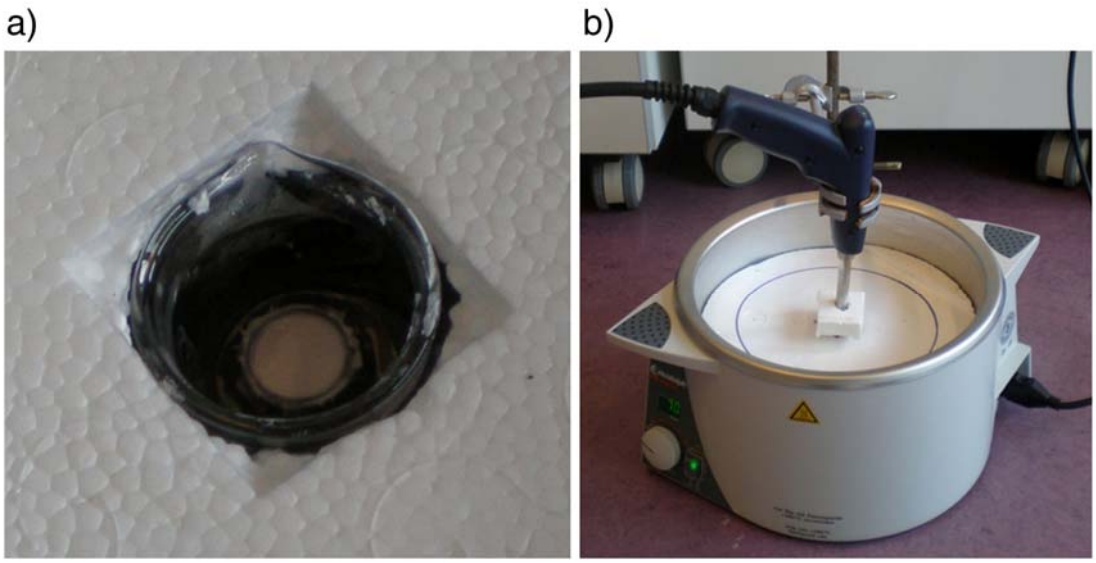

Figure S1 – Thermostated silicone-based drug reservoir a) interfaced with the FT-NIR spectrometer b).

Crosslinking study: supplemental data justifying the use of first derivative (window: 15 points) signal pre-processing

To study the crosslinking kinetic, a Savitzky Golay smoothing filter prior to the first derivative transformation was used as signal pre-processing.

The first derivative transformation was selected as it reduces the baseline shifts between the spectra occurring during the crosslinking process. However, such transformation is highly sensitive to spectral noise. Therefore, the Savitzky Golay smoothing filter was selected to reduce the spectral noise before applying the first derivative transformation.

The polynomial degree was set to 2 and different window sizes were investigated, knowing that the larger the window size is, the stronger the smoothing effect will be.

Figure S2a), b) and c) display NIR spectra collected during a crosslinking process with a window size of 7, 15 and 25 points respectively.

One can see from these figures that the spectral noise is stronger when the smoothing window size is 7 compared to 14 and 21 window sizes.

a)

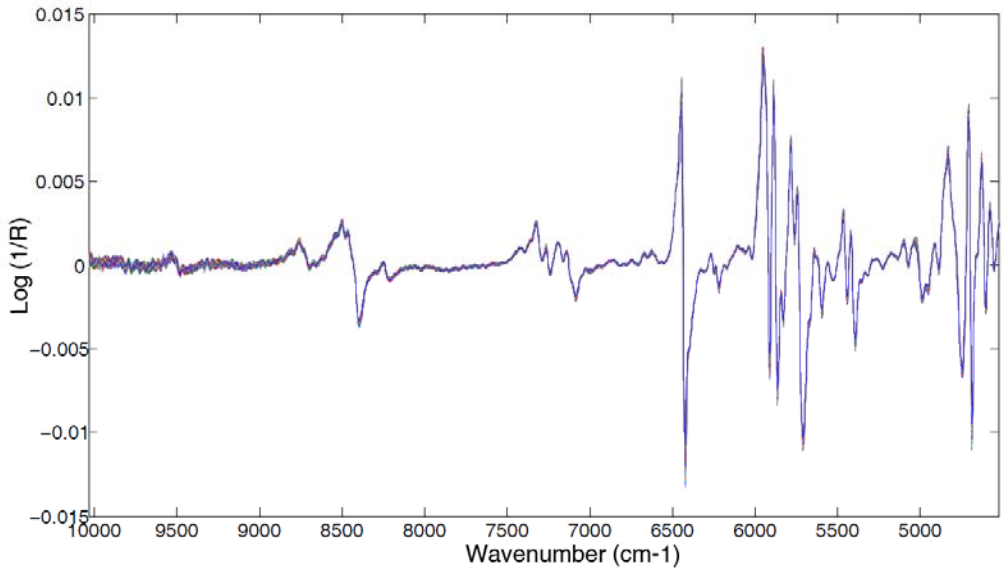

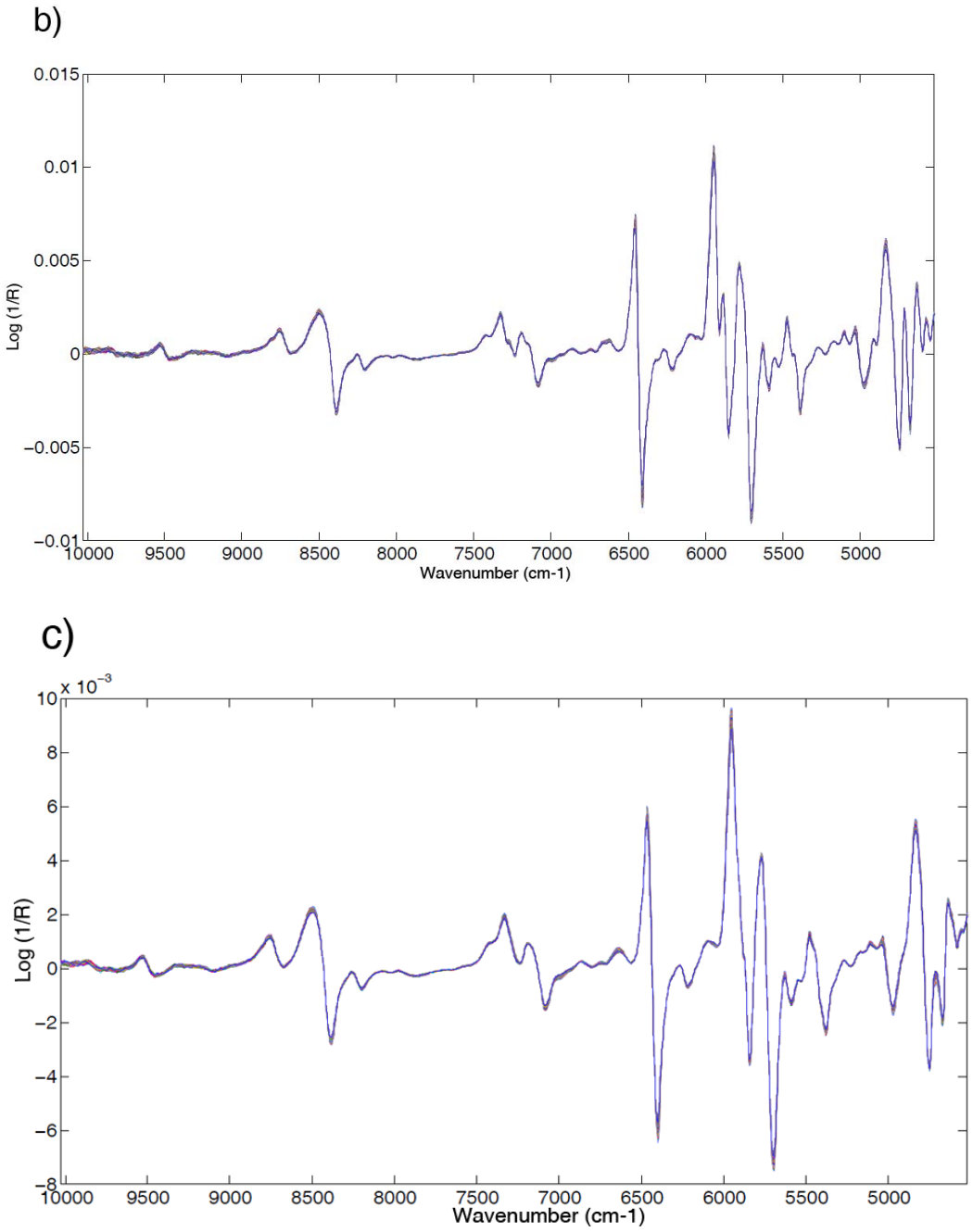

Figure S2 – Pre-processed NIR spectra collected during the crosslinking of a drug reservoir. The signal pre-processing consists in a Savitzky Golay smoothing filter followed by first derivative transformation. The smoothing filter polynomial order is 2 and the window size is 7, 15 and 21 for Figure S2a), b) and c) respectively.

In addition to spectra visual observation, NIR PCA models calculated with drug reservoirs thermostated at 24, 30, 36, 54 and 74 °C were built using the 3 window sizes. As can be seen from Table S1, the percentage of variance explained by PC 2 and PC 3 slightly differs according to the selected window size. However, a smoothing window size of 15 provided the highest explained variance percentage value. Accordingly, based on the spectra

visual observation and on the PCA results, the Savitzky Golay smoothing filter window size was set to 15.

Table S1- NIR PCA model calculated with drug reservoirs thermostated at 24, 30, 36, 54 and 74 °C: percentage of variance explained by PC 2 and 3 according to the selected window size of the Savitzky Golay smoothing filter.

Smoothing filter window size	% variance explained PC 2	% variance explained PC 3
a)7	14.32	0.97
b)15	15.65	1.22
c)21	14.28	1.18

Crosslinking study: supplemental data explaining the loadings factors of the PCA model displayed in Figure 8

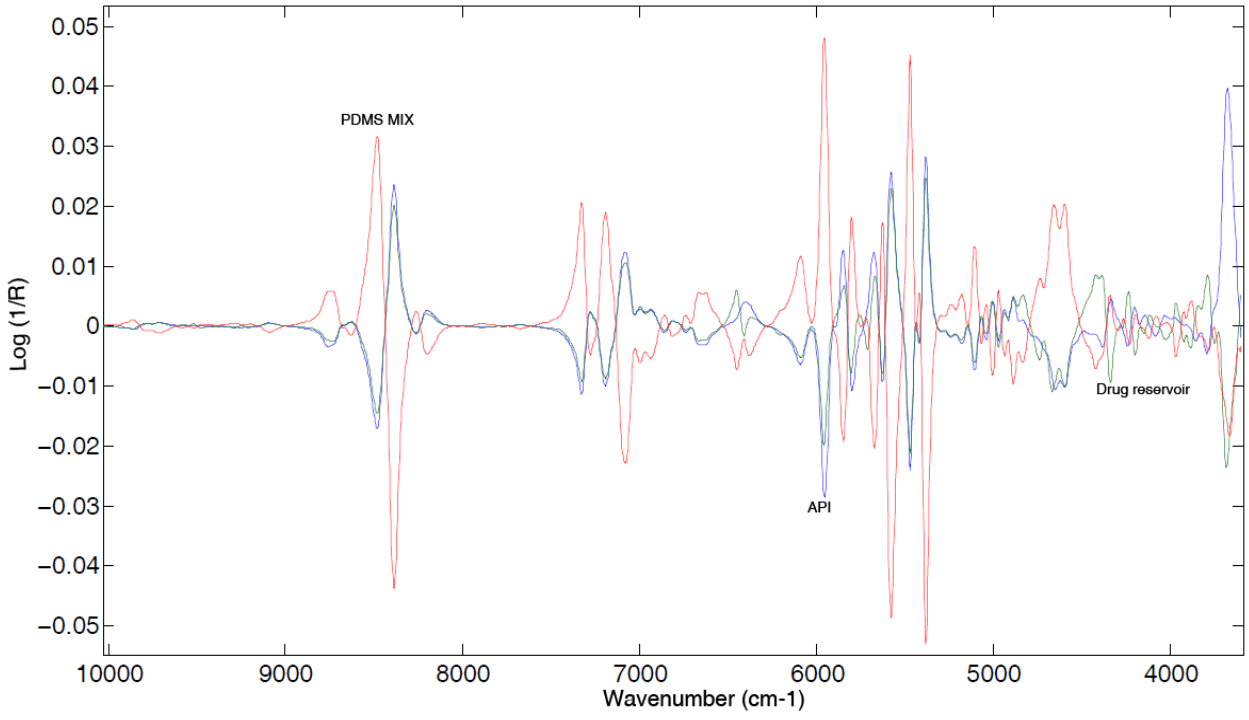

Figure S3 - PDMS mixture, API and drug reservoir NIR reflectance spectra after first derivative transformation.

Regarding the crosslinking study, in order to fully interpret the loading factors of the PCA model, Figure S3 displays the NIR spectra of the PDMS mixture, API and drug reservoir after first derivative transformation.

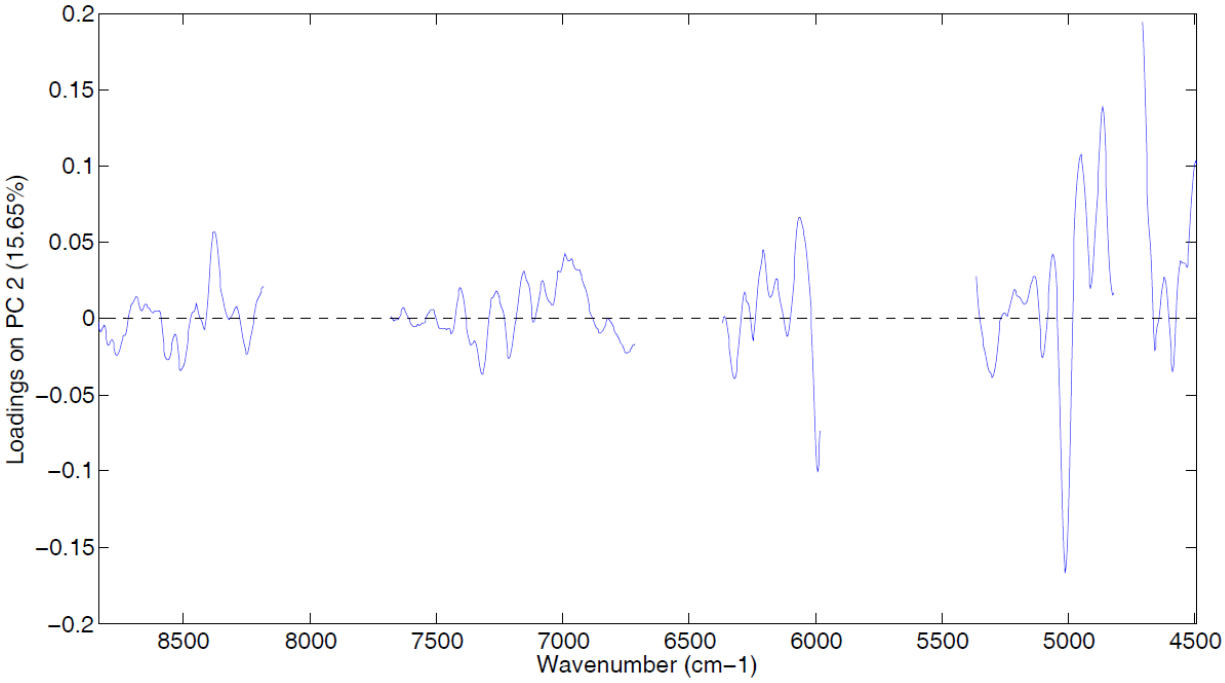

Figure S4 – Second loading factor of the NIR PCA model calculated with drug reservoirs thermostated at 24, 30, 36, 54 and 74 °C.

Figure S4 and S5 respectively display the second and third loading factor of the NIR PCA model calculated with drug reservoirs thermostated at 24, 30, 36, 54 and 74 °C.

The second loading factor plotted in Figure S4 does not clearly highlight API or PDMS spectral bands. In addition, it does not represent spectral noise. Based on the previous considerations and on the PCA results displayed in Figure 8, it was therefore presumed that the second loading factor highlighted temperature sensitive spectral bands.

Regarding PC 3 which models the crosslinking state of the samples, its corresponding loading factor clearly refers to the PDMS mixture spectrum as plotted in Figure S3. Therefore, the interpretation of the third loading factor clearly confirmed that PC 3 is specific to the crosslinking process.

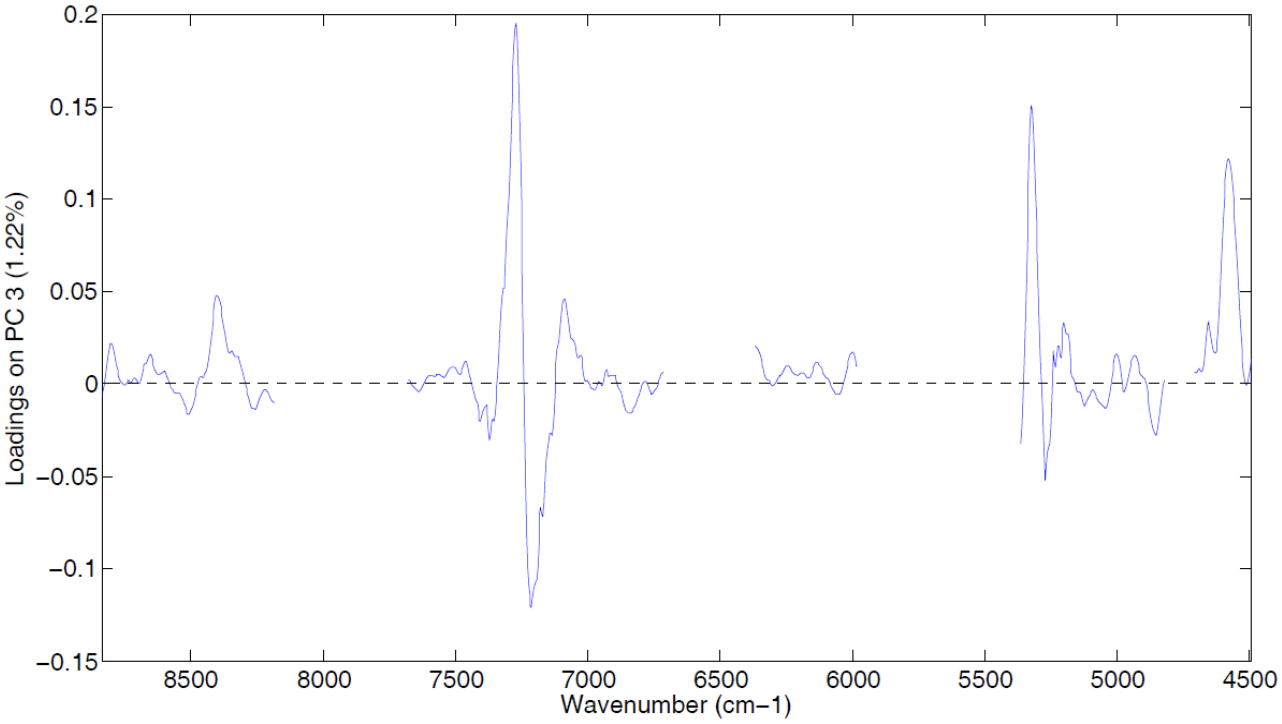

Figure S5 - Third loading factor of the NIR PCA model calculated with drug reservoirs thermostated at 24, 30, 36, 54 and 74 °C.

Acknowledgements

Special thanks are due to Fabienne Wijzen for the manufacturing of the silicone-based drug reservoirs. Thanks are due to the Walloon Region for a research grant provided to Jérôme Mantanus and Eric Ziémons. A research grant from the Belgium National Fund for Scientific Research (FRS-FNRS) to E. Rozet is gratefully acknowledged.

References

[1] International Conference on Harmonisation (ICH) of technical requirements for registration of pharmaceuticals for human use, Topic Q8(R2): Pharmaceutical development, Geneva, 2009.

[2] S.H. Tabasi, R. Fahmy, D. Bensley, C. O'brien, S.W. Hoag, J. Pharm. Sci 97 (2008) 4040-4051.

[3] International Conference on Harmonisation (ICH) of technical requirements for registration of pharmaceuticals for human use, Topic Q10: Pharmaceutical quality system, Geneva, 2008.

[4] J.F. Kunzler, Trends Polym. Sci. 4 (1996) 52-59.

[5] Z. Chen, R. Ward, Y. Tian, F. Malizia, D.H. Gracias, Y.R. Shen, J. Biomed. Mater Res. 62 (2002) 254-264.

[6] F. Abbasi, H. Mirzadeh, A.-A. Katbab, Polym. Int. 50 (2001) 1279-1287.
[7] United States Food and Drug Administration (FDA), Guidance for industry PAT-A framework for innovative pharmaceutical manufacturing and quality assurance, FDA, 2004.
[8] X. Li, Design of controlled release drug delivery systems, first ed., McGraw-Hill Professional, NewYork, 2005.
[9] United States Food and Drug Administration (FDA), Pharmaceutical CGMPs for the 21st century – a risk-based approach, FDA, 2004.
[10] D.A. Burns, E.W. Ciurczak, Handbook of Near-Infrared Analysis, third ed., CRC Press, New York, 2008.
[11] J. Luypaert, D.L. Massart, Y. Vander Heyden, Talanta 72 (2007) 865-883.
[12] S. Sasic, Pharmaceutical Applications of Raman Spectroscopy, John Wiley & Sons, New Jersey, 2007.
[13] R.M. Balabin, R.Z. Safieva, E.I. Lomakina, Anal. Chim. Acta 671 (2010) 27-35.
[14] D.L. Flumignan, A.G. Tininis, F. de Oliveira Ferreira, J.E. de Oliveira, Anal. Chim. Acta 595 (2007) 128-135.
[15] J. Müller, K. Knop, J. Thies, C. Uerpmann, P. Kleinebudde, Drug Dev. Ind. Pharm. 36 (2010) 234–243.
[16] T.R.M. De Beer, C. Bodson, B. Dejaegher, B. Walczak, P. Vercruysse, A. Burggraeve, A. Lemos, L. Dellatre, Y. Vander Heyden, J.P. Remon, C. Vervaet, W.R.G. Baeyens, J. Pharm. Biomed. Anal. 48 (2008) 772-779.
[17] T.R.M. De Beer, M. Wiggenhorn, R. Veillon, C. Debacq, Y. Mayeresse, B. Moreau, A. Burggraeve, T. Quinten, W. Friess, G. Winter, C. Vervaet, J.P. Remon, W.R.G. Baeyens, Anal. Chem. 81 (2009) 7639-7649.
[18] C. Bodson, E. Rozet, E. Ziemons, B. Evrard, Ph. Hubert, L. Delattre, J. Pharm. Biomed. Anal. 45 (2007) 356-361. http://hdl.handle.net/2268/1642
[19] J.J. Moes, M.M. Ruijken, E. Gout, H.W. Frijlink, M.I. Ugwoke, Int. J. Pharm. 357 (2008) 108-118.
[20] E.T.S. Skibsted, J.A. Westerhuis, A.K. Smilde, D.T. Witte, J. Pharm. Biomed. Anal. 43 (2007) 1297-1305.
[21] W. Li, L. Bagnol, M. Berman, R.A. Chiarella, M. Gerber, Int. J. Pharm. 380 (2009) 49-54.
[22] H. Grohganz, D. Gildemyn, E. Skibsted, J.M. Flink, J. Rantanen, Anal. Chim. Acta 676 (2010) 34-40.
[23] S.S. Rosa, P.A. Barata, J.M. Martins, J.C. Menezes, Talanta 75 (2008) 725-733.
[24] J. Mantanus, E. Ziémons, P. Lebrun, E. Rozet, R. Klinkenberg, B. Streel, B. Evrard, Ph. Hubert, Anal. Chim. Acta 642 (2009) 186-192. http://hdl.handle.net/2268/18780
[25] J. Mantanus, E. Ziémons, E. Rozet, B. Streel, R. Klinkenberg, B. Evrard, J. Rantanen, Ph. Hubert, Talanta 83 (2010) 305-311. http://hdl.handle.net/2268/69980
[26] J. Rantanen, S. Lehtola, P. Rämet, J.P. Mannermaa, J. Yliruusi, Powder Technol. 99 (1998) 163-170.
[27] J. Rantanen, E. Räsänen, O. Antikainen, J.P. Mannermaa, J. Yliruusi, Chemom. Intel. Lab. Syst. 56 (2001) 51-58.
[28] N. Sandler, J. Rantanen, J. Heinämäki, M. Römer, M. Marvola, J. Yliruusi, AAPS PharmSciTech 6 (2) (2005) 174-183.
[29] S.H. Tabasi, V. Moolchandani, R. Fahmy, S.W. Hoag, Int. J. Pharm. 382 (2009) 1-6.
[30] L. Maurer, H. Leuenberger, Int. J. Pharm. 370 (2009) 8-16.
[31] C. Ravn, E. Skibsted, R. Bro, J. Pharm. Biomed. Anal. 48 (2008) 554-561.

[32] M. Blanco, M. Alcalá, Anal. Chim. Acta 557 (2006) 353-359.
[33] M. Blanco, M. Alcalá, M. Bautista, Eur. J. Pharm. Sci. 33 (2008) 409-414.
[34] L. Saerens, L. Dierickx, B. Lenain, C. Vervaet, J.P. Remon, T. De Beer, Eur. J. Pharm. Biopharm. 77 (2011) 158-163.
[35] H. Martens, T. Naes, Multivariate Calibration, JohnWiley&Sons, Chichester, 1996.
[36] S. Wold, M. Sjöström, L. Eriksson, Chemom. Intel. Lab. Syst. 58 (2001) 109-130. http://wiki.eigenvector.com/index.php?title=Using_Cross-Validation (accessed 11/01/11).
[37] International Conference on Harmonization (ICH) of Technical requirements for registration of pharmaceuticals for human use, Topic Q2 (R1): Validation of analytical
[38] Procedures: Text and Methodology, Geneva, 2005.
[39] Ph. Hubert., J.J. Nguyen-Huu, B. Boulanger, E. Chapuzet, P. Chiap, N. Cohen, P.A. Compagnon, W. Dewé, M. Feinberg, M. Lallier, M. Laurentie, N. Mercier, G. Muzard, C. Nivet, L. Valat, J. Pharm. Biomed. Anal. 36 (2004) 579-586. http://hdl.handle.net/2268/6169
[40] Analytical Methods Committee, Analyst 120 (1995) 2303-2308.
[41] Eurachem/Citac guide, Quantifying the uncertainty in analytical measurement, second ed., 2000.
[42] CB EA-4/16, EA guidelines on the expression of uncertainty in quantitative testing, http://www.european-accreditation.org.
[43] M. Feinberg, B. Boulanger, W. Dewé, Ph. Hubert, Anal. Bioanal. Chem. 380 (2004) 502-514. http://hdl.handle.net/2268/6186
[44] R. Rozet, W. Dewe, S. Rudaz, R. Marini Djang'Eing'A, E. Ziemons, B. Boulanger, Ph. Hubert, Trends Analyt. Chem. 30 (2011) 797-806. http://hdl.handle.net/2268/81653

Chapter IV

Conclusions and perspectives

In 2004, FDA described the PAT concept as "*a system for designing, analyzing, and controlling manufacturing through timely measurements (i.e., during processing) of critical quality attributes and performance attributes of raw and in-process materials and processes, with the goal of ensuring the final product quality*". This concept involves many changes, especially in terms of batch release as most of the conformity tests would be carried out during the manufacturing itself. Nowadays, the use of PAT is increasingly encouraged by the recent guidelines. In addition, the recent Manual of Policies and Procedures document (MAPP 5016.1) expects the use of PAT as key "*enhanced knowledge element*" supporting the pharmaceutical development.

Taking into account its advantages (non-invasive and fast measurements, physical and chemical information contained in the NIR spectra, optical fibres accessories) it is obvious that NIR spectroscopy matches the requirements of the PAT framework, enabling to collect real time or near real time information about manufacturing processes in lieu of end product testing.

Within the framework of PAT, the aim of the present thesis was to confirm the potentiality of NIR spectroscopy on various types of pharmaceutical formulations.

First of all, as a first PAT control for any pharmaceutical process, a NIR method for the identification of the API raw materials in the manufacturing area was developed. To match the manufacturing line framework, the identification method was developed to analyze the API raw materials directly through 2 different standardized polyethylene bags. The results showed that chemical nature of the APIs but also their grades and providers could be identified. It was concluded that the present method consists in the first critical checkpoint for any pharmaceutical process. In addition, as an example of API raw material polymorphism , a comparative study based on the pre-validation results showing the interchangeability between NIR spectroscopy and X-Ray powder diffraction for the quantification of pure crystalline form II of fluconazole in binary polymorphic mixture (form II + III) was successfully conducted.

In the second place, a NIR method for the API determination of a low-dose (2 % (w/v) acetaminophen) liquid pharmaceutical formulation was developed. A full validation protocol was performed and the accuracy profile enabled to visualize the accuracy of the NIR method all over the considered API range. In addition, as a risk management tool, it guaranteed that at least 95 % of the actual and future results will be situated within the ± 5 % acceptance limits. Further, the validated method successfully monitored the API concentration during the mixing between lab-scale samples suggesting the possibility to transpose the present method in the manufacturing line using a transmission NIR liquid cell.

The next chapter was dedicated to the introduction of PAT checkpoints in the process flow chart of a pharmaceutical pellets formulation. A first checkpoint was introduced after the first drying step to quantify with NIR spectroscopy the active content of non-coated pharmaceutical pellets. The accuracy profile was used on the validation results to select among 3 NIR prediction models the one with the highest accuracy. Further, a NIR method robustness testing was successfully conducted on 2 new API concentration levels, blends of validation batches and industrial batches. A Bland and Altman plot between the HPLC

reference method and the NIR reference method results clearly demonstrated that the NIR method could easily and safely replace HPLC as a reliable IPC method. A second checkpoint in the pellets manufacturing was set after the pellets coating step to evaluate the moisture content of the coated pellets. Based on the validation results, the accuracy profile was used to select the most adequate model for the moisture content determination, a NIR model that allowed to check the pellets moisture content specification in an off-line or at-line way. A final checkpoint in the pellets flowchart was dedicated to the API determination in the final pharmaceutical product, coated pharmaceutical pellets, in motion situations found in the manufacturing line before the final packaging step. The first qualitative results showed that NIR spectroscopy could be interfaced with various particle streams found in the manufacturing line and still provide adequate and reliable qualitative results. Further, a quantitative application was developed based on a specific lab-scale particles stream of which accuracy was similar to off-line methods. The previous results clearly suggested that quantitative NIR methods could be effectively implemented in-line and provide a major contribution in a Real Time Release quality-based system.

Finally, we focused on a polymeric pharmaceutical formulation: silicone-based drug reservoir which is a rather uncommon pharmaceutical formulation. This last study highlighted the use of NIR but also Raman spectroscopy as PAT tools for the control of 3 critical quality attributes of a silicone-based drug reservoir formulation. Raman mapping successfully allowed to evaluate the API homogeneity within the drug reservoir while NIR spectroscopy enabled the real time monitoring of the reservoirs crosslinking process. Finally, an innovative NIR method able to quantify the reservoirs API content was successfully developed and validated with the accuracy profile approach. It was concluded in this first PAT study published in the literature on silicone-based drug reservoirs that the developed PAT tools paved the way towards Real Time Release and could be advantageously used for process optimization leading to the definition of the process design space.

As a conclusion, the results of the present thesis confirmed that NIR spectroscopy is a highly reliable analytical technique to control multiple critical quality attributes of various types of pharmaceutical formulation within the framework of the pharmaceutical development. All the developed quantitative applications were thoroughly validated using the accuracy profile approach which demonstrated their adequate accuracy for their purpose. Based on these results, the latter methodology can then be extended to the validation of NIR methods. Moreover, as it evaluates the risk to obtain future analytical results outside the analytical method acceptance limits, the accuracy profile approach is fully compliant with the actual trend in the analytical method development which is the risk assessment (cf. ICH Q9). Based on the previous considerations, it is obvious that NIR spectroscopy will remain an effective PAT tool for the next years to come. The information obtained by the developed PAT applications pave the way towards a Real Time Release based quality system.

Future work could be carried out on the optimization and validation of pharmaceutical processes based on the responses provided by various types of process analyzer (NIR and Raman spectroscopy, in-line particle size analyzers…).

Taking into account the PAT tools (NIR and Raman spectroscopy) developed in the present thesis, a first process to be optimized and validated could be the manufacturing process of silicone-based drug reservoirs. For this particular process, process parameters such as the raw materials blending speed and the heating temperature are known to influence the formulation critical quality attributes (API distribution, crosslinking kinetic, crosslinking state, drug diffusion profile). Besides, product variables such as the API particle size and moisture content and the crosslinker/catalyst chemical nature and level of concentration are also impacting on the formulation critical quality attributes.

Facing the previous considerations, it is obvious that a holistic approach would be needed to map the process parameters and product variables interactions. In this context, design of experiments would be perfectly adapted to gather the data and translate how the combination of the process parameters and product variables affect the critical quality attributes (CQAs). It would eventually help defining the combinations of process parameters and product variables that would keep the product performance within the specifications with a quantified guarantee for the future use of the process: the design space (cf. ICH Q8). That is, the target would be to identify, into the parameter space, a region of reliable robustness. To provide guarantees of future quality, DS could be defined in a risk-based framework. This approach would finally be compliant with the QbD expectations, as the results would emphasis on the assessment of quality and on the guarantees and underlying risks that this quality could or could not be achieved.

As the silicone-based drug reservoir process involves multiple critical quality attributes responses, a Design Space would be built from multiple response surfaces to find out the process parameters that would meet the specification of all the desired product attributes. Multiple response surface optimization usually involves the overlapping mean response approach. This approach performs as follows: if, for example, a process response is influenced by 3 process parameters, then this approach will display the mean predicted process response for any combination of the 3 process parameters within the defined parameters range. However, such approach would not take into consideration the model uncertainty parameters: it would not provide any indication about how often or how well the process can meet specifications with respect to the investigated response. This would represent a major drawback as ICH Q8 is clearly asking for a level of assurance to meet the product quality specifications. In contrast to the commercially available software packages such as Design Expert, SAS-JMP, Minitab, Statistica which construct the Design Space using the overlapped mean responses, a Bayesian predictive approach to define the Design Space would take into account the uncertainty of the statistical models, of the process and process analyzers. This approach would integrate the uncertainty in the Design Space by propagating the error associated to each model response prediction. Consequently, the Bayesian predictive approach would significantly improve the prediction ability of the Design Space. The calculated Design Space DS would allow to define a robustness area which could be validated by testing the predicted optimal operating conditions, enabling to define the Normal Operating Conditions.

For that purpose and because of their frequent use in the Pharmaceutical Industry, process optimization involving compaction, extrusion and granulation could also be investigated as case studies.

Chapter V

Thesis summary

Taking into account the *« Process Analytical Technology »* concept as described by the FDA in 2004, the main objective of the present work was to study and by the way to confirm the potentiality of NIR spectroscopy for the study of various types of pharmaceutical formulations. Parallel to the development of quantitative NIR applications, a secondary objective was to investigate whether the accuracy profile approach could be in any cases extended to the validation of NIR quantitative methods.

In the first place, a qualitative NIR method was developed to identify routinely through polyethylene bags the API raw materials being dispatched in a pharmaceutical manufacturing line. The results showed that chemical but also grade and provider identification could be achieved. Further, as a specific case study of API raw material polymorphism, the interchangeability between NIR spectroscopy and X-Ray powder diffraction was demonstrated for the quantification of pure crystalline form II of fluconazole in binary polymorphic mixture (form II + III). It was then concluded from this part of our work that such methods could consist in the very first PAT checkpoint of any pharmaceutical manufacturing process allowing to easily avoid any further misuse of these raw materials.

Later on, NIR as a PAT tool to control pharmaceutical formulations was considered. A NIR method for the API determination in a low dose syrup was first developed (2 % (w/v)). From the validation results, the accuracy profile enabled to visualize the accuracy of the NIR method all over the considered API range, it guaranteed that at least 95 % of the actual and future results will be included within the ± 5 % acceptance limits. Further, the validated method allowed successfully to monitor the API concentration during the mixing between lab-scale samples.

Further, following the pharmaceutical pellets process flow chart, an «off/at-line» method able to determine the API content of the non-coated pellets was developed and validated. The method robustness was successfully tested with 2 new API concentration levels, blends of validation batches and industrial batches. The interchangeability of the NIR method with the reference HPLC method was further demonstrated. Prior to the packaging steps, the coated pellets moisture content specifications were evaluated with a developed and validated *«off/at-line»* NIR method while the feasibility of an *«in-line»* NIR method for API evaluation was investigated. NIR spectroscopy was able to qualitatively assess the API content of coated pellets in a great variety of particles streams. One quantitative NIR method fitted for one specific particle stream was developed and validated: the validation results demonstrated that accurate quantitative measurements from moving particles could be achieved with NIR spectroscopy.

The last chapter of the work was focused on the development of PAT tools to assess 3 critical quality attributes of silicone-based drug reservoirs. NIR spectroscopy successfully allowed the real time monitoring of the crosslinking process while Raman mapping enabled

to evaluate the API distribution within the drug reservoirs. Finally, a NIR method able to determine the API content of the reservoirs was successfully developed and validated. The accuracy profile demonstrated that the NIR method could efficiently replace the actual HPLC reference analysis involving a very time consuming sample preparation step.

As a conclusion, the interest of NIR spectroscopy as a PAT tool was confirmed and its reliability as a PAT process analyzer for the evaluation of multiple critical quality attributes of various types of pharmaceutical formulations was clearly demonstrated by means of several practical examples. The present work also showed that the use of the accuracy profile could be extended without any problem to the validation of NIR quantitative methods and this profile could be a very interesting decision tool in the framework of the selection of the most appropriate calibration model.

Reposant sur le concept du *« Process Analytical Technology »* tel que préconisé par la FDA depuis 2004, l'objectif principal de ce travail était d'étudier et de confirmer par la même occasion les potentialités de la spectroscopie NIR pour le suivi de principes actifs tant au niveau de leur identification primaire que de leur quantification au sein de différentes formulations pharmaceutiques. Parallèlement à cet objectif, nous voulions appliquer mais aussi et surtout évaluer l'intérêt du profil d'exactitude pour la validation des méthodes quantitatives en spectroscopie NIR.

Dans un premier temps, nous nous sommes attelés au développement d'une méthodologie qualitative en spectroscopie NIR pour l'identification au travers de sacs en polyéthylène de différents principes actifs présents dans une zone de production pharmaceutique. Les résultats obtenus lors de cette étude nous ont permis de montrer qu'en plus d'une identification chimique, une identification de la qualité et des différents fournisseurs de principe actif étaient également possibles. Par la suite nous sommes intéressés au cas plus particulier d'un principe actif présentant un phénomène de polymorphisme. Nous avons démontré l'interchangeabilité existant entre la spectroscopie NIR et la diffraction aux rayons X pour la quantification de la forme cristalline II du fluconazole dans des mélanges binaires de formes cristallines (formes II et III). A l'issue de ces premières études, il apparaît clairement que de telles méthodes constituent indéniablement un premier point de contrôle PAT adapté aux procédés de fabrication permettant d'éviter assez facilement toute mauvaise utilisation des matières premières pharmaceutiques.

Par la suite, nous nous sommes plus spécifiquement attachés à l'étude des potentialités de la spectroscopie NIR pour la quantification de principes actifs dans différentes formulations pharmaceutiques.

Une nouvelle méthode NIR a tout d'abord été développée afin d'analyser des sirops faiblement dosés en paracétamol (2 % (m/v)). Sur la base des résultats de validation, l'utilisation du profil d'exactitude nous a non seulement permis de visualiser les performances analytiques de la méthode NIR sur toute la gamme de concentration envisagée mais aussi de garantir qu'au moins 95 % des futurs résultats seraient compris à l'intérieur des limites d'acceptation fixées à ± 5 %. De plus, cette méthode NIR nous a également permis de suivre directement la concentration en paracétamol pendant le mélange de différents sirops, simulant de la sorte un procédé industriel pour forme liquide.

Ultérieurement, de multiples points de contrôle NIR ont été introduits dans un procédé de fabrication de pellets pharmaceutiques. Dans le cadre de cette seconde étude, une méthode NIR permettant de déterminer la quantité d'actif présente dans des pellets non-enrobés a été développée et validée avec succès. Sa robustesse a ensuite été éprouvée sur des niveaux de concentration différents mais aussi sur des mélanges de plusieurs lots de

validation et sur des lots industriels. Sur la base de ces résultats, nous pouvons raisonnablement affirmer que la méthode de référence (HPLC) pourrait être remplacée par la méthode NIR pour ce type contrôle. De plus, cette interchangeabilité ne s'arrête pas là. En effet, avant l'étape de conditionnement des pellets enrobés, leur teneur en eau a été déterminée à l'aide d'une méthode NIR « *off/at-line* » également complètement validée tandis que la faisabilité d'une méthode NIR « *in-line* » capable de doser la teneur en principe actif a aussi été investiguée avec succès. En effet, la spectroscopie NIR nous a permis d'étudier une grande variété de flux particulaires de pellets enrobés lors du développement de cette méthode de quantification « *in-line* ». Les résultats de la validation attestent clairement que des mesures quantitatives de qualité à partir de particules en mouvement sont tout à fait envisageables via la spectroscopie NIR.

Le dernier chapitre du travail a été quant à lui consacré au développement d'outils PAT capables d'évaluer trois caractéristiques critiques d'un dispositif médicamenteux particulier, à savoir un réservoir polymérique à libération prolongée. Dans le cadre de cette dernière étude, la spectroscopie NIR nous a permis de suivre en temps réel l'étape de réticulation du réservoir et la spectroscopie Raman de visualiser la distribution du principe actif au sein de ce dernier. Enfin, comme dans les études précédentes, une méthode NIR originale a été développée et validée pour la détermination de la teneur du principe actif. L'utilisation du profil d'exactitude nous a à nouveau permis de prouver que la méthode NIR pourrait efficacement remplacer la méthode chromatographique de référence qui nécessite une étape d'extraction du principe actif assez fastidieuse.

En conclusion, les exemples pratiques développés dans le présent travail ont permis de confirmer l'intérêt de la spectroscopie NIR, en tant qu'analyseur PAT compliant, pour le contrôle des caractéristiques critiques d'une large gamme de formulations pharmaceutiques. Ils nous ont également permis de prouver que l'approche de validation basée sur le profil d'exactitude était parfaitement transposable à la validation des méthodes quantitatives NIR. Cette dernière approche pourrait par ailleurs constituer un outil décisionnel judicieux pour la sélection du modèle de calibration le plus approprié.

Chapter VI

Scientific production

Publications

1. **J. Mantanus, E. Ziemons, P. Lebrun, E. Rozet, R. Klinkenberg, B. Streel, B. Evrard, Ph. Hubert, *"Moisture content determination of pharmaceutical pellets by near infrared spectroscopy: Method development and validation"***, Analytica Chimica Acta 2009 (642) 186-192.

2. **J. Mantanus, E. Ziemons, P. Lebrun, E. Rozet, R. Klinkenberg, B. Streel, B. Evrard, Ph. Hubert, *"Active content determination of non-coated pharmaceutical pellets by near infrared spectroscopy: Method development, validation and reliability evaluation"***, Talanta 2010 (80) 1750-1757.

3. **J. Mantanus, E. Ziemons, P. Lebrun, E. Rozet, B. Evrard, Ph. Hubert, "*Acetaminophen determination in low-dose pharmaceutical syrup by NIR spectroscopy"***, Journal of Pharmaceutical and Biomedical Analysis 2010 (53) 510-516.

4. **J. Mantanus, E. Ziemons, E. Rozet, B. Streel, R. Klinkenberg, B. Evrard, J. Rantanen, Ph. Hubert, *"Building the quality into pellet manufacturing environment – feasibility study and validation of an in-line quantitative near infrared (NIR) method"***, Talanta 2010 (83) 305-311.

5. **E. Ziemons, H. Bourichi, J. Mantanus, E. Rozet, P. Lebrun, E. Essassi, Y. Cherrah, A. Bouklouze, Ph. Hubert, *" Determination of binary polymorphic mixtures of fluconazole using near infrared spectroscopy and X-ray powder diffraction : A comparative study based on the pre-validation stage results"***, Journal of Pharmaceutical and Biomedical Analysis 2011 (55) 1208-1212.

6. **J. Mantanus, E. Rozet, K. Van Butsele, C. De Bleye, A. Ceccato, B. Evrard, Ph. Hubert, E. Ziemons, *"Near infrared and Raman spectroscopy as Process Analytical Technology tools for the manufacturing of silicone-based drug reservoirs"***, Analytica Chimica Acta 2011 (699) 96-106.

7. **P. Lebrun, F. Krier, J. Mantanus, H. Grohganz, M. Yang, E. Rozet, B. Boulanger, B. Evrard, J. Rantanen, Ph. Hubert, *"Design space approach in the optimization of the spray drying process",*** submitted to European Journal of Pharmaceutical Sciences.

Talks

1. **J. Mantanus, E. Ziemons, P. Lebrun, E. Rozet, R. Klinkenberg, B. Streel, B. Evrard, Ph. Hubert, *"Determination of moisture content in pharmaceutical pellets using near infrared spectroscopy: method development and validation"*,** PAT workshop 2008, Ghent, Belgium.

2. **J. Mantanus, E. Ziemons, B. Streel, R. Klinkenberg, B. Evrard, Ph. Hubert, J. Rantanen, *"Production line real time near infrared (NIR) monitoring – Effect of sample flow and density"*,** Pharmaceutical Solid State Research Cluster 2009, Copenhagen, Denmark.

3. **J. Mantanus, E. Ziemons, K. Van Butsele, B. Evrard, A. Ceccato, Ph. Hubert, *"NIR and Raman spectroscopy as PAT tools for the manufacturing of silicone-based drug reservoirs"*,** Drug Analysis 2010, Antwerpen, Belgium.